Missouri S&T Library and Learning Resources

Scholars' Mine

Doctoral Dissertations | Student Theses and Dissertations

Fall 2009

Decentralized adaptive neural network control of interconnected nonlinear dynamical systems with application to power system

Shahab Mehraeen

Follow this and additional works at: https://scholarsmine.mst.edu/doctoral_dissertations

 Part of the Electrical and Computer Engineering Commons

Department: Electrical and Computer Engineering

Recommended Citation

Mehraeen, Shahab, "Decentralized adaptive neural network control of interconnected nonlinear dynamical systems with application to power system" (2009). *Doctoral Dissertations*. 2149.
https://scholarsmine.mst.edu/doctoral_dissertations/2149

This thesis is brought to you by Scholars' Mine, a service of the Missouri S&T Library and Learning Resources. This work is protected by U. S. Copyright Law. Unauthorized use including reproduction for redistribution requires the permission of the copyright holder. For more information, please contact scholarsmine@mst.edu.

DECENTRALIZED ADAPTIVE NEURAL NETWORK CONTROL OF INTERCONNECTED NONLINEAR DYNAMICAL SYSTEMS WITH APPLICATION TO POWER SYSTEM

by

SHAHAB MEHRAEEN

A DISSERTATION

Presented to the Faculty of the Graduate School of the

MISSOURI UNIVERSITY OF SCIENCE AND TECHNOLOGY

In Partial Fulfillment of the Requirements for the Degree

DOCTOR OF PHILOSOPHY

in

ELECTRICAL ENGINEERING

2009

Approved by

Jagannathan Sarangapani, Advisor

Mariesa Crow
Kelvin Erickson
Cihan Dagli
Jonathan Kimball

PUBLICATION DISSERTATION OPTION

This dissertation consists of the following six articles:

Paper 1, S. Mehraeen, S. Jagannathan, M. L. Crow, "Novel Dynamic Representation and Control of Power Systems with FACTS Devices", *Accepted in IEEE Transactions on Power Systems, 2009.*

Paper 2, S. Mehraeen, S. Jagannathan, M. L. Crow, "Decentralized Control of Large Scale Systems Using Adaptive Neural Network-based Dynamic Surface Control", *Submitted to IEEE Transactions on Neural Networks, 2009.*

Paper 3, S. Mehraeen, S. Jagannathan, M. L. Crow, "Decentralized Control of Power Systems Using Adaptive Neural Network-Dynamic Surface based Control", *in Revision for the IEEE Transactions on Power Systems, 2009.*

Paper 4, S. Mehraeen, S. Jagannathan, M. L. Crow, "Decentralized Adaptive Neural Network Control of a Class of Interconnected Nonlinear Discrete-time Systems with Application to Power Systems", *Submitted to IEEE Transactions on Power Systems, 2009.*

Paper 5, S. Mehraeen**,** S. Jagannathan, "Decentralized Near Optimal Control of a Class of Interconnected Nonlinear Discrete-time Systems by Using Online Hamilton-Bellman-Jacobi Formulation" *Submitted to IEEE Transactions on Neural Networks, 2009.*

Paper 6, S. Mehraeen, T. Dierks, S. Jagannathan, and M. L. Crow "Generalized Hamilton-Jacobi-Isaacs Formulation for Near Optimal Control of Affine Nonlinear Discrete-Time Systems with Application to Power Systems", *Submitted to IEEE Transactions on Systems, Man and Cybernetics, 2009.*

ABSTRACT

Traditional nonlinear techniques cannot be directly applicable to control large scale interconnected nonlinear dynamic systems due their sheer size and unavailability of system dynamics. Therefore, in this dissertation, the decentralized adaptive neural network (NN) control of a class of nonlinear interconnected dynamic systems is introduced and its application to power systems is presented in the form of six papers.

In the first paper, a new nonlinear dynamical representation in the form of a large scale interconnected system for a power network free of algebraic equations with multiple UPFCs as nonlinear controllers is presented. Then, oscillation damping for UPFCs using adaptive NN control is discussed by assuming that the system dynamics are known. Subsequently, the dynamic surface control (DSC) framework is proposed in continuous-time not only to overcome the need for the subsystem dynamics and interconnection terms, but also to relax the explosion of complexity problem normally observed in traditional backstepping. The application of DSC-based decentralized control of power system with excitation control is shown in the third paper.

On the other hand, a novel adaptive NN-based decentralized controller for a class of interconnected discrete-time systems with unknown subsystem and interconnection dynamics is introduced since discrete-time is preferred for implementation. The application of the decentralized controller is shown on a power network. Next, a near optimal decentralized discrete-time controller is introduced in the fifth paper for such systems in affine form whereas the sixth paper proposes a method for obtaining the L_2-gain near optimal control while keeping a tradeoff between accuracy and computational complexity. Lyapunov theory is employed to assess the stability of the controllers.

ACKNOWLEDGMENTS

I would like to thank my advisor, Dr. Jagannathan Sarangapani, for his guidance, support, and patience over the last several years. I would like to thank my co-advisor, Dr. Mariesa Crow for her guidance and help. I would also like to thank, Dr. Kelvin Erickson, Dr. Cihan Dagli, and Dr. Jonathan Kimball for serving on my doctoral committee. In addition, I would like to thank the National Science Foundation and Sandia National Laboratories for providing additional support.

I also thank my wife, Simin, my daughter, Bahharr, my parents, as well as the rest of my family for their support. I would also like to thank God for the opportunities I have been presented with and the courage to pursue them.

PUBLICATION DISSERTATION OPTION

This dissertation consists of the following six articles:

Paper 1, S. Mehraeen, S. Jagannathan, M. L. Crow, "Novel Dynamic Representation and Control of Power Systems with FACTS Devices", *Accepted in IEEE Transactions on Power Systems, 2009.*

Paper 2, S. Mehraeen, S. Jagannathan, M. L. Crow, "Decentralized Control of Large Scale Systems Using Adaptive Neural Network-based Dynamic Surface Control", *Submitted to IEEE Transactions on Neural Networks, 2009.*

Paper 3, S. Mehraeen, S. Jagannathan, M. L. Crow, "Decentralized Control of Power Systems Using Adaptive Neural Network-Dynamic Surface based Control", *in Revision for the IEEE Transactions on Power Systems, 2009.*

Paper 4, S. Mehraeen, S. Jagannathan, M. L. Crow, "Decentralized Adaptive Neural Network Control of a Class of Interconnected Nonlinear Discrete-time Systems with Application to Power Systems", to be *Submitted to IEEE Transactions on Power Systems, 2009.*

Paper 5, S. Mehraeen**,** S. Jagannathan, "Decentralized Near Optimal Control of a Class of Interconnected Nonlinear Discrete-time Systems by Using Online Hamilton-Bellman-Jacobi Formulation" *to be Submitted to IEEE Transactions on Neural Networks, 2009.*

Paper 6, S. Mehraeen, T. Dierks, S. Jagannathan, and M. L. Crow "Generalized Hamilton-Jacobi-Isaacs Formulation for Near Optimal Control of Affine Nonlinear Discrete-Time Systems with Application to Power Systems", to be *Submitted to IEEE Transactions on Systems, Man and Cybernetics, 2009.*

ABSTRACT

Traditional nonlinear techniques are not directly applicable to control large-scale interconnected nonlinear dynamic systems due their sheer size, unknown system dynamics and the unavailability of state measurements. Therefore, in this dissertation, the decentralized adaptive neural network (NN) control of unknown nonlinear interconnected systems with application to power systems is presented.

In paper one, a new nonlinear dynamical representation in the form of a large scale interconnected system for a power network free of algebraic equations with multiple Unified Power Flow Controllers (UPFCs) as nonlinear controllers for oscillation damping is presented by assuming that the system dynamics are unknown. Subsequently, in paper two the dynamic surface control (DSC) framework is proposed in continuous-time not only to overcome the need for the subsystem dynamics and interconnection terms, but also to relax the "explosion of complexity" problem normally observed in traditional backstepping. Then, the application of DSC-based decentralized control of power system with excitation control is shown in paper three.

On the other hand, in paper four, a novel adaptive NN-based decentralized controller for a class of interconnected discrete-time systems with unknown subsystem and interconnection dynamics is introduced since discrete-time design is preferred for implementation. The application of the controller is shown on a power system. Next, a near optimal decentralized discrete-time controller is introduced in paper five where NNs are employed to approximate the cost function and optimal control input by using online learning feature. Finally, paper six proposes the L_2-gain near optimal controller. Lyapunov theory is employed to assess the stability of all the controllers.

ACKNOWLEDGMENTS

I would like to thank my advisor, Dr. Jagannathan Sarangapani, for his guidance, support, and patience over the last several years. I would like to thank my co-advisor, Dr. Mariesa Crow for her guidance and help. I would also like to thank, Dr. Kelvin Erickson, Dr. Cihan Dagli, and Dr. Jonathan Kimball for serving on my doctoral committee. In addition, I would like to thank the National Science Foundation and Sandia National Laboratories for providing additional support.

I also thank my wife, Simin, my daughter, Bahharr, my parents, as well as the rest of my family for their support. I would also like to thank God for the opportunities I have been presented with and the courage to pursue them.

TABLE OF CONTENTS

SECTION

LIST OF ILLUSTRATIONS

Paper 4

Paper 5

LIST OF TABLES

SECTION

1. INTRODUCTION

For the past several decades, linear systems theory was the major methodology in the area of control as its mathematical basis is well developed and implemented on industrial controllers. Well-known methods such as quantitative feedback theory (QFT) [1], root locus, Nyquist criteria, Bode and Nichols chart [2] have been widely used in the control system design and analysis in the frequency domain, while Kalman filtering [3], the linear-quadratic regulator (LQR), and the linear-quadratic-Gaussian controller (LQG) [4] are solutions in the time domain.

With the increased system complexity of today's industrial systems, limitation of the linear control methods have been observed in a variety of applications. Power systems, robot manipulators, HVAC (heating, ventilation, and air conditioning systems), and electric machines are just a few examples of highly nonlinear systems where linear techniques provide good results for a very limited region of operation. If the operational conditions change or the system exits the linear region, stability may not be guaranteed by using linear control theory.

The nonlinear control theory, on the other hand, has been developed in the past few decades. Topics such as nonlinear adaptive control [5], robust control, nonlinear optimal control [6] as well as techniques including feedback linearization, sliding mode control, backstepping [7], dynamic surface control [8] and many others have been attracting a great attention lately. From application point of view, not only have the

nonlinear control designs been found useful in the diverse industrial applications, but also they have proven to be more promising when it comes to stability assurance and control performance compared to their linear counterparts.

Next, applications of nonlinear control in power systems are considered, and the benefits over linear control techniques are discussed.

1.1. APPLICATIONS OF NONLINEAR CONTROL IN POWER SYSTEMS

The power system is the one of the most important infrastructures for any region of the world since it generates and transmits (Fig. 1.1) energy for lighting, heating, home appliances, transportation, industrial applications, medical centers, etc. Thus, power system operation, reliability, and stability are of paramount importance.

Stability is one of key features in operating power systems. When a disturbance occurs in the system, generators deviate from their stable operating point due to the power imbalance which in turn causes generator oscillations. The resulting oscillations remain sustained unless they are damped by means of a stabilizer. In the recent years, the competitive market for power generation and energy services demand a more reliable power network. Due to offshore wind generation plants (Fig. 1.2) and solar cells, a noticeable uncertainty in the load flows will occur in a power system thus impacting the dynamic behavior and stability [9]. Therefore, power system controllers play an important role in maintaining dynamic performance and power system stability, and thus, increasing reliability.

Fig.1.1 Power system transmission lines convey energy for hundreds of miles[1]

Power systems are usually represented by nonlinear dynamic equations of the generation units and loads combined with nonlinear algebraic equations of the power network [9]. Linear approaches have been used widely to achieve a useful representation of the nonlinear power system dynamics; however, it is assumed that the power system stays close to the operating point. Nonlinear control of power systems, on the other hand, is a new topic in power system analysis and control. Due to the recent developments in the nonlinear control theory, power system researchers find nonlinear techniques more reliable and robust to operate and control the power network.

[1]Photo courtesy of: www2.ee.ic.ac.uk/cap/cappp/projects/15/trline.jpg

Fig.1.2 Wind turbines are one of the most common sources of renewable energy[2]

In the next section, an overview of recent nonlinear topics is introduced.

1.2. OVERVIEW OF NONLINEAR CONTROL TOPICS AND POWER SYSTEM APPLICATIONS

1.2.1. Decentralized Control. Nonlinear control approaches such as feedback linearization, robust control, optimal control, adaptive control, and many others usually require the knowledge of the system dynamics and measurement of system states for control. If the system consists of several subsystems, the controller requires state measurements from all subsystems. Consider a power network which is spread over a few hundreds of miles where the generators spread over the entire system. In other words, the distance between the generators can be hundreds of miles. In addition, in order to achieve an effective control design, one needs the power system bus data (voltages and phase angles) from various points in the power system. Although the data can be acquired from

[2] Photo courtesy of: jcwinnie.biz/wordpress/?p=2318

generators as well as the power system nodes and be sent to the main controller or all subsystem controllers, the process of data acquisition and transmission to the large-scale system or among different subsystems is quite long which can cause significant delays. Moreover, the amount of data in such an infrastructure is usually large enough to cause processing delays in the controller regardless of the distance where the data are sent from. The delay is one major cause of instability.

In decentralized control methods, each subsystem has a controller that uses local measurements [10]. Then, the effect of other subsystems is normally modeled by interconnection terms in the subsystem dynamic representation. The interconnection term is an unknown function of other subsystems states. Depending on the type of application, different assumptions can be made on how the interconnection terms behave. The interconnection term can be bounded by a constant, a function of other subsystem tracking errors, or a function of other subsystems states. The subsystem controllers are designed simultaneously such that they mitigate the effect of the interconnection terms in the overall large-scale system.

In power systems, the subsystems can be the generators (Fig. 1.3) or groups of generators. Then, the power system is divided among these subsystems. The effect of other subsystems appears as injected power that influences the subsystem dynamics. Finally, the controller can be a generator excitation controller or FACTS device.

Fig. 1.3 Generators are the subsystems in the decentralized control of power systems[3]

1.2.2. Adaptive Neural Network Design. The use of adaptive neural networks (NN's) in control systems has been motivated by biological processes such as the nervous system where the biological neural network has the ability to learn and control. The ability of neural networks to learn from the input data is widely used in nonlinear control to approximate unknown nonlinear functions [11]. Neural networks can approximate continuous functions in a compact set. The approximation precision depends on the number of neurons. It has been shown that the function approximation error can be arbitrarily small if the number of neurons is adequately large [11].

The weights in the neural networks are trained via offline methods by using a series of input and output data. However, in unknown nonlinear systems the input-output data set is usually not available. Thus, the ideal NN weights are unknown and only an

[3] Photo courtesy of: www.pppl.gov/.../pages/motor_generators.html

estimation of the ideal weights can be utilized. Consequently, the actual weights can be tuned in an online fashion such that certain requirements in the control design are satisfied including stability. The most common way of tuning the NN weight estimates is to obtain an update law such that, together with other dynamics of the control system, it satisfies the Lyapunov stability requirements.

When a power system is represented in a purely dynamical form, the nonlinear functions are complicated functions of all the power system states [12]. Obtaining these functions is involved which requires the knowledge of the topology of the power system. By using NNs in the control design, one can relax a priori knowledge of power system topology as well as burdensome nonlinear function calculations. Moreover, adaptive neural networks combined with the decentralized control can help stabilizing power systems when the size of the power system is large.

1.2.3. Optimal Nonlinear Control. Closed-loop stability is often the sole purpose of many controller designs. However, other objectives, such as optimality, require a control policy to stabilize the system in an optimal manner when the control cost matters in addition to the system stability. In the robust optimal control formulation, the objective of the controller is to minimize a certain cost function which represents a penalty associated with the states and control input. The optimization problem can include disturbances. In this case, controller is to minimize a certain cost function representing a penalty associated with the states and control input while maximizing the disturbances that the system can tolerate [6].

1.2.4. Discrete-time Decentralized Control Design. Although continuous-time controller design can be considered for some applications through using analog controllers, in practice discrete-time control approaches are preferred for computer implementations [13], since controller designs in continuous-time become unsatisfactory when implemented on digital computers using low sampling hardware. Moreover, due to large size of large-scale interconnected systems such as electric power systems, the feedback delays degrade the controller performance, and thus, the design requires more decentralized control techniques. Therefore, decentralized controller development in discrete-time has to be explicitly considered for large-scale systems. The decentralized controller development in discrete-time for power system application is not yet undertaken due to the fact that the stability proofs in discrete-time are more involved than their continuous-time counterparts [14].

1.3. ORGANIZATION OF THE DISSERTATION

Nonlinear control of dynamic control systems and its application to physical systems in both continuous and discrete-time domains has been attracting a great attention due to the fact that most of the physical systems are nonlinear in nature. Although numerous nonlinear control methods are available in the literature, they do not meet all the required performance specifications for complex physical systems and networks. Some of the requirements include asymptotic stability, optimality, controllability and stability in the presence of uncertainty, and desired performance. On the other hand, in order to employ the nonlinear control techniques, a mature mathematical model of the physical system needs to be available.

Power systems are considered as a large scale system but also it suffers from the lack of an appropriate dynamical representation. A power system includes nonlinear dynamical relationships for generators and nonlinear algebraic relationship representing power balance equations in the system buses which make it hard to directly employ the nonlinear control techniques. Therefore, in this dissertation a novel representation of the nonlinear dynamical power system will be considered and various sort of decentralized techniques will be introduced. This dissertation is presented in the form of six papers, and their relation to one another is illustrated in Fig. 1.4.

In the first paper, a new nonlinear dynamical representation of a power network free of algebraic equations with UPFC as a nonlinear controller is presented. This representation is appropriate to model a nonlinear power network with several FACTS devices. Then, oscillation damping using nonlinear control schemes for UPFCs is discussed. The proposed approach in this paper involves obtaining a nonlinear dynamical representation using network power balance equations. The advantage of this approach is that no algebraic equations are needed for the representation while still retaining the nonlinear behavior. Though classical power system representation in which the internal voltages of the generators are held constant to develop the control approach are considered, the proposed approach can be extended to more complex generator models without loss of generality. Then, a nonlinear control scheme is developed to stabilize and damp the oscillations resulting from a disturbance. The universal approximation property of neural networks (NN) is invoked to approximate the power system uncertainties online without any offline learning phase. Finally, the representation is shown to be a decentralized nonlinear system.

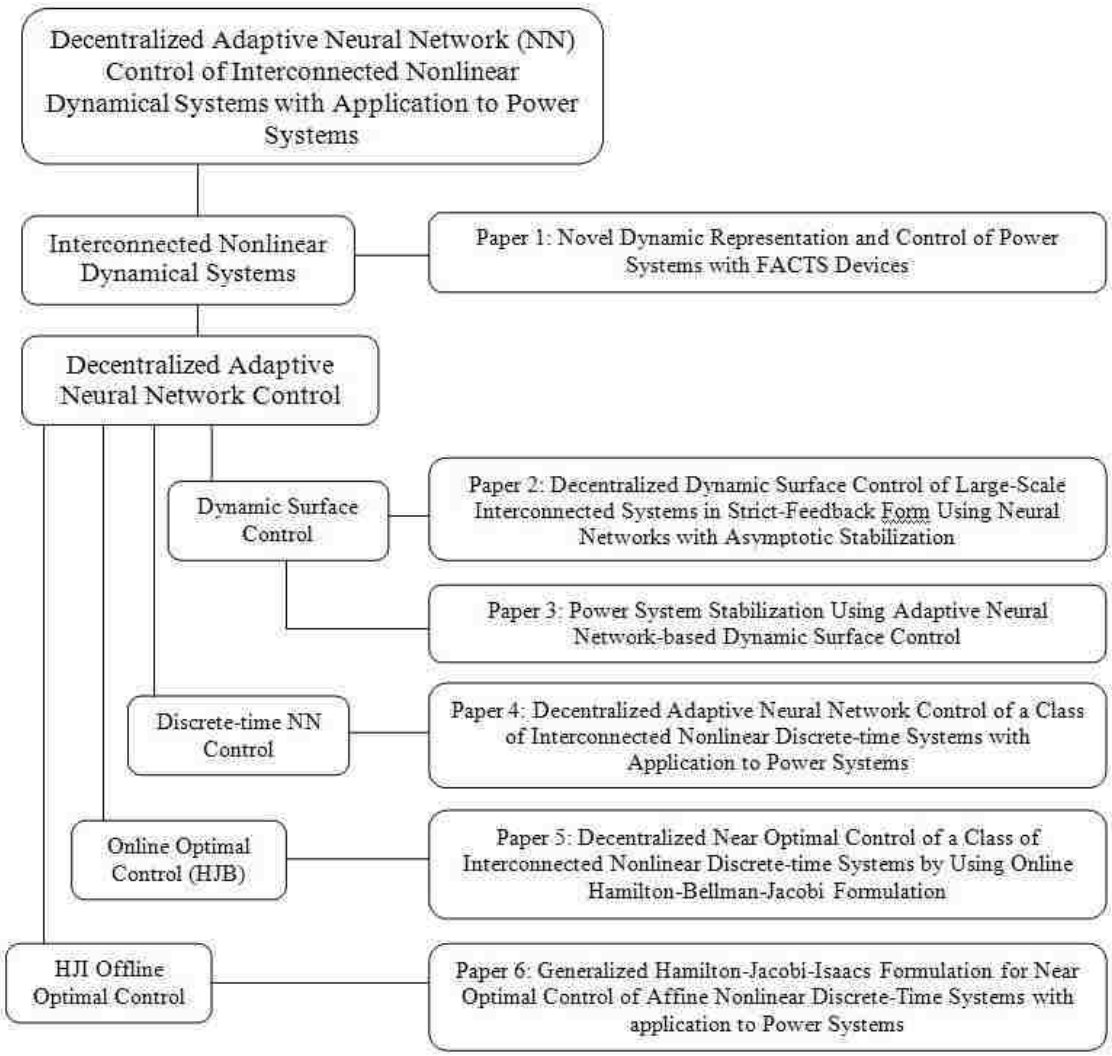

Fig. 1.4 Dissertation outline

In the second paper, the dynamic surface control (DSC) design framework is proposed for a class of nonlinear uncertain interconnected systems in strict-feedback form while relaxing the matching condition; thus, the repeated differentiation of the virtual control signal involved in the traditional backstepping design utilized in Paper I, is relaxed while guaranteeing asymptotic stability. Next, NNs are introduced to overcome

system uncertainties. Thus, the use of neural network-based DSC in decentralized control not only overcomes the lack of knowledge about the subsystem dynamics and interconnection terms, but also relaxes the explosion of complexity problem normally observed in traditional backstepping. Moreover, the control gain matrix, $g(x)$, is considered as an unknown nonlinear function of the states and its time derivative is not required. It is demonstrated that the states of the subsystems approach zero asymptotically through novel online NN weight update laws in contrast with boundedness with the available DSC schemes in the literature.

In the third paper, the power system with excitation control is represented as a class of large-scale, uncertain, interconnected nonlinear continuous-time system in strict-feedback form. Subsequently, dynamic surface control (DSC)-based adaptive neural network (NN) controller is designed to overcome the repeated differentiation of the control input that is observed in the conventional backstepping approach. Then, the power system dynamical model presented in paper I is expanded to the generator flux-decay model representation [9]. Subsequently, by using the proposed model, it is shown that the power system with generator excitation control satisfies the theoretical requirements introduced in paper II, and thus, the proposed NN controller introduced in paper II is applied to a medium size power system to mitigate the oscillations after a fault occurs. Simulation results on the IEEE 14-bus power system with generator excitation control are provided to show the effectiveness of the approach in damping oscillations that occur after disturbances are removed. The end result is a nonlinear decentralized adaptive state-feedback excitation controller for damping power systems oscillations in the presence of uncertain subsystem and interconnection terms.

The work in the fourth paper is focused on a novel decentralized controller design for a class of interconnected nonlinear discrete-time systems in affine form with unknown subsystem and interconnection dynamics. A single neural network (NN) is utilized in the proposed decentralized controller to overcome the unknown internal dynamics as well as the control gain matrix of each subsystem. All NN weights are tuned online by using a novel update law. By using Lyapunov techniques, all subsystems signals are shown to be uniformly ultimately bounded (*UUB).* Simulation results are shown on a general interconnected nonlinear discrete-time system in affine form first to show the effectiveness of the approach. Subsequently, interconnected electric power system with excitation control is considered as an example and the proposed controller is utilized to mitigate the power fluctuations after a disturbance has occurred.

In paper five, the direct neural dynamic programming technique is utilized to solve the HJB (Hamilton Jacobi-Bellman) equation forward-in-time for the decentralized near optimal control of affine nonlinear interconnected discrete-time systems where the interconnected terms in the subsystems are unknown function of other subsystem states which are unavailable. The optimal controller design consists of two NNs; an action NN that is aimed to provide a nearly optimal control signal, and a critic NN which evaluates the performance of the system. All NN parameters are tuned online. By using Lyapunov techniques all subsystems signals are shown to be uniformly ultimately bounded (*UUB)* and that the synthesized subsystems inputs approach their corresponding near optimal control inputs with small bounded error. Simulation results are shown on an interconnected system to show the effectiveness of the approach.

The work in the sixth paper proposes a practical method for obtaining the L_2-gain near optimal control while keeping a tradeoff between accuracy and computational complexity for a class of affine nonlinear discrete-time systems. Using the Taylor series expansion of the value function and a small signal perturbation assumption, a generalized Hamilton-Jacobi-Isaacs (GHJI) equation is proposed, and an iterative approach to solve the GHJI is presented. Successive solutions for the value function ensure that the value function reaches its saddle-point in a zero-sum two-player differential game where the players are system disturbance and control input. The successive approximations of the value function are accomplished using the approximation properties of neural networks (NN) and least squares. Moreover, a NN identifier is presented in this work to learn the nonlinear internal dynamics of the system. Using Lyapunov theory, it is shown that the identification errors converge to a small bounded region around the origin. Then, using the learned NN model of the internal dynamics, offline training is undertaken resulting in a novel solution to the HJI optimal control problem. The novelty of the proposed method is that the scheme does not require explicit knowledge of the system internal dynamics as only an online learned NN model is utilized for the offline training. Additionally, convergence of the successive approximations is demonstrated while explicitly considering the identifier NN reconstruction errors.

1.4. CONTRIBUTIONS OF THE DISSERTATION

This dissertation contributes to the field of general nonlinear interconnected systems controller design as well as to the control of power systems. The nonlinear model development for power systems presented in paper 1 provides a suitable

framework to apply nonlinear control techniques to the power systems. In the proposed representation, the power system algebraic equations are converted to dynamical equations, and thus, a pure dynamical system is obtained. This modeling procedure is then enhanced in other papers to achieve decentralized adaptive NN control of power systems.

Next, the decentralized control design is discussed in paper 2 and the dynamic surface control (DSC) technique is applied to the general decentralized continuous-time nonlinear systems in backstepping form with unknown system dynamics, control gains, and interconnection terms. Then, a NN controller is considered in the control design to approximate the system nonlinearities. Through a novel NN update law and by using Lyapunov techniques, asymptotic stability in state and output feedback design is achieved as opposed to bounded results available in the literature. Further, in paper 3, the power system model with excitation control is represented in general decentralized model representation by using the enhanced model introduced in Paper 1. Then, the DSC adaptive NN decentralized control method is applied to the power systems to mitigate oscillations after a disturbance occurs and effective damping performance is illustrated.

In paper 4, the general unknown discrete-time nonlinear decentralized control design is discussed and adaptive NN is utilized to approximate the unknown dynamics in the subsystems. Unlike, the previous works, the interconnection terms are not bounded by constants and can grow in a quadratic manner while the large-scale system states as well as NN weight estimates are proven to be uniformly ultimately bounded. Finally, power system with excitation control representation is developed in discrete-time and the proposed controller is applied where satisfactory damping performance is shown.

Subsequently, the direct neural dynamic programming (DNDP) approach is utilized for the optimal regulation and tracking of nonlinear interconnected discrete-time systems in affine form by solving the HJB equation online and forward-in-time. The NNs are used to approximate the critic as well as the action networks where the optimal control signal is approximated while minimizing the cost function based on the information provided by the critic in the presence of the large-scale system unknown interconnection terms but known subsystems dynamics with explicitly considering the effect of the interconnection terms in the optimal control design. Additionally, overall closed-loop stability of the nonlinear decentralized system is presented.

The work in paper 6 seeks to provide the HJI optimal framework for nonlinear systems in affine form by proposing a practical method of obtaining the L_2-gain near optimal control while keeping a tradeoff between accuracy and computational complexity where the method can be expanded to decentralized nonlinear interconnected systems. Using the Taylor series expansion of the value function and using a small signal perturbation assumption, a generalized Hamilton-Jacobi-Isaacs (GHJI) equation is proposed, and an iterative approach to solve the GHJI is presented. Successive solutions for the value function ensure that the value function reaches its saddle-point in a zero-sum two-player differential game where the players are system disturbances and the control input. Next, an NN identifier is presented in this work to learn the nonlinear internal dynamics of the system. Using Lyapunov theory, it is shown that the identification errors converge to a small bounded region around the origin. Then, using the learned NN model of the internal dynamics, offline training is undertaken resulting in a novel solution to the HJI optimal control problem. Power system with FACTs device as

damping controller is presented by applying the proposed method to achieve optimal damping performance.

1.5. DEFINITIONS

In this part, we review some of the definitions that are used in this dissertation.

Equilibrium Point: Consider the dynamical system $\dot{x} \in f(x,u,t)$ (which can be a function of states as well as time) with $x \in R^n$ represents the states of an uncontrolled open-loop system, or a closed-loop system after the application of the control input, and control input $u(t)$ has been specified in terms of the state $x(t)$. Let the initial time be t_0, and the initial condition be $x_0 \equiv x(t_0)$. A state x_e is an equilibrium point of the system if $f(x_e,t) = 0, t \geq t_0$.

Asymptotic stability: An equilibrium point x_e is locally asymptotically stable at t_0 if there exists a compact set $S \subset \Re^n$ such that, for every initial condition in $x_0 \subset S$, $\|x(t) - x_e\| \to 0$ as $t \to \infty$ [14].

Uniformly Ultimately Bounded : Consider the dynamical system $\dot{x} = f(x)$ with $x \in \Re^n$ being a state vector. Let the initial time be t_0 and initial condition be $x_0 = x(t_0)$. Then, the equilibrium point x_e is said to be UUB if there exists a compact set $S \subset \Re^n$ so that for all $x_0 \in S$ there exists a bound B and a time $T(B, x_0)$ such that $\|x(t) - x_e\| \leq B$ for $\forall t > t_0 + T$ [14].

Neural Network Universal Approximation: A general function $f(x) \in R$ where $x \in R^n$ can be written as $f(x) = W^T \phi(\bar{V}^T x) + \varepsilon(x)$ with $\varepsilon(x)$ a neural network (NN) functional reconstruction error and ϕ is the neural network activation function vector which is a

basis function vector, $W \in R^{N_2 \times 1}$ and $\bar{V} \in R^{n \times N_2}$ are weight matrices [14]. The input-to-the hidden-layer weight matrix $\bar{V}$ is selected initially at random and held fixed during learning. It is demonstrated in [15] that if the input-to-the-hidden-layer weights, $\bar{V}$, are chosen initialized randomly and kept constant and if the number of neurons N_2 in the hidden layer is sufficiently large, the NN approximation error $\varepsilon(x)$ can be made arbitrarily small since the activation function vector ϕ forms a basis.

REFERENCES

[1] I. M. Horowitz, *Quantitative feedback design theory (QFT)*, QFT Publications, 1992.

[2] S. M. Shinners, *Modern control system theory and design*, John Wiley and Sons Inc. 1998.

[3] A. Gelb, *Applied Optimal Estimation*, MIT Press, 1974.

[4] P. Dorato, V. Cerone, and C. T. Abdallah, *Linear Quadratic Control: An Introduction*, Krieger Publishing Company, 2000.

[5] K. S. Narendra and A.M. Annaswamy, *Stable Adaptive Systems*, Prentice Hall, New Jersey, 1989.

[6] F. L. Lewis and V. L. Syrmos, *Optimal Control*, New York, Weily, 1995.

[7] H.K. Khalil, *Nonlinear Systems*, Prentice Hall, New Jersey, 2002.

[8] D. Swaroop, J.K. Hedrick, P.P. Yip, and J.C. Gerdes; "Dynamic surface control for a class of nonlinear systems," *IEEE Transactions on Automatic Control*, vol. 45, no. 10, pp. 1893 – 1899, Oct. 2000.

[9] P.W. Sauer and M.A. Pai, *Power System Dynamics and Stability*, Prentice Hall, 1997.

[10] S.N. Huang, K.K. Tan, and T.H. Lee, "Nonlinear adaptive control of interconnected systems using neural networks," *IEEE Transactions on Neural* Networks, vol. 17, no. 1, pp. 243 - 246, Jan. 2006.

[11] F. Lewis, S. Jagannathan, S., and A. Yesildirek, "*Neural Network Control of Robot. Manipulators and Nonlinear Systems*," Taylor & Francis, 1998.

[12] S. Mehraeen, S. Jagannathan, and M. L. Crow, "Novel Dynamic Representation and Control of Power Networks Embedded with FACTS Devices," *Proceedings of IEEE Conference on System, Man and Cybernetics*, pp.: 3171 - 3176, Oct. 2008.

[13] Y. H. Lin and K. S. Narendra, "A New Error Model for Adaptive Systems," *IEEE Transactions on Automatic Control*, vol. 25, no. 3, pp.: 585-587, June 1980.

[14] S. Jagannathan, *Neural Network Control of Nonlinear Discrete-time Systems*, CRC Press, April 2006.

[15] B. Igelnik and Y. H. Pao, "Stochastic choice of basis functions in adaptive function approximation and the functional-link net," *IEEE Trans. Neural Networks*, vol. 6, no. 6, pp. 1320–1329, Nov. 1995.

PAPER

1. Novel Dynamic Representation and Control of Power Systems with FACTS Devices

S. Mehraeen, S. Jagannathan, and M. L. Crow[1]

Abstract— *FACTS devices have been shown to be useful in damping power system oscillations. However, in large power systems, the FACTS control design is complex due to the combination of differential and algebraic equations required to model the power system. In this paper, a new method to generate a nonlinear dynamic representation of the power network is introduced to enable more sophisticated control design. Then, the representation is expanded to decentralized formulation of power systems. Once the new representation is obtained, a back stepping methodology for the UPFC is utilized to mitigate the generator oscillations. Finally, the neural network approximation property is utilized to relax the need for knowledge of the power system topology and to approximate the nonlinear uncertainties. The net result is a power system representation that can be used for the design of an enhanced FACTS control scheme. Simulation results are given to validate the theoretical conjectures.*

Index Terms – Power System Control, Nonlinear Systems, Neural Networks, FACTS**.**

[1] Authors are with Department of Electrical and Computer Engineering, Missouri University of Science and Technology, 1870 Miner Circle, Rolla, MO 65409. Contact author: sm347@mst.edu. Research Supported in part by NSF ECCS#0624644.

I. Introduction

Power system stability is defined as the ability of an electric power system, for a given initial operating condition, to regain a state of operating equilibrium after being subjected to a physical disturbance [1]. Power system stability can be improved through the use of dynamic controllers such as power system stabilizers, excitation systems, and more recently FACTS devices. To effectively design the controller, proper modeling of the generators, controller dynamics, and the network must be utilized. A power system is usually modeled using a combination of differential and algebraic equations. The differential equations represent generator angles and speeds whereas the algebraic equations represent bus active and reactive power balance relationships. Incorporating the differential-algebraic equations into the control process is difficult and is made more complex by the inclusion of FACTS devices such as the unified power flow controller (UPFC).

Advanced controller design usually requires that a system be represented by purely differential equations. However, power systems with embedded FACTS devices typically require the algebraic transmission network power balance equations to be included in the system model and it is not straightforward to develop an algebraic equation free system model representation for control purposes.

Several approaches have been analyzed for system wide FACTS control design. Past work [2-6], has proposed to linearize the differential-algebraic equation network and eliminate the algebraic equations through reduction methods. Then linear control methods are applied to the linearized power system. This approach, however, tacitly assumes that the network variables remain in the neighborhood of the desired operating point. In

addition, the placement and number of UPFC devices are determined heuristically. By contrast, in [7-12] a single-machine infinite bus model is used to apply nonlinear control schemes. However, the infinite bus assumption required for this approach is not valid for large multi-machine systems when the fault affects the power system.

FACTS devices have been considered in [13-14] via utilizing energy functions to develop the controllers. This approach is not practical because it requires the calculation of the derivatives of power system bus voltages and angles and requires numerical differentiators or approximations. Nonlinear control of a multi-machine power system excitation and governor control has been proposed using back stepping in [17]. This method holds considerable potential, but does not consider FACTS devices. FACTS devices can serve many control functions in an electric power system including steady-state power flow, voltage regulation, and oscillation damping control. Thus, stabilizing capabilities can be added with the other control capabilities without any additional cost. This property is exploited in this work.

In this paper, we propose the following contributions to overcome the above-mentioned challenges:

I- a new nonlinear dynamical representation of a power network free of algebraic equations with UPFC as a controller is introduced. This representation is appropriate to model a nonlinear power network with several FACTS devices,

II- oscillation damping using nonlinear control schemes for UPFCs, and

III- a neural network approximation property is utilized to relax the need for knowledge of the power system topology and to approximate the nonlinear uncertainties.

Our approach involves first obtaining a nonlinear dynamical representation using network power balance equations. The advantage of this approach is that no algebraic equations are involved in the control design while the nonlinear behavior is retained. In the proposed approach, we use the power system classical model in which the internal voltages of the generators are held constant in order to develop the control design. However, the proposed approach can be extended to more complex generator models without loss of generality. Subsequently, a nonlinear control scheme is developed to stabilize and damp the oscillations resulting from a disturbance such as a three-phase to ground fault. Finally, we have employed the universal approximation property of neural networks (NN) to approximate the power system uncertainties and to relax the need for the a priori knowledge of the system uncertainties.

II. The Power System Differential-Algebraic Model

The classical generator representation is often sufficient for the control development in order to mitigate the inter-area oscillations since only the rotor speed deviations are of interest. In addition, the resistances of power network lines are neglected. Despite this assumption made for ease of control development, the proposed control will be validated on a full nonlinear power system model.

It is more convenient to represent the generator dynamical equations in the Center of Inertia (COI) coordinates:

$$\dot{\delta}_i = \omega_i \tag{1}$$

$$M_i\dot{\omega}_i = P_{mi} - \frac{M_i}{M_T}P_{COI} - B_{i,i+n}E_{gi}V_{i+n}\sin(\delta_i - \psi_{i+n});\ i = 1,\ldots,n \tag{2}$$

where $\delta_i = \bar{\delta}_i - \delta_0$, $\omega_i = \bar{\omega}_i - \omega_0$, $\psi_i = \bar{\psi}_i - \delta_0$, $M_T = \sum_{i=1}^{n} M_i$, $\delta_0 = 1/M_T \sum_{i=1}^{n} M_i \bar{\delta}_i$, $\omega_0 = 1/M_T \sum_{i=1}^{n} M_i \bar{\omega}_i$,

$P_{COI} = \sum_{i=1}^{n} P_{mi} - \sum_{i=n+1}^{n+N} P_{Li}$ where P_{Li} is the active load at each bus and P_{mi} is the input mechanical power. Also, $\bar{\delta}_i$ is the rotor angle of the *i*-th machine, $\bar{\omega}_i$ is the angular speed, δ_0 is the center of angle, ω_0 is the center of angular speed, *B* represents the reactance of the admittance matrix, E_{gi} is the *i*-th machine internal voltage, *n* is the number of generators, $M_i = 2H/\omega_0$ is the *i*-th machine inertia, and V_{i+n} and $\bar{\psi}_{i+n}$ are the generator bus voltage and phase angle, respectively. In addition, *N* is the number of non-generator buses in the power system.

The bus voltages and phase angles of all of the power system buses are constrained by the following set of algebraic power balance equations (neglecting resistances)

$$\begin{aligned} &P_{Li} + \sum_{j=1}^{N+n} B_{ij} V_i V_j \sin(\psi_i - \psi_j) = S_{\mathrm{P}i} = 0 \\ &-Q_{Li} + \sum_{j=1}^{N+n} B_{ij} V_i V_j \cos(\psi_i - \psi_j) = S_{\mathrm{Q}i} = 0; i = n+1, \ldots, n+N \end{aligned} \tag{3}$$

where P_{Li} and Q_{Li} are the active and reactive loads on the *i*-th bus and $V_j = E_{gj}$; $\psi_j = \delta_j$ for $1 \le j \le n$.

III. New Dynamic Representation of Power Networks

Equations (1) through (3) form the set of power system differential-algebraic equations. However, a controller design in a differential-algebraic environment is difficult to achieve, therefore it is desirable to substitute the set of equations (3) with a more appropriate set. One way to have a pure dynamical system is to take derivative of equation (3) to obtain $\dot{V}_i$ and $\dot{\psi}_i$ terms. Thus, we have

$$\frac{\partial S_{\mathrm{P}i}}{\partial t}=\frac{\partial S_{\mathrm{P}i}}{\partial V}\dot{V}+\frac{\partial S_{\mathrm{P}i}}{\partial \psi}\dot{\psi}+\frac{\partial S_{\mathrm{P}i}}{\partial \delta}\dot{\delta}=0 \tag{4}$$

and

$$\frac{\partial S_{\mathrm{Q}i}}{\partial t}=\frac{\partial S_{\mathrm{Q}i}}{\partial V}\dot{V}+\frac{\partial S_{\mathrm{Q}i}}{\partial \psi}\dot{\psi}+\frac{\partial S_{\mathbf{Q}i}}{\partial \delta}\dot{\delta}=0 \qquad i=n+1,\ldots,n+N \tag{5}$$

Solving equations (4) and (5) for $\dot{V}_i$ and $\dot{\psi}_i$, we obtain a new set of dynamic equations as

$$\begin{bmatrix}\dot{V}\\ \dot{\psi}\end{bmatrix}=-\begin{bmatrix}\overline{A}(x_S) & \overline{B}(x_S)\\ \overline{D}(x_S) & \overline{E}(x_S)\end{bmatrix}^{-1}\begin{bmatrix}C(x_S)\\ F(x_S)\end{bmatrix}\omega \tag{6}$$

where

$V=[V_{n+1}\ \ V_{n+2}\ \ \ldots\ \ V_{n+N}]^T$, $\psi=[\psi_{n+1}\ \ \psi_{n+2}\ \ \ldots\ \ \psi_{n+N}]^T$, and $\omega=[\omega_1\ \ \omega_2\ \ \ldots\ \ \omega_n]^T$. Also, we define $\delta=[\delta_1\ \ \delta_2\ \ \ldots\ \ \delta_n]^T$ and $x_S=[\delta^T\ \ \omega^T\ \ V^T\ \ \psi^T]^T$. Assuming P_{Li} and Q_{Li} to be functions of V_i and ψ_i, we get $\overline{A}_{N\times N}=\frac{\partial S_{\mathbf{P}}}{\partial V}$, $\overline{B}_{N\times N}=\frac{\partial S_{\mathbf{P}}}{\partial \psi}$, $C_{N\times n}=\frac{\partial S_{\mathbf{P}}}{\partial \delta}$, $\overline{D}_{N\times N}=\frac{\partial S_{\mathbf{Q}}}{\partial V}$, $\overline{E}_{N\times N}=\frac{\partial S_{\mathbf{Q}}}{\partial \psi}$, and $F_{N\times n}=\frac{\partial S_{\mathbf{Q}}}{\partial \delta}$ as given in (I-3a) through (I-4e) in Appendix I. Once again, it is important to note that this step is for controller development and is not required for actual (practical) implementation. The proposed approach is a complementary way of solving the differential-algebraic equations $\{\dot{x}=f(x,z);\quad g(x,z)=0\}$ where $z=h(x)$ is obtained by solving $g(x,z)=0$ and replaced in the differential equations $\dot{x}=f(x,z)$ where x is the states of the power system. Solving the nonlinear algebraic equations $g(x,z)=0$ is a huge challenge (if not impossible in large-scale power systems) which is relaxed in the proposed approach without losing the nonlinear characteristics of the power system.

IV. Power System Decentralized Model

In this section, a decentralized representation of a power system is obtained for nonlinear controller development. Generator excitation control is a means to alleviate the power system oscillations. Since the disturbance is a function of the power network voltages and angles as well as generator states, it is generally hard to design a centralized damping controller for the complex interconnected power network. Thus, in this section, we aim at a decentralized excitation controller to mitigate the oscillations by using locally measurable states of the generator as well as its bus voltages and angles. For this controller development, the large-scale power system has to be represented in a decentralized form which is discussed next.

A. Model Development

A power system is usually modeled using a combination of differential and algebraic equations. The differential equations represent generator states (i.e. angles, speeds, and *dq* voltages E'_q and E'_d) whereas the algebraic equations represent bus active and reactive power balance relationships. For the purpose of controller design it is desirable to have pure dynamical equations. In the previous section an algebraic-free power system representation based on the classical generator model is represented. In order to incorporate the generator flux-decay states, the proposed model is extended herein.

A two-axis model [18] is chosen for the purpose of power system representation. As a consequence, the generator dynamical equations are given as

$$\begin{aligned}
&\dot{\delta}_i = \bar{\omega}_i;\ \bar{\omega}_i = \frac{1}{M_i}\left(P_{mi} - P_{ei}\right);\\
&\dot{E}'_{qi} = \frac{1}{T_{d0i}}\left(-\frac{x_{di}}{x'_{di}}E'_{qi} + \frac{x_{di}-x'_{di}}{x'_{di}}V_{i+n}\cos(\bar{\delta}_i - \bar{\psi}_{i+n}) + E_{fdi}\right)\\
&\dot{E}'_{di} = \frac{1}{T_{q0i}}\left(-\frac{x_{qi}}{x'_{di}}E'_{di} + \frac{x_{qi}-x'_{di}}{x'_{di}}V_{i+n}\sin(\bar{\delta}_i - \bar{\psi}_{i+n})\right);\ \dot{E}_{fdi} = \frac{1}{T_{Ei}}\left(V_{Ri} - K_{Ei}E_{fdi}\right)
\end{aligned} \tag{7}$$

where $\bar{\delta}_i$ is the rotor angle of the *i*-th machine, $\bar{\omega}_i$ is the difference between the generator angular speed and synchronous speed, E'_{qi} and E'_{di} are generator's *dq* variables as defined in [18], E_{fdi} is the excitation voltage, and V_{i+n} and $\bar{\psi}_{i+n}$ are the generator bus voltage and phase angle, respectively, as depicted by Fig. 1. In addition

$$P_{ei} = B_{i,i+n}V_{i+n}\left(E'_{qi}\sin(\bar{\delta}_i - \bar{\psi}_{i+n}) - E'_{di}\cos(\bar{\delta}_i - \bar{\psi}_{i+n})\right), \tag{8}$$

where *B* represents the reactance of the admittance matrix, *n* is the number of generators, and *N* denotes the number of non-generator buses in the power system as shown in Fig. 1. The bus voltage and phase angles of the power system buses are illustrated in Fig. 1 which are constrained by the set of algebraic power balance equations (neglecting resistances) as

$$\begin{aligned}
&P_{Li} + \sum_{j=1}^{n} B_{ij}V_i\left(E'_{qj}\sin(\psi_i - \delta_j) + E'_{dj}\cos(\psi_i - \delta_j)\right) + \sum_{j=n+1}^{N+n} B_{ij}V_iV_j\sin(\psi_i - \psi_j) = S_{Pi} = 0\\
&Q_{Li} - \sum_{j=1}^{n} B_{ij}V_i\left(E'_{qj}\cos(\psi_i - \delta_j) - E'_{dj}\sin(\psi_i - \delta_j)\right) - \sum_{j=n+1}^{N+n} B_{ij}V_iV_j\cos(\psi_i - \psi_j) = S_{Qi} = 0\\
&i = n+1,\ldots,n+N
\end{aligned} \tag{9}$$

Then, taking the derivative of (9) to obtain $\dot{V}_i$ and $\dot{\psi}_i$ as

$$\frac{\partial S_{Pi}}{\partial t} = \frac{\partial S_{Pi}}{\partial V}\dot{V} + \frac{\partial S_{Pi}}{\partial \psi}\dot{\psi} + \frac{\partial S_{Pi}}{\partial \delta}\dot{\delta} + \frac{\partial S_{Pi}}{\partial E'_q}\dot{E}'_q + \frac{\partial S_{Pi}}{\partial E'_d}\dot{E}'_d = 0 \tag{10}$$

and

$$\frac{\partial S_{Qi}}{\partial t} = \frac{\partial S_{Qi}}{\partial V}\dot{V} + \frac{\partial S_{Qi}}{\partial \psi}\dot{\psi} + \frac{\partial S_{Qi}}{\partial \delta}\dot{\delta} + \frac{\partial S_{Qi}}{\partial E'_q}\dot{E}'_q + \frac{\partial S_{Qi}}{\partial E'_d}\dot{E}'_d = 0 \qquad i = n+1,\ldots,n+N \tag{11}$$

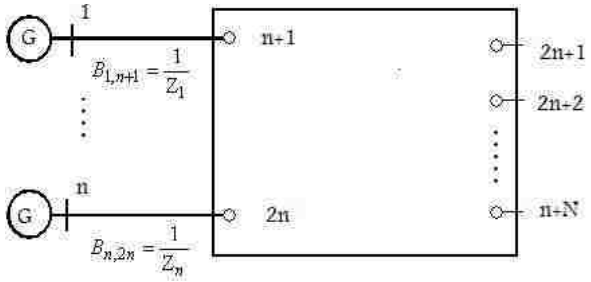

Fig.1-Power System

By using (7) for $\dot{E}'_{qi}$ and $\dot{E}'_{di}$ and solving (10) and (11) and for $\dot{V}_i$ and $\dot{\psi}_i$, we obtain a new set of dynamic equations as

$$\begin{bmatrix} A(x) & B(x) \\ D(x) & E(x) \end{bmatrix}\begin{bmatrix} \dot{V} \\ \dot{\bar{\psi}} \end{bmatrix}+\left(\begin{bmatrix} C(x) \\ F(x) \end{bmatrix}\bar{\omega}+R(x)\right)=0 \tag{12}$$

where $V=[V_{n+1}\ \ V_{n+2}\ \ \dots\ \ V_{n+N}]^T$, $\bar{\psi}=[\bar{\psi}_{n+1}\ \ \bar{\psi}_{n+2}\ \ \dots\ \ \bar{\psi}_{n+N}]^T$, and $\bar{\omega}=[\bar{\omega}_1\ \ \bar{\omega}_2\ \ \dots\ \ \bar{\omega}_n]^T$ is the generators' speed error vector. Also, define $\bar{\delta}=[\bar{\delta}_1\ \ \bar{\delta}_2\ \ \dots\ \ \bar{\delta}_n]^T$, $E'_q=[E'_{q1}\ \ E'_{q2}\ \ \dots\ \ E'_{qn}]^T$, $E'_d=[E'_{d1}\ \ E'_{d2}\ \ \dots\ \ E'_{dn}]^T$, $E_{fd}=[E_{fd1}\ E_{fd2}\dots E_{fdn}]^T$, $\Delta P_e=[\Delta P_{e1}\ \ \Delta P_{e2}\ \ \dots\ \ \Delta P_{en}]^T$, and $x=[\bar{\delta}^T\ \bar{\omega}^T\ E'^T_q\ E'^T_d\ E^T_{fd}\ V^T\ \bar{\psi}^T]^T$. The entities for $A_{N\times N}$, $B_{N\times N}$, $D_{N\times N}$, $E_{N\times N}$, $C_{N\times n}$, $F_{N\times N}$, $R_{2N\times 1}$, and $G_{2N\times n}$ can be derived by collecting the corresponding coefficients. Equation (12) can be rewritten in a more appropriate way as

$$\begin{bmatrix} \dot{V} \\ \dot{\bar{\psi}} \end{bmatrix}=-\begin{bmatrix} A(x) & B(x) \\ D(x) & E(x) \end{bmatrix}^{-1}\left(\begin{bmatrix} C(x) \\ F(x) \end{bmatrix}\bar{\omega}+R(x)\right)=a(x) \tag{13}$$

It is important to note that this step is needed only for model development and is not required for implementation.

B. Generator Representation

Next, the flux-decay model [18] of the generator is given as

$$\begin{aligned}&\dot{\bar{\delta}}_i = \bar{\omega}_i;\ \dot{\bar{\omega}}_i = \frac{1}{M_i}\left(P_{mi} - P_{ei}\right);\ \dot{E}'_{qi} = \frac{1}{T_{d0i}}\left(-E'_{qi} + \left(x_{di} - x'_{di}\right)I_{di} + E_{fdi}\right)\\&\dot{E}_{fdi} = \frac{1}{T_{Ei}}\left(V_{Ri} - K_{Ei}E_{fdi}\right)\end{aligned} \tag{14}$$

where P_{ei} is the active load at each bus, and $M_i = 2H/\omega_0$ is the i-th machine inertia. In addition, the following equalities are valid

$$P_{ei} = E'_{qi}I_{qi} + (x_{qi} - x'_{di})I_{qi}I_{di} \tag{15}$$

and

$$I_{qi} = B_{i,i+n}V_{i+n}\sin(\bar{\delta}_i - \bar{\psi}_{i+n});\ I_{di} = B_{i,i+n}\left(E'_{qi} - V_{i+n}\cos(\bar{\delta}_i - \bar{\psi}_{i+n})\right) \tag{16}$$

Moreover, the power balance equations (9) will be simplified by employing the flux-decay assumption

$$E'_{di} = (x_{qi} - x'_{di})I_{qi}\,. \tag{17}$$

In this design we assume that the mechanical power $P_{mi}\,(1 \le i \le n)$ is slowly changing compared to the other control variables; thus $\dot{P}_{mi} \approx 0$. Now define

$$x_{i1} = \bar{\delta}_i - \bar{\delta}_{0i};\ x_{i2} = \bar{\omega}_i;\ x_{i3} = \frac{\Delta P_{ei}}{M_i};\ x_{i4} = P_{e0i} - I_{qi}E_{fdi} \tag{18}$$

where $\Delta P_{ei} = P_{e0i} - P_{ei}$ and $P_{e0i} = P_{mi}$. Consequently, the generator dynamics (8) can be rewritten in the state-space form as

$$\begin{aligned}&\dot{x}_{i1} = x_{i2};\ \dot{x}_{i2} = x_{i3}\\&\dot{x}_{i3} = -\frac{x_{i3}}{T_{d0i}} + \frac{x_{i4}}{T_{d0i}M_i} + \frac{1}{T_{d0i}}\left(x_{di} - x_{qi}\right)I_{qi}I_{qi} - E'_{qi}\dot{I}_{qi}\\&\qquad -\left(x_{qi} - x'_{di}\right)\left(\dot{I}_{qi}I_{di} + I_{qi}\dot{I}_{di}\right)\\&\dot{x}_{i4} = I_{qi}\left(\frac{K_{Ei}}{T_{Ei}}E_{fdi} - \frac{V_{Ri}}{T_{Ei}}\right) - \dot{I}_{qi}E_{fdi}\end{aligned} \tag{19}$$

The electrical diagram of the generator using the flux-decay model is depicted in Fig. 2 [18] where the voltage source and injected current are represented as $E_i = \left((x_{qi} - x'_{di})I_{qi} + jE'_{qi}\right)e^{\left(\bar{\delta}_i - \frac{\pi}{2}\right)}$ and $, I_i = \frac{E_i}{\mathrm{Z}_i}$. According to the figure and (17), the voltage source in Fig.2 can be represented as

$E_i = \left(\left(x_{qi} - x'_{di}\right)B_{i,i+n}V_{i+n}\sin(\bar{\delta}_i - \psi_{i+n}) + jE'_{qi}\right)e^{\left(\bar{\delta}_i - \frac{\pi}{2}\right)}$. Then, by applying $I = Y_{\mathbf{bus}}\bar{V}$ to the power network, where $I = [I_1 \quad I_2 \quad \dots \quad I_n]^T$ and $\bar{V} = \left[V_{n+1}e^{\psi_{n+1}} \quad V_{n+2}e^{\psi_{n+2}} \quad \dots \quad V_{2n}e^{\psi_{2n}}\right]^T$ we obtain

$$\begin{aligned}&\left(\left(x_{qi} - x'_{di}\right)B_{i,i+n}V_{i+n}\sin(\bar{\delta}_i - \bar{\psi}_{i+n}) + jE'_{qi}\right)e^{\left(\bar{\delta}_i - \frac{\pi}{2}\right)}\\&= \sum_{k=1}^{N} Y_{\mathrm{bus},ik}V_{k+n}e^{j\bar{\psi}k+n}\end{aligned} \tag{20}$$

which yields

$$\begin{aligned}&\left(x_{qi} - x'_{di}\right)B_{i,i+n}V_{i+n}\sin(\bar{\delta}_i - \psi_{i+n})\sin(\bar{\delta}_i) + E'_{qi}\cos(\bar{\delta}_i)\\&= \mathrm{Re}\left(\sum_{k=1}^{N} Y_{\mathrm{bus},ik}V_{k+n}e^{j\bar{\psi}k+n}\right)\end{aligned} \tag{21}$$

and

$$\begin{aligned}&-\left(x_{qi} - x'_{di}\right)B_{i,i+n}V_{i+n}\sin(\bar{\delta}_i - \bar{\psi}_{i+n})\cos(\bar{\delta}_i) + E'_{qi}\sin(\bar{\delta}_i)\\&= \mathrm{Im}\left(\sum_{k=1}^{N} Y_{\mathrm{bus},ik}V_{k+n}e^{j\bar{\psi}k+n}\right)\end{aligned} \tag{22}$$

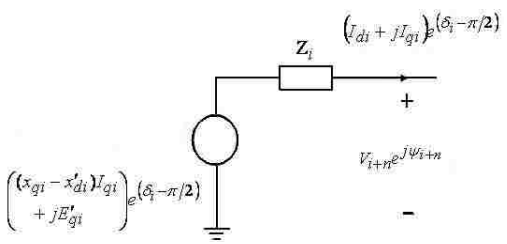

Fig.2 Generator flux-decay model

Remark 1. Here $Y_{\mathbf{bus}}$ may contain nonlinear impedances (including constant loads). Thus, even if the system $Y_{\mathbf{bus}}$ is reduced to an $n \times n$ matrix, non-generator bus voltages and angles are involved in computations. Thus, conventional $Y_{\mathbf{bus}}$ reduction techniques cannot be applied to overcome non-generator nodes.

C. Decentralized Nonlinear System Representation

The dynamical representation of the power system from (19) can be rewritten as a general class of L interconnected nonlinear subsystems in affine form as

$$\begin{cases} \dot{x}_{i1} = f_{i1}(x_{i1}) + g_{i1}(x_{i1})x_{i2} + \Delta_{i1}(\bar{X}_1) \\ \vdots \\ \dot{x}_{il} = f_{il}(X_{il}) + g_{il}(X_{il})u_i + \Delta_{il}(\bar{X}_l) \end{cases} \qquad (23)$$
$$h_i(X_{il}) = x_{i1}$$

where index i, $1 \le i \le L$, represents the subsystem (generator) number, L is the number of subsystems (generators) in the power system, p, $1 \le p \le l$, shows the generator state number, $l = 4$ is the order of the power system according to (19), $f(.)$ and $g(.)$, represent unknown nonlinearities, $\Delta(.)$ denotes interconnected terms, with $X_{ip} = [x_{i1}, \ldots, x_{ip}]^T$, $\bar{X}_p = [\bar{X}_1^T, \ldots, \bar{X}_p^T]^T$, $\bar{X}_j = [x_{1j}, \ldots, x_{Lj}]^T$, $\bar{X}_0 = 0$ and $h_i(X_{il})$ is the subsystem output for $1 \le i \le L$ and $1 \le p \le l$. By comparing the power system representation (19) and the general system description given by (23), it follows that $f_{i1} = f_{i2} = f_{i4} = 0$, $f_{i3} = -x_{i3}/T_{d0i}$, $g_{i1} = g_{i2} = 1$, $g_{i3} = 1/T_{d0i}M_i$, and $g_{i4} = I_{qi}$. Also, $\Delta_{i1} = \Delta_{i2} = 0$, with

$$\Delta_{i3} = \frac{1}{T_{d0i}}\left(x_{di} - x_{qi}\right)I_{qi}I_{qi} - E'_{qi}\dot{I}_{qi} - \left(x_{qi} - x'_{di}\right)\left(\dot{I}_{qi}I_{di} + I_{qi}\dot{I}_{di}\right), \qquad (24)$$

$$\Delta_{i4} = -\dot{I}_{qi}E_{fdi}, \qquad (25)$$

and

$$u_i = I_q\left(\frac{K_{Ei}}{T_{Ei}}E_{fdi} - \frac{V_{Ri}}{T_{Ei}}\right) \tag{26}$$

In the following, we find V and ψ as a function of the states $\bar{\delta}$, $\bar{\omega}$, and ΔP_e. Equations (21) and (22) yield expressions $E'_{qi}\cos(\bar{\delta}_i)$ and $E'_{qi}\sin(\bar{\delta}_i)$ as functions of $\bar{\delta}$, V, and $\bar{\psi}$ which in turn yields E'_{qi} and $\bar{\delta}$ to be functions of V, and $\bar{\psi}$ as

$$E'_{qi} = \vartheta_{1i}(V,\bar{\psi}),\ \bar{\delta}_i = \vartheta_{2i}(V,\bar{\psi}). \tag{27}$$

Consequently, by using (15), (16), and (27) the variables I_{qi} and I_{di} as well as P_{ei} can be represented as functions of V and ψ as

$$P_{ei} = \vartheta_{3i}(V,\bar{\psi}) \tag{28}$$

Now, equations (17) and (27) (for $1 \le i \le L$) along with the $2N$ nodal power flow equations (3) give solutions for V and ψ in terms of δ_i for $1 \le i \le L$ as

$$V_{i+n} = \bar{\vartheta}_{1i}(\bar{\delta});\ \bar{\psi}_{i+n} = \bar{\vartheta}_{2i}(\bar{\delta});\quad 1 \le i \le N \tag{29}$$

D. Interconnection Terms

In order to address the interconnection terms, the following assumption is needed for analyzing their upper bound.

Assumption 1: The excitation voltage, E_{fdi}, satisfies the following inequality [19] defined by

$$E_{fdi} \le \bar{\mathrm{K}}\left(E'_{qi} + (x_{di} - x'_{di})I_{di}\right) \tag{30}$$

where $\bar{\mathbf{K}}$ is a positive constant. Consequently, by (16) and (27) we have

$$E_{fdi} \le \vartheta_4(V,\bar{\psi}) \tag{31}$$

Also, by employing (17), (27), and (31), equation (12) can be simplified to

$$\dot{V}_{i+n} \le c_{1i}(x_s); \dot{\bar{\psi}}_{i+n} \le c_{2i}(x_s); \quad 1 \le i \le N \tag{32}$$

where $c_{1i}(.)$ and $c_{2i}(.)$ are positive nonlinear functions and $x_s = [\bar{\delta}^T \quad \bar{\omega}^T \quad V^T \quad \bar{\psi}^T]^T$. Then, by using (28) and (29) we obtain

$$\dot{V}_{i+n} \le \bar{c}_{1i}(\bar{\delta}, \bar{\omega}, P_e); \dot{\psi}_{i+n} \le \bar{c}_{2i}(\bar{\delta}, \bar{\omega}, P_e); \quad 1 \le i \le N \tag{33}$$

where $\bar{c}_{1i}$ and $\bar{c}_{2i}$ are positive nonlinear functions. Now, by considering the interconnection term (24) along with (16), (29), (30), and (33) it can be shown that $|\Delta_{ip}| \le \zeta_i(\bar{\delta}, \bar{\omega}, \Delta P_e)$ for $3 \le p \le 4$. This step is only for model development and is not necessary for practical implementation.

Next, we show that Δ_{i3} and Δ_{i4} are zero at steady state condition. Obviously, at steady state, we have $x_{3i} = \Delta P_{ei}/M_i = 0$. Consequently, by using (18) at steady state, we obtain

$$\Delta_{i3s} = 1/T_{d0i}\,(x_{di} - x_{qi})I_{qis}\,I_{qis}$$

where the index "*s*" stands for steady state conditions. At steady state, the states x_{i1}, x_{i2}, and x_{i3} in (18) are zero. The term $(x_{qi} - x_{di})$ is zero for round rotors and it is a small value for salient pole rotors. Therefore, $\Delta_{i3s} = 0$. Also, since $\dot{x}_{3i} = 0$ at steady state, we have $x_{4is} = 0$. In addition, $\dot{I}_{qi} = 0$ and $\Delta_{i4s} = 0$. Consequently, at steady state $x_{i1} = x_{i2} = x_{i3} = x_{i4} = 0$, we have $\Delta_{i3}(0) = \Delta_{i4}(0) = 0$.

V. The UPFC as a Nonlinear Controller

In the proposed effort, the UPFC is chosen as a FACTS device which acts as a controller to mitigate system oscillations. The method, however, is applicable to other FACTS devices since the proposed approach is generic and deals with power balance equations as well as generator dynamics. As illustrated in Fig.3a, the UPFC shunt

transformer is connected to bus $t+n$ and the series transformer is connected between buses $t+n$ and $h+n$. The effect of the UPFC on the power system can be represented as injected powers to the connecting buses [20] as shown in Fig. 3b. This is referred to as the "power injection" model of the UPFC [20].

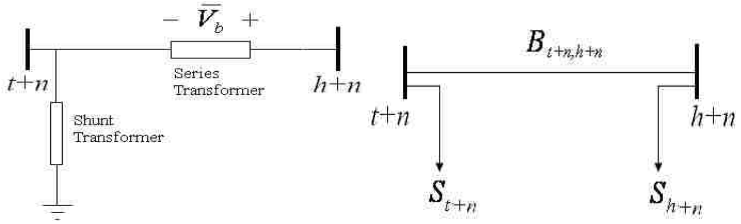

(a) (b)

Fig. 3 a) UPFC connected between two network nodes b) Injected powers to the connected buses

The injected active and reactive powers are given by

$$\begin{aligned} P_{t+n} &= B_{t+n,h+n}V_bV_{h+n}\sin(\psi_{t+n}-\psi_{h+n}+\theta) \\ P_{h+n} &= -B_{t+n,h+n}V_bV_{h+n}\sin(\psi_{t+n}-\psi_{h+n}+\theta) \\ Q_{t+n} &= B_{t+n,h+n}V_bV_{t+n}\cos(\theta) \\ Q_{h+n} &= -B_{t+n,h+n}V_bV_{h+n}\cos(\psi_{t+n}-\psi_{h+n}+\theta) \end{aligned} \tag{34}$$

where $\bar{V}_b = V_b\angle(\psi_{t+n}+\theta)$ is the voltage produced by the series transformer and can be assumed to be a function of time. Thus, the power flow equation at buses $t+n$ and $h+n$ can be represented as

$$\begin{aligned} &P_{\mathrm{OLD}t+n} + B_{t+n,h+n}V_{h+n}[\gamma\sin(\psi_{t+n}-\psi_{h+n})+\mu\cos(\psi_{t+n}-\psi_{h+n})] = 0 \\ &P_{\mathrm{OLD}h+n} - B_{t+n,h+n}V_{h+n}[\gamma\sin(\psi_{t+n}-\psi_{h+n})+\mu\cos(\psi_{t+n}-\psi_{h+n})] = 0 \\ &Q_{\mathrm{OLD}t+n} - B_{t+n,h+n}V_{t+n}\gamma = 0 \\ &Q_{\mathrm{OLD}h+n} + B_{t+n,h+n}V_{h+n}[\gamma\cos(\psi_{t+n}-\psi_{h+n})-\mu\sin(\psi_{t+n}-\psi_{h+n})] = 0 \end{aligned} \tag{35}$$

where $\gamma = V_b \cos\theta$, $\mu = V_b \sin\theta$, and $P_{\mathbf{OLD}}$ and $Q_{\mathbf{OLD}}$ represent the left hand side of equations (3). By taking the derivative of (35), equations (4) and (5) must be modified on the buses $t+n$ and $h+n$. Therefore, at bus $t+n$, we get

$$\begin{aligned}&\dot{P}_{\mathrm{OLD}t+n} + B_{t+n,h+n}[\gamma \sin(\psi_{t+n} - \psi_{h+n}) + \mu \cos(\psi_{t+n} - \psi_{h+n})]\dot{V}_{h+n} \\ &+ B_{t+n,h+n}V_{h+n}[\gamma \cos(\psi_{t+n} - \psi_{h+n}) - \mu \sin(\psi_{t+n} - \psi_{h+n})](\dot{\psi}_{t+n} - \dot{\psi}_{h+n}) \\ &+ B_{t+n,h+n}V_{h+n}[\dot{\gamma} \sin(\psi_{t+n} - \psi_{h+n}) + \dot{\mu} \cos(\psi_{t+n} - \psi_{h+n})] = 0\end{aligned} \tag{36a}$$

and at bus $h+n$, we get

$$\begin{aligned}&\dot{P}_{\mathrm{OLD}h+n} - B_{t+n,h+n}[\gamma \sin(\psi_{t+n} - \psi_{h+n}) + \mu \cos(\psi_{t+n} - \psi_{h+n})]\dot{V}_{h+n} \\ &- B_{t+n,h+n}V_{h+n}[\gamma \cos(\psi_{t+n} - \psi_{h+n}) - \mu \sin(\psi_{t+n} - \psi_{h+n})](\dot{\psi}_{t+n} - \dot{\psi}_{h+n}) \\ &- B_{t+n,h+n}V_{h+n}[\dot{\gamma} \sin(\psi_{t+n} - \psi_{h+n}) + \dot{\mu} \cos(\psi_{t+n} - \psi_{h+n})] = 0\end{aligned} \tag{36b}$$

Similarly, terms are also added to the left hand side of (5) at buses $t+n$ and $h+n$ to achieve

$$\dot{Q}_{\mathrm{OLD}+n} - B_{t+n,h+n}\gamma\dot{V}_{t+n} - B_{t+n,h+n}V_{t+n}\dot{\gamma} = 0 \tag{37a}$$

and

$$\begin{aligned}&\dot{Q}_{\mathrm{OLD}h+n} + B_{t+n,h+n}[\gamma \cos(\psi_{t+n} - \psi_{h+n}) - \mu \sin(\psi_{t+n} - \psi_{h+n})]\dot{V}_{h+n} \\ &+ B_{t+n,h+n}V_{h+n}[-\gamma \sin(\psi_{t+n} - \psi_{h+n}) - \mu \cos(\psi_{t+n} - \psi_{h+n})](\dot{\psi}_{t+n} - \dot{\psi}_{h+n}) \\ &+ B_{t+n,h+n}V_{h+n}[\dot{\gamma} \cos(\psi_{t+n} - \psi_{h+n}) - \dot{\mu} \sin(\psi_{t+n} - \psi_{h+n})] = 0\end{aligned} \tag{37b}$$

By updating matrices $\overline{A}$, $\overline{B}$, $\overline{D}$, and $\overline{E}$ with the additional terms, new matrices A, B, D, and E are obtained and given by (I-5a) - (I-5d) in Appendix I. Note that matrices C and F remain unchanged. Consequently, (6) becomes

$$\begin{bmatrix} A(x) & B(x) \\ D(x) & E(x) \end{bmatrix} \begin{bmatrix} \dot{V} \\ \dot{\psi} \end{bmatrix} = -\begin{bmatrix} C(x) \\ F(x) \end{bmatrix} \omega - G(x) \tag{38}$$

where $x = [x_S^T \quad \gamma \quad \mu]^T$ and vector G represents additional terms in (36) and (37) which are dependent on $\dot{\gamma}$ and $\dot{\mu}$. We define $u_1 = \dot{\gamma}$ and $u_2 = \dot{\mu}$ and obtain:

$$\begin{cases} G_t = +B_{t+n,h+n}V_{h+n}[u_1 \sin(\psi_{t+n}-\psi_{h+n})+u_2\cos(\psi_{t+n}-\psi_{h+n})] \\ G_h = -B_{t+n,h+n}V_{h+n}[u_1 \sin(\psi_{t+n}-\psi_{h+n})+u_2\cos(\psi_{t+n}-\psi_{h+n})] \\ G_{t+N} = -B_{t+n,h+n}V_{t+n}u_1 \\ G_{h+N} = +B_{t+n,h+n}V_{h+n}[u_1\cos(\psi_{t+n}-\psi_{h+n})-u_2\sin(\psi_{t+n}-\psi_{h+n})] \\ G_i = 0; \quad elsewhere \end{cases} \tag{39}$$

By solving (38) for $\dot{V}$ and $\dot{\psi}$, we obtain the set of nonlinear equations

$$\begin{bmatrix} \dot{V} \\ \dot{\psi} \end{bmatrix} = \begin{bmatrix} \bar{f}_1(x) \\ \bar{f}_2(x) \end{bmatrix} + \begin{bmatrix} \bar{g}_1(x) & \bar{g}_2(x) \\ \bar{g}_3(x) & \bar{g}_4(x) \end{bmatrix} \begin{bmatrix} u_1 \\ u_2 \end{bmatrix} \tag{40}$$

where

$\begin{bmatrix} \bar{f}_1(x) \\ \bar{f}_2(x) \end{bmatrix} = -\begin{bmatrix} A & B \\ D & E \end{bmatrix}^{-1}\begin{bmatrix} C \\ F \end{bmatrix}$, $\begin{bmatrix} \bar{g}_1(x) & \bar{g}_2(x) \\ \bar{g}_3(x) & \bar{g}_4(x) \end{bmatrix} = -\begin{bmatrix} A & B \\ D & E \end{bmatrix}^{-1}\bar{G}$, $\bar{G}_{2N\times 2}$ is introduced as equation (I-6) in Appendix I and satisfies $G = \bar{G}[u_1 \quad u_2]^T$, and $\bar{f}_1, \bar{f}_2, \bar{g}_1, \bar{g}_2, \bar{g}_3, \bar{g}_4 \in R^N$.

Equation (40) is an affine nonlinear system in continuous-time with control inputs u_1 and u_2. Once the control inputs are defined, the UPFC control parameters γ and μ can be obtained by integrating the control inputs. By Incorporating (1) and (2), we obtain the system dynamic equations as

$$\begin{cases} \dot{\delta}_i = \omega_i \\ M_i\dot{\omega}_i = P_{mi} - \dfrac{M_i}{M_T}P_{COI} - B_{i,i+n}E_{gi}V_{i+n}\sin(\delta_i - \psi_{i+n}); \quad i = 1,\ldots,n \\ \begin{bmatrix} \dot{V} \\ \dot{\psi} \end{bmatrix} = \begin{bmatrix} \bar{f}_1(x) \\ \bar{f}_2(x) \end{bmatrix} + \begin{bmatrix} \bar{g}_1(x) & \bar{g}_2(x) \\ \bar{g}_3(x) & \bar{g}_4(x) \end{bmatrix}\begin{bmatrix} u_1 \\ u_2 \end{bmatrix} \\ \dot{\gamma} = u_1 \\ \dot{\mu} = u_2 \end{cases} \tag{41}$$

Equation (41) is now in special case of strict feedback form (as explained after (45)) where backstepping can be used for the controller design.

Remark 2. In the case of multiple UPFCs in the network, equations (34) through (39) are repeated for each pair of UPFC buses $t_j + n$ and $h_j + n$ for all $1 \le j \le k$, where k is the total number of UPFCs. Similarly, the corresponding entries of matrices *A*, *B*, *D*, and *E* change

following the same logic described for equation (38). Moreover, vector *G* has entries corresponding to each UPFC. Consequently, the resulting differential equation is affine in terms of all UPFC control inputs which is given by

$$\begin{bmatrix}\dot{V}\\ \dot{\psi}\end{bmatrix}=\begin{bmatrix}\bar{f}_{T1}(x_T)\\ \bar{f}_{T2}(x_T)\end{bmatrix}+\sum_{j=1}^{k}\begin{bmatrix}\bar{g}_{j1}(x_T) & \bar{g}_{j2}(x_T)\\ \bar{g}_{j3}(x_T) & \bar{g}_{j4}(x_T)\end{bmatrix}\begin{bmatrix}u_{j1}\\ u_{j2}\end{bmatrix} \tag{42}$$

where k is the number of UPFCs and $x_T=[x_S^T \quad \gamma_1 \quad \mu_1 \quad \cdots \quad \gamma_k \quad \mu_k]^T$. The nonlinear functions $\bar{f}_{T1}, \bar{f}_{T2}, \bar{g}_{j1}, \bar{g}_{j2}, \bar{g}_{j3}, \bar{g}_{j4} \in R^N$ are defined in Appendix I.

VI. Controller Design

The conventional approach to damping oscillations in an interconnected power system is to employ a linear control scheme [21]. By contrast, we target the stability of the generators in a nonlinear sense by defining an appropriate Lyapunov function. In the control development, we restrict our design to the case of constant loads. Also, we assume that the mechanical power $P_{mi}\,(1\le i\le n-1)$ is slowly changing compared to the other control variables; thus, $\dot{P}_{mi}\approx 0$. For the purpose of convenience we define new state variables as

$$\begin{aligned} x_{1i} &= \delta_i-\delta_{i0}\\ x_{2i} &= \omega_i\\ x_{3i} &= V_{i+n}\sin(\delta_i-\psi_{i+n}) \end{aligned} \tag{43}$$

where δ_{i0} is the pre-fault generator angle for $1\le i\le n-1$. The selection of x_{3i} renders (2) in the backstepping form as will be explained. Using (42), we obtain

$$\dot{x}_{3i}=\dot{V}_{i+n}\sin(\delta_i-\psi_{i+n})+V_{i+n}(\omega_i-\dot{\psi}_{i+n})\cos(\delta_i-\psi_{i+n})$$

$$\begin{aligned} &= \bar{f}_{T1i}\,sin(\delta_i-\psi_{i+n})-V_{i+n}\bar{f}_{T2i}\,cos(\delta_i-\psi_{i+n})+V_{i+n}\omega_i\,cos(\delta_i-\psi_{i+n})\\ &+\sum_{j=1}^{k}\Big\{[\bar{g}_{j1i}\,sin(\delta_i-\psi_{i+n})-V_{i+n}\bar{g}_{j3i}\,cos(\delta_i-\psi_{i+n})u_{j1}]\\ &+[\bar{g}_{j2i}\,sin(\delta_i-\psi_{i+n})-V_{i+n}\bar{g}_{j4i}\,cos(\delta_i-\psi_{i+n})]u_{j2}\Big\} \end{aligned}$$

$$= \mathrm{f}_{Ti}(x_T) + \sum_{j=1}^{k} \mathrm{a}_{j1i}(x_T)u_{j1} + \mathrm{a}_{j2i}(x_T)u_{j2} \tag{44}$$

where $\bar{f}_{T1i}$, $\bar{f}_{T2i}$, $\bar{g}_{j1i}$, $\bar{g}_{j2i}$, $\bar{g}_{j3i}$, and $\bar{g}_{j4i}$ are the i-th elements of $\bar{f}_{T1}$, $\bar{f}_{T2}$, $\bar{g}_{j1}$, $\bar{g}_{j2}$, $\bar{g}_{3j}$, and $\bar{g}_{j4}$, respectively. Also, k is the number of UPFCs and j is the UPFC number.

A. Single generator/Single UPFC control

To introduce the design concept, we initially design a controller for a single generator/single UPFC power system using the standard backstepping design method with the control inputs $u_{j1} = u_1$ and $u_{j2} = u_2$. This approach will be extended to multiple generators/multiple UPFCs in the next section.

Remark 3. In [15], [20], [24], it is demonstrated that if the UPFC injects the maximum series voltage (i.e. constant V_b), it can inject the maximum active power; thus, it improves transient stability. The condition $V_b = Const$ may be applied by noting that $\gamma^2 + \mu^2 = V_b^2$. This in turn results in $\gamma u_1 + \mu u_2 = 0$ by taking derivative from both sides (note that $dV_b^2/dt = 0$ for constant V_b) which may be considered as an algebraic relationship between the control inputs u_1 and u_2. However, for damping the after-fault oscillations V_b can be kept high at the beginning (for a short time) and reduced afterwards in accordance with the state errors as this helps reduce the electrical stress on the UPFC. According to [20], UPFC injected power can also be controlled by varying V_b under the constant phase angle θ. Then, when θ is around $\pm 90^o$ maximum active power is injected for a given V_b. This requires that $\gamma = 0$; thus, $u_1 = 0$. Consequently, in this design we let $u_1 = 0$ thereby decreasing the number of inputs in (44). Then, from (2), (43) and (44), the new set of state equations can be constructed as

$$\begin{cases} \dot{x}_{1i} = x_{2i} \\ M_i \dot{x}_{2i} = f_{1i} + g_{1i} x_{3i} \\ \dot{x}_{3i} = f_{2i}(x) + g_{2i}(x)u; i = 1,\ldots,n \end{cases} \quad (45)$$

where $f_{1i} = P_{mi} - (M_i / M_T) P_{COI}$, $g_{1i} = -B_{i,i+n} E_{gi}$, $f_{2i}(x) = \mathrm{f}_{Ti}(x)$, $g_{2i}(x) = \mathrm{a}_{2i}(x)$, and $u = u_2$ for $1 \le i \le n-1$ where $x = [x_S^T, \gamma, \mu]^T$. Equation (45) is a special case of strict feedback form where f_{1i} and g_{1i} are constants instead of function of the states.

Assumption 2. $g_{2i}(x)$ is bounded away from zero. Without loss of generality it will be assumed that $g_{2i}(x) > 0$.

This claim is supported by the fact that due to its continuity if $g_{2i}(x)$ changes sign, then it must pass through the origin. As a consequence, equation (45) encounters a singularity tending to make $[\gamma \quad \mu]^T$ infinitely large. By selecting a proper place for the UPFC and setting appropriate design gains, we can avoid large control inputs.

Step 1. Introducing $K_{\delta i}$ and K_{Z1i} as design constants, we introduce $z_{1i} = x_{2i} + K_{\delta i} x_{1i}$ which results in

$$\dot{x}_{1i} = -K_{\delta i} x_{1i} + z_{1i} \quad (46)$$

Consequently, by defining $z_{2i} = (x_{3i} - x_{3si})$ we have

$$M_i \dot{z}_{1i} = f_{1i} + M_i K_{\delta i} x_{2i} + g_{1i} x_{3si} + g_{1i} z_{2i} \quad (47)$$

where

$$x_{3si} = \frac{1}{g_{1i}} \times [-x_{1i} - f_{1i} - M_i K_{\delta i} x_{2i} - K_{Z1i} z_{1i}] \quad (48)$$

is chosen such that the Lyapunov function $\mathrm{L}_{1i} = \frac{1}{2} {x_{1i}}^2 + \frac{1}{2} M_i z_{1i}^2$ has a negative definite derivative when $z_{2i} = 0$.

Step 2. Define the new Lyapunov function

$$\mathrm{L}_{2i} = K_{\text{atten}i}(\frac{1}{2}x_{1i}^2 + \frac{1}{2}M_i z_{1i}^2) + \frac{1}{2}z_{2i}^2 \tag{49}$$

with $K_{\text{atten}i}$ being a design constant, we can easily show that $\dot{\mathrm{L}}_{2i} = K_{\text{atten}i}(\dot{x}_{1i}x_{1i} + M_i\dot{z}_{1i}z_{1i}) + \dot{z}_{2i}z_{2i} < 0$ guaranteeing that the states x_{1i}, z_{1i}, and z_{2i} asymptotically converge to zero provided that $\dot{z}_{2i} = \nu_i$ where

$$\nu_i = -K_{\text{atten}i}z_{1i}g_{1i} - K_{Z2i}z_{2i} \tag{50}$$

and from (45)

$$\dot{z}_{2i} = f_{2i}(x) + g_{2i}(x)u - \dot{x}_{3si} \tag{51}$$

where

$$\dot{x}_{3si} = \frac{1}{g_{1i}} \times [-x_{2i} - K_{Z1i}K_{\delta i}x_{2i} - \frac{K_{\delta i}M_i + K_{Z1i}}{M_i}(f_{1i} + g_{1i}x_{3i})] \tag{52}$$

Equation (51) along with $\dot{z}_{2i} = \nu_i$ and (50) provides a solution for control inputs u in terms of nonlinear functions of states as

$$u = g_{2i}(x)^{-1}(\nu_i - f_{2i}(x) + \dot{x}_{3si}) . \tag{53}$$

Remark 4. If the assumption made in *Remark 2* is not applied (i.e. $u_1 \neq 0$), equation (53) will revert to

$$\mathrm{a}_{1i}(x)u_1 + \mathrm{a}_{2i}(x)u_2 = \nu_i - f_{2i}(x) + \dot{x}_{3si} \tag{54}$$

which gives a linear relationship in terms of the control inputs. Then, a second relationship such as $\gamma u_1 + \mu u_2 = 0$ (mentioned in Remark 2) between u_1 and u_2 is needed to select them. Since optimal performance of UPFC is obtained by varying both the injected voltage V_b and angle θ, a second relationship between u_1 and u_2 can play an important role in achieving the controller.

B. Multiple generator/multiple UPFC control

For the case of multiple generator control, the equation (24) is replaced by

$$\dot{z}_2 = f_3(x) + g_2(x)\overline{H}u \tag{55}$$

where, $f_3(x) = f_2(x) - \dot{x}_{3s}$, $f_2 = [f_{21} \ \ldots \ f_{2,n-1}]^T$, $g_2 = diag(g_{21} \ \ldots \ g_{2,n-1})$, $x_{3s} = [x_{3s1} \ \ldots \ x_{3s,n-1}]^T$ and $\overline{H}_{(n-1)\times 1} = [1 \ \ldots \ 1]^T$. Also, define $x_1 = [x_{11} \ \ldots \ x_{1,n-1}]^T$, $z_1 = [z_{11} \ \ldots \ z_{1,n-1}]^T$, and $z_2 = [z_{21} \ \ldots \ z_{2,n-1}]^T$. Note that for the multiple UPFC case x is replaced by x_T and the dimensions of g_2 change. Moreover, note that only $n-1$ generators are chosen to be controlled. Since the n generators are present in the interconnected power network, the *n*th generator is forced to be controlled by the power balance if the remaining $n-1$ speeds are controlled. Since there are fewer inputs than outputs, it is generally difficult to find an input that makes the first derivative of the Lyapunov function candidate negative definite. In other words, because of the inconsistency that arises due to multiple solutions for a single u the above single generator control method cannot be employed for multiple generator control. Thus, we propose the input

$$u = \frac{-1}{\sum_{i=1}^{n-1}(1 + 2K_{Z3}z_{2i})g_{2i}}\left((\overline{H}^T + 2K_{Z3}z_2^T) f_3(x) + (\overline{H}^T + K_{Z3}z_2^T)K_{Z2}z_2\right) \tag{56}$$

where K_{Z2} and K_{Z3} are design parameters .

Definition. (*Uniform Ultimate Bounded (UUB)***)**[22]. Consider the dynamical system $\dot{x} = f(x)$ with $x \in \Re^n$ being a state vector. Let the initial time be t_0 and initial condition be $x_0 = x(t_0)$. Then, the equilibrium point x_e is said to be UUB if there exists a compact set $S \subset \Re^n$ so that for all $x_0 \in S$ there exists a bound B and a time $T(B, x_0)$ such that $\|x(t) - x_e\| \le B$ for $\forall t > t_0 + T$.

Theorem 1. Consider the dynamical system described by (19), (47), and (51) which is rewritten as

$$\begin{cases} \dot{x}_{1i} = -K_{\delta i} x_{1i} + z_{1i} \\ M_i \dot{z}_{1i} = f_{1i} + M_i K_{\delta i} x_{2i} + g_{1i} x_{3si} + g_{1i} z_{2i} \\ \dot{z}_{2i} = f_{2i}(x) + g_{2i}(x) u - \dot{x}_{3si} \end{cases} \tag{57}$$

with the input given by (56) for $1 \le i \le n-1$. Then the states are globally uniformly ultimately bounded provided Assumption 1 holds.

Proof. See Appendix II. ■

Remark 5. Equation (57) needs the term $\sum_{i=1}^{n-1}(1+2K_{Z3}z_{2i}^T)g_{2i}$ to be bounded away from zero. Based on Assumption 1, this can be easily achieved by selecting a proper K_{Z2} and K_{Z3} and replacing each x_{3i} with $K_{MZ2i}x_{3i}$ where K_{MZ2i} is a proper modification factor if $\sum_{i=1}^{n-1}(1+2K_{Z3}z_{2i}^T)g_{2i}=0$. From equation (45) this changes g_{2i} to $K_{MZ2i}g_{2i}$ such that the term $\sum_{i=1}^{n-1}(1+2K_{Z3}z_{2i}^T)K_{MZ2i}g_{2i}$ moves from zero in (56).

VII. Neural Network Control

Although equation (56) provides the UPFC control inputs, finding the analytical and/or numerical nonlinear control inputs in practice (for fast computing) is a challenging task in large power systems. Moreover, in order to implement the control law, a complete knowledge of the total power system dynamics and topology are needed. However, by using the neural network approximation property for nonlinear functions with on-line learning scheme [22], we are able to approximate the nonlinear "unknown dynamic" terms in the power system dynamics, thus relaxing the need for a complete system description as well as onerous function calculations.

A general function $f(x) \in R$ where $x \in R^n$ can be written as $f(x) = W^T \phi(\bar{V}^T x) + \varepsilon(x)$ with $\varepsilon(x)$ a neural network (NN) functional reconstruction error where $W \in R^{N_2 \times 1}$ and $\bar{V} \in R^{n \times N_2}$ are weight matrices [22]. In our design, input-to-the hidden-layer weight matrix $\bar{V}$ is selected initially at random and held fixed during learning. It is demonstrated in [23] that if the input-to-the-hidden-layer weights, $\bar{V}$, are chosen initialized randomly and kept constant and if the number of neurons N_2 in the hidden layer is sufficiently large, the NN approximation error $\varepsilon(x)$ can be made arbitrarily small since the activation function vector ϕ forms a basis.

A. Single generator/single UPFC control

Consider the system (45). Unlike equation (56), here we assume that the nonlinear functions g_{2i} and f_{2i} (for $1 \le i \le n-1$) are not available. Thus, in order to provide the desired input we employ the neural network approximation property for nonlinear functions as $u_1 = -K_{Z2i} z_{2i} - \left(W_i^T \phi_i(\bar{V}_i^T x) + \varepsilon\right)$ where the term $W_i^T \phi_i(\bar{V}_i^T x) + \varepsilon$ represents the unknown nonlinear function in the control input with W_i being unknown ideal weight matrix (where $\|W_i\|$ is assumed to be upper bounded [22]) and $\varepsilon_i \le \varepsilon_M$ is the approximation error in a compact set $\Omega = \left\{x_{1i}, z_{1i}, z_{2i} \;\middle|\; x_{1i}^2 + z_{1i}^2 + z_{1i}^2 \le \rho\right\}$. In practice, the actual weight matrix W_i and approximation error ε_i are unknown and only an estimation of the weight matrix is utilizable, i.e.

$$u = -K_{Z2i} z_{2i} - \hat{W}_i^T \phi_i(\bar{V}_i^T x) \tag{58}$$

It is shown in Appendix III that the states $[z_{2i} \;\; \hat{W}_{2i}]^T$ are stable with arbitrarily small upper bounds by selecting the neural network weight update law as [22]

$$\dot{\hat{W}}_i = \Gamma_i \phi_i(\bar{V}_i^T x) z_{2i} - \alpha_i \Gamma_i \hat{W}_i \tag{59}$$

where α_i is a design constant and Γ_i is a constant matrix.

B. Multiple generator/multiple UPFC control

By using the similar approach to single generator neural network controller we define the desired control input for system (45) as (60)

$$u = -K_{Z2}\bar{H}^T z_2 - \left(W^T \varphi(\bar{V}^T x) + \varepsilon\right) \tag{60}$$

where $\bar{H}_{(n-1)\times 1} = [1 \ \ldots \ 1]^T$ and $\varepsilon \le \varepsilon_M$ in a compact set [22] $\Omega = \left\{x_1, z_1, z_2 \ \middle| x_1^T x_1 + z_1^T z_1 + z_2^T z_2 \le \rho\right\}$. Then we utilize the estimation of the weight matrix as

$$u = -K_{Z2}\bar{H}^T z_2 - \hat{W}^T \varphi(\bar{V}^T x) \tag{61}$$

It is shown in Appendix IV that by selecting the weight update law as

$$\dot{\hat{W}} = \Gamma \phi(\bar{V}^T x)\bar{H}^T z_2 - \alpha\Gamma\hat{W} \tag{62}$$

boundedness of the states $[\bar{H}^T z_2 \ \ \|\tilde{W}\|]^T$ with bounds defined in the Appendix is achieved. In general, it is hard to conclude stability of the states $z_{2i}\,(1 \le i \le n-1)$ from boundedness of $\bar{H}^T z_2$. However, in this problem we have considered $n-1$ generator to avoid dependency of generators electrical powers (and z_{2i}) to each other. For many power system topologies if the UPFC is placed on the proper bus we may conclude stability of $z_{2i}\,(1 \le i \le n-1)$ based on the stability of $\bar{H}^T z_2$ as confirmed by simulations. Exceptions may include topologies with isolated generators. Similar to proof of Theorem 1, this yields stability of the states x_1 and z_1.

Remark 6. We can see from (61) and (62) that the control and update laws are only functions of generators data and loads. Although for the controller design δ_{i0} is needed,

this parameter can be achieved by knowing the generator operating conditions. Thus, no prior knowledge of power system topology is needed for controller design.

VIII. Simulation Results

For control validation, two power system topologies are considered. In both examples the simulations are performed using the complete power system model (with line resistances) to evaluate the effectiveness of the modeling and design. Also, steam governor is in action in all simulations. First, the system in Fig. 4 is chosen where a three-phase fault is injected close to bus 3 (as depicted in Fig. 4) at $t = 0.2s$ and removed at $t = 0.4s$ seconds. The infinite bus is simulated by a huge generator whose angle and speed do not change by the fault. The infinite bus voltage and angle are given as $V_2 = 1.0470\text{pu}$ and $\psi_2 = \text{-}0.0091\text{Rad}$. The data for generator 1 are given as $x'_d = 0.006$, $H = 1$, $E_g = 1.0657\text{pu}$, and $\bar{\delta}_i = 0.0017\text{Rad}$ at $t = 0$. The UPFC is placed on bus 1 between buses 1 and 3 and is activated after fault clearance.

Two scenarios are assumed; the fault is removed without changing the topology and with removal of one of the lines between buses 1 and 3(i.e. the faulted line). In accordance with Remark 2, the proposed control is performed via constant UPFC angle $\theta = \pm 90^o$ and variable (controlled) UPFC voltage V_b. The design is performed by using the method introduced in Section V-A for single generator control where gains are chosen as $K_{\delta 1} = 0.1$, $K_{\text{Z11}} = 0.2$, $K_{\text{Z12}} = 100$, and K_{atten} =1. The results from the proposed method are compared with the case with $V_{b\max} = 0.5\text{pu}$ and variable θ where the controller examines the slope of the power flow in the line, where the UPFC series transformer is placed, and switches the output $\bar{\theta}$ (shown in Fig. 5) between $\pm 90^o$ (which gives maximum UPFC

injected power at constant $V_b = V_{b\max}$ as explained in Remark 2) correspondingly to prevent increasing or decreasing the flow of power in the UPFC line, and thus, to prevent the power flow oscillations. The output $\bar{\theta}$ is then passed through a first order filter $K_P/(1+\tau_P s)$ (with $K_P = 0.1;\ \ \tau_P = 0.1$ after fine tuning), depicted in Fig. 5, to reduce sharp power fluctuations and to provide the UPFC angle θ which in turn provides the total line power P_e (including the injected power by UPFC.)

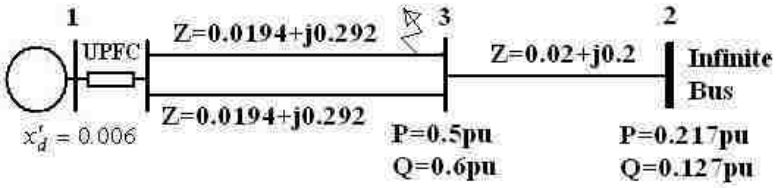

Fig. 4 One-generator power system

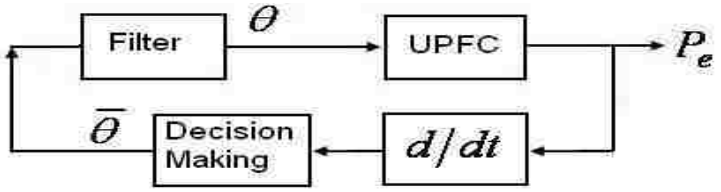

Fig. 5 UPFC active power controller

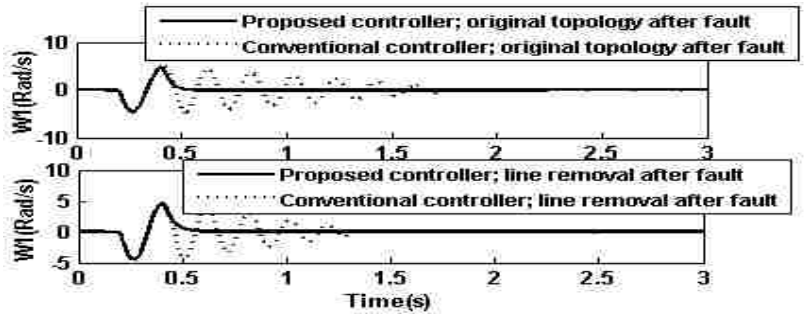

Fig. 6 Damping effect of the proposed nonlinear controller when compared to the method with UPFC fixed injected voltage V_b and variable angle θ

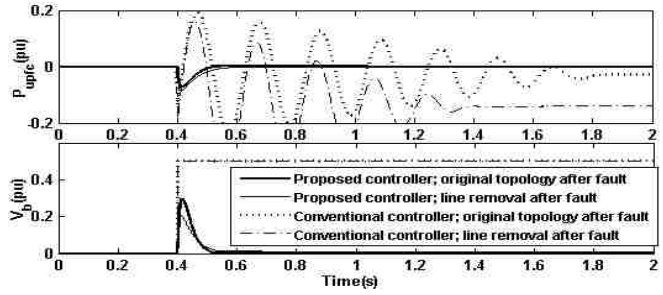

Fig. 7 UPFC injected power and voltage in the proposed nonlinear controller when compared to the method with UPFC fixed injected voltage V_b and variable angle θ

Figures 6 and 7 show the UPFC damping effect, injected power, and voltage of the proposed controller for the two scenarios (original topology and line removal after fault) as compared to those of the conventional controller through controlling θ. As shown in the figures faster damping as well as lower injected voltage and power are achieved by using the proposed nonlinear controller. Also, unlike the conventional

controller, no significant difference in controller performance between the two cases (original topology and line removal after fault) is observed when using the proposed controller.

In the second example the IEEE 14-bus, 5-generator power system shown in Fig. 8 is used and subjected to three phase faults.

Table 1. Generators Specifications

Gen no.	1	2	3	4	5
x'_d	0.006	0.006	0.006	0.006	0.006
$H = \omega_s M/2$	5	1	1	5	5

The generator data is given in Table 1. All of the generators have steam governors and the UPFC control is implemented via the power injection model. The power system loads are considered as constants. The control objective is to damp the generators oscillations after the fault is cleared.

In the system given by Fig. 8, the UPFC is installed on bus 6 between 6 and 7 which is found to be an appropriate placement by trial and error, i.e. it can stabilize the power system for different fault locations. The power system modes are 11.3561, 5.9101, 2.6977, and 2.1026Hz. A three-phase short circuit fault is applied to buses 1, 6, and 11 at $t = 0.2s$ and removed at $t = 0.4s$ seconds. Generators 1 through 4 are chosen for control. The control inputs γ and μ are initially set to zero such that $V_b(t_0) = 0$ and the proposed control

method is performed through using variable V_b and $\theta = \pm 90^o$. Two cases are considered for simulations.

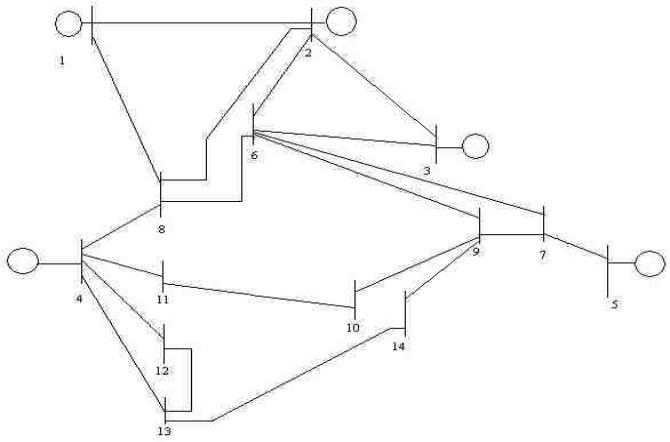

Fig. 8 The IEEE 14-bus, 5-generator power system

Case 1. All power system dynamic states are assumed to be available for the control design and equation (56) along with $\theta = \pm 90^o$ ($u_1 = 0$) are used to design the controller. The design gains are chosen as $K_{\delta 1}$ through $K_{\delta 4}$ =0.1, K_{Z11} through K_{Z14} =0.2, K_{Z2} =100, $K_{Z3} = 1$.

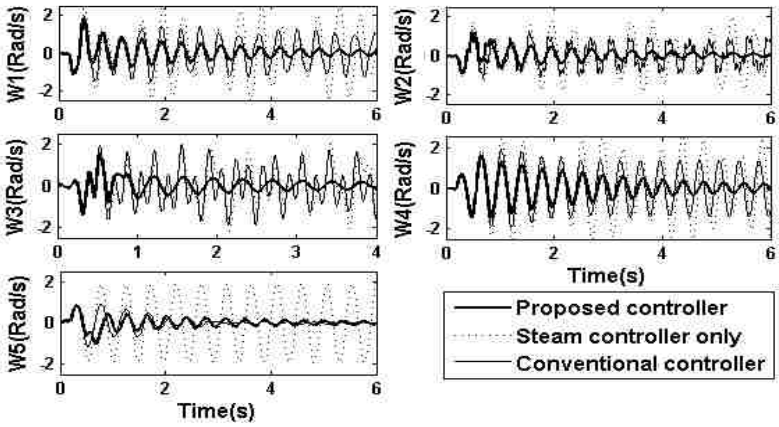

Fig. 9 Generator speeds with and without control; Case 1 with fault on bus 1

Figures 9 through 11 show that significant percentage of oscillation damping can be achieved for a medium size power network by using a single UPFC as a controller. Moreover, the nonlinear controller without changing the controller gains from the previous case is able to damp the oscillations resulting from a fault occurring at different locations through satisfactory control effort as shown in Figs. 12 and 13. Note, however, that damping performance varies with the fault location. In particular, Figs. 9 through 11 illustrate that for faults occurring at the locations relatively close to the UPFC bus (bus 6), the oscillation damping is more effective than for the faults occurring far from UPFC bus. Also, the control effort for the latter case is higher as shown in Figs. 12 and 13. This is due to different after fault conditions imposed to the controller.

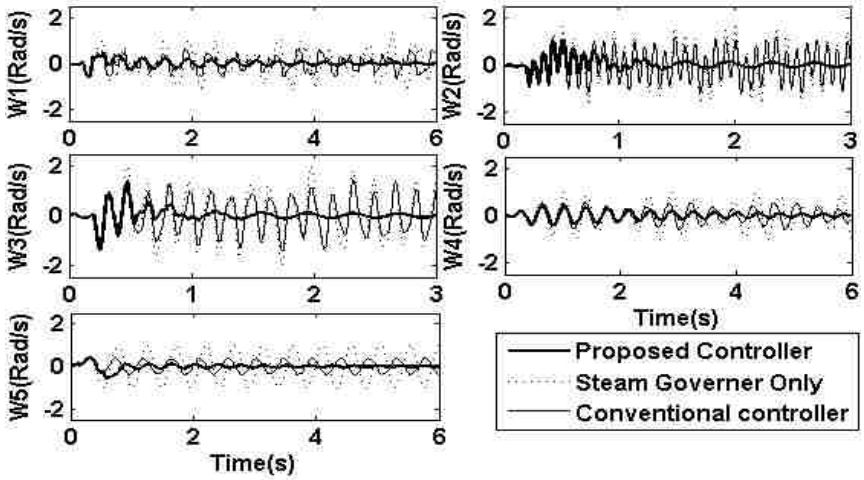

Fig. 10 Generator speeds with and without control; Case 1 with fault on bus 6

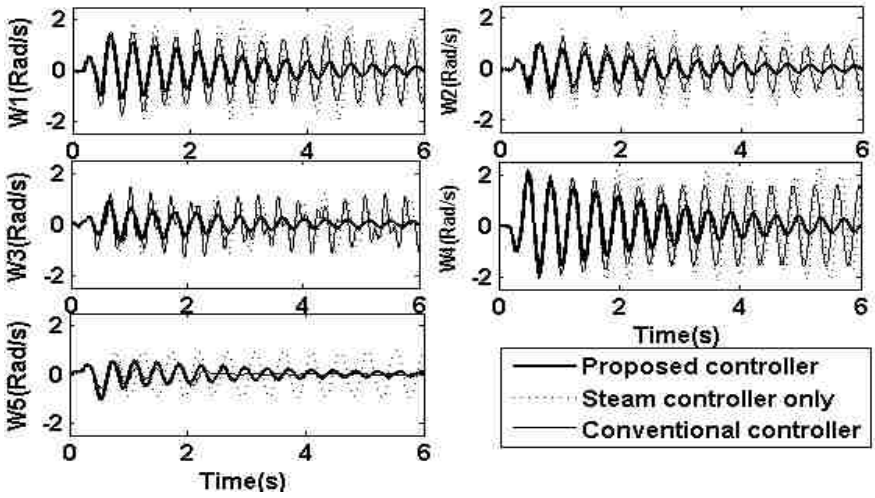

Fig. 11 Generator speeds with and without control; Case 1 with fault on bus 11

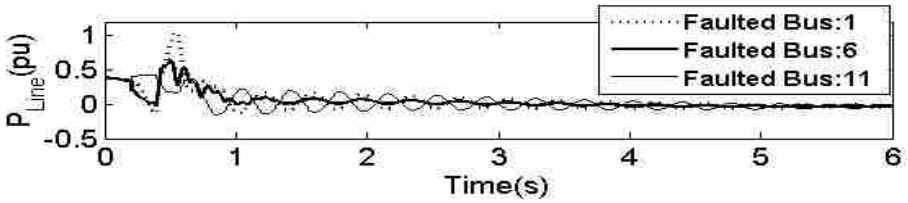

Fig. 12 Active power flow from bus 6 to 7; Case 1

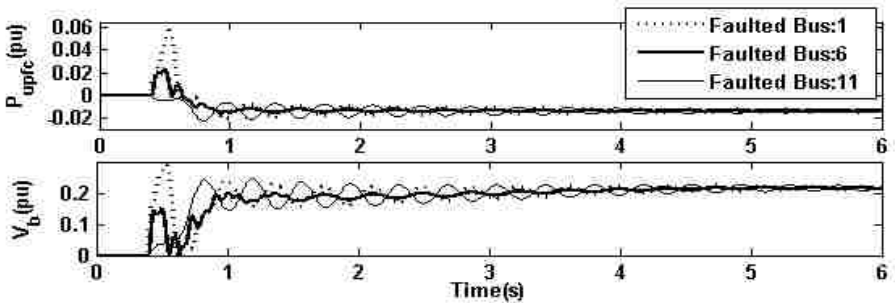

Fig. 13 UPFC injected power and series injected voltage; Case 1

However, the voltage and line flows do not go back to their pre-fault values due to bounded stability performance of the controller. Overall, from these results, the proposed control is very effective in damping the oscillations even in the presence of numerous modes and with significant fault (as illustrated in Figs. 6-11) occurring in the power network. The results from the proposed controller are then compared with those of the conventional controller explained in the first example with $K_P = 0.2;\ \ \tau_P = 0.1$(after fine tuning) where instead of observing the line power flow slope, the sign change in angle difference of the UPFC line buses (i.e. $\text{sign}(\psi_{t+n} - \psi_{h+n})$) is considered since a stabilizing controller using the power flow derivative sign was not achieved. Unlike the previous example, the conventional controller cannot stabilize all generators and only affects the generator close to UPFC (i.e. Gen5). For the fault on bus 6, no significant damping effect is introduced by the conventional controller.

Case 2. Power system dynamics are assumed unavailable. By using equations (61) and (62) and assuming $u_1 = 0$ ($\theta = \pm 90^o$), the NN controller is utilized to approximate the unknown system. Ten neurons are selected for the hidden layer with sigmoid [22] as activation function and design gains are chosen as $K_{\delta 1}$=0.1, $K_{\delta 2}$=0.2, $K_{\delta 3}$=0.1, $K_{\delta 4}$=0.1, K_{Z11} through K_{Z14}=0.1, K_{Z2}=500, α=1e-4, and Γ=5e5. The weight estimate $\hat{W}$ is initialized randomly. No offline training is utilized to tune the weights and no a priori data about the power system topology is needed for controller design.

Figures 14 and 15 illustrate that the neural network controller nearly has the same ability to damp the oscillations as that of Case 1. This implies that the neural network controller is able to quickly learn the power system nonlinear dynamics by only using the network voltages and angles as well as the synthesized input u.

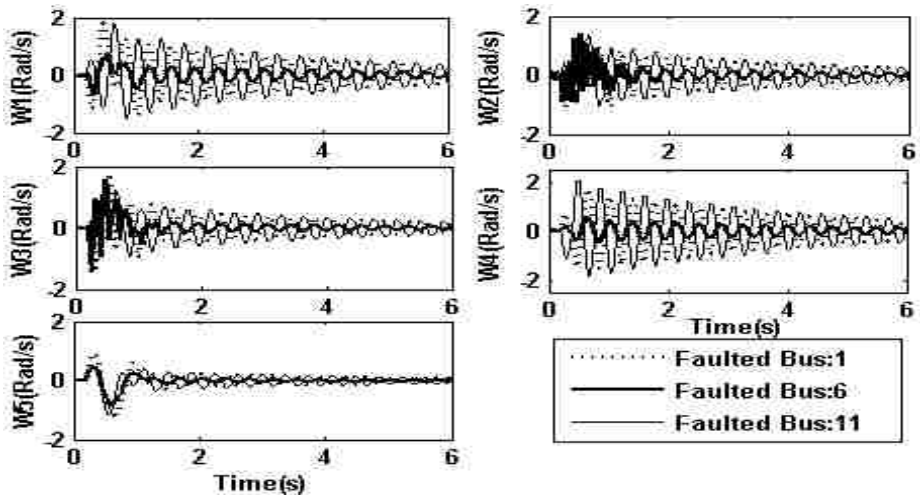

Fig. 14 Generator speeds; Case 2

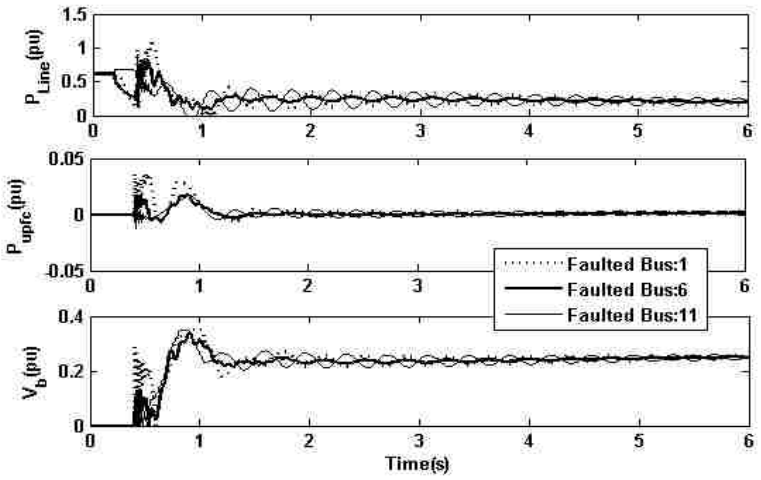

Fig. 15 UPFC injected power and series voltage; Case 2

IX. Conclusions

We have introduced a general nonlinear dynamical model for power systems with UPFC as stabilizing controller. This model is free of algebraic equations, thus conventional nonlinear control strategies are applicable to stabilize the power system after fault occurrence. Then, the model representation is expanded to decentralized formulation of power systems. We have addressed a multi-machine control scheme in which the number of control inputs is less than the number of outputs. Furthermore, we have utilized neural networks approximation property to relax the burdensome nonlinear function calculations and a priori knowledge about the power system dynamics needed for control design. Our analytical approach as well as our simulation results shows the effectiveness of our approach.

References

[1] IEEE/CIGRE Joint Task Force on Stability Terms and Definitions, "Definition and Classification of Power System Stability," IEEE *Trans. on Power Systems,* vol. 19, no. 2, May 2004.

[2] C. Li-Jun and I. Erlich, "Simultaneous coordinated tuning of PSS and FACTS damping controllers in large power systems," *IEEE Trans. on Power Systems,* vol. 20, no. 1, pp. 294 – 300, Feb 2005.

[3] H. Wang, "A Unified Model for the Analysis of FACTS Devices in Damping Power System Oscillations-Part III: Unified Power Flow Controller," *IEEE Trans. on Power Delivery,* vol. 15, no. 3, pp. 978-983, July 2000.

[4] B. C. Pal, "Robust damping of interarea oscillations with unified power-flow controller," *IEE Proc-Gener. Transm. Diatrib.,* vol. 149, no. 6, pp. 733-738, November 2002.

[5] N. Yang, Q. Liu, and J.D. McCalley, "TCSC controller design for damping interarea oscillations," *IEEE Trans. on Power Systems,* vol. 13, no. 4, pp. 1304 – 1310, Nov. 1998.

[6] J. Guo, "Decentralized Control and Placement of Multiple Unified Power Flow Controllers," *Missouri University of Science and Technology, PhD Dissertation,* pp. 40-67, 2006.

[7] E. Ghollipour and S. Saadat, "Improving transient stability of power systems using UPFC," *IEEE Trans. on Power Delivery,* vol. 20, no.2, pp. 1677-1682, 2005.

[8] U. Gabrijel, and R. Mihalic, "Direct methods for transient stability assessment in power systems comprising controllable series devices," *IEEE Trans. on Power Systems,* vol. 17, no. 4, pp.1116 –1122, 2002.

[9] N. Tambey and M.L. Kothari, "Damping of power system oscillations with unified power flow controller (UPFC) ," *IEE Proc-Gener. Transm. Distrib.,* vol. 150, no. 2, pp. 129-140, March 2003.

[10] M. Januszewski, J. Machowski, and J.W. Bialek, "Application of direct Lyapunov method to improve damping of power swings by control of UPFC," *IEE Proc-Gener. Transm. Distrib.,* vol. 151, no. 2, pp. 252-260, March 2004.

[11] J.J. Ford, G. Ledwich, and Z.Y Dong, "Nonlinear control of single-machine-infinite-bus transient stability," *IEEE Power Engineering Society General Meeting*, June 18 -22, 2006.

[12] M. Poshtan, B.N. Singh, and P. Rastgoufard, "A Nonlinear Control Method for SSSC to Improve Power System Stability", *International Conference on Power Electronics, Drives and Energy Systems,* pp. 1 – 7, 12-15 Dec. 2006.

[13] M.A. Pai., "*Energy function analysis of power systems*," Kluwer International Series, 1989.

[14] M. Ghandhari, G. Anderson, and I.A. Hiskens, "Control Lyapunov functions for controllable series devices", *IEEE Trans. power systems*, vol. 16, no. 4, pp. 689-694, November 2001.

[15] V. Azbe, U. Gabrijel, D. Povh, and R. Mihalic, "The energy function of a general multi machine system with a unified power flow controller," *IEEE Trans. power systems*, vol. 20, no. 3, pp. 1478-1485, August 2005.

[16] M. Noroozian, M. Ghandhari, G. Andersson, J. Gronquist, and I. Hiskens "A robust control strategy for shunt and series reactive compensators to damp electromechanical oscillations," *IEEE Trans. on Power Delivery*, vol. 16, no. 4, pp.: 812 – 817, Oct. 2001.

[17] Y. Guo, D. Hill, and Y. Wang, "Nonlinear decentralized control of large-scale power systems," *Automatica*, vol. 36, pp.: 1275-1289, 2000.

[18] P.W. Sauer and M.A. Pai, *Power System Dynamics and Stability*, Prentice Hall, 1997.

[19] Y. Guo, D. J. Hill, and Y. Wang, "Nonlinear decentralized control of large scale power systems", *Automatica*, vol. 36, no. 9, pp. 1275-1289, 2000.

[20] M. Noroozian, L. Angquist, M. Ghandhari, and G. Anderson, "Use of UPFC for optimal power flow control," *IEEE Trans. On Power Delivery*, vol. 12, no. 4, pp. 1629-1634, October 1997.

[21] K. Mekki, N.M. HadjSaid, D. Georges, and R**.** Feuillet**, "**LMI versus non-linear techniques for the design of FACTS controller", *IEEE Power Engineering Society Winter Meeting*, vol. 2, pp.: 1501 – 1505, Jan. 2002.

[22] F.L. Lewis, S. Jagannathan, and A. Yesildirek, "*Neural Network Control Of Robot Manipulators and nonlinear Systems*," Taylor and Francis, 1999.

[23] B. Igelnik and Y. H. Pao, "Stochastic choice of basis functions in adaptive function approximation and the functional-link net," *IEEE Trans. Neural Networks*, vol. 6, no. 6, pp. 1320–1329, Nov. 1995.

[24] V. Azbe and R. Mihalic, , "The Control Strategy for an IPFC based on the energy function," *IEEE Transactions on Power Systems*, vol. 23, no. 4, pp.1662 – 1669, 2008.

Appendix I

According to equations (4) and (5) we have the equations (I-1) and (I-2).

$$\begin{aligned}\dot{S}_P &= \dot{P}_{Li} + \dot{V}_i\Big(\sum_{j=1}^{n} B_{ij}E_{gj}\sin(\psi_i-\delta_j) + \sum_{j=n+1}^{n+N} B_{ij}V_j\sin(\psi_i-\psi_j)\Big)\\ &+ \dot{\psi}_i V_i\sum_{j=1}^{n} B_{ij}E_{gj}\cos(\psi_i-\delta_j) - V_i\sum_{j=1}^{n} B_{ij}E_{gj}\omega_j\cos(\psi_i-\delta_j)\\ &+ V_i\sum_{j=n+1}^{n+N} B_{ij}\sin(\psi_i-\psi_j)\dot{V}_j + \dot{\psi}_i V_i\sum_{j=n+1}^{n+N} B_{ij}V_j\cos(\psi_i-\delta_j)\\ &- V_i\sum_{j=n+1}^{n+N} B_{ij}V_j\cos(\psi_i-\psi_j)\dot{\psi}_j = 0\end{aligned} \tag{I-1}$$

$$\begin{aligned}\dot{S}_Q &= -\dot{Q}_{Li} + \dot{V}_i\Big(\sum_{j=1}^{n} B_{ij}E_{gj}\cos(\psi_i-\delta_j) + \sum_{j=n+1}^{n+N} B_{ij}V_j\cos(\psi_i-\psi_j)\Big)\\ &- \dot{\psi}_i V_i\sum_{j=1}^{n} B_{ij}E_{gj}\sin(\psi_i-\delta_j) + V_i\sum_{j=1}^{n} B_{ij}E_{gj}\omega_j\sin(\psi_i-\delta_j)\\ &+ V_i\sum_{j=n+1}^{n+N} B_{ij}V_j\sin(\psi_i-\psi_j)\dot{\psi}_j = 0\end{aligned} \tag{I-2}$$

Entries of matrices $\overline{A}_{N\times N}$, $\overline{B}_{N\times N}$, $C_{N\times n}$, $\overline{D}_{N\times N}$, $\overline{E}_{N\times N}$, and $F_{N\times n}$ for the case without UPFC are summarized as follows.

$$a_{ij} = B_{i+n,j+n}V_{i+n}\sin(\psi_{i+n}-\psi_{j+n}) \quad ; i=1,\ldots,N;\ j=1,\ldots,N \tag{I-3a}$$

$$\begin{aligned}a_{ii} &= \sum_{j=1}^{n} B_{i+n,j}E_{gj}\sin(\psi_{i+n}-\delta_j)\\ &+ \sum_{j=1}^{N} B_{i+n,j+n}V_{j+n}\sin(\psi_{i+n}-\psi_{j+n}) + \frac{\partial P_{Li+n}}{\partial V_{i+n}} \qquad i=1,\ldots,N\end{aligned} \tag{I-3b}$$

$$b_{ij} = -V_{i+n}B_{i+n,j+n}V_{j+n}\cos(\psi_{i+n}-\psi_{j+n}) \quad ; i=1,\ldots,N;\ j=1,\ldots,N \tag{I-3c}$$

$$b_{ii} = V_{i+n}\sum_{j=1}^{n} B_{i+n,j}E_{gj}\cos(\psi_{i+n}-\delta_j) + V_{i+n}\sum_{j=n+1}^{n+N} B_{i+n,j}V_j\cos(\psi_{i+n}-\psi_j) - V_{i+n}^2 B_{i+n,i+n} + \frac{\partial P_{Li+n}}{\partial \psi_{i+n}} \quad i=1,\ldots,N \tag{I-3d}$$

$$c_{ij} = -V_{i+n}B_{i+n,j}E_{gj}\cos(\psi_{i+n}-\delta_j) \quad ;i=1,\ldots,N;\ j=1,\ldots,n \tag{I-4e}$$

$$d_{ij} = B_{i+n,j+n}V_{i+n}\cos(\psi_{i+n}-\psi_{j+n}) \quad ;i=1,\ldots,N;\ j=1,\ldots,n \tag{I-4a}$$

$$d_{ii} = \sum_{j=1}^{n} B_{i+n,j}E_{gj}\cos(\psi_{i+n}-\delta_j) + \sum_{j=1}^{N} B_{i+n,j+n}V_{j+n}\cos(\psi_{i+n}-\psi_{j+n}) + B_{i+n,i+n}V_{i+n} - \frac{\partial Q_{Li+n}}{\partial V_{i+n}} \quad ;i=1,\ldots,N \tag{I-4b}$$

$$e_{ij} = V_{i+n}B_{i+n,j+n}V_{j+n}\sin(\psi_{i+n}-\psi_{j+n}) \quad ;i=1,\ldots,N;\ j=1,\ldots,N \tag{I-4c}$$

$$e_{ii} = -V_{i+n}\sum_{j=1}^{n} B_{i+n,j}E_{gj}\sin(\psi_{i+n}-\delta_j) - V_{i+n}\sum_{j=1}^{N} B_{i+n,j+n}V_{j+n}\sin(\psi_{i+n}-\psi_{j+n}) - \frac{\partial Q_{Li+n}}{\partial \psi_{i+n}} \quad i=1,\ldots,N; \tag{I-4d}$$

$$f_{ij} = V_{i+n}B_{i+n,j}E_{gj}\sin(\psi_{i+n}-\delta_j) \quad ;i=1,\ldots,N;\ j=1,\ldots,n \tag{I-4e}$$

Modifications on the entries of matrices $A_{N\times N}$, $B_{N\times N}$, $D_{N\times N}$, and $E_{N\times N}$ for the case with UPFC are summarized as follows.

$$\begin{cases} a_{t,h} = a_{t,h(old)} + B_{t+n,h+n}[\gamma\sin(\psi_{t+n}-\psi_{h+n}) + \mu\cos(\psi_{t+n}-\psi_{h+n})] \\ b_{t,t} = b_{t,t(old)} + B_{t+n,h+n}V_{h+n}[\gamma\cos(\psi_{t+n}-\psi_{h+n}) - \mu\sin(\psi_{t+n}-\psi_{h+n})] \\ b_{t,h} = b_{t,h(old)} - B_{t+n,h+n}V_{h+n}[\gamma\cos(\psi_{t+n}-\psi_{h+n}) - \mu\sin(\psi_{t+n}-\psi_{h+n})] \end{cases} \tag{I-5a}$$

$$\begin{cases} a_{h,h} = a_{h,h(old)} - B_{t+n,h+n}[\gamma\sin(\psi_{t+n}-\psi_{h+n}) + \mu\cos(\psi_{t+n}-\psi_{h+n})] \\ b_{h,t} = b_{h,t(old)} - B_{t+n,h+n}V_{h+n}[\gamma\cos(\psi_{t+n}-\psi_{h+n}) - \mu\sin(\psi_{t+n}-\psi_{h+n})] \\ b_{h,h} = b_{h,h(old)} + B_{t+n,h+n}V_{h+n}[\gamma\cos(\psi_{t+n}-\psi_{hv}) - \mu\sin(\psi_{t+n}-\psi_{h+n})] \end{cases} \tag{I-5b}$$

$$d_{t,t} = d_{t,t(old)} - B_{t+n,h+n}\gamma \tag{I-5c}$$

$$\begin{cases} d_{h,h} = d_{h,h(old)} + B_{t+n,h+n}[\gamma\cos(\psi_{t+n}-\psi_{h+n}) - \mu\sin(\psi_{t+n}-\psi_{h+n})] \\ e_{h,t} = e_{h,t(old)} - B_{t+n,h+n}V_{h+n}[\gamma\sin(\psi_{t+n}-\psi_{h+n}) + \mu\cos(\psi_{t+n}-\psi_{h+n})] \\ e_{h,h} = e_{t,h(old)} + B_{t+n,h+n}V_{h+n}[\gamma\sin(\psi_{t+n}-\psi_{h+n}) + \mu\cos(\psi_{t+n}-\psi_{h+n})] \end{cases} \quad \text{(I-5d)}$$

The subscript (*old*) refers to the original values (without UPFC) as defined by (I-3) and (I-4). The matrix $\overline{G}$ is defined as follows:

$$\begin{cases} \overline{G}_{t,1} = +B_{t+n,h+n}V_{h+n}\sin(\psi_{t+n}-\psi_{h+n}); \overline{G}_{t,2} = +B_{t+n,h+n}V_{h+n}\cos(\psi_{t+n}-\psi_{h+n}) \\ \overline{G}_{h,1} = -B_{t+n,h+n}V_{h+n}\sin(\psi_{t+n}-\psi_{h+n}); \overline{G}_{h,2} = -B_{t+n,h+n}V_{h+n}\cos(\psi_{t+n}-\psi_{h+n}) \\ \overline{G}_{t+N,1} = -B_{t+n,h+n}V_{t+n}; \overline{G}_{t+N,2} = 0 \\ \overline{G}_{h+N,1} = +B_{t+n,h+n}V_{h+n}\cos(\psi_{t+n}-\psi_{h+n}); \overline{G}_{h+N,2} = -B_{t+n,h+n}V_{h+n}\sin(\psi_{t+n}-\psi_{h+n}) \\ \overline{G}_{i,j} = 0; \quad \textit{elsewhere} \end{cases} \quad \text{(I-6)}$$

For the case of multiple UPFCs matrices A, B, D, and E are changed to A_T, B_T, D_T, and E_T as described in Remark 1. The nonlinear functions used in (15) are described as (I-7)

$$\begin{bmatrix} \bar{f}_{T1}(x_T) \\ \bar{f}_{T2}(x_T) \end{bmatrix} = -\begin{bmatrix} A_T(x_T) & B_T(x_T) \\ D_T(x_T) & E_T(x_T) \end{bmatrix}^{-1}\begin{bmatrix} C(x_T) \\ F(x_T) \end{bmatrix} \quad \text{(I-7)}$$

Also, we have

$$-\begin{bmatrix} A_T(x_T) & B_T(x_T) \\ D_T(x_T) & E_T(x_T) \end{bmatrix}^{-1} G_T = -\begin{bmatrix} A_T(x_T) & B_T(x_T) \\ D_T(x_T) & E_T(x_T) \end{bmatrix}^{-1} \overline{G}_T U \quad \text{(I-8)}$$

where $U_{2k\times 1} = \begin{bmatrix} u_{11} & u_{21} & \cdots & u_{1j} & u_{2j} & \cdots & u_{1k} & u_{2k} \end{bmatrix}^T$, k is the number of UPFCs and $\overline{G}_T = \begin{bmatrix} \overline{G}_{T1} & \cdots & \overline{G}_{Tj} & \cdots & \overline{G}_{Tk} \end{bmatrix}_{2N\times 2k}$ with $\overline{G}_{Tj} \in R^{2N\times 2}$ corresponds to the jth UPFC whose entries are defined in (I-6). Using $\overline{G}_T$, we are able to define

$$\begin{bmatrix} \overline{g}_{j1}(x_T) & \overline{g}_{j2}(x_T) \\ \overline{g}_{j3}(x_T) & \overline{g}_{j4}(x_T) \end{bmatrix}_{2N\times 2} = -\begin{bmatrix} A_T(x_T) & B_T(x_T) \\ D_T(x_T) & E_T(x_T) \end{bmatrix}^{-1} \times G_{Tj} \quad \text{(I-9)}$$

Appendix II

Proof of Theorem 1: For the case of multiple generator control, we define the Lyapunov function as

$$\mathrm{L} = \frac{1}{2}\left[\sum_{i=1}^{n-1}\left(z_{2i} + K_{\mathbf{Z}3} z_{2i}^2\right)\right]^2 \tag{II-1}$$

where $K_{\mathbf{Z}3i}$ is a design constant. Taking derivative of (II-1), we have

$$\dot{\mathrm{L}} = \left(\sum_{i=1}^{n-1}(1+2K_{Z3}z_{2i})\dot{z}_{2i}\right)\left(\sum_{i=1}^{n-1}\left(z_{2i} + K_{\mathbf{Z}3} z_{2i}^2\right)\right). \tag{II-2}$$

Using the following equation

$$\sum_{i=1}^{n-1}(1+2K_{Z3}z_{2i})\dot{z}_{2i} = \sum_{i=1}^{n-1}\overline{v}_{\mathbf{i}} \tag{II-3}$$

where $\overline{v}_i = -K_{Z2}\left(z_{2i} + K_{\mathbf{Z}3} z_{2i}^2\right)$, makes $\dot{\mathrm{L}}$ negative definite.

In order to obtain u_1 in the case of multiple generator control we use equation (51) and (II-3) and obtain

$$u_1 = \left(\sum_{i=1}^{n-1}(1+2K_{Z3}z_{2i})g_{2i}(x)\right)^{-1}\sum_{i=1}^{n-1}\left(\overline{v}_i - (1+2K_{Z3}z_{2i})\left(f_{2i}(x) - \dot{x}_{3si}\right)\right) \tag{II-4}$$

The control input (II-4) causes the term $\sum_{i=1}^{n-1} z_{2i} + K_{\mathbf{Z}3} z_{2i}^2$ converge to zero asymptotically. Consequently, z_{2i} converges to the bound obtained below.

$$\sum_{i=1}^{n-1} z_{2i} + K_{\mathbf{Z}3} z_{2i}^2 = \sum_{i=1}^{n-1} K_{\mathbf{Z}3}\left(\left(z_{2i} + \frac{1}{2K_{\mathbf{Z}3}}\right)^2 - \frac{1}{4K_{Z3}^2}\right) = 0$$

which in turns results in the bound

$$\sum_{i=1}^{n-1}\left(z_{2i} + \frac{1}{2K_{\mathbf{Z}3}}\right)^2 = \frac{n-1}{4K_{Z3}^2} \tag{II-5}$$

Thus, z_{2i} approaches to the bound presented by (II-5) asymptotically.

Next, equations (58) imply

$$\begin{bmatrix} \dot{x}_{1i} \\ \dot{z}_{1i} \end{bmatrix} = \begin{bmatrix} -K_{\delta i} & 1 \\ -\frac{1}{M_i} & -\frac{K_{Z1i}}{M_i} \end{bmatrix} \begin{bmatrix} x_{1i} \\ z_{1i} \end{bmatrix} + \begin{bmatrix} 0 \\ \frac{g_{1i}}{M_i} \end{bmatrix} z_{2i} \quad ; 1 \le i \le n-1 \tag{II-6}$$

which is a linear input-to-state stable system by proper choice of the control gains $K_{\delta i}$ and K_{Z1i} such that the eigenvalues of the linear system have negative real parts. Thus, the states x_{1i} and z_{1i} are bounded following the stability of z_{2i} for $1 \le i \le n-1$. ■

Appendix III

Equation (51) for the *i*-th generator in a single-UPFC power system can be written as

$$\dot{z}_{2i} = g_{2i}\left(\frac{f_{2i}(x) - \dot{x}_{3si}}{g_{2i}(x)} + u\right) \tag{III-1}$$

where x is the vector of the global parameters as defined earlier. We repeat the back stepping control design mentioned in the previous section and define the Lyapunov function L_{2i} as

$$\mathrm{L}_{2i} = z_{2i}^2 / \left(2g_{2i}(x)\right). \tag{III-2}$$

which has the derivative as

$$\dot{\mathrm{L}}_{2i} = \left(\frac{\dot{z}_{2i}}{g_{2i}(x)} - \frac{\dot{g}_{2i}(x)}{2g_{2i}^2(x)} z_{2i}\right) z_{2i} \tag{III-3}$$

Applying (III-1) into (III-3) renders the Lyapunov function derivative $\dot{\mathrm{L}}_{2i} < 0$ provided the control input is selected as

$$u = -K_{Z2i} z_{2i} - \frac{f_{2i}(x) - \dot{x}_{3si}}{g_{2i}(x)} + \frac{\dot{g}_{2i}(x)}{2g_{2i}^2(x)} z_{2i} \tag{III-4}$$

The term $\frac{f_{2i}(x) - \dot{x}_{3si}}{g_{2i}(x)} - \frac{\dot{g}_{2i}(x)}{2g_{2i}^2(x)} z_{2i}$ in (III-4) is the unknown term which must be approximated by a neural network as

$$\frac{f_{2i}(x) - \dot{x}_{3si}}{g_{2i}(x)} - \frac{\dot{g}_{2i}(x)}{2g_{2i}^2(x)} z_{2i} = W_i^T \phi_i(\bar{V}_i^T x) + \varepsilon_i \tag{III-5}$$

where $\varepsilon_i \le \varepsilon_M$ is the approximation error in a compact set [22] $\Omega = \left\{ x_{1i}, z_{1i}, z_{2i} \;\middle|\; x_{1i}^2 + z_{1i}^2 + z_{1i}^2 \le \rho \right\}$. Since the ideal weights W_i are not known, the estimated weight matrix $\hat{W}_i$ is utilized to approximate u_1 as (58). Now, define the Lyapunov function

$$\mathrm{L_i} = \mathrm{L}_{2i} + (1/2)\tilde{W}_i^T \Gamma_i^{-1} \tilde{W}_i \tag{III-6}$$

where $\tilde{W}_i = \hat{W}_i - W_i$ and Γ_i is a design constant. Taking the derivative of (III-6) and applying (58) results in

$$\dot{\mathrm{L}}_i = -K_{Z2i} z_{2i}^2 - \tilde{W}_i^T \phi_i(\bar{V}_i^T X) z_{2i} + \varepsilon z_{2i} + \tilde{W}_i^T \Gamma_i^{-1} \dot{\hat{W}}_i \tag{III-7}$$

By selecting the neural network weight update law as (59) and applying (III-7) we obtain

$$\begin{aligned}
\dot{\mathrm{L}}_{2i} &= -K_{Z2i} z_{2i}^2 - \alpha \tilde{W}_i^T \tilde{W}_i + \varepsilon_i z_{2i} - \alpha \tilde{W}_i^T W_i \\
&\le -K_{Z2i} z_{2i}^2 + \varepsilon_M |z_{2i}| - \alpha \left\| \tilde{W}_i \right\|^2 + \alpha \left\| \tilde{W}_i \right\| \| W_i \| \\
&= -K_{Z2i} \left(\left(z_{2i} - \frac{\varepsilon_M}{2K_{Z2i}} \right)^2 - \left(\frac{\varepsilon_M}{2K_{Z2i}} \right)^2 - \frac{\alpha_i}{K_{Z2i}} \left(\frac{\| W_i \|}{2} \right)^2 \right) - \alpha_i \left(\| \tilde{W}_i \| - \frac{\| W_i \|}{2} \right)^2 \\
&\quad or \\
&= -K_{Z2i} \left(z_{2i} - \frac{\varepsilon_M}{2K_{Z2i}} \right)^2 - \alpha_i \left(\left(\| \tilde{W}_i \| - \frac{\| W_i \|}{2} \right)^2 - \left(\frac{\| W_i \|}{2} \right)^2 - \frac{1}{\alpha_i K_{Z2i}} \left(\frac{\varepsilon_M}{2} \right)^2 \right)
\end{aligned} \tag{III-8}$$

$\dot{\mathrm{L}}_{2i}$ is negative if

$$|z_{2i}| > \frac{\varepsilon_M}{2K_{Z2i}} + \sqrt{\left(\frac{\varepsilon_M}{2K_{Z2i}}\right)^2 + \frac{\alpha_i}{K_{Z2i}}\left(\frac{\|W_i\|}{2}\right)^2} \text{ or } \|\tilde{W}_i\| > \frac{\|W_i\|}{2} + \sqrt{\left(\frac{\|W_i\|}{2}\right)^2 + \frac{1}{\alpha_i K_{Z2i}}\left(\frac{\varepsilon_M}{2}\right)^2}$$

which yield uniform ultimate boundedness of the states $[z_{2i} \quad \hat{W}_{2i}]^T$ with bounds defined above. Note that the bound on z_{2i} can be arbitrarily small by increasing the design gain K_{Z2i}. Similar to proof of Theorem 1 boundedness of the states $[x_{1i} \quad z_{1i}]^T$ can be concluded.

Appendix IV

The Lyapunov function in this case is proposed as

$$\mathrm{L}_4 = \left(\sum_{i=1}^{n-1} z_{2i}\right)^2 \Big/ \left(2\sum_{i=1}^{n-1} g_{2i}\right) + \frac{1}{2}\tilde{W}^T \Gamma_i^{-1} \tilde{W} \tag{IV-1}$$

where $\tilde{W} = \hat{W} - W$. We define the desired control input for system (45) as (IV-2)

$$u = -K_{Z2}\bar{H}^T z_2 - \left(\left(\sum_{i=1}^{n-1} f_{3i}\right) \Big/ \left(\sum_{i=1}^{n-1} g_{2i}\right) - \left(\sum_{i=1}^{n-1} \dot{g}_{2i} \sum_{i=1}^{n-1} z_{2i}\right) \Big/ \left(2\sum_{i=1}^{n-1} g_{2i}\right)^2\right) \tag{IV-2}$$

where $\bar{H}_{(n-1)\times 1} = [1 \quad \dots \quad 1]^T$. However, the desired control input u is a function of unknown dynamics and is approximated by a neural network as $u_1 = -K_{Z2}\bar{H}^T z_2 - \left(W^T \varphi(\bar{V}^T x) + \varepsilon\right)$. Taking the derivative of (IV-9), employing (IV-2), and choosing the weight update law as (62), we obtain

$$\begin{aligned} \dot{\mathrm{L}}_{2i} &= -K_{Z2}\bar{H}^T z_2^2 - \alpha\tilde{W}^T\tilde{W} + \varepsilon\bar{H}^T z_2 - \alpha\tilde{W}^T W \\ &\le -K_{Z2}\left(\bar{H}^T z_2\right)^2 + \varepsilon_M\left|\bar{H}^T z_2\right| - \alpha\left\|\tilde{W}\right\|^2 + \alpha\left\|\tilde{W}\right\|\|W\| \end{aligned} \tag{IV-3}$$

Similar to (III-8) $\dot{\mathrm{L}}_4$ is negative if $\left|\bar{H}^T z_2\right| > \frac{\varepsilon_M}{2K_{Z2}} + \sqrt{\left(\frac{\varepsilon_M}{2K_{Z2}}\right)^2 + \frac{\alpha}{K_{Z2}}\left(\frac{\|W\|}{2}\right)^2}$ or $\|\tilde{W}\| > \frac{\|W\|}{2} + \sqrt{\left(\frac{\|W\|}{2}\right)^2 + \frac{1}{\alpha K_{Z2}}\left(\frac{\varepsilon_M}{2}\right)^2}$ which yield uniform ultimate boundedness of $\bar{H}^T z_2$.

2. Decentralized Dynamic Surface Control of Large-Scale Interconnected Systems in Strict-Feedback Form Using Neural Networks with Asymptotic Stabilization

S. Mehraeen, S. Jagannathan, and M. L. Crow [1]

Abstract— *A novel neural network (NN)-based nonlinear decentralized adaptive controller is proposed for a class of large-scale, uncertain, interconnected nonlinear systems in strict-feedback form by using the dynamic surface control (DSC) principle; thus, the "explosion of complexity" problem which is observed in the conventional backstepping approach is relaxed in both state and output feedback control design. The matching condition is not assumed when considering the interconnection terms. Then, neural networks are utilized to approximate the uncertainties in both subsystem and interconnected terms. By using novel NN weight update laws with quadratic error terms, it is demonstrated using Lyapunov stability that the closed-loop signals are asymptotically stable with both state and output feedback controller, even in the presence of NN approximation errors in contrast with the uniform ultimate boundedness result, which is common in the literature with NN-based DSC and backstepping schemes. Simulation results show the effectiveness of the approach.*

Index Terms – Dynamic Surface Control, Decentralized Control, Nonlinear Adaptive Control, Neural Networks**.**

[1] Authors are with Department of Electrical and Computer Engineering, Missouri University of Science and Technology, 1870 Miner Circle, Rolla, MO 65409. Contact author: sm347@mst.edu. Research Supported in part by NSF ECCS#0624644.

I. Introduction

Dynamic surface control (DSC) [1] has been attracting great attention in this decade. The well-known problem of increased complexity in the backstepping design which occurs due to the repeated differentiation of the virtual control signal is replaced by a series of algebraic terms; thus, the burdensome calculations in the analytical development and practical implementations are relaxed. Unlike in standard backstepping method which results in globally uniformly bounded system states in the presence of unmodeled dynamics, the work in DSC results in uniform ultimate boundedness (UUB) in a semi-global manner [1]. Further attempts in [2] provide asymptotic stabilization for a class of uncertain nonlinear systems using DSC and adaptive control provided the control gain coefficient being unity or $g(.)=1$ and the uncertainty is assumed to be linear in the unknown parameters (LIP). Subsequently, neural network (NN) universal approximation property is asserted in [3] to relax this LIP assumption for subsystem uncertainties so that boundedness of the states is assured in the presence of NN reconstruction errors.

Decentralized control, on the other hand, has been investigated for large-scale systems with unknown system uncertainties and interconnection terms. In [4], by using state feedback control design a class of interconnected systems represented in Brunovski Canonical form is considered and an asymptotic tracking controller using adaptive NNs is demonstrated provided the interconnection terms satisfy a stringent matching condition. In [5], decentralized NN control of a more general class of nonlinear systems has been proposed by relaxing the matching condition using a standard backstepping approach. A uniformly ultimately boundedness of the system states is provided. Adaptive decentralized control of a class of uncertain nonlinear systems with asymptotic regulation

in the backstepping framework is proposed in [6]; however, the explosion of complexity is not addressed and the control gains $g(.)$ are assumed constants.

On the other hand, output feedback control design, has been investigated for certain class of interconnected systems. In [7] and [8], the constant control gain coefficient matrix ($g(.) = Const.$) matrix is considered and asymptotic results are achieved where the interconnection terms are functions of the output. In [9], an optimal strategy based on existence of Algebraic Riccati Equations (ARE) is considered and exponential stability of the decentralized system is achieved although constant gain coefficient matrix is used.

In this paper, the DSC design framework is proposed for a class of nonlinear uncertain interconnected systems in strict-feedback form while relaxing the matching condition; thus, the repeated differentiation of the virtual control signal is relaxed. Both state and output feedback controller designs are introduced. Next, NNs are introduced to overcome the uncertainties present in both subsystem and the interconnection dynamics. Thus, the use of neural network-based DSC in decentralized control not only overcomes the lack of knowledge about the subsystem dynamics and interconnection terms, but also relaxes the explosion of complexity problem normally observed in traditional backstepping. Moreover, the control gain matrix, $g(x)$, is considered as an unknown nonlinear function of the states and its time derivative is not required. For the case of output feedback, the control gain coefficient for the last state is considered unity.

It is demonstrated that the states of the subsystems approach the origin asymptotically, for both state and output feedback control design through novel NN weight update laws with second order error terms in contrast with UUB, which is

common with the available DSC schemes in the literature. Simulation results verify satisfactory performance of this controller.

First background information is given in the next section. Subsequently, the class of large-scale decentralized system along with the DSC state feedback design is introduced in Section III followed by output control design in Section IV. A numerical example resulting from the application of DSC to a nonlinear system is presented in Section V. Conclusions and future works are given in Section VI.

II. Background

Consider the dynamical system $\dot{x} \in f(x,t)$ with $x \in R^n$ represents the states of an uncontrolled open-loop system, or a closed-loop system after the application of the control input, and control input $u(t)$ has been specified in terms of the state $x(t)$. Let the initial time be t_0, and the initial condition be $x_0 \equiv x(t_0)$. A state x_e is an equilibrium point of the system if $f(x_e,t) = 0, t \geq t_0$.

Definition 1: An equilibrium point x_e is locally asymptotically stable at t_0 if there exists a compact set $S \subset \Re^n$ such that, for every initial condition in $x_0 \subset S$, $\|x(t) - x_e\| \to 0$ as $t \to \infty$.

Next, a brief background on NN is given. A general function $f(x) \in R$ where $x \in R^n$ can be written as $f(x) = W^T \phi(V^T x) + \varepsilon(x)$ with $\varepsilon(x)$ NN denotes functional reconstruction error vector, $W \in R^{N_2 \times 1}$ and $V \in R^{n \times N_2}$ represent target NN weight matrices. It is demonstrated in [10] that if, the input-to-the-hidden layer weight matrix, V, are chosen initialized randomly and kept constant and if the number of neurons N_2 in the hidden layer is sufficiently large, the NN approximation error $\varepsilon(x)$ can be made arbitrarily

small since the activation function vector ϕ forms a basis. In this work, V, is initialized at random and held and the output-layer weights are tuned online. Next, we introduce the class of decentralized nonlinear system under consideration.

III. The Large-scale Decentralized Nonlinear System with State Feedback Control Design

In order to consider the class of N interconnected subsystems defined by

$$\begin{cases} \dot{x}_{i1} = f_{i1}(x_{i1}) + g_{i1}(x_{i1})x_{i2} + \Delta_{i1}(\bar{X}_1) \\ \vdots \\ \dot{x}_{ip} = f_{ip}(X_{ip}) + g_{ip}(X_{ip})x_{i,p+1} + \Delta_{ip}(\bar{X}_p) \quad ; i = 1,\ldots,N \\ \vdots \\ \dot{x}_{i,n_i} = f_{i,n_i}(X_{i,n_i}) + g_{i,n_i}(X_{i,n_i})u_i + \Delta_{i,n_i}(\bar{X}_{n_i}) \end{cases} \tag{1}$$
$$h_i = x_{i1}$$

where index i represents the subsystem number, *f(.)*, and *g(.)*, represent unknown nonlinearities, $\Delta(.) = [\Delta_{i1},...,\Delta_{ip},...,\Delta_{in}]^T$ denotes interconnected terms, with $X_{ip} = [x_{i1},\ldots,x_{ip}]^T$, $\bar{X}_j = [x_{1j},\ldots,x_{Nj}]^T$, $\bar{X}_p = [\bar{X}_1^T,\ldots,\bar{X}_p^T]^T$, $\bar{X}_0 = 0$, and h_i is the subsystem measured output for $1 \le i \le N$ and $1 \le p \le n_i$. For the purpose of readability the notations a_{ij} and $a_{i,j}$ are used throughout the paper for the same variable where a_{ij} (i and j are integers representing element of a matrix) is an arbitrary real variable. Before we proceed, the following are needed.

Assumption 1: Assume that the interconnection terms in (1) are upper bounded in the compact set Ω (defined later) such that $\left|\Delta_{ip}(\bar{X}_p)\right| \le \sum_{j=1}^{N} \delta_{ipj}(X_{jp})$ (which corresponds to non-matching condition in contrast with [4]) where δ_{ipj} is an unknown function with $\delta_{ipj}(0) = 0$ for $1 \le i \le N$ and $1 \le p \le n_i$. Consequently, by using the mean value theorem [11], the interconnection terms can be written as

$$\left|\Delta_{ip}(\bar{X}_p)\right| \le \sum_{j=1}^{N} \delta_{ipj}(X_{jp}) \le \sum_{j=1}^{N}\sum_{q=1}^{p} \left|x_{jq}\right| \bar{\delta}_{ip,jq}(X_{jq}) \tag{2}$$

where $\bar{\delta}_{ip,jq} = \left|\left(\partial \delta_{ipj}(X_{jp})/\partial x_{jq}\right)\right|_{X_{jp}=X'_{jp}=l(X_{jp})}$ in Ω.

Assumption 2*:* The control gain matrix $g_{ip}(X_{ip})$ for $1 \le i \le N$ and $1 \le p \le \mathrm{n}_i$ satisfy $0 \le g_{ip}^{m} \le g_{ip}(X_{ip}) \le \bar{g}_{ip}(X_{ip})$ [4][5].

Assumption 3: The nonlinear function in (1) satisfies $f_{ip}(0) = 0$ for $1 \le i \le N$ and $1 \le p \le \mathrm{n}_i$. Thus, by using the mean value theorem [11] $f_{ip}(X_{ip})$ can be written as $f_{ip}(X_{ip}) = \sum_{s=1}^{p} x_{is} \upsilon_{ips}(X_{ip})$ where $\upsilon_{ips}(X_{ip}) = \partial f_{ip}(X_{ip})/\partial x_{is}\big|_{X_{ip}=X''_{ip}=l'(X_{ip})}$.

In other words, function $f_{ip}(X_{ip})$ can be written in the form of linear combination of X_{ip} elements where the coefficients are functions X_{ip}. This helps in the proof of asymptotic stability. Next, the design of the controller is introduced.

A. Controller Design

Before we proceed, define $\Pi_{i1} = x_{i1} = z_{i1}$, $\Pi_{ip} = [X_{ip}^T, z_{ip}, y_{ip}]^T$, $Z_{ip} = [z_{i1},\ldots,z_{ip}]^T$, $Y_{ip} = [y_{i1},\ldots,y_{ip}]^T$, $Z = [Z_{1\mathrm{n}_1}^T,\ldots,Z_{N\mathrm{n}_N}^T]^T$, $Y = [Y_{1\mathrm{n}_1}^T,\ldots,Y_{N\mathrm{n}_N}^T]^T$ where z_{ip} and y_{ip} are defined in the following section. Moreover, $\Pi_{i0} = 0$ is defined.

Step 1: Define the error as $z_{i1} = x_{i1} - x_{i1d}$ and $y_{i1} = \bar{x}_{i1} = 0$ where x_{i1d} is the desired set point for regulation. Now define

$$\bar{x}_{i2} = z_{i1}\hat{\Phi}_{i1}(\Pi_{i1}) - K_{i1}z_{i1} + \dot{x}_{i1d} \tag{3}$$

where $\bar{x}_{i2}$ is the desired virtual input to make $z_{i1} \to 0$ as $t \to \infty$ with $\hat{\Phi}_{ip}$ (for $1 \le i \le N$ and $1 \le p \le \mathrm{n}_i$) a nonlinear estimate of the unknown nonlinearity Φ_{ip} defined later in (B-19) in the appendix where unknown nonlinear terms in Lyapunov function are to be

approximated. In equation (3), a two-layer NN, $\hat{\Phi}_{ip}(\Pi_{ip}) = \hat{W}_{ip}^T \phi_{ip}(\Pi_{ip})$, where the second hidden layer weights matrix V_{ip} (second layer) are chosen at random initially and held fixed, will be utilized to approximate the nonlinear function $\Phi_{ip}(\Pi_{ip}) = W_{ip}^T \phi_{ip}(V_{ip}{}^T \Pi_{ip}) + \varepsilon$. Thus, throughout the paper we use $\hat{W}_{ip}^T \phi_{ip}(\Pi_{ip})$ to refer to $\hat{W}_{ip}^T \phi_{ip}(V_{ip}^T \Pi_{ip})$ and to emphasize that the weights $\hat{W}_{ip}$ are updated.

For the stabilization problem, the desired values become $x_{i1d} = \dot{x}_{i1d} = 0$. The intermediate virtual input x_{i2d} is obtained by passing the $\bar{x}_{i2}$ through a first order filter consistent with the DSC literature [1] as

$$\tau_{i2}\dot{x}_{i2d} + x_{i2d} = \bar{x}_{i2} \tag{4}$$

Also, define

$$z_{i2} = x_{i2} - x_{i2d};\ y_{i2} = x_{i2d} - \bar{x}_{i2} \tag{5}$$

Thus,

$$x_{i2} = z_{i2} + y_{i2} + \bar{x}_{i2}. \tag{6}$$

Then, the error dynamic is given by

$$\dot{z}_{i1} = f_{i1}(z_{i1}) + \Delta_{i1}(\bar{X}_p) + g_{i1}(z_{i1})(z_{i2} + y_2 + \bar{x}_2). \tag{7}$$

This procedure is performed repeatedly until step *p*.

Step p: Define

$$z_{ip} = x_{ip} - x_{ipd}. \tag{8}$$

Then, it follows that

$$\bar{x}_{i,p+1} = z_{ip}\hat{\Phi}_{ip}(\Pi_{ip}) - K_{ip} z_{ip} + \dot{x}_{ipd}, \tag{9}$$

$$\tau_{i,p+1}\dot{x}_{i,p+1,d} + x_{i,p+1,d} = \bar{x}_{i,p+1}, \tag{10}$$

$$y_{i,p+1} = x_{i,p+1,d} - \bar{x}_{i,p+1}, \tag{11}$$

$$\dot{x}_{i,p+1,d} = -y_{i,p+1}/\tau_{i,p+1}, \tag{12}$$

and

$$x_{i,p+1} = z_{i,p+1} + y_{i,p+1} + \bar{x}_{i,p+1}. \tag{13}$$

Also, the error dynamics can be written as

$$\dot{z}_{ip} = f_{ip}(X_{ip}) + \Delta_{ip}(\bar{X}_p) + g_{ip}(X_{ip})x_{i,p+1} - \dot{x}_{ipd} \tag{14}$$

where $\hat{\Phi}_{ip}(\Pi_{ip})$ is an approximation of the unknown nonlinear function as mentioned. Finally, in the last step, errors are defined as

Step n.

$$\bar{x}_{i,\mathrm{n}_i+1} = u_i = z_{i,\mathrm{n}_i}\hat{\Phi}^T_{i,\mathrm{n}_i}(\Pi_{i,\mathrm{n}_i}) - K_{i,\mathrm{n}_i}z_{i,\mathrm{n}_i} + \dot{x}_{i,\mathrm{n}_i,d}, \tag{15}$$

$$\begin{cases} z_{i\mathrm{n}_i} = x_{i\mathrm{n}_i} - x_{i\mathrm{n}_i d} \\ \dot{z}_{i,\mathrm{n}_i} = f_{i,\mathrm{n}_i}(X_{\mathrm{n}_i}) + \Delta_{i,\mathrm{n}_i}(\bar{X}_{\mathrm{n}_i}) + g_{i,\mathrm{n}_i}(X_{\mathrm{n}_i})\bar{x}_{i,\mathrm{n}_i+1} - \dot{x}_{i,\mathrm{n}_i,d} \\ z_{i,\mathrm{n}_i+1} = y_{i,\mathrm{n}_i+1} = 0 \end{cases}$$

where in the above equations (3) through (15), a NN function approximation $\hat{\Phi}_{ip}(\Pi_{ip}) = \hat{W}^T_{ip}\phi_{ip}(\Pi_{ip})$, will be utilized to approximate the nonlinear function $\Phi_{ip}(\Pi_{ip}) = W^T_{ip}\phi_{ip}(\Pi_{ip}) + \varepsilon$, with $\Phi_{ip}(\Pi_{ip})$ to be defined as explained previously. Consequently, the desired virtual input becomes $\bar{x}_{i,p+1} = z_{pi}\hat{W}^T_{ip}\phi_{ip}(\Pi_{ip}) - K_{ip}z_{pi} + \dot{x}_{ipd}$ as opposed to Wang and Huang [3]. Before going to the next step, define $\bar{x}_{i1} = y_{i0} = y_{i1} = z_{i0} = K_{i0} = e_{i0} = 0$, $\tau_{i0} = \tau_{i1} = 1$ for $1 \le i \le N$ and $\tilde{W} = [\tilde{W}_{11}, \ldots \tilde{W}_{N,\mathrm{n}_N}]$ where $\tilde{W}_{ip} = \hat{W}_{ip} - W_{ip}$. Here for convenience, we assume $\mathrm{n}_i = n$ for $1 \le i \le N$. The proof for the case with different n_i follows similarly such that $\mathrm{n}_i = n$ for the stabilization problem and therefore omitted here.

B. Stability Analysis

Before presenting the system stability, the following lemmas are introduced.

Lemma 1: The intermediate and desired virtual inputs $\bar{x}_{i,p+1}$ and $\bar{x}_{i,p+1,d}$, and states, $x_{i,p+1}$, for the decentralized system (1) with $1 \le i \le N$ and $1 \le p \le n-1$ satisfy the following inequalities defined by

$$\begin{cases} |\bar{x}_{i,p+1}| \le (e_{ip} + K_{ip})|z_{ip}| + |y_{ip}|/\tau_{ip} \\ |x_{i,p+1,d}| \le (e_{ip} + K_{ip})|z_{ip}| + |y_{ip}|/\tau_{ip} + |y_{i,p+1}| \\ |x_{i,p+1}| \le (e_{ip} + K_{ip})|z_{ip}| + |z_{i,p+1}| + |y_{ip}|/\tau_{ip} + |y_{i,p+1}| \end{cases}$$

with e_{ip} being an appropriate positive constant.

Proof. See Appendix. ■

Lemma 2. The derivative of the desired virtual control inputs $\dot{\bar{x}}_{ip}$ in the decentralized system (1) with $1 \le i \le N$ and $2 \le p \le n$ satisfy the following inequality defined as

$$|\dot{\bar{x}}_{ip}| \le \sum_{s=1}^{p} \xi_{\mathbf{z},ips}(\Pi_{i,p-1})|z_{is}| + \sum_{s=1}^{p} \xi_{\mathbf{y},ips}(\Pi_{i,p-1})|y_{is}|$$

$$+ \sum_{j=1}^{N} \sum_{q=1}^{p-1} \begin{pmatrix} \xi_{\Delta\mathbf{z},ip,jq}(\Pi_{i,p-1}, X_{jq})|z_{jq}| \\ + \xi_{\Delta\mathbf{y},ip,jq}(\Pi_{i,p-1}, X_{jq})|y_{jq}| \end{pmatrix}$$

with $\xi_{\mathbf{z},ips}$, $\xi_{\mathbf{y},ips}$, $\xi_{\Delta\mathbf{z},ip,jq}$, and $\xi_{\Delta\mathbf{y},ip,jq}$ being appropriate positive functions of states and errors.

Proof. See Appendix. ■

Next, we discuss the NN weight update law by using a novel projection scheme for tuning the NN weights since NNs are utilized for nonlinear function approximation. An interesting property of updating the NN weights using the proposed projection scheme via a second order error term is the boundedness of the NN weights without the need for the persistency of excitation condition (PE) which is demonstrated next.

Theorem 1: Assume that single-layer NNs are utilized to approximate the unknown nonlinearities of the system dynamics and the interconnection terms in (1). Let the NN weight tuning for the '*i*th' subsystem be provided by

$$\dot{\hat{W}}_{ip} = -\rho_{ip} z_{ip}^2 \phi_{ip}(\Pi_{ip}) - \rho_{ip} z_{ip}^2 \hat{W}_{ip} + \rho_{ip} z_{ip}^2 \chi \frac{\hat{W}_{ip}\hat{W}_{ip}^T}{\left\|\hat{W}_{ip}\right\|^2} \phi_{ip}(\Pi_{ip}) \tag{16}$$

where

$$\chi = \begin{cases} 0 & if \quad \left\|\hat{W}_{ip}\right\| < W_{ip}^M \quad or \quad \left\|\hat{W}_{ip}\right\| = W_{ip}^M \ \& \hat{W}_{ip}^T z_{ip}^2 \phi_{ip}(\Pi_{ip}) \geq 0 \\ 1 & if \quad \left\|\hat{W}_{ip}\right\| = W_{ip}^M \ \& \hat{W}_{ip}^T z_{ip}^2 \phi_{ip}(\Pi_{ip}) < 0 \\ 1 & if \quad \left\|\hat{W}_{ip}\right\| > W_{ip}^M \end{cases}$$

for all $1 \leq i \leq N$; $1 \leq p \leq n$, with W_{ip}^M denoting the user selected bound for the weights $\left\|\hat{W}_{ip}\right\|$. Then: (a) the weight estimates remain within the user selected bound such that $\left\|\hat{W}_{ip}\right\| \leq W_{ip}^M$ for $t \geq 0$ provided the initial weights start within the set defined by $\left\|\hat{W}_{ip}\right\| \leq W_{ip}^M$ at $t = 0$; (b) the weight estimation error term, $\tilde{W}_{ip} = \hat{W}_{ip} - W_{ip}$ or $\tilde{W} = [\tilde{W}_{11}, \ldots \tilde{W}_{N,\mathrm{n}_N}]$ is bounded inside the compact set Ω for $1 \leq i \leq N$ and $1 \leq p \leq n$ with W_{ip} being the target NN weight matrix.

Proof: See Appendix A. ■

Remark 1: The NN weight update law is a variant of the projection algorithm [12] with the exception that a quadratic error term is employed along with a new term $\rho_{ip} z_{ip}^2 \hat{W}_{ip}$ for relaxing the PE condition. The benefit of using the quadratic term of the state in the NN update law helps ensure asymptotic stability in Theorem 2. The user selected bound on the NN weights can play an important role for the function approximation. Conservative bound selection (i.e. small W_{ip}^M) can result in significant reconstruction errors, which

should be avoided. This may cause the weight estimates $\hat{W}_{ip}$ stay away from the actual weights W_{ip}. Nevertheless, the system errors regulate asymptotically and the weight estimation errors $\tilde{W}_{ip}$ are bounded as shown in Theorem 2.

Lemma 3: The following are equivalent $\sum_{p=1}^{n}\sum_{s=1}^{p} a_s = \sum_{p=1}^{n}\sum_{s=p}^{n} a_p$ where a_i (i is an integer) is an arbitrary real number and *n*, *p* and *s* are integers.

Proof. See Appendix. ■

The main result of this section is introduced next.

Theorem 2: *Consider the nonlinear interconnected system given by (1). Consider the Assumptions 1-3 hold and let the unknown nonlinearities in the subsystems and interconnection terms be approximated by NNs. Let the NN weight update be provided by (16), then there exist a set of control gains* K_{ip} *and filter time constants,* τ_{ip} *,associated with the given control inputs such that the states* z_{ip} *and* y_{ip} *approach to zero asymptotically (local) for all* $1 \le i \le N$ *and* $1 \le p \le n$.

Outline of the proof. Since the DSC approach involves two error systems as described earlier (i.e. z_{ip} and y_{ip} for $1 \le i \le N$ and $1 \le p \le \mathrm{n}$) the proof is divided into two parts. In the first part, we proceed by defining a positive definite Lyapunov function $\mathbf{V}_{ip} = \int_0^{z_{ip}} \frac{\sigma}{g_{ip}(X_{i,p-1}, \sigma + x_{ipd})} d\sigma$ [14] in the compact set defined by $\Omega = \left\{ z_{ip}, y_{ip} \middle| \mathbf{W_1}(Z,Y) = \frac{1}{4}\sum_{i=1}^{N}\sum_{p=1}^{n}\left(\mathbf{V}_{ip} + y_{ip}^2\right) \le \mu; 1 \le i \le N, 1 \le p \le \mathrm{n}, \right\}$ where $X_{i0} = 0$. Then, by expanding the involved terms in the derivative of the Lyapunov function candidate and employing

Assumption 1 through 3 and Lemma 1, we factorize z_{ip}^2 terms for $1 \le i \le N$ and $1 \le p \le n$ in all the involved terms. Next, the unknown terms in the Lyapunov first derivative is approximated by employing the NNs in the desired virtual control as $\bar{x}_{i,p+1} = z_{pi}\hat{W}_{ip}^T \phi_{ip}(\Pi_{ip}) - K_{ip} z_{pi} + \dot{x}_{ipd}$ for $1 \le i \le N$ and $1 \le p \le n$ where $\dot{x}_{ipd} = -y_{ip}/\tau_{ip}$ from (12) and the NN output, $\hat{W}_{ip}^T \phi_{ip}(\Pi_{ip})$, approximates the nonlinear function $\Phi(\Pi_{ip}) = W_{ip}^T \phi_{ip}(\Pi_{ip}) + \varepsilon_{ip}$ which is introduced in the proof of Theorem 2 and the functional reconstruction errors are bounded above $|\varepsilon_{ip}| \le \varepsilon_{ip}^M$. By using this approach we are able to obtain quadratic terms z_{ip}^2 and y_{ip}^2 even when dealing with the NN approximation errors. Then, all the quadratic terms can be overcome by a negative quadratic stabilizing term, which can be designed adequately by choosing a proper design gain K_{ip} and filter time constant τ_{ip}.

Next, we elaborate on the second error system y_{ip} (for $1 \le i \le N$ and $2 \le p \le n$). By defining a quadratic Lyapunov function candidate $\mathbf{L}_{ip} = y_{ip}^2/2$ for $1 \le i \le N$ and $1 \le p \le n$ ($y_{i1} = 0$ as defined earlier), expanding its first derivative, and employing Lemma 2, the resulting terms in the first derivative is converted into quadratic terms z_{ip}^2 and y_{ip}^2.

Finally, by adding a quadratic Lyapunov function for NN weight estimation errors $\mathbf{L}_{\mathbf{W},ip} = \frac{1}{2\rho_{ip}} \tilde{W}_{ip}^T \tilde{W}_{ip}$ defined in Theorem 1 (part b), obtaining its first derivative, and using the weight update law (16), we sum and reorganize all the resulting quadratic terms z_{ip}^2 and y_{ip}^2 for $1 \le i \le N$ and $1 \le p \le n$.

By summing the individual Lyapunov function candidates, an overall Lyapunov function candidate $\mathbf{L}_\mathbf{T} = \mathbf{L} + \mathbf{L}_\mathbf{W}$ will be obtained where $\mathbf{L} = \sum_{i=1}^{N} \sum_{p=1}^{n} \left(\mathbf{V}_{ip} + \mathbf{L}_{ip} \right)$ and

$\mathbf{L_W} = \sum_{i=1}^{N}\sum_{p=1}^{n}\frac{1}{2\rho_{ip}}\tilde{W}_{ip}^{T}\tilde{W}_{ip}$ is defined in Theorem 1. Then, the overall first derivative of the Lyapunov function is given by $\dot{\mathbf{L}}_{\mathbf{T}} \le \sum_{i=1}^{N}\sum_{p=1}^{n}\left(-\beta_{\mathbf{z},ip}z_{ip}^{2} - \beta_{\mathbf{y},ip}y_{ip}^{2}\right)$ which can be set negative in the compact set Ω by choosing design gains K_{ip} and filter time constants τ_{ip} for $1 \le i \le N$ and $1 \le p \le n$.

It is important to note that unlike other works in NN literature [4, 5, 6], the key to achieve the asymptotic stability despite the presence of approximation errors is to build the quadratic terms in the first derivative of the overall Lyapunov function by using the novel NN weight update law. This further implies that if the initial states are within the set Ω, then they will stay in the same set for $t \ge 0$ by using (Theorem 4.8 in [14]). Therefore $\dot{\mathbf{L}}_{\mathbf{T}} \le 0$ for all $t \ge 0$. Now by applying Barballat's Lemma [15] the states z_{ip} and y_{ip} are guaranteed to asymptotically converge to zero as time goes to infinity for all $1 \le i \le N$ and $1 \le p \le n$. ■

Remark 2: Theorem 2 proves asymptotic regulation for unknown nonlinear interconnected systems by relaxing the stringent matching condition. A similar procedure can be utilized to show asymptotic stability of unknown strict feedback nonlinear systems without interconnection terms.

IV. Output Feedback Control Design

In this section, we consider the DSC controller design using partial knowledge of subsystem states. In other words, only subsystem outputs (x_{i1} for all $1 \le i \le N$) are available.

A. Controller Design

In the previous sections for the control system (1), it is assumed that all subsystem states are available for controller design. This assumption may not be practical if only partial state measurements are available in the subsystem. Thus, in this section, we proceed with the DSC controller design with only the partial knowledge of subsystem states by employing the linear observer as

$$\begin{cases} \dot{\hat{x}}_{i1} = \bar{L}_{i1}\hat{x}_{i1} + \hat{x}_{i2} + \mu L_{i1}\tilde{x}_{i1} \\ \vdots \\ \dot{\hat{x}}_{ip} = \bar{L}_{ip}\hat{x}_{ip} + \hat{x}_{i,p+1} + \mu^{p} L_{ip}\tilde{x}_{i1} \\ \vdots \\ \dot{\hat{x}}_{in} = \bar{L}_{in}\hat{x}_{in} + u_i + \mu^{n} L_{in}\tilde{x}_{i1} \end{cases} \tag{17}$$

where $\hat{x}_{ip}$ is the estimated state for x_{ip}, with state estimation error defined as $\tilde{x}_{ip} = x_{ip} - \hat{x}_{ip}$, L_{ip} and $\bar{L}_{ip}$ are positive and negative design constants, respectively, for all $1 \le i \le N$ and $1 \le p \le n$ and $\mu \ge 1$ is a positive design constant. Next, define $\hat{\Pi}_{i1} = \hat{x}_{i1} = \hat{z}_{i1}$, $\hat{X}_{ip} = [\hat{x}_{i1}, \ldots, \hat{x}_{ip}]^T$, $\hat{\Pi}_{ip} = [\hat{X}_{ip}^T, \hat{z}_{ip}, y_{ip}]^T$, $\hat{z}_i = [\hat{z}_{i1}, \ldots, \hat{z}_{in}]^T$, where $\hat{z}_{ip}$ is defined as $\hat{z}_{ip} = \hat{x}_{ip} - x_{ipd}$, with x_{ipd} is the intermediate virtual input, and $\tilde{z}_i = [\tilde{z}_{i1}, \ldots, \tilde{z}_{in}]^T$ for all $1 \le i \le N$ and $1 \le p \le n$. Moreover, $\hat{\Pi}_{i0} = 0$ is defined.

Step 1: Define the errors as

$$\hat{z}_{i1} = \hat{x}_{i1} - x_{i1d};\ z_{i1} = x_{i1} - x_{i1d}, \tag{18}$$

and

$$y_{i1} = \bar{x}_{i1} = 0 \tag{19}$$

where x_{i1d} is the desired set point for regulation. For the stabilization problem, the desired values become $x_{i1d} = \dot{x}_{i1d} = 0$. In addition, the error dynamics can be written as

$$\dot{\hat{z}}_{i1} = \bar{L}_{i1}\hat{x}_{i1} + \hat{x}_{i2} + \mu L_{i1}\tilde{x}_{i1} \tag{20}$$

Step p ($2 \le p < n$): Define

$$\hat{z}_{ip} = \hat{x}_{ip} - x_{ipd};\ z_{ip} = x_{ip} - x_{ipd} \tag{21}$$

where x_{ipd} is the intermediate virtual input at step *p*. Now, inspired by the state feedback in section III design, it is desirable to redefine

$$\bar{x}_{i,p+1} = \hat{z}_{ip}\hat{W}_{ip}^T\phi_{ip}(\hat{\Pi}_{ip}) - K_{ip}\hat{z}_{pi} + \dot{x}_{ipd} \tag{22}$$

where $\bar{x}_{i,p+1}$ is the desired virtual input to make $z_{ip} \to 0$ as defined in (21) as $t \to \infty$ (for all $1 \le i \le N$ and $1 \le p < n$) with $\hat{W}_{ip}^T\phi_{ip}(\hat{\Pi}_{ip})$ being a NN nonlinear estimate of the unknown nonlinearity $\Phi_{ip}(\Pi_{ip}) = W_{ip}^T\phi_{ip}(\Pi_{ip}) + \varepsilon_{ip}$ described in the previous section. Note that in (22), $\hat{z}_{ip}$ is used instead of the measured state as in (18) since partial knowledge of states is available. Once the estimated state errors $\hat{z}_{ip}$ reach adequately close to the actual state errors z_{ip}, the NNs act the same way as in the state feedback design. The intermediate virtual input $x_{i,p+1,d}$ is obtained by passing the $\bar{x}_{i,p+1,d}$ through a first order filter consistent with the DSC literature [1] as

$$\tau_{i,p+1}\dot{x}_{i,p+1,d} + x_{i,p+1,d} = \bar{x}_{i,p+1}, \tag{23}$$

and thus, it yields

$$y_{i,p+1} = x_{i,p+1,d} - \bar{x}_{i,p+1}, \tag{24}$$

and

$$\dot{x}_{i,p+1,d} = -y_{i,p+1}/\tau_{i,p+1}, \tag{25}$$

Finally, the error dynamics can be written as

$$\dot{\hat{z}}_{ip} = \bar{L}_{ip}\hat{x}_{ip} + \hat{x}_{i,p+1} + \mu^p L_{ip}\tilde{x}_{i1} - \dot{x}_{ipd} \tag{26}$$

Step n.

In the last step, errors are defined as:

$$\begin{cases} \hat{z}_{in} = \hat{x}_{in} - x_{ind} \\ z_{in} = x_{in} - x_{ind} \\ \dot{\hat{z}}_{in} = \bar{L}_{in}\hat{x}_{in} + g_{in}(X_{in})u_i + \mu^n L_{in}\tilde{x}_{i1} - \dot{x}_{ind} \end{cases}$$

and

$$\bar{x}_{i,n+1} = u_i = \mu^n\left(-a_{i1}\hat{z}'_{i1} - \cdots - a_{in}\hat{z}'_{in} + \hat{z}'_{in}\hat{\Phi}^T_{in}(\hat{\Pi}_{in}) - K_{in}\hat{z}'_{in} - y'_{in}/\tau_{in}\right) \tag{27}$$

where $\hat{z}'_{ip} = \hat{z}_{ip}\big/\mu^{p-1}$ and $y'_{ip} = y_{ip}\big/\mu^{p-1}$ for all $1 \le i \le N$ and $1 \le p < n$. Also, due to the dependency of the NN approximator to the state estimates $\hat{z}_{ip}$ (as opposed to z_{ip} in state feedback control (18)), we redefine the NN weight estimate update with the measured states replaced with their estimates as

$$\dot{\hat{W}}_{ip} = -\rho_{ip}\hat{z}^2_{ip}\phi_{ip}(\hat{\Pi}_{ip}) - \rho_{ip}\hat{z}^2_{ip}\hat{W}_{ip} + \rho_{ip}\hat{z}^2_{ip}\chi\frac{\hat{W}_{ip}\hat{W}^T_{ip}}{\left\|\hat{W}_{ip}\right\|^2}\phi_{ip}(\hat{\Pi}_{ip}) \tag{28}$$

where

$$\chi = \begin{cases} 0 & if \quad \left\|\hat{W}_{ip}\right\| < W^M_{ip} \quad or \quad \left\|\hat{W}_{ip}\right\| = W^M_{ip} \;\&\; \hat{W}^T_{ip}\hat{z}^2_{ip}\phi_{ip}(\hat{\Pi}_{ip}) \ge 0 \\ 1 & if \quad \left\|\hat{W}_{ip}\right\| = W^M_{ip} \;\&\; \hat{W}^T_{ip}\hat{z}^2_{ip}\phi_{ip}(\hat{\Pi}_{ip}) < 0 \\ 1 & if \quad \left\|\hat{W}_{ip}\right\| > W^M_{ip} \end{cases}$$

for all $1 \le i \le N$ and $1 \le p \le n$. Next, we discuss the interconnected system stability.

B. Stability Analysis

Here we introduce the Lemmas 3 and 4 which are output feedback equivalents of Lemmas 1 and 2.

Lemma 4: The intermediate and desired virtual inputs as well as the subsystem *p* error in the states $\bar{x}_{i,p+1}, x_{i,p+1,d}, \hat{x}_{i,p+1}$ for the decentralized system (1) for $1 \le i \le N$ and $1 \le p \le n-1$ satisfy the following inequalities defined by

$$\left|\bar{x}_{i,p+1}\right| \le \left(e_{ip} + K_{ip}\right)\left|\hat{z}_{ip}\right| + \left|y_{ip}\right| / \tau_{ip}$$

$$\left|x_{i,p+1,d}\right| \le \left(e_{ip} + K_{ip}\right)\left|\hat{z}_{ip}\right| + \left|y_{ip}\right| / \tau_{ip} + \left|y_{i,p+1}\right|, \qquad \left|\hat{x}_{i,p+1}\right| \le \left(e_{ip} + K_{ip}\right)\left|\hat{z}_{ip}\right| + \left|\hat{z}_{i,p+1}\right| + \left|y_{ip}\right| / \tau_{ip} + \left|y_{i,p+1}\right|,$$

and

$$\left|x_{i,p+1}\right| \le \left(e_{ip} + K_{ip}\right)\left|\hat{z}_{ip}\right| + \left|\hat{z}_{i,p+1}\right| + \left|y_{ip}\right| / \tau_{ip} + \left|y_{i,p+1}\right| + \left|\tilde{z}_{i,p+1}\right|$$

with e_{ip} being an appropriate positive constant.

Proof. See Appendix. ■

Lemma 5. The derivative of the desired virtual control inputs $\dot{\bar{x}}_{ip}$ in the decentralized system (1) with $1 \le i \le N$ and $2 \le p \le n$ satisfy the following inequality defined as

$$\left|\dot{\bar{x}}_{ip}\right| \le \sum_{s=1}^{p} \xi_{\mathbf{z},ips}(\hat{\Pi}_{i,p-1})\left|\hat{z}_{ip}\right| + \sum_{s=1}^{p} \xi_{\mathbf{y},ips}(\hat{\Pi}_{i,p-1})\left|y_{ip}\right| + \mu^{p-1}\xi_{\tilde{\mathbf{z}},ip}(\hat{\Pi}_{i,p-1})\left|\tilde{z}_{i1}\right| \quad \text{with} \quad \xi_{\mathbf{z},ips}, \quad \xi_{\mathbf{y},ips}, \quad \text{and}$$

$\xi_{\tilde{\mathbf{z}},ips}$ being appropriate positive functions of states estimates and errors.

Proof. See Appendix. ■

The main result of DSC with output feedback controller design is introduced following this assumption.

Assumption 4*:* The control gain coefficient $g_{in}(X_{in}) = 1$ for $1 \le i \le N$ is assumed. In other words, the last state of each subsystem dynamics where the control input comes in has a unity control gain coefficient.

Remark 3. Note that in each subsystem all the control gains except the last one are assumed to be functions of the states in contrast with [7] and [9].

The main result of section IV is introduced next.

Theorem 3: *Consider the nonlinear interconnected system given by (1). Consider the Assumptions 1-4 hold and let the unknown nonlinearities in the subsystems and interconnection terms be approximated by NNs. Let the NN weight update be provided by (28) and the subsystem states estimated by the observer (17), then there exist design control gains* K_{ip} *and* a_{ip}*, filter time constants* τ_{ip}*, observer gains* $\bar{L}_{ip}$, L_{ip}*, and constant* μ *,associated with the given control inputs such that the states* z_{ip}, y_{ip}, *and* $\hat{z}_{ip}$ *approach to zero asymptotically for all* $1 \le i \le N$ *and* $1 \le p \le n$.

Outline of the proof. Here the approach involves three error systems due to the presence of observer states, i.e. $\tilde{z}_{ip}$, $\hat{z}_{ip}$ and y_{ip} for $1 \le i \le N$ and $1 \le p \le n$ where $\tilde{z}_{ip} = z_{ip} - \hat{z}_{ip}$. We proceed by defining a positive definite Lyapunov function $\sum_{i=1}^{N}\left(\|P_{\mathbf{x}i}\|^2 \mathbf{L}_{\tilde{\mathbf{x}}i} + \mathbf{L}_{\mathbf{x}i} + \sum_{p=1}^{n}\left(\mathbf{L}_{ip} + \mathbf{L}_{\mathbf{W}ip}\right)\right)$ where $\mathbf{L}_{\tilde{\mathbf{x}}i} = \tilde{z}_i'^T P_{\tilde{\mathbf{x}}i} \tilde{z}_i'$, $\mathbf{L}_{\mathbf{x}i} = \hat{z}_i'^T P_{\hat{\mathbf{x}}i} \hat{z}_i'$, $\mathbf{L}_{ip} = y_{ip}'^2 / 2$, and $\mathbf{L}_{\mathbf{W}ip} = \frac{1}{2\rho_{ip}} \tilde{W}_{ip}^T \tilde{W}_{ip}$ with $\hat{z}_{ip}' = \hat{z}_{ip} / \mu^{p-1}$, $\tilde{z}_{ip}' = \tilde{z}_{ip} / \mu^{p-1}$, $y_{ip}' = y_{ip} / \mu^{p-1}$ and with $P_{\hat{\mathbf{x}}i}$, ρ_{ip} being constants in the compact set defined by $\hat{\Omega} = \left\{ \tilde{z}_{ip}, \hat{z}_{ip}, y_{ip} \middle| \mathbf{W_1} = \frac{1}{4}\sum_{i=1}^{N}\sum_{p=1}^{n}\left(\tilde{z}_{ip}^{\ 2} + \hat{z}_{ip}^{\ 2} + y_{ip}^{\ 2}\right) \le \bar{\delta}; 1 \le i \le N, 1 \le p \le n \right\}$ where $X_{i0} = 0$,. When L_{ip} and a_{ip} are appropriately chosen an appropriate μ and sufficiently small τ_{ip} make $\dot{\mathbf{L}}$ negative semi definite (lacking NN weights errors) in the compact set $\hat{\Omega}$ for $1 \le i \le N$ and $1 \le p \le n$. The sufficient conditions are summarized in the proof in Appendix. This further implies that if the initial states are within the set $\hat{\Omega}$, then they will stay in the same

set for $t \geq 0$ by using [14 and Theorem 4.8)]. Consequently, $\dot{\mathbf{L}} < 0$ for $t \geq 0$ and by applying Barballat's Lemma [15] the states the states $\tilde{z}_{ip}$, $\hat{z}_{ip}$, and y_{ip} asymptotically converge to zero while the states $\tilde{W}_{ip}$ remain bounded for all $1 \leq i \leq N$ and $1 \leq p \leq n$. ■

V. Simulation Results

Two examples are considered for verifying the proposed controllers.

Example 1 (Decentralized State Feedback Control): Consider a four subsystem-based interconnected nonlinear system (29) whose dynamics are given by

$$\begin{cases} \dot{x}_{11} = x_{11}^2 + \sin(x_{11}) + \left(2 + x_{11}^2 + \cos(x_{11})\right)x_{12} + 2x_{21}^2 + x_{31}^2 + x_{41}^2 \\ \dot{x}_{12} = x_{11}^3 + \sin(x_{11} + x_{12}^2) + \left(2 + x_{12}^2 + \cos(x_{12})\right)u_1 + 2(x_{21} + x_{22} + x_{31} + x_{41})^2 \end{cases}$$

$$\begin{cases} \dot{x}_{21} = x_{21} * \sin(x_{21}) + \left(2 + \cos^2(x_{21})\right)x_{22} + 2(x_{11} + x_{31},) \\ \dot{x}_{22} = \sin(x_{21}^2 + x_{22}^2) + \left(2 + (x_{21} * \cos(x_{22}))^2\right)u_2 + 2(x_{11} + x_{12} + x_{42}) \end{cases}$$

$$\begin{cases} \dot{x}_{31} = x_{31}^2 + \sin(x_{31}^2) + \left(2 + x_{31}^2 + \cos(x_{31})\right)x_{32} + 2x_{21}^2 + x_{41}^2 \\ \dot{x}_{32} = x_{31}^2 + \sin(x_{31}^2 + x_{32}^2) + \left(2 + x_{32}^2 + \cos(x_{32})\right)u_3 \\ \quad + 2(x_{21} + x_{22} + x_{32} + x_{42})^2 \end{cases}$$

$$\begin{cases} \dot{x}_{41} = x_{41}^2 + \sin(x_{41}) + \left(2 + x_{41}^2 + \cos(x_{41})\right)x_{42} + 2x_{21}^2 \\ \dot{x}_{42} = x_{41}^3 + \sin(x_{41} + x_{42}^2) + \left(2 + x_{42}^2 + \cos(x_{42})^2\right)u_4 \\ \quad + 2(x_{21} + x_{22} + x_{31}^2 + x_{32} + x_{41} + x_{42}); \end{cases} \tag{29}$$

The states of the system are initialized to $x_{11} = 1; x_{12} = 1.5$; $x_{21} = 1; x_{22} = 1$; $x_{31} = .5; x_{32} = .5$; $x_{41} = .5; x_{42} = .5$. The controller (18) for $1 \leq i \leq N$ and $1 \leq p \leq n$ along with the weight update law (16) is utilized with $\bar{x}_{i,n+1} = u_i$. The objective of the controller is to regulate the system states to zero.

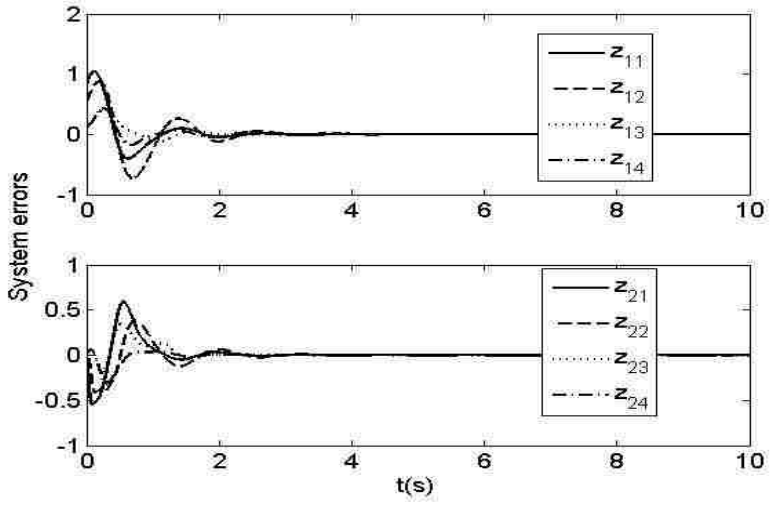

Fig.1 Interconnected system errors for state feedback NN controller

The design gains and filter time constants are taken as $K_{11} = K_{21} = K_{31} = K_{41} = 1$; $K_{12} = K_{22} = K_{32} = K_{42} = 7$; $\tau_{12} = \tau_{22} = \tau_{32} = \tau_{42} = 0.5$; $\rho_{13} = \rho_{23} = \rho_{33} = \rho_{43} = 100$. The satisfactory performance of the controller is depicted in Fig. 1 where the state errors eventually converge to zero. Fig. 2 illustrates the NN control inputs. The control inputs converge to zero while the NN approximation error is bounded. Also, Fig. 3 shows the selected NN weights. These results are as expected according to Theorem 2 where the system errors go to zero asymptotically while the NN weights stay bounded.

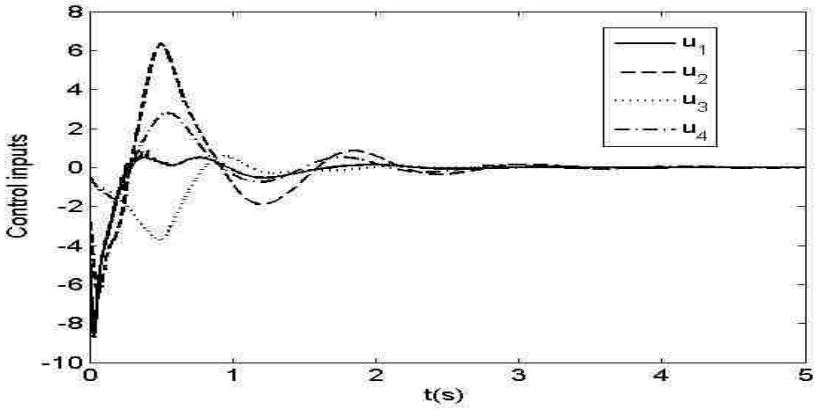

Fig.2 State feedback NN control inputs

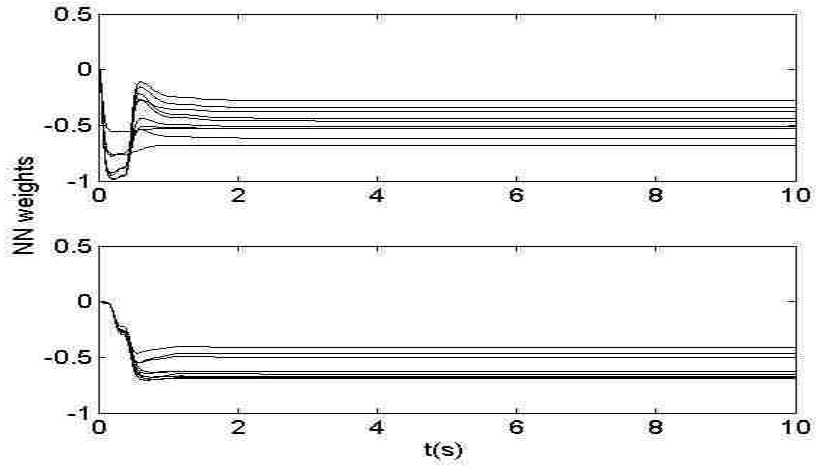

Fig.3 NN weights stability for state feedback controller

Example 2 (Decentralized output Feedback Control): The system in Example 1 is chosen. The objective of the controller is to regulate the system states to zero. The controller (27) for $1 \le i \le N$ and $1 \le p \le n$ along with the observer (17) and the weight update law (28) is utilized with $\bar{x}_{i,n+1} = u_i$. The design gains and filter time constants are given as

$K_{11} = K_{21} = K_{31} = K_{41} = 1$; $K_{12} = K_{22} = K_{32} = K_{42} = 7$; $\tau_{12} = \tau_{22} = \tau_{32} = \tau_{42} = 0.01$;

$\rho_{13} = \rho_{23} =$; $\rho_{33} = \rho_{43} = 100$ $L_{11} = L_{21} = L_{31} = L_{41} = 1$; $L_{12} = L_{22} = L_{32} = L_{42} = 1$; $\bar{L}_{11} = \bar{L}_{21} = \bar{L}_{31} = \bar{L}_{41} = 1$;

$\bar{L}_{12} = \bar{L}_{22} = \bar{L}_{32} = \bar{L}_{42} = 1$; $\mu = 1$; $a_{11} = a_{21} = a_{31} = a_{41} = 1352$; $a_{12} = a_{22} = a_{32} = a_{42} = 78$

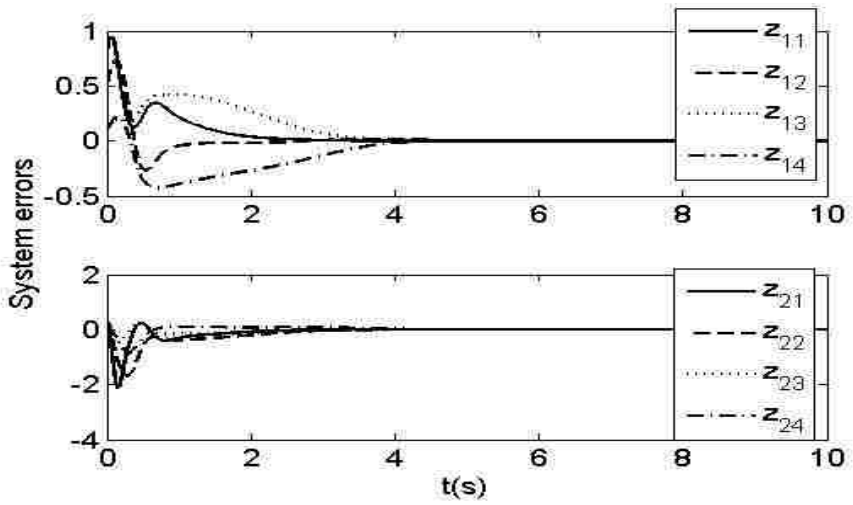

Fig.4 Interconnected system errors for output feedback NN controller

The satisfactory performance of the output feedback controller is depicted in Fig. 4 where the state errors eventually converge to zero even in the presence of observer. Figs. 5 and 6 illustrate the NN control inputs and state estimation errors, respectively, which converge. Moreover, the neural network weight estimations are depicted in Fig. 7. The control inputs converge to zero while the NN approximation attains stable.

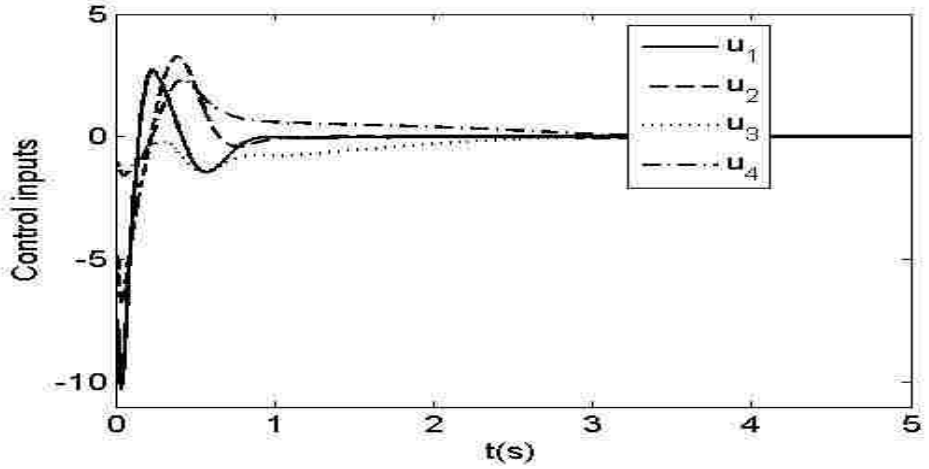

Fig.5 Output feedback NN control inputs

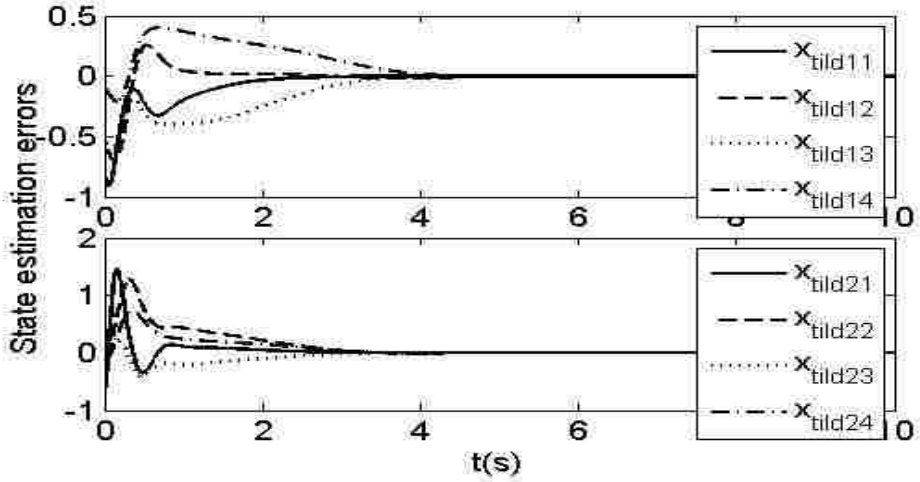

Fig.6 State estimation errors $\tilde{x}_{ip}$ for output feedback NN controller

VI. Conclusions

In this paper, the stability of a class of large-scale nonlinear interconnected system with uncertainties in both subsystem and the interconnection terms is introduced even when the system does not satisfy the matching condition. By using a variant of the

projection scheme and dynamic surface control with NNs, the need for the repeated differentiation in the backstepping design procedure was overcome. The neural network approximation property is used to approximate the nonlinearities of the subsystems and interconnected terms. It is shown that the closed loop system is asymptotically regulated to zero with both state and output feedback control even in the presence of NN function reconstruction errors using a novel NN weight update law. Separation principle is not needed for the output feedback design. Simulation results show the effectiveness of the approach.

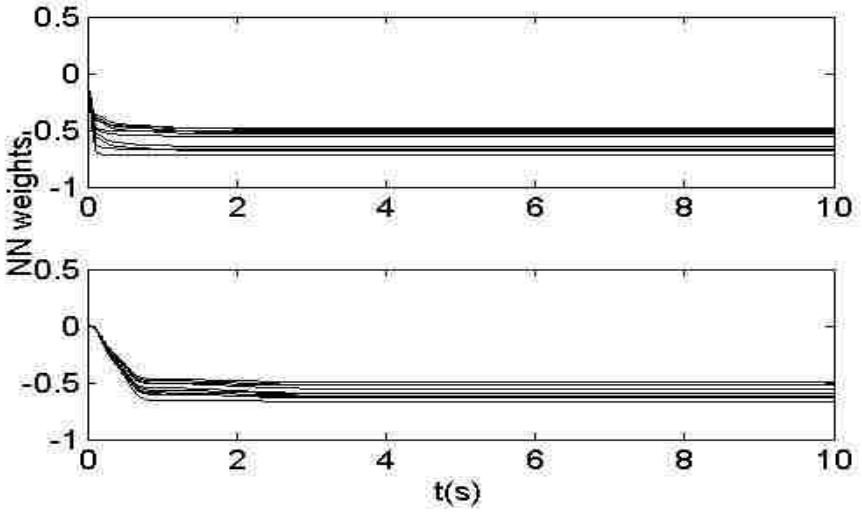

Fig.7 NN weights stability for output feedback NN controller

References

[1] D. Swaroop, J.K. Hedrick, P.P. Yip and J.C. Gerdes; "Dynamic surface control for a class of nonlinear systems," *IEEE Transactions on Automatic Control*, vol. 45, no. 10, pp. 1893 – 1899, Oct. 2000.

[2] P. P. Yip and J. K. Hedrick, "Adaptive dynamic surface control: A simplified algorithm for adaptive backstepping control of nonlinear systems," *Int. J. Control*, vol. 71, no. 5, pp. 959–979, 1998.

[3] D. Wang and J. Huang, "Neural network-based adaptive dynamic surface control for a class of uncertain nonlinear systems in strict-feedback form," *IEEE Transactions on Neural Networks*, vol. 16, no. 1, pp. 195 – 202, Jan. 2005.

[4] S.N. Huang, K.K. Tan, and T.H. Lee, "Nonlinear adaptive control of interconnected systems using neural networks," *IEEE Transactions on Neural Networks*, vol. 17, no. 1, pp. 243 - 246, Jan. 2006.

[5] W. Liu, S. Jagannathan, D.C. Wunsch, and M.L. Crow, "Decentralized neural network control of a class of large-scale systems with unknown interconnections," *proceeding of IEEE Conference on Decision and Control(CDC)*, vol. 5, pp. 4972 – 4977, 14-17 Dec. 2004.

[6] C. Wen, W. Wang, and J. Zhou, "Decentralized adaptive backstepping stabilization of nonlinear interconnected systems," *proceeding of Chinese Control and Decision Conference* (*CCDC)*, pp. 4111 – 4116, 2-4 July 2008.

[7] Z. Jiang, "Decentralized and adaptive nonlinear tracking of large-scale systems via output feedback," *IEEE Transactions on Automatic Control*, vol. 45, no. 11, pp.:2122 – 2128, Nov. 2000.

[8] X. Wang, X. Wang, J. Zhang, and Z. Cheng, "Decentralized output feedback semiglobal stabilization for a class of large-scale nonlinear systems," *The Sixth World Congress on Intelligent Control and Automation (WCICA 2006)*, pp:1232 – 1236, 2006.

[9] P. R. Pagilla and Y. Zhu, "A decentralized output feedback controller for a class of large-scale interconnected nonlinear systems," *ASME J. Dynam. Syst., Meas., Control*, vol. 127, pp. 167–172, 2005.

[10] B. Igelnik and Y. H. Pao, "Stochastic choice of basis functions in adaptive function approximation and the functional-link net," *IEEE Trans. Neural Network*, vol. 6, no. 6, pp. 1320–1329, Nov. 1995.

[11] P.K. Sahoo and T. Riedel, *Mean Value Theorems and Functional Equations*, World Scientific Publishing Co., 1998.

[12] K.S. Narendra and A.M. Annaswamy, *Stable Adaptive Systems*, Dover Publications. 2005.

[13] T. Zhang, S. S. Ge, and C. C. Hang, "Stable adaptive control for a class of nonlinear systems using a modified Lyapunov function," *IEEE Trans. Automatic. Control*, vol. 45, no. 1, pp. 129–132, 2000.

[14] H.K. Khalil, *Nonlinear Systems*, Prentice Hall, New Jersey, 2002.

[15] F. Lewis, S. Jagannathan, S., A. Yesildirek, *Neural Network Control of Robot. Manipulators and Nonlinear Systems*, Taylor & Francis, 1998.

Appendix

Proof of Theorem 1: (a) Define the Lyapunov function $L_{W,ip} = (1/2)\hat{W}_{ip}^T\hat{W}_{ip}$. The first derivative of the Lyapunov function after the substitution of the NN weight update law (16) is given by $\dot{L}_{W,ip} = -\rho_{ip} z_{ip}^2 \hat{W}_{ip}^T \phi_{ip}(\Pi_{ip}) - \rho_{ip} z_{ip}^2 \hat{W}_{ip}^T \hat{W}_{ip} + \rho_{ip} z_{ip}^2 \chi \hat{W}_{ip}^T \phi_{ip}(\Pi_{ip}) \le 0$. Since $\dot{L}_{W,ip} \le 0$, $\|\hat{W}_{ip}\|$ remains bounded such that $\|\hat{W}_{ip}\| \le W_{ip}^M \quad \forall t \ge 0$. (b) Define the Lyapunov function $\mathbf{L_W} = \sum_{i=1}^{N}\sum_{p=1}^{n}(1/2\rho_{ip})\tilde{W}_{ip}^T\tilde{W}_{ip}$. By differentiating $\mathbf{L_W}$, using update law (16), and noting that

$z_{ip}^2 \chi\left(\hat{W}_{ip}\hat{W}_{ip}^T / \|\hat{W}_{ip}\|^2\right)\phi_{ip}(\Pi_{ip}) - z_{ip}^2\hat{W}_{ip} \le z_{ip}^2\left(\max_{\Omega}\|\phi_{ip}\| + W_{ip}^M\right)$, we have

$$\dot{\mathbf{L}}_{\mathbf{W}} = \sum_{i=1}^{N}\sum_{p=1}^{n}\frac{1}{\rho_{ip}}\tilde{W}_{ip}^T\dot{\hat{W}}_{ip} \le \sum_{i=1}^{N}\sum_{p=1}^{n}\begin{pmatrix} -z_{ip}^2\tilde{W}_{ip}^T\phi_{ip}(\Pi_{ip}) \\ + z_{ip}^2\left[\|(W_{ip}^T - \hat{W}_{ip}^T)\|\left(\max_{\Omega}\|\phi_{ip}\| + W_{ip}^M\right)\right]\end{pmatrix}$$

$$\le \sum_{i=1}^{N}\sum_{p=1}^{n}\left(-z_{ip}^2\tilde{W}_{ip}^T\phi_{ip}(\Pi_{ip}) + z_{ip}^2\eta_{ip}^M\right) \qquad \text{(A-1)}$$

where $\eta_{ip}^M = \left(\|W_{ip}\| + W_{ip}^M\right)\left(\max_{\Omega}\|\phi_{ip}\| + W_{ip}^M\right)$. Using (A-1), it can be inferred that the weight

estimation errors are bounded such that $\left\|\tilde{W}_{ip}\right\| > \eta_{ip}^{M} / \left\|\phi_{ip}(.)\right\|$. This upper bound is a function of user selected bound for the NN weights and an upper bound on the target NN weights.

Proof of Lemma 1: *Step 1.*From (3) we have

$$\bar{x}_{i2} = z_{i1}\hat{W}_{i1}^{T}\phi_{i1}(\Pi_{i1}) - K_{i1}z_{i1}$$

Consider the set Ω being the same as the compact set over which the neural network approximation property applies and by using (16) and (A-1) it is assured that there is a maximum for the states $\tilde{W}_{i1}^{T}$ and for $\hat{W}_{i1}^{T}$ as well in Ω. Also, note that we can assume $\left|\hat{W}_{i1}^{T}\phi_{i1}(\Pi_{i1})\right|_{\infty} \le W_{i1}^{M}\left|\phi_{i1}(\Pi_{i1})\right|_{\infty} = e_{i1}$ by using a proper NN activation function. Hence, the following steps can be concluded.

Step 1,

$$|\bar{x}_{i2}| \le (e_{i1} + K_{i1})|z_{i1}| \tag{A-2}$$

Then, from (5) and (6) we have

$$|x_{i2d}| \le (e_{i1} + K_{i1})|z_{i1}| + |y_{i2}| \tag{A-3}$$

and

$$|x_{i2}| \le (e_{i1} + K_{i1})|z_{i1}| + |z_{i2}| + |y_{i2}| \tag{A-4}$$

Step $(2 \le p \le n-1)$

From (9) and by setting $\hat{\Phi}_{i1}(\Pi_{i1}) = \hat{W}_{i1}^{T}\phi_{i1}(\Pi_{i1})$ we have $\bar{x}_{i,p+1} = z_{ip}\hat{W}_{ip}^{T}\phi_{ip}(\Pi_{ip}) - K_{ip}z_{ip} - \dfrac{y_{ip}}{\tau_{ip}}$

Noting that $\left|\hat{W}_{ip}^{T}\phi_{ip}(\Pi_{ip})\right|_{\infty} \le W_{ip}^{M} \max_{\Omega}\left\|\phi_{ip}(\Pi_{ip})\right\| = e_{ip}$, it yields

$$\left|\bar{x}_{i,p+1}\right| \le \left(e_{ip} + K_{ip}\right)\left|z_{ip}\right| + \left|y_{ip}\right|/\tau_{ip} \tag{A-5}$$

Consequently, from (11) and (A-5)

$$\left|x_{i,p+1,d}\right| \le \left(e_{ip} + K_{ip}\right)\left|z_{ip}\right| + \left|y_{ip}\right|/\tau_{ip} + \left|y_{i,p+1}\right| \tag{A-6}$$

and

$$\left|x_{i,p+1}\right| \le \left(e_{ip} + K_{ip}\right)\left|z_{ip}\right| + \left|z_{i,p+1}\right| + \left|y_{ip}\right|/\tau_{ip} + \left|y_{i,p+1}\right| \tag{A-7}$$

Proof of Lemma 2: *Step 1*. From (2), (6), and (7) we have

$$\dot{z}_{i1} = f_{i1}(z_{i1}) + \Delta_{i1}(\bar{X}_p) + g_{i1}(z_{i1})(z_{i2} + y_2 + \bar{x}_2)$$

Thus, by using Assumption 3 and $x_{i1} = z_{i1}$ we have

$$|\dot{z}_{i1}| \le |\upsilon_{i11}(z_{i1})||z_{i1}| + \sum_{j=1}^{N}\left(\left|z_{j1}\right|\right)\bar{\delta}_{i1,j1}(X_{j1})| + |g_{i1}(X_{i1})|\left(|z_{i2}| + |y_{i2}| + |\bar{x}_{i2}|\right) \tag{A-8}$$

From (3) and $\hat{\Phi}_{i1}(\Pi_{i1}) = \hat{W}_{i1}^T\phi_{i1}(\Pi_{i1})$ we have

$$\bar{x}_{i2} = z_{i1}\hat{W}_{i1}^T\phi_{i1}(\Pi_{i1}) - K_{i1}z_{i1}$$

Thus,

$$\left|\dot{\bar{x}}_{i2}\right| \le \left\|\dot{\hat{W}}_{i1}\right\| \max_{\Omega}\|\phi_{i1}(\Pi_{i1})\|.|z_{i1}| + A_{i1}(\Pi_{i1})|\dot{z}_{i1}| \tag{A-9}$$

where $A_{i1}(\Pi_{i1}) = \left(W_{i1}^M \max_{\Omega}\|\partial\phi_{i1}/\partial z_{i1}\|.|z_{i1}| + W_{i1}^M \max_{\Omega}\|\phi_{i1}(\Pi_{i1})\| + K_{i1}\right)$.

Using the weight update laws (16), we have

$$\dot{\hat{W}}_{ip} = -\rho_{ip}z_{ip}^2\phi_{ip}(\Pi_{ip}) - \rho_{ip}z_{ip}^2\hat{W}_{ip} + \chi\frac{\hat{W}_{ip}\hat{W}_{ip}^T}{\left\|\hat{W}_{ip}\right\|^2}z_{ip}^2\phi_{ip}(\Pi_{ip})$$

This in turn yields

$$\left\|\dot{\hat{W}}_{ip}\right\| \le \rho_{ip}z_{ip}^2\left(2\max_{\Omega}\left\|\phi_{ip}(\Pi_{ip})\right\| + W_{ip}^M\right) \tag{A-10}$$

for $1 \le i \le N$ and $1 \le p \le n$. Therefore, using (A-9) and employing (A-2), (A-8), and (A-10) for $p = 1$, it yields

$$\begin{aligned}&\left|\dot{\bar{x}}_{i2}\right| \le \xi_{\mathbf{z},i21}(\Pi_{i1})|z_{i1}| + \xi_{\mathbf{z},i22}(\Pi_{i1})|z_{i2}| + \xi_{\mathbf{y},i22}(\Pi_{i1})|y_{i2}| \\ &+\left(\sum_{j=1}^{N} A_{i1}|z_{j1}|\bar{\delta}_{i1,j1}(X_{j1})\right)\end{aligned} \tag{A-11}$$

where

$$\begin{aligned}&\xi_{\mathbf{z},i21}(\Pi_{i1}) = \rho_{ip} z_{ip}^2\left(2\max_{\Omega}\left\|\phi_{ip}(\Pi_{ip})\right\| + W_{ip}^{M}\right).\max_{\Omega}\left\|\phi_{ip}(\Pi_{ip})\right\| \\ &+ A_{i1}\left(\left|\upsilon_{i11}(z_{i1})\right| + \left|g_{i1}(X_{i1})\right|\left(e_{i1} + K_{i1}\right)\right) \\ &\xi_{\mathbf{z},i22}(\Pi_{i1}) = A_{i1}\left|g_{i1}(X_{i1})\right| \\ &\xi_{\mathbf{y},i22}(\Pi_{i1}) = A_{i1}\left|g_{i1}(X_{i1})\right|\end{aligned}$$

Note that $\left|\dot{\bar{x}}_{i2}\right|$ is a function of K_{i1}. Also,

$$\begin{aligned}&|\dot{y}_{i2}| = \left|\dot{x}_{i2d} - \dot{\bar{x}}_{i2}\right| \le \frac{|y_{i2}|}{\tau_{i2}} + \left|\dot{\bar{x}}_{i2}\right| \\ &\le \xi_{\mathbf{z},i21}(\Pi_{i1})|z_{i1}| + \xi_{\mathbf{z},i22}(\Pi_{i1})|z_{i2}| + \xi_{\mathbf{y},i22}(\Pi_{i1})|y_{i2}| \\ &+\left(\sum_{j=1}^{N} A_{i1}|z_{j1}|\bar{\delta}_{i1,j1}(X_{j1})\right) + |y_{i2}|/\tau_{i2}\end{aligned} \tag{A-12}$$

Step 2: From (2), (14), and (12) we have

$$\dot{z}_{i2} = f_{i2}(X_{i2}) + \sum_{j=1}^{N}\sum_{q=1}^{2}\left|x_{jq}\right|\bar{\delta}_{i2,jq}(X_{jq}) + g_{i2}(X_{i2})x_{i3} + y_{i2}/\tau_{i2}$$

Thus, by using Assumption 1 and Lemma 1 we have

$$\begin{aligned}&|\dot{z}_{i2}| \le \bar{\upsilon}_{\mathrm{Z},i21}|z_{i1}| + \bar{\upsilon}_{\mathrm{Z},i22}|z_{i2}| + \left(\bar{\upsilon}_{\mathrm{Y},i22} + 1/\tau_{i2}\right)|y_{i2}| + \sum_{j=1}^{N}\sum_{q=1}^{2}\left|x_{jq}\right|\bar{\delta}_{i2,jq}(X_{jq})| \\ &+ |g_{i2}(X_{i2})\|x_{i3}| \le \bar{\upsilon}_{\mathrm{Z},i21}|z_{i1}| + \bar{\upsilon}_{\mathrm{Z},i22}|z_{i2}| + \left(\bar{\upsilon}_{\mathrm{Y},i22} + 1/\tau_{i2}\right)|y_{i2}| \\ &+ \sum_{j=1}^{N}\sum_{q=1}^{2}\left(a_{jq}|z_{jq}| + |y_{jq}|\right)\bar{\delta}_{i2,jq}(X_{jq})| + |g_{i2}(X_{i2})|\left(|z_{i3}| + |y_{i3}| + |\bar{x}_{i3}|\right)\end{aligned} \tag{A-13}$$

where $\bar{\upsilon}_{\mathrm{Z},i21}$, $\bar{\upsilon}_{\mathrm{Z},i22}$, and $\bar{\upsilon}_{\mathrm{Y},i21}$ are appropriate positive functions of the states and a_{jq} is an appropriate positive constant. From (9), (12), and $\hat{\Phi}_{i2}(\Pi_{i2}) = \hat{W}_{i2}^{T}\phi_{i2}(\Pi_{i2})$ we have $\bar{x}_{i3} = z_{i2}\hat{W}_{i2}^{T}\phi_{i2}(\Pi_{i2}) - K_{i2}z_{i2} - y_{i2}/\tau_{i2}$; thus,

$$\left|\dot{\bar{x}}_{i3}\right| \le \left\|\hat{\dot{W}}_{i2}\right\|\max_{\Omega}\left\|\phi_{i2}(\Pi_{i2})\right\|.|z_{i2}| + A_{\mathbf{z},i21}|\dot{z}_{i1}| + A_{\mathbf{z},i22}|\dot{z}_{i2}| + A_{\mathbf{y},i22}|\dot{y}_{i2}| \tag{A-14}$$

where

$$A_{\mathbf{z},i21}(\Pi_{i2}) = W_{i2}^{M}\max_{\Omega}\|\partial\phi_{i2}/\partial z_{i1}\|\|z_{i2}|; A_{\mathbf{y},i22}(\Pi_{i2}) = W_{i2}^{M}\max_{\Omega}\|\partial\phi_{i2}/\partial y_{i2}\|\|z_{i2}| + 1/\tau_{i2}$$
$$A_{\mathbf{z},i22}(\Pi_{i2}) = W_{i2}^{M}\max_{\Omega}\|\partial\phi_{i2}/\partial z_{i2}\|\|z_{i2}| + W_{i2}^{M}\max_{\Omega}\|\phi_{i1}(\Pi_{i1})\| + K_{i2}$$

According to (A-10), we have

$$\left\|\dot{\hat{W}}_{i2}\right\| \le \rho_{i2}z_{i2}^{2}\left(2\max_{\Omega}\left\|\phi_{i2}(\Pi_{ip})\right\| + W_{i2}^{M}\right) \quad . \tag{A-15}$$

By using (A-8) and (A-13) we conclude that the terms $|\dot{z}_{i1}|$ and $|\dot{z}_{i2}|$ can be over bounded by terms bearing $|z_{i1}|$, $|z_{i2}|$, $|z_{i3}|$, $|y_{i2}|$, $|y_{i3}|$, and the interconnection terms as cofactors. Thus, by following a similar procedure to what we used in *Step 1* (A-14) may be rewritten as

$$\begin{aligned}
&\left|\dot{\bar{x}}_{i3}\right| \le \xi_{\mathbf{z},i31}(\Pi_{i2})|z_{i1}| + \xi_{\mathbf{z},i32}(\Pi_{i2})|z_{i2}| + \xi_{\mathbf{z},i33}(\Pi_{i2})|z_{i3}| \\
&+ \xi_{\mathbf{y},i32}(\Pi_{i2})|y_{i2}| + \xi_{\mathbf{y},i33}(\Pi_{i2})|y_{i3}| \\
&+ \left(A_{\mathbf{z},i21}(\Pi_{i2}) + A_{\mathbf{y},i22}(\Pi_{i2})\right)\sum_{j=1}^{N}A_{i1}|z_{j1}|\left\|\bar{\delta}_{i1,j1}(X_{j1})\right| \\
&+ A_{\mathbf{z},i22}(\Pi_{i2})\sum_{j=1}^{N}\sum_{q=1}^{2}\left(a_{jq}|z_{jq}| + |y_{jq}|\right)\left|\bar{\delta}_{i2,jq}(X_{jq})\right| \\
&\le \xi_{\mathbf{z},i31}(\Pi_{i2})|z_{i1}| + \xi_{\mathbf{z},i32}(\Pi_{i2})|z_{i2}| + \xi_{\mathbf{z},i33}(\Pi_{i2})|z_{i3}| \\
&+ \xi_{\mathbf{y},i32}(\Pi_{i2})|y_{i2}| + \xi_{\mathbf{y},i33}(\Pi_{i2})|y_{i3}| \\
&+ \sum_{j=1}^{N}\sum_{q=1}^{2}\left(\xi_{\Delta\mathbf{z},i3,jq}(\Pi_{i2},X_{jq})|z_{jq}| + \xi_{\Delta\mathbf{y},i3,jq}(\Pi_{i2},X_{jq})|y_{jq}|\right)
\end{aligned}$$

Note that $\left|\dot{\bar{x}}_{i3}\right|$ is a function of $[K_{i1},K_{i2},\tau_{i1},\tau_{i2}]^{T}$.

Step p, $2 < p \le n-1$

By induction we obtain

$$\begin{aligned}
&\left|\dot{x}_{ip}\right| \le \xi_{\mathbf{z},ip1}(\Pi_{i,p-1})|z_{i1}| + \cdots + \xi_{\mathbf{z},ipp}(\Pi_{i,p-1})|z_{ip}| + \\
&\xi_{\mathbf{y},ip1}(\Pi_{i,p-1})|y_{i2}| + \cdots + \xi_{\mathbf{y},ipp}(\Pi_{i,p-1})|y_{ip}| + \\
&+ \sum_{j=1}^{N}\sum_{q=1}^{p-1}\begin{pmatrix}\xi_{\Delta\mathbf{z},ip,jq}(\Pi_{i,p-1},X_{jq})|z_{jq}| \\ + \xi_{\Delta\mathbf{y},ip,jq}(\Pi_{i,p-1},X_{jq})|y_{jq}|\end{pmatrix}
\end{aligned}$$

$$
\begin{aligned}
&= \sum_{s=1}^{p} \xi_{\mathbf{z},ips}(\Pi_{i,p-1})\left|z_{is}\right| + \sum_{s=1}^{p} \xi_{\mathbf{y},ips}(\Pi_{i,p-1})\left|y_{is}\right| \\
&+ \sum_{j=1}^{N}\sum_{q=1}^{p-1}\begin{pmatrix} \xi_{\Delta\mathbf{z},ip,jq}(\Pi_{i,p-1}, X_{jq})\left|z_{jq}\right| \\ + \xi_{\Delta\mathbf{y},ip,jq}(\Pi_{i,p-1}, X_{jq})\left|y_{jq}\right| \end{pmatrix}
\end{aligned}
\tag{A-16}
$$

Note that $\left|\dot{\bar{x}}_{ip}\right|$ is a function of $[K_{i1},\ldots,K_{i,p-1},\tau_{i1},\ldots,\tau_{i,p-1}]^T$.

Proof of Lemma 3.

$$
\sum_{p=1}^{n}\sum_{s=1}^{p} a_s = \begin{Bmatrix} a_1 + \\ a_1 + a_2 + \\ a_1 + a_2 + a_3 + \\ \vdots \qquad\qquad \ddots \\ a_1 + a_2 + a_3 + \cdots a_{n-1} + \\ a_1 + a_2 + a_3 + \cdots a_{n-1} + a_n \end{Bmatrix} = \sum_{p=1}^{n}\sum_{s=p}^{n} a_p
$$

Proof of Theorem 2: Since there are two error systems (i.e. z_{ip} and y_{ip} for $1 \le i \le N$ and $1 \le p \le n$) to be dealt with, here the proof is divided into two parts.

First error system (z_{ip}): Consider the Lyapunov function candidate $\mathbf{V}_{ip} = \int_0^{z_{ip}} \frac{\sigma}{g_{ip}(X_{i,p-1}, \sigma + x_{ipd})} d\sigma$ [13] in the compact set defined by $\Omega = \left\{ z_{ip}, y_{ip} \middle| \begin{matrix} 1 \le i \le N, 1 \le p \le \mathrm{n}, \\ \mathbf{W_1}(Z,Y) = \frac{1}{4}\sum_{i=1}^{N}\sum_{p=1}^{n}\left(\mathbf{V}_{ip} + y_{ip}^2\right) \le \mu \end{matrix} \right\}$ where $X_{i0} = 0$. In the remainder of this proof the first derivative, $\dot{\mathbf{V}}_{ip}$, inside the set Ω is evaluated. By differentiating $\mathbf{V}_{ip}$, the first derivative is given by

$$
\begin{aligned}
\dot{\mathbf{V}}_{ip} &= \frac{z_{ip}}{g_{ip}(X_{ip})}\dot{z}_{ip} + z_{ip}^2 \int_0^1 \alpha \sum_{k=1}^{p-1} \left\{ \begin{matrix} \frac{\partial}{\partial x_{ik}} \frac{1}{g_{ip}(X_{i,p-1}, z_{ip}\alpha + x_{ipd})} \times \\ \left(f_{ik}(X_{ik}) + g_{ik}(X_{ik})x_{i,k+1} + \Delta_{ik}(\bar{X}_k)\right) \end{matrix} \right\} d\alpha \\
&+ \frac{z_{ip}\dot{x}_{ipd}}{g_{ip}(X_{ip})} - z_{ip}\dot{x}_{ipd}\int_0^1 \frac{d\alpha}{g_{ip}(X_{i,p-1}, z_{ip}\alpha + x_{ipd})}
\end{aligned}
$$

where $\sum_{k=1}^{p-1} = 0$ when $p = 1$. By using (12), the first derivative is expressed as

$$\dot{\mathbf{V}}_{ip} \le \frac{z_{ip}}{g_{ip}(X_{ip})}\dot{z}_{ip} + z_{ip}^2 \sum_{k=1}^{p-1}\left\{\zeta_{ip,1k}(\Pi_{ip})\Delta_{ik}(\bar{X}_k)\right\} + \zeta_{2ip}(\Pi_{ip})z_{ip}^2 + \zeta_{3ip}(\Pi_{ip})z_{ip}^2 + y_{ip}^2 \tag{B-1}$$

where

$$\zeta_{ip,1k}(\Pi_{ip}) = \int_0^1 \alpha\left(\frac{\partial}{\partial x_{ik}}\frac{1}{g_{ip}(X_{i,p-1}, z_{ip}\alpha + x_{ipd})}\right)d\alpha \tag{B-2}$$

$$\zeta_{2ip}(\Pi_{ip}) = \sum_{k=1}^{p-1}\left(\zeta_{ip,1k}\right)\left(f_{ik}(X_{ik}) + g_{ik}(X_{ik})x_{i,k+1}\right) \tag{B-3}$$

and

$$\zeta_{3ip}(\Pi_{ip}) = \frac{1}{4}\left(\frac{1}{\tau_{ip}g_{ip}(X_{ip})}\right)^2 + \frac{1}{4}\left(\frac{1}{\tau_{ip}}\int_0^1 \frac{d\alpha}{g_{ip}(X_{i,p-1}, z_{ip}\alpha + x_{ipd})}\right)^2 \tag{B-4}$$

Employing $\dot{z}_{ip}$ from (13) and (14) and expanding the first term in (B-1) yields the resulting terms as follows. According to Assumption 3 and Lemma 1 we have

$$\begin{aligned}
&\frac{z_{ip}f_{ip}(X_{ip})}{g_{ip}(X_{ip})} = \frac{z_{ip}}{g_{ip}(X_{ip})}\sum_{s=1}^{p} x_{is}\upsilon_{ips}(X_{ip}) \\
&\le \sum_{s=1}^{p}\frac{|z_{ip}|}{g_{ip}(X_{ip})}|\upsilon_{ips}(X_{ip})|\left(\left(e_{i,s-1} + K_{i,s-1}\right)|z_{i,s-1}| + |z_{is}| + \frac{|y_{i,s-1}|}{\tau_{i,s-1}} + |y_{is}|\right) \\
&\le \frac{z_{ip}^2}{4g_{ip}^2(X_{ip})}\sum_{s=1}^{p}\left(\upsilon_{ips}(X_{ip})\right)^2\left(2 + \left(e_{i,s-1} + K_{i,s-1}\right)^2 + \frac{1}{\tau_{i,s-1}^2}\right) \\
&+ \sum_{s=1}^{p} z_{i,s-1}^2 + \sum_{s=1}^{p} z_{is}^2 + \sum_{s=1}^{p} y_{i,s-1}^2 + \sum_{s=1}^{p} y_{is}^2
\end{aligned} \tag{B-5}$$

Define

$$\zeta_{4ip}(\Pi_{ip}) = \frac{1}{4g_{ip}^2(X_{ip})}\sum_{s=1}^{p}\left(\upsilon_{ips}(X_{ip})\right)^2\left(2 + \left(e_{i,s-1} + K_{i,s-1}\right)^2 + \frac{1}{\tau_{i,s-1}^2}\right) \tag{B-6}$$

Next, by applying Assumption 1 and Lemma 1, the following term can be written as

$$\frac{z_{ip}\Delta_{ip}(\bar{X}_p)}{g_{ip}(X_{ip})} \le \sum_{j=1}^{N}\sum_{q=1}^{p}\frac{|z_{ip}|}{g_{ip}(X_{ip})}|x_{jq}|\bar{\delta}_{ip,jq}(X_{jq})$$
$$\le \sum_{j=1}^{N}\sum_{q=1}^{p}\left(\frac{|z_{ip}|}{g_{ip}(X_{ip})}\left(\begin{array}{l}\left(e_{j,q-1}+K_{j,q-1}\right)|z_{j,q-1}|+\\ |z_{jq}|+\dfrac{|y_{j,q-1}|}{\tau_{j,q-1}}+|y_{jq}|\end{array}\right)\bar{\delta}_{ip,jq}(X_{jq})\right)$$

$$\le z_{ip}^2\sum_{j=1}^{N}\sum_{q=1}^{p}\left(\frac{1}{4g_{ip}^2(X_{ip})}\left(\begin{array}{l}\left(e_{j,q-1}+K_{j,q-1}\right)^2+\\ \dfrac{1}{\tau_{j,q-1}^2}+2\end{array}\right)\left(\bar{\delta}_{ip,jq}^{M}\right)^2\right) \qquad \text{(B-7)}$$
$$+\sum_{j=1}^{N}\sum_{q=1}^{p}\left(z_{j,q-1}^2+z_{jq}^2+y_{j,q-1}^2+y_{jq}^2\right)$$

where $\bar{\delta}_{ip,jq}^{M}=\max_{X_{jq}\in\Omega}\left|\bar{\delta}_{ip,jq}(X_{jq})\right|$. Define

$$\zeta_{5ip}(\Pi_{ip})=\sum_{j=1}^{N}\sum_{q=1}^{p}\left(\frac{1}{4g_{ip}^2(X_{ip})}\left(\begin{array}{l}\left(e_{j,q-1}+K_{j,q-1}\right)^2+\\ 1/\tau_{j,q-1}^2+2\end{array}\right)\left(\bar{\delta}_{ip,jq}^{M}\right)^2\right) \qquad \text{(B-8)}$$

Finally, from (13) we have

$$\frac{z_{ip}}{g_{ip}(X_{ip})}\left(g_{ip}(X_{ip})x_{i,p+1}-\dot{x}_{ipd}\right) \qquad \text{(B-9)}$$
$$\le z_{ip}^2+z_{i,p+1}^2/2+y_{i,p+1}^2/2+z_{ip}\left(\bar{x}_{i,p+1}-\dot{x}_{ipd}/g_{ip}(X_{ip})\right)$$

Summarizing (B-5) through (B-9), the term on the left hand side of (B-10) can be expressed as

$$\frac{z_{ip}}{g_{ip}(X_{ip})}\dot{z}_{ip} \le z_{ip}^2\zeta_{4ip}(\Pi_{ip})+\sum_{s=1}^{p}\left(z_{i,s-1}^2+z_{is}^2+y_{i,s-1}^2+y_{is}^2\right)$$
$$+z_{ip}^2\zeta_{5ip}(\Pi_{ip})+\sum_{j=1}^{N}\sum_{q=1}^{p}\left(z_{j,q-1}^2+z_{jq}^2+y_{j,q-1}^2+y_{jq}^2\right) \qquad \text{(B-10)}$$
$$+z_{ip}^2+z_{i,p+1}^2/2+y_{i,p+1}^2/2+z_{ip}\bar{\bar{x}}_{i,p+1}$$

where

$$\bar{\bar{x}}_{i,p+1}=\bar{x}_{i,p+1}-\dot{x}_{ipd}/g_{ip}(X_{ip}).$$

Similar to (B-7), the second term in (B-1) can be expanded as follows.

$$\sum_{k=1}^{p-1} z_{ip}^2 \left|\zeta_{ip1k}(\Pi_{ip})\right\| \Delta_{ik}(\overline{X}_k)\left|\right.$$

$$\le z_{ip}^2 \sum_{k=1}^{p-1}\sum_{j=1}^{N}\sum_{q=1}^{k} \left|\zeta_{ip1k}(\Pi_{ip})\right\| x_{jq}\left|\overline{\delta}_{ik,jq}(X_{jq})\right.$$

$$\le z_{ip}^2 \sum_{k=1}^{p-1}\sum_{j=1}^{N}\sum_{q=1}^{k} \left|\zeta_{ip1k}(\Pi_{ip})\right\| \begin{pmatrix} \left(e_{j,q-1}+K_{j,q-1}\right)\left|z_{j,q-1}\right| + \\ \left|z_{jq}\right| + \left|y_{j,q-1}\right|/\tau_{j,q-1} + \left|y_{jq}\right| \end{pmatrix} \overline{\delta}_{ik,jq}(X_{jq})$$

$$\le (z_{ip}^4/4)\sum_{k=1}^{p-1}\sum_{j=1}^{N}\sum_{q=1}^{k}\left(\left(\zeta_{ip1k}(\Pi_{ip})\right)^2 \left(\overline{\delta}_{ik,jq}^{M}\right)^2 \left(\left(e_{j,q-1}+K_{j,q-1}\right)^2 + 1/\tau_{j,q-1}^2 + 2\right)\right)$$

$$+ \sum_{k=1}^{p-1}\sum_{j=1}^{N}\sum_{q=1}^{k}\left(z_{j,q-1}^2 + z_{jq}^2 + y_{j,q-1}^2 + y_{jq}^2\right) \tag{B-11}$$

Define

$$\zeta_{6ip}(\Pi_{ip}) = (z_{ip}^4/4)\sum_{k=1}^{p-1}\sum_{j=1}^{N}\sum_{q=1}^{k}\begin{pmatrix} \left(\zeta_{ip1k}(\Pi_{ip})\right)^2 \left(\overline{\delta}_{ik,jq}^{M}\right)^2 \times \\ \left(\left(e_{j,q-1}+K_{j,q-1}\right)^2 + 1/\tau_{j,q-1}^2 + 2\right) \end{pmatrix} \tag{B-12}$$

Using (B-11) and (B-12), we have

$$z_{ip}^2 \sum_{k=1}^{p-1}\left\{\zeta_{ip,1k}(\Pi_{ip})\Delta_{ik}(\overline{X}_k)\right\} \le$$
$$z_{ip}^2\zeta_{6ip}(\Pi_{ip}) + \sum_{k=1}^{p-1}\sum_{j=1}^{N}\sum_{q=1}^{k}\left(z_{j,q-1}^2 + z_{jq}^2 + y_{j,q-1}^2 + y_{jq}^2\right) \tag{B-13}$$

By using (B-1), (B-10) through (B-13), the first derivative is rewritten as

$$\dot{\mathbf{V}}_{ip} \le \begin{pmatrix} \zeta_{2ip}(\Pi_{ip}) + \zeta_{3ip}(\Pi_{ip}) + \zeta_{4ip}(\Pi_{ip}) \\ + \zeta_{5ip}(\Pi_{ip}) + \zeta_{6ip}(\Pi_{ip}) \end{pmatrix} z_{ip}^2 + \sum_{s=1}^{p}\begin{pmatrix} z_{i,s-1}^2 + z_{is}^2 \\ + y_{i,s-1}^2 + y_{is}^2 \end{pmatrix}$$
$$+ \sum_{j=1}^{N}\sum_{q=1}^{p}\begin{pmatrix} z_{j,q-1}^2 + z_{jq}^2 \\ + y_{j,q-1}^2 + y_{jq}^2 \end{pmatrix} + z_{ip}^2 + z_{i,p+1}^2/2 + y_{i,p+1}^2/2 + z_{ip}\overline{\overline{x}}_{i,p+1} + y_{ip}^2$$
$$+ \sum_{k=1}^{p-1}\sum_{j=1}^{N}\sum_{q=1}^{k}\left(z_{j,q-1}^2 + z_{jq}^2 + y_{j,q-1}^2 + y_{jq}^2\right) \tag{B-14}$$

Now the second error system is simplified.

Second error system (y_{ip}): Define the Lyapunov function candidate as $\mathbf{L}_{ip} = y_{ip}^2/2$ for $1 \le i \le N$ and $2 \le p \le n$. Then by using (9) and (12) the first derivative is given by

$$\dot{\mathbf{L}}_{ip} = y_{ip}(\dot{x}_{ipd} - \dot{\bar{x}}_{ip}) \le -y_{ip}^2/\tau_{ip} + \left|y_{ip}\right|\left\|\dot{\bar{x}}_{ip}\right| \tag{B-15}$$

By employing Lemma 2, the first derivative, $\dot{\mathbf{L}}_{ip}$, can be written as

$$\begin{aligned}
\dot{\mathbf{L}}_{ip} &= y_{ip}(\dot{x}_{ipd} - \dot{\bar{x}}_{ip}) \le -y_{ip}^2/\tau_{ip} + \left|y_{ip}\right|\left\|\dot{\bar{x}}_{ip}\right| \\
&\le -\frac{y_{ip}^2}{\tau_{ip}} + \left|y_{ip}\right|\sum_{s=1}^{p}\xi_{\mathbf{z},ips}(\Pi_{i,p-1})\left|z_{is}\right| + \left|y_{ip}\right|\sum_{s=1}^{p}\xi_{\mathbf{y},ips}(\Pi_{i,p-1})\left|y_{is}\right| \\
&+ \left|y_{ip}\right|\sum_{j=1}^{N}\sum_{q=1}^{p-1}\begin{pmatrix}\xi_{\mathbf{\Delta z},ip,jq}(\Pi_{i,p-1},X_{jq})\left|z_{jq}\right| \\ +\xi_{\mathbf{\Delta y},ip,jq}(\Pi_{i,p-1},X_{jq})\left|y_{jq}\right|\end{pmatrix} \\
&\le -y_{ip}^2/\tau_{ip} + \sigma_{ip}(\Pi_{i,p-1},\bar{X}_{p-1})y_{ip}^2 + \sum_{s=1}^{p}\left(z_{is}^2 + y_{is}^2\right) + \sum_{j=1}^{N}\sum_{q=1}^{p-1}\left(z_{jq}^2 + y_{jq}^2\right)
\end{aligned} \tag{B-16}$$

where

$$\begin{aligned}
\sigma_{ip}(\Pi_{i,p-1},\bar{X}_{p-1}) &= \frac{1}{4}\sum_{s=1}^{p}\left(\left(\xi_{\mathbf{z},ips}(\Pi_{i,p-1})\right)^2 + \left(\xi_{\mathbf{y},ips}(\Pi_{i,p-1})\right)^2\right) \\
&+ \frac{1}{4}\sum_{j=1}^{N}\sum_{q=1}^{p-1}\begin{pmatrix}\left(\xi_{\mathbf{\Delta z},ip,jq}(\Pi_{i,p-1},X_{jq})\right)^2 \\ +\left(\xi_{\mathbf{\Delta y},ip,jq}(\Pi_{i,p-1},X_{jq})\right)^2\end{pmatrix} \quad for\ p \ge 2\ \&\ \sigma_{i1} = 0
\end{aligned} \tag{B-17}$$

Now, define the combined Lyapunov function candidate $\mathbf{L} = \sum_{i=1}^{N}\sum_{p=1}^{\mathrm{n}}\left(\mathbf{V}_{ip} + \mathbf{L}_{ip}\right)$. By taking the derivative of $\mathbf{L}$ to get

$$\dot{\mathbf{L}} \le \sum_{i=1}^{N}\sum_{p=1}^{n}\begin{pmatrix}
-\Phi(\Pi_{ip})z_{ip}^2 + (z_{ip}^2 + y_{ip}^2) - \sum_{j=1}^{N}\left(z_{jp}^2 + y_{jp}^2\right) + \sum_{s=1}^{p}\begin{pmatrix}z_{i,s-1}^2 + 2z_{is}^2 \\ + y_{i,s-1}^2 + 2y_{is}^2\end{pmatrix} \\
+ \sum_{j=1}^{N}\sum_{q=1}^{p}\begin{pmatrix}z_{j,q-1}^2 + 2z_{jq}^2 \\ + y_{j,q-1}^2 + 2y_{jq}^2\end{pmatrix} + \frac{z_{i,p+1}^2}{2} + \frac{y_{i,p+1}^2}{2} + z_{ip}\bar{\bar{x}}_{i,p+1} \\
+ \sum_{k=1}^{p-1}\sum_{j=1}^{N}\sum_{q=1}^{k}\begin{pmatrix}z_{j,q-1}^2 + z_{jq}^2 \\ + y_{j,q-1}^2 + y_{jq}^2\end{pmatrix} - \left(\frac{1}{\tau_{ip}} - \sigma_{ip}(\Pi_{i,p-1},\bar{X}_{p-1})\right)y_{ip}^2
\end{pmatrix} \tag{B-18}$$

where $z_{i,n+1} = 0$, $y_{i,n+1} = 0$, and

$$\begin{aligned}
-\Phi(\Pi_{ip}) &= \zeta_{2ip}(\Pi_{ip}) + \zeta_{3ip}(\Pi_{ip}) + \zeta_{4ip}(\Pi_{ip}) \\
&+ \zeta_{5ip}(\Pi_{ip}) + \zeta_{6ip}(\Pi_{ip})
\end{aligned} \tag{B-19}$$

Define the virtual control input $\bar{x}_{i,p+1}$ as

$$\bar{x}_{i,\,p+1} = z_{pi}\hat{W}_{ip}^{T}\phi_{ip}(\Pi_{ip}) - K_{ip}z_{pi} + \dot{x}_{ipd} \tag{B-20}$$

for $1 \le i \le N$ and $1 \le p \le n$ where $\dot{x}_{ipd} = -y_{ip}/\tau_{ip}$ from (12) and the neural network $\hat{W}_{ip}^{T}\phi_{ip}(\Pi_{ip})$ approximates function $\Phi(\Pi_{ip}) = W_{ip}^{T}\phi_{ip}(\Pi_{ip}) + \varepsilon_{ip}$ (introduced in (B-19)) where the functional reconstruction errors are bounded above $|\varepsilon_{ip}| \le \varepsilon_{ip}^{M}$. By plugging (B-20) into (B-18) the first derivative is given by

$$\dot{\mathbf{L}} \le \sum_{i=1}^{N}\sum_{p=1}^{n}\begin{pmatrix} -\left(K_{ip} - 1/4\tau_{ip}'^{\,2} - \varepsilon_{ip}^{M}\right)z_{ip}^{2} + \tilde{W}_{ip}^{T}\phi_{ip}(\Pi_{ip})z_{ip}^{2} - \sum_{j=1}^{N}\left(z_{jp}^{2} + y_{jp}^{2}\right) \\ + (z_{ip}^{2} + y_{ip}^{2}) + z_{i,\,p+1}^{2}/2 + y_{i,\,p+1}^{2}/2 + \sum_{s=1}^{p}\left(3z_{is}^{2} + 3y_{is}^{2}\right) - \left(z_{ip}^{2} + y_{ip}^{2}\right) \\ + \sum_{j=1}^{N}\sum_{q=1}^{p}\left(3z_{jq}^{2} + 3y_{jq}^{2}\right) - \sum_{j=1}^{N}\left(z_{jp}^{2} + y_{jp}^{2}\right) + \sum_{k=1}^{p-1}\sum_{j=1}^{N}\sum_{q=1}^{k}\left(2z_{jq}^{2} + 2y_{jq}^{2}\right) \\ - \sum_{k=1}^{p-1}\sum_{j=1}^{N}\left(z_{jk}^{2} + y_{jk}^{2}\right) - \left(1/\tau_{ip} - \sigma_{ip}^{M}\right)y_{ip}^{2} \end{pmatrix} \tag{B-21}$$

where

$$\frac{1}{\tau_{ip}'} = \max_{\Omega}\frac{g_{ip}(X_{ip}) - 1}{\tau_{ip}g_{ip}(X_{ip})} \le \frac{1}{\tau_{ip}} \tag{B-22}$$

and $\sigma_{ip}^{M} = \max_{\Omega}\left|\sigma_{ip}(\Pi_{i,\,p-1}, \bar{X}_{p-1})\right|$ (which is a known result in DSC literature [1-3]) for all $1 \le i \le N$ and $1 \le p \le n$ in the compact set Ω.

Now, combine the individual Lyapunov function candidates as $\mathbf{L_T} = \mathbf{L} + \mathbf{L_W}$ where $\mathbf{L_W}$ is defined in Theorem 1 (part b). By differentiating $\mathbf{L_T}$ and using Theorem 1 the first term in (17) gets cancelled with second term in (B-21) and the second term can be brought into the first term in (B-23). By differentiating $\mathbf{L_T}$, rearranging the summations, and noting that $\sum_{i=1}^{N}\sum_{j=1}^{M}a_{ij} = \sum_{i=1}^{N}\sum_{j=1}^{M}a_{ji}$ we obtain

$$\begin{aligned}\dot{\mathbf{L}}_{\mathbf{T}} \le & \sum_{i=1}^{N}\sum_{p=1}^{n} -\left(K_{ip} - 1/4{\tau_{ip}}^2 - \varepsilon_{ip}^M - \eta_{ip}^M\right) z_{ip}^2 - \sum_{i=1}^{N}\sum_{p=1}^{n}\sum_{j=1}^{N}\left(z_{ip}^2 + y_{ip}^2\right) \\ & + \sum_{i=1}^{N}\sum_{p=1}^{n}\left(\frac{z_{i,p+1}^2}{2} + \frac{y_{i,p+1}^2}{2}\right) + \sum_{i=1}^{N}\sum_{p=1}^{n}\sum_{s=1}^{p}\left(3z_{is}^2 + 3y_{is}^2\right) + \sum_{i=1}^{N}\sum_{p=1}^{n}\sum_{j=1}^{N}\sum_{q=1}^{p}\left(3z_{iq}^2 + 3y_{iq}^2\right) \\ & - \sum_{i=1}^{N}\sum_{p=1}^{n}\sum_{j=1}^{N}\left(z_{ip}^2 + y_{ip}^2\right) + \sum_{i=1}^{N}\sum_{p=1}^{n}\sum_{k=1}^{p-1}\sum_{j=1}^{N}\sum_{q=1}^{k}\left(2z_{iq}^2 + 2y_{iq}^2\right) \\ & - \sum_{i=1}^{N}\sum_{p=1}^{n}\sum_{k=1}^{p-1}\sum_{j=1}^{N}\left(z_{ik}^2 + y_{ik}^2\right) - \sum_{i=1}^{N}\sum_{p=1}^{n}\left(1/\tau_{ip} - \sigma_{ip}^M\right) y_{ip}^2\end{aligned} \tag{B-23}$$

Additional simplification can be done by noting that $\sum_{j=1}^{N} a_i = Na_i$ and $\sum_{k=1}^{p-1} a_k = \sum_{k=1}^{p} a_k - a_p$ which results in the first derivative as

$$\begin{aligned}\dot{\mathbf{L}}_{\mathbf{T}} \le & \sum_{i=1}^{N}\sum_{p=1}^{n} -\left(K_{ip} - \frac{1}{4{\tau_{ip}}^2} - \varepsilon_{ip}^M - \eta_{ip}^M\right) z_{ip}^2 \\ & - \sum_{i=1}^{N}\sum_{p=1}^{n}\left(2Nz_{ip}^2 + 2Ny_{ip}^2\right) + \sum_{i=1}^{N}\sum_{p=1}^{n}\left(\frac{z_{i,p+1}^2}{2} + \frac{y_{i,p+1}^2}{2}\right) \\ & + \sum_{i=1}^{N}\sum_{p=1}^{n}\sum_{s=1}^{p}\left(3(N+1)z_{is}^2 + 3(N+1)y_{is}^2\right) \\ & + \sum_{i=1}^{N}\sum_{p=1}^{n}\sum_{k=1}^{p-1}\sum_{q=1}^{k}\left(2Nz_{iq}^2 + 2Ny_{iq}^2\right) - \sum_{i=1}^{N}\sum_{p=1}^{n}\sum_{k=1}^{p}\left(Nz_{ik}^2 + Ny_{ik}^2\right) \\ & + \sum_{i=1}^{N}\sum_{p=1}^{n}\left(Nz_{ip}^2 + Ny_{ip}^2\right) - \sum_{i=1}^{N}\sum_{p=1}^{n}\left(1/\tau_{ip} - \sigma_{ip}^M\right) y_{ip}^2\end{aligned} \tag{B-24}$$

The first derivative in (B-24) can be represented as (B-25) by using Lemma 3 and the fact that $\sum_{k=1}^{p-1}\sum_{q=k}^{p-1} a_k = \sum_{k=1}^{p}\sum_{q=k}^{p-1} a_k$ as

$$\begin{aligned}\dot{\mathbf{L}}_{\mathbf{T}} \le & \sum_{i=1}^{N}\sum_{p=1}^{n} -\left(K_{ip} - 1/4{\tau_{ip}}^2 - \varepsilon_{ip}^M - \eta_{ip}^M\right) z_{ip}^2 - \sum_{i=1}^{N}\sum_{p=1}^{n}\left(2Nz_{ip}^2 + 2Ny_{ip}^2\right) \\ & + \sum_{i=1}^{N}\sum_{p=1}^{n}\left(\frac{z_{i,p+1}^2}{2} + \frac{y_{i,p+1}^2}{2}\right) + \sum_{i=1}^{N}\sum_{p=1}^{n}\sum_{s=p}^{n}\left(3(N+1)z_{ip}^2 + 3(N+1)y_{ip}^2\right) \\ & + \sum_{i=1}^{N}\sum_{p=1}^{n}\sum_{k=1}^{p}\sum_{q=k}^{p-1}\left(2Nz_{ik}^2 + 2Ny_{ik}^2\right) - \sum_{i=1}^{N}\sum_{p=1}^{n}\sum_{k=p}^{n}\left(Nz_{ip}^2 + Ny_{ip}^2\right) \\ & + \sum_{i=1}^{N}\sum_{p=1}^{n}\left(Nz_{ip}^2 + Ny_{ip}^2\right) - \sum_{i=1}^{N}\sum_{p=1}^{n}\left(1/\tau_{ip} - \sigma_{ip}^M\right) y_{ip}^2\end{aligned} \tag{B-25}$$

The term $\sum_{i=1}^{N}\sum_{p=1}^{n}\sum_{k=1}^{p}\sum_{q=k}^{p-1}\left(2Nz_{ik}^2+2Ny_{ik}^2\right)$ in (B-25) is rewritten as

$$\begin{aligned}&\sum_{i=1}^{N}\sum_{p=1}^{n}\sum_{k=1}^{p}\sum_{q=k}^{p-1}\left(2Nz_{ik}^2+2Ny_{ik}^2\right)=\sum_{i=1}^{N}\sum_{p=1}^{n}\sum_{k=1}^{p}\left(2(p-k)Nz_{ik}^2+2(p-k)Ny_{ik}^2\right)\\&=\sum_{i=1}^{N}\sum_{p=1}^{n}\sum_{k=p}^{n}\left(2(k-p)Nz_{ip}^2+2(k-p)Ny_{ip}^2\right)\end{aligned}\tag{B-26}$$

By combining (B-25) and (B-26) and performing additional manipulations, the first derivative from (B-25) is given by

$$\dot{\mathbf{L}}_{\mathbf{T}}\le\sum_{i=1}^{N}\sum_{p=1}^{n}\left(-\beta_{\mathbf{z},ip}z_{ip}^2-\beta_{\mathbf{y},ip}y_{ip}^2\right)\tag{B-27}$$

Where

$$\begin{cases}\beta_{\mathbf{z},ip}=\left(K_{ip}+(N-3)n-\varepsilon_{ip}^{M}-\eta_{ip}^{M}-2N-\kappa_p\right)\\\beta_{\mathbf{y},ip}=0\end{cases}\qquad for\ p=1$$

and

$$\begin{cases}\beta_{\mathbf{z},ip}=\begin{pmatrix}K_{ip}+N+(2N-3)(n-p+1)\\-1/2-1/\left(4\tau_{ip}{}^2\right)-\varepsilon_{ip}^{M}-\eta_{ip}^{M}-3Np-\kappa_p\end{pmatrix}\\\beta_{\mathbf{y},ip}=1/\tau_{ip}+N+(2N-3)(n-p+1)-1/2-\sigma_{ip}^{M}-3Np-\kappa_p\end{cases}\qquad for\ p\ge 2\tag{B-28}$$

with $\kappa_p=\sum_{k=p}^{n}(2(k-p)N)$ for all $1\le i\le N$ and $1\le p\le n$ in the compact set Ω. The first derivative of the Lyapunov function $\dot{\mathbf{L}}_{\mathbf{T}}$ is negative semi-definite if the initial states $[Z(0),Y(0)]$ are inside the compact set Ω provided the design constants τ_{ip} and K_{ip} satisfy

$$\begin{cases}K_{ip}\ge\varepsilon_{ip}^{M}+\eta_{ip}^{M}-(N-3)n+2N+\kappa_p & for\ p=1\\\dfrac{1}{\tau_{ip}}\ge\dfrac{1}{2}+\sigma_{ip}^{M}-(N-3)(n-p+1)-N+3Np+\kappa_p & \\K_{ip}\ge\dfrac{1}{2}+\dfrac{1}{4\tau_{ip}{}^2}+\varepsilon_{ip}^{M}+\eta_{ip}^{M}-(N-3)(n-p+1)+3Np+\kappa_p & for\ p\ge 2\end{cases}\tag{B-29}$$

This further implies that if the initial states are within the set Ω, then they will stay in the same set for $t\ge 0$ by using [14 and Theorem 4.8). Consequently, $\dot{\mathbf{L}}_{\mathbf{T}}\le 0$ for $t\ge 0$.

Now by applying Barballat's Lemma [15] the states z_{ip} and y_{ip} are guaranteed to asymptotically converge to zero locally as time goes to infinity for all $1 \le i \le N$ and $1 \le p \le n$. ■

Remark 4: Design (B-29) suggests that the design constants are selected in a specific design order as $K_{i1} \to \tau_{i2} \to K_{i2} \to \cdots \to \tau_{in} \to K_{in}$. This means that each design gain K_{ip} and time constant τ_{ip} for all $1 \le i \le N$ and $1 \le p \le n$ depend on gains and time constants from previous steps. This sequence is also satisfied in the proof of Lemma 2.

Proof of Lemma 4: *Step 1*. From (3) we have

$$\bar{x}_{i2} = \hat{z}_{i1}\hat{W}_{i1}^T \phi_{i1}(\Pi_{i1}) - K_{i1}\hat{z}_{i1} \tag{C-1}$$

Consider the set $\hat{\Omega}$ being the same as the compact set over which the neural network approximation property applies and by using (16) and (A-1) it is assured that there is a maximum for the states $\tilde{W}_{i1}^T$ and for $\hat{W}_{i1}^T$ as well in Ω. Also, note that we can assume $\left|\hat{W}_{i1}^T \phi_{i1}(\hat{\Pi}_{i1})\right|_\infty \le W_{i1}^M \left|\phi_{i1}(\hat{\Pi}_{i1})\right|_\infty = e_{i1}$ by using a proper NN activation function. Hence, the following steps can be concluded.

Step 1:

$$|\bar{x}_{i2}| \le (e_{i1} + K_{i1})|\hat{z}_{i1}| \tag{C-2}$$

Then, from (5) and (6) we have

$$|x_{i2d}| \le (e_{i1} + K_{i1})|\hat{z}_{i1}| + |y_{i2}|, \tag{C-3}$$

$$|\hat{x}_{i2}| \le (e_{i1} + K_{i1})|\hat{z}_{i1}| + |\hat{z}_{i2}| + |y_{i2}|, \tag{C-4}$$

and

$$|x_{i2}| \le (e_{i1} + K_{i1})|\hat{z}_{i1}| + |\hat{z}_{i2}| + |y_{i2}| + |\tilde{z}_{i2}|. \tag{C-5}$$

Step p, $2 \le p \le n-1$

By using $\left|\hat{W}_{ip}^T \phi_{ip}(\hat{\Pi}_{ip})\right|_\infty \le W_{ip}^M \max_{\hat{\Omega}} \left\|\phi_{ip}(\hat{\Pi}_{ip})\right\| = e_{ip}$ and a similar reasoning to proof of Lemma1, we obtain

$$\left|\bar{x}_{i,p+1}\right| \le \left(e_{ip} + K_{ip}\right)\left|\hat{z}_{ip}\right| + \frac{\left|y_{ip}\right|}{\tau_{ip}} \tag{C-6}$$

Consequently, from (11) and (A-5)

$$\left|x_{i,p+1,d}\right| \le \left(e_{ip} + K_{ip}\right)\left|\hat{z}_{ip}\right| + \left|y_{ip}\right|/\tau_{ip} + \left|y_{i,p+1}\right|, \tag{C-7}$$

$$\left|\hat{x}_{i,p+1}\right| \le \left(e_{ip} + K_{ip}\right)\left|\hat{z}_{ip}\right| + \left|\hat{z}_{i,p+1}\right| + \left|y_{ip}\right|/\tau_{ip} + \left|y_{i,p+1}\right|, \tag{C-8}$$

and

$$\left|x_{i,p+1}\right| \le \left(e_{ip} + K_{ip}\right)\left|\hat{z}_{ip}\right| + \left|\hat{z}_{i,p+1}\right| + \left|y_{ip}\right|/\tau_{ip} + \left|y_{i,p+1}\right| + \left|\tilde{z}_{i,p+1}\right|. \tag{C-9}$$

Proof of Lemma 5: *Step 1.* From (20) we have

$$\dot{\hat{z}}_{i1} = \bar{L}_{i1}\hat{x}_{i1} + \hat{x}_{i2} + \mu L_{i1}\tilde{x}_{i1}$$

Thus,

$$\left|\dot{\hat{z}}_{i1}\right| \le \left|\bar{L}_{i1}\right|\left|\hat{x}_{i1}\right| + \left|\hat{x}_{i2}\right| + \mu L_{i1}\left|\tilde{x}_{i1}\right| \tag{C-10}$$

From (22) and $\dot{x}_{i1d} = 0$, we obtain

$$\bar{x}_{i2} = \hat{z}_{i1}\hat{W}_{i1}^T \phi_{i1}(\hat{\Pi}_{i1}) - K_{i1}\hat{z}_{i1} \tag{C-11}$$

Thus,

$$\left|\dot{\bar{x}}_{i2}\right| \le \left\|\dot{\hat{W}}_{i1}\right\| \max_{\hat{\Omega}} \left\|\phi_{i1}(\hat{\Pi}_{i1})\right\| \left|\hat{z}_{i1}\right| + A_{i1}(\hat{\Pi}_{i1})\left|\dot{\hat{z}}_{i1}\right| \tag{C-12}$$

where $A_{i1}(\hat{\Pi}_{i1}) = \left(W_{i1}^M \max_{\hat{\Omega}} \left\|\partial\hat{\phi}_{i1}/\partial\hat{z}_{i1}\right\| \left|\hat{z}_{i1}\right| + W_{i1}^M \max_{\hat{\Omega}} \left\|\phi_{i1}(\hat{\Pi}_{i1})\right\| + K_{i1}\right)$

and $\hat{\phi}_{i1} = \phi_{i1}(\hat{\Pi}_{i1})$. Using the weight update laws (28), we have

$$\left\|\dot{\hat{W}}_{ip}\right\| \le \rho_{ip}\hat{z}_{ip}^2\left(2\max_{\hat{\Omega}}\left\|\phi_{ip}(\hat{\Pi}_{ip})\right\| + W_{ip}^M\right) \tag{C-13}$$

for $1 \le i \le N$ and $1 \le p \le n$. Therefore, by using (C-12), (C-10), (C-13) for $p = 1$, and $\tilde{z}_{i1} = \tilde{x}_{i1}$, it yields

$$\begin{aligned}\left|\dot{\tilde{x}}_{i2}\right| \le{}& \xi_{\mathbf{z}i,21}(\hat{\Pi}_{i1})\left|\hat{z}_{i1}\right| + \xi_{\mathbf{z}i,22}(\hat{\Pi}_{i1})\left|\hat{z}_{i2}\right| + \mu\xi_{\tilde{\mathbf{z}},i2}(\hat{\Pi}_{i1})\left|\tilde{z}_{i1}\right| \\ & \xi_{\mathbf{y}i,22}(\hat{\Pi}_{i1})\left|y_{i2}\right|\end{aligned} \tag{C-14}$$

where $\xi_{\mathbf{z}i,22}(\hat{\Pi}_{i1}) = A_{i1}$, $\xi_{\tilde{\mathbf{x}},i21}(\hat{\Pi}_{i1}) = A_{i1}L_{i1}$, $\xi_{\mathbf{y}i,22}(\hat{\Pi}_{i1}) = A_{i1}$,and

$$\begin{aligned}&\xi_{\mathbf{z}i,21}(\Pi_{i1}) = \rho_{i1}\hat{z}_{i1}^2\left(2\max_{\hat{\Omega}}\left\|\phi_{i1}(\hat{\Pi}_{i1})\right\| + W_{i1}^M\right).\max_{\hat{\Omega}}\left\|\phi_{i1}(\hat{\Pi}_{i1})\right\|. \\ &+ A_{i1}\bar{L}_{i1} + A_{i1}\left(e_{i1} + K_{i1}\right)\end{aligned}$$

Note that $\left|\dot{\tilde{x}}'_{i2}\right|$ is a function of $[K_{i1}, L_{i1}, L_{i2}, \bar{L}_{i1}]^T$. Also,

$$\begin{aligned}&\left|\dot{y}_{i2}\right| = \left|\dot{x}_{i2d} - \dot{\tilde{x}}_{i2}\right| \le \left|y_{i2}\right|/\tau_{i2} + \left|\dot{\tilde{x}}_{i2}\right| \\ &\le \xi_{\mathbf{z}i,21}(\hat{\Pi}_{i1})\left|\hat{z}_{i1}\right| + \xi_{\mathbf{z}i,22}(\hat{\Pi}_{i1})\left|\hat{z}_{i2}\right| + \mu\xi_{\tilde{\mathbf{z}},i2}(\hat{\Pi}_{i1})\left|\tilde{z}_{i1}\right| \\ &\quad \xi_{\mathbf{y}i,22}(\hat{\Pi}_{i1})\left|y_{i2}\right| + \left|y_{i2}\right|/\tau_{i2}\end{aligned} \tag{C-15}$$

Step 2: From (26) we have

$$\dot{\hat{z}}_{i2} = \bar{L}_{i2}\hat{x}_{i2} + \hat{x}_{i3} + \mu^2 L_{i2}\tilde{x}_{i1} + y_{i2}/\tau_{i2}\ .$$

From (22) we have $\bar{x}_{i3} = \hat{z}_{i2}\hat{W}_{i2}^T\phi_{i2}(\hat{\Pi}_{i2}) - K_{i2}\hat{z}_{i2} + y_{i2}/\tau_{i2}$; thus,

$$\left|\dot{\bar{x}}_{i3}\right| \le \left\|\dot{\hat{W}}_{i2}\right\|\max_{\hat{\Omega}}\left\|\phi_{i2}(\hat{\Pi}_{i2})\right\|.\left|\hat{z}_{i2}\right| + A_{\mathbf{z},i21}\left|\dot{\hat{z}}_{i1}\right| + A_{\mathbf{z},i22}\left|\dot{\hat{z}}_{i2}\right| + A_{y,i22}\left|\dot{y}_{i2}\right| \tag{C-16}$$

where

$$A_{\mathbf{z},i21}(\hat{\Pi}_{i2}) = W_{i2}^M\max_{\hat{\Omega}}\left\|\frac{\partial\hat{\phi}_{i2}}{\partial\hat{z}_{i1}}\right\|\left|\hat{z}_{i2}\right|; A_{\mathbf{y},i22}(\hat{\Pi}_{i2}) = W_{i2}^M\max_{\hat{\Omega}}\left\|\frac{\partial\hat{\phi}_{i2}}{\partial y_{i2}}\right\|\left|\hat{z}_{i2}\right| + \frac{1}{\tau_{i2}}$$

$$A_{\mathbf{z},i22}(\hat{\Pi}_{i2}) = W_{i2}^M\max_{\hat{\Omega}}\left\|\frac{\partial\hat{\phi}_{i2}}{\partial\hat{z}_{i2}}\right\|\left|\hat{z}_{i2}\right| + W_{i2}^M\max_{\hat{\Omega}}\left\|\phi_{i1}(\hat{\Pi}_{i1})\right\| + K_{i2}$$

According to (C-13), we have

$$\left\|\dot{\hat{W}}_{i2}\right\| \le \rho_{i2}\hat{z}_{i2}^2\left(2\max_{\hat{\Omega}}\left\|\phi_{i2}(\hat{\Pi}_{i2})\right\| + W_{i2}^M\right)\cdot \tag{C-17}$$

By using Lemma 1 for $\left|x_{ipd}\right|$ and $\hat{z}_{ip} = \hat{x}_{ip} - x_{ipd}$, we conclude that

$$\begin{aligned}\left|\dot{\bar{x}}_{i3}\right| &\le \xi_{\mathbf{z},i31}(\hat{\Pi}_{i2})\left|\hat{z}_{i1}\right| + \xi_{\mathbf{z},i31}(\hat{\Pi}_{i2})\left|\hat{z}_{i2}\right| + \xi_{\mathbf{z},i33}(\hat{\Pi}_{i2})\left|\hat{z}_{i3}\right| \\ &+ \xi_{\mathbf{y},i32}(\hat{\Pi}_{i2})\left|y_{i2}\right| + \xi_{\mathbf{y},i33}(\hat{\Pi}_{i3})\left|y_{i3}\right| + \mu^2\xi_{\tilde{\mathbf{z}},i31}(\hat{\Pi}_{i2})\left|\tilde{z}_{i1}\right|\end{aligned} \tag{C-18}$$

Note that $\left|\dot{\bar{x}}_{i3}\right|$ is a function of $[K_{i1}, K_{i2}, \tau_{i2}, L_{i1}, L_{i2}, \bar{L}_{i1}, \bar{L}_{i2}]^T$. Also,

$$\begin{aligned}\left|\dot{y}_{i3}\right| &= \left|\dot{x}_{i3d} - \dot{\bar{x}}_{i3}\right| \le \left|y_{i3}\right|/\tau_{i3} + \left|\dot{\bar{x}}_{i3}\right| \\ &\le \xi_{\mathbf{z},i31}(\hat{\Pi}_{i2})\left|\hat{z}_{i1}\right| + \xi_{\mathbf{z},i31}(\hat{\Pi}_{i2})\left|\hat{z}_{i2}\right| + \xi_{\mathbf{z},i33}(\hat{\Pi}_{i2})\left|\hat{z}_{i3}\right| \\ &+ \xi_{\mathbf{y},i32}(\hat{\Pi}_{i2})\left|y_{i2}\right| + \xi_{\mathbf{y},i33}(\hat{\Pi}_{i3})\left|y_{i3}\right| + \mu^2\xi_{\tilde{\mathbf{z}},i31}(\hat{\Pi}_{i2})\left|\tilde{z}_{i1}\right| + \left|y_{i3}\right|/\tau_{i3}\end{aligned} \tag{C-19}$$

Step p, $2 \le p \le n-1$

By induction we obtain

$$\begin{aligned}\left|\dot{\bar{x}}_{ip}\right| &\le \xi_{\mathbf{z},ip1}(\hat{\Pi}_{i,p-1})\left|\hat{z}_{i1}\right| + \cdots + \xi_{\mathbf{z},ipp}(\hat{\Pi}_{i,p-1})\left|\hat{z}_{ip}\right| + \\ &\xi_{\mathbf{y},ip2}(\hat{\Pi}_{i,p-1})\left|y_{i2}\right| + \cdots + \xi_{\mathbf{y},ip,p-1}(\hat{\Pi}_{i,p-1})\left|y_{ip}\right| + \mu^{p-1}\xi_{\tilde{\mathbf{z}},ip}(\hat{\Pi}_{i,p-1})\left|\tilde{z}_{i1}\right|\end{aligned} \tag{C-20}$$

Note that $\left|\dot{\bar{x}}_{ip}\right|$ is a function of $[K_{i1}, \ldots, K_{i,p-1}, \tau_{i2}, \ldots, \tau_{i,p-1}, L_{i1}, \ldots, L_{i,p-1}, L_{i1}, \ldots, L_{i,p-1}]^T$.

Proof of Theorem 3: Due to the presence of observer in the output feedback controller design, there is a third error besides the two errors involved in the state feedback design. For convenience, we analyze the dynamics $\hat{z}_{ip}$, $\tilde{z}_{ip}$, and y_{ip} where $\tilde{z}_{ip} = z_{ip} - \hat{z}_{ip}$ for $1 \le i \le N$ and $1 \le p \le n$. Thus, here the proof involves three error systems. Before we continue, we define $\hat{z}_{i_i n+1} = \hat{y}_{i_i n+1} = 0$. Moreover, define $\bar{x}_{i1} = y_{i0} = y_{i1} = z_{i0} = \hat{z}_{i0} = \tilde{x}_{i0} = \tilde{x}'_{i0} = K_{i0} = \bar{K}_{i0} = e_{i0} = 0$, and $\tau_{i0} = \tau_{i1} = 1$.

First error system ($\tilde{z}'_{ip}$): Employing $\dot{z}_{ip}$ $(1 \le p \le n-1)$ from (14), $\dot{\hat{z}}_{ip}$ from (26), and noting that $\tilde{z}_{ip} = \tilde{x}_{ip}$ we obtain

$$\begin{aligned}\dot{\tilde{z}}_{ip} &= f_{ip}(X_{ip}) + \Delta_{ip}(\bar{X}_p) + g_{ip}(X_{ip})\tilde{z}_{i,p+1} \\ &- \bar{L}_{ip}\hat{x}_{ip} - \mu^p L_{ip}\tilde{z}_{i1} + \left(g_{ip}(X_{ip}) - 1\right)\hat{x}_{i,p+1}\end{aligned} \tag{D-1}$$

For $p = n$, the error $\dot{\tilde{x}}_{ip}$ becomes

$$\dot{\tilde{z}}_{in} = f_{in}(X_{ip}) + \Delta_{in}(\bar{X}_p) - \bar{L}_{in}\hat{x}_{in} - \mu^n L_{in}\tilde{z}_{i1}. \tag{D-2}$$

Define $x'_{ip} = x_{ip}/\mu^{p-1}$, $\hat{x}'_{ip} = \hat{x}_{ip}/\mu^{p-1}$, $\hat{z}'_{ip} = \hat{z}_{ip}/\mu^{p-1}$, $\tilde{z}'_{ip} = \tilde{z}_{ip}/\mu^{p-1}$, $y'_{ip} = y_{ip}/\mu^{p-1}$, and $\tilde{z}'_i = [\tilde{z}'_{i1}, \ldots, \tilde{z}'_{in}]^T$ for $1 \le i \le N$ and $1 \le p \le n$. Equations (D-1) together with (D-2) can be rewritten as

$$\dot{\tilde{z}}'_i = F_1 + \mu A_1 \tilde{z}'_i + \mu B_1 \hat{x}_i \tag{D-3}$$

where

$$F_1 = \begin{bmatrix} \left(f_{i1}(X_{i1}) + \Delta_{i1}(\bar{X}_1)\right) \\ \vdots \\ 1/\mu^{n-2}\left(f_{i,n-1}(X_{i,n-1}) + \Delta_{i,n-1}(\bar{X}_{i,n-1})\right) \\ 1/\mu^{n-1}\left(f_{in}(X_{in}) + \Delta_{in}(\bar{X}_n)\right) \end{bmatrix}, \quad A_1 = \begin{bmatrix} -L_{i1} & g_{i1}(X_{i1}) & \cdots & 0 \\ -L_{i2} & 0 & \ddots & 0 \\ \vdots & \vdots & & \vdots \\ -L_{i,n-1} & 0 & & g_{i,n-1}(X_{i,n-1}) \\ -L_{in} & 0 & & 0 \end{bmatrix},$$

$$B_1 = \frac{1}{\mu}\begin{bmatrix} -\bar{L}_{i1} & \mu\bar{g}_{i1} & \cdots & 0 & 0 \\ 0 & -\bar{L}_{i2} & \mu\bar{g}_{i2} & 0 & 0 \\ \vdots & & & \ddots & \vdots \\ 0 & 0 & & -\bar{L}_{i,n-1} & \mu\bar{g}_{i,n-1} \\ 0 & 0 & \cdots & 0 & -\bar{L}_{in} \end{bmatrix},$$

and $\bar{g}_{in} = g_{ip}(X_{ip}) - 1$. Now, define the Lyapunov function $\mathbf{L}_{\tilde{\mathbf{x}}i} = \tilde{z}_i'^T P_{\tilde{\mathbf{x}}i} \tilde{z}'_i$ with $P_{\tilde{\mathbf{x}}i}$ being a constant. Taking the Lyapunov function first derivative, we have

$$\frac{d}{dt}\left(\tilde{z}_i'^T P_{\tilde{\mathbf{x}}i} \tilde{z}'_i\right) \le -\mu\lambda_{\mathbf{Q}1\min}\left\|\tilde{z}'_i\right\|^2 + 2\tilde{z}_i'^T P_{\tilde{\mathbf{x}}i}(F_1 + \mu B_1 \hat{x}_i) \tag{D-4}$$

where $\lambda_{\mathbf{Q}1i,\min} = \lambda_{\min_{\hat{\Omega}}}(Q_{\tilde{\mathbf{x}}i}(X_{in}))$ and $Q_{\tilde{\mathbf{x}}i}(X_{in})$ is the solution of Lyapunov equation $A_1(X_{in})^T P_{\tilde{\mathbf{x}}i} + P_{\tilde{\mathbf{x}}i} A_1(X_{in}) = -Q_{\tilde{\mathbf{x}}i}(X_{in})$. By using Assumption 1 and 3, (D-4) can be written as

$$
\begin{aligned}
&\frac{d}{dt}\left(\tilde{z}_i^{T} P_{\tilde{\mathbf{x}}i}\tilde{z}_i'\right) \le -\mu\lambda_{\mathbf{Q}1i,\min}\left\|\tilde{z}_i'\right\|^2 \\
&+\mu\left\|\tilde{z}_i'\right\|^2\left\|B_1(X_{in})\right\|\sum_{p=1}^{n}\frac{1}{2}\left(2+\left(e_{i,p-1}+K_{i,p-1}\right)^2+1/\tau_{i,s-1}^2\right) \\
&+\mu\left\|P_{\tilde{\mathbf{x}}i}\right\|^2\left\|B_1(X_{in})\right\|\sum_{p=1}^{n}\left(\hat{z}_{i,p-1}^2+\hat{z}_{ip}^2+y_{i,p-1}^2+y_{ip}^2\right) \\
&+\left\|\tilde{z}_i'\right\|^2\left\|P_{\tilde{\mathbf{x}}i}\right\|\sum_{p=1}^{n}\sum_{s=1}^{p}\frac{1}{2}\left(\upsilon_{ips}(X_{ip})\right)^2\left(3+\left(e_{i,s-1}+K_{i,s-1}\right)^2+1/\tau_{i,s-1}^2\right) \\
&+\left\|P_{\tilde{\mathbf{x}}i}\right\|\sum_{p=1}^{n}\sum_{s=1}^{p}\left(\hat{z}_{i,s-1}^2+\hat{z}_{is}^2+y_{i,s-1}^2+y_{is}^2+\tilde{z}_{is}'^2\right) \\
&+\left\|\tilde{z}_i'\right\|^2\left\|P_{\tilde{\mathbf{x}}i}\right\|\sum_{p=1}^{n}\sum_{j=1}^{N}\sum_{q=1}^{p}\frac{1}{2}\left(\bar{\delta}_{ip,jq}^{M}\right)^2\left(3+\left(e_{j,q-1}+K_{j,q-1}\right)^2+1/\tau_{j,q-1}^2\right) \\
&+\left\|P_{\tilde{\mathbf{x}}i}\right\|\sum_{p=1}^{n}\sum_{j=1}^{N}\sum_{q=1}^{p}\left(\hat{z}_{j,q-1}^2+\hat{z}_{jq}^2+y_{j,q-1}^2+y_{jq}^2+\tilde{z}_{jq}'^2\right).
\end{aligned}
\tag{D-5}
$$

By using Lemma 3, performing more manipulations, and summing over *i*, we obtain

$$
\begin{aligned}
&\sum_{i=1}^{N}\frac{d}{dt}\left(\tilde{z}_i^{T} P_{\tilde{\mathbf{x}}i}\tilde{z}_i'\right) \le -\sum_{i=1}^{N}\left(\begin{array}{l}\mu\lambda_{\mathbf{Q}1i,\min}-\mu\left\|\bar{B}_1(X_{in})\right\|- \\ \mu\left\|B_1(X_{in})\right\|C_{1i}-\left\|P_{\tilde{\mathbf{x}}i}\right\|C_{2i}(X_{in})\end{array}\right)\left\|\tilde{z}_i'\right\|^2 \\
&+\sum_{i=1}^{N}\mu\left\|P_{\tilde{\mathbf{x}}i}\right\|^2\left\|B_1(X_{in})\right\|\left(2(n-p+1)\left\|\hat{z}_i'\right\|^2+\sum_{p=1}^{n}2{y'_{ip}}^2\right) \\
&+\sum_{i=1}^{N}\left\|P_{\tilde{\mathbf{x}}i}\right\|\sum_{p=1}^{n}\left(2(n-p+1)\left\|\hat{z}_i'\right\|^2+2(n-p+1){y'_{ip}}^2+(n-p+1)\left\|\tilde{z}_i'\right\|^2\right) \\
&+\sum_{i=1}^{N}\sum_{p=1}^{n}\left(2(n-p+1)\left\|\hat{z}_i'\right\|^2+2(n-p+1){y'_{ip}}^2+(n-p+1)\left\|\tilde{z}_i'\right\|^2\right)\sum_{j=1}^{N}\left\|P_{\tilde{\mathbf{x}}j}\right\|
\end{aligned}
\tag{D-6}
$$

where $C_{1i}=\sum_{p=1}^{n}\sum_{s=1}^{p}\frac{1}{2}\left(2+\left(e_{i,s-1}+K_{i,s-1}\right)^2+1/\tau_{i,s-1}^2\right)$

and

$$
\begin{aligned}
C_{2i} &= \sum_{p=1}^{n}\sum_{s=1}^{p}\frac{1}{2}\left(\upsilon_{ips}^{M}\right)^2\left(3+\left(e_{i,s-1}+K_{i,s-1}\right)^2+1/\tau_{i,s-1}^2\right) \\
&+\sum_{p=1}^{n}\sum_{j=1}^{N}\sum_{q=1}^{p}\frac{1}{2}\left(\bar{\delta}_{ip,jq}^{M}\right)^2\left(3+\left(e_{j,q-1}+K_{j,q-1}\right)^2+1/\tau_{j,q-1}^2\right)+\sum_{p=1}^{n}(n-p+1)
\end{aligned}
$$

where $\upsilon_{ips}^{M}=\max_{\Omega}\upsilon_{ips}(X_{ip})$ which results

$$\sum_{i=1}^{N}\frac{d}{dt}\left(\tilde{z}_i'^{T}P_{\tilde{\mathbf{x}}i}\tilde{z}_i'\right)\le-\sum_{i=1}^{N}\begin{pmatrix}\mu\lambda_{\mathbf{Q}1i,\min}-\mu\|B_1(X_{in})\|-\mu\|B_1(X_{in})\|C_{1i}\\-\|P_{\tilde{\mathbf{x}}i}\|C_{2i}(X_{in})-(n-p+1)\sum_{j=1}^{N}\|P_{\tilde{\mathbf{x}}j}\|\\-(n-p+1)\|P_{\tilde{\mathbf{x}}i}\|\end{pmatrix}\|\tilde{z}_i'\|^2+\sum_{i=1}^{N}\mu C_{3i}\|\hat{z}_i'\|^2+\sum_{i=1}^{N}\sum_{p=1}^{n}C_{4ip}y_{ip}'^{\,2}\qquad\text{(D-7)}$$

where

$$C_{3i}=\sum_{p=1}^{n}\left(\|P_{\tilde{\mathbf{x}}i}\|(n-p+1)+(2/\mu)(n-p+1)\sum_{j=1}^{N}\|P_{\tilde{\mathbf{x}}j}\|+\|P_{\tilde{\mathbf{x}}i}\|^2\times b2(n-p+1)\right),$$

$$C_{4ip}=2\mu\|P_{\tilde{\mathbf{x}}i}\|^2b+2\|P_{\tilde{\mathbf{x}}i}\|(n-p+1)+2(n-p+1)\sum_{j=1}^{N}\|P_{\tilde{\mathbf{x}}j}\|,\ \text{and}\ b=\max_{\hat{\Omega}}\|B_1(X_{in})\|.$$

Second error system ($\hat{z}_{ip}'$): From (26) and (25), the observer dynamics can be rewritten as

$$\begin{aligned}\dot{\hat{z}}_{ip}'&=\bar{L}_{ip}\hat{x}_{ip}'+\mu\hat{x}_{i,p+1}'+\mu L_{ip}\tilde{x}_{i1}'+y_{ip}'/\tau_{ip}\\&=\bar{L}_{ip}\left(\hat{z}_{ip}'+x_{ipd}'\right)+\mu\left(\hat{z}_{i,p+1}'+x_{i,p+1,d}'\right)+\mu L_{ip}\tilde{z}_{i1}'+y_{ip}'/\tau_{ip}\\&=\bar{L}_{ip}\hat{z}_{ip}'+\mu\hat{z}_{i,p+1}'+\mu L_{ip}\tilde{z}_{i1}'+\bar{L}_{ip}x_{ipd}'+\mu x_{i,p+1,d}'+y_{ip}'/\tau_{ip}\end{aligned}$$

which results

$$\dot{\hat{z}}_i'=F_2+\mu A_2\hat{z}_i'+\mu L_i\tilde{z}_{i1}'\qquad\text{(D-8)}$$

where

$$A_2=\begin{bmatrix}\bar{L}_{i1}/\mu & 1 & 0 & 0\\ \vdots & & \ddots & \vdots\\ 0 & 0 & \bar{L}_{i,n-1}/\mu & 1\\ -a_{i1} & -a_{i2} & & -a_{in}-K_{in}+\hat{W}_{in}^{T}\phi_{in}(\hat{\Pi}_{in})+\bar{L}_{in}/\mu\end{bmatrix},\ L_i=\left[L_{i1},\ldots,L_{in}\right]^T,$$

And

$F_2^{\,n\times1}=[\mu\hat{x}_{i2,d}',\,y_{i2}'/\tau_{i2}+\bar{L}_{i2}x_{i2d}'+\mu\hat{x}_{i3d}',\ldots,y_{in}'/\tau_{in}+\bar{L}_{in}x_{ind}']^T$. Now, define the Lyapunov function $\mathbf{L}_{\mathbf{x}i}=\hat{z}_i'^{T}P_{\mathbf{x}i}\hat{z}_i'$ with $P_{\mathbf{x}i}$ being a constant. Taking the Lyapunov function first derivative, we have

$$\frac{d}{dt}\left(\hat{z}_i'^{T}P_{\mathbf{x}i}\hat{z}_i'\right)\le-\mu\lambda_{\mathbf{Q}2i,\min}\|\hat{z}_i'\|^2+2\mu\hat{z}_i'^{T}P_{\mathbf{x}i}L_i\tilde{z}_{i1}'+2\hat{z}_i'^{T}P_{\mathbf{x}i}F_2\qquad\text{(D-9)}$$

where $\lambda_{\mathbf{Q}2i,\min}=\min_{\Omega}(Q_{\mathbf{x}i}(X_{in}))$ and $Q_{\mathbf{x}i}(\hat{X}_{in})$ is the solution of Lyapunov equation

$A_2^T P_{\mathbf{x}i} + P_{\mathbf{x}i} A_2 = -Q_{\mathbf{x}i}(\hat{\Pi}_{in})$. Equation (D-8) can be written as

$$\frac{d}{dt}\left(\hat{z}_i'^T P_{\mathbf{x}i} \hat{z}_i'\right) \le -\mu\lambda_{\mathbf{Q}2i,\min}\left\|\hat{z}_i'\right\|^2 + \mu\left\|L_i\right\|\left\|\hat{z}_i'\right\|^2 + \mu\left\|P_{\mathbf{x}i}\right\|^2\left\|L_i\right\|\left\|\tilde{z}_i'\right\|^2$$
$$+ \left\|\hat{z}_i'\right\|^2\left\|P_{\mathbf{x}i}\right\|\frac{1}{2}\sum_{p=1}^{n}\left(1/\tau_{ip}^{\,2} + \left(e_{ip} + K_{ip}\right)^2 + 1\right) + \left\|P_{\mathbf{x}i}\right\|\sum_{p=1}^{n}\left(2y_{ip}'^{\,2}\right) + \left\|P_{\mathbf{x}i}\right\|\left\|\tilde{z}_i'\right\|^2 \tag{D-10}$$

Summing over *i* results

$$\sum_{i=1}^{N}\frac{d}{dt}\left(\hat{z}_i'^T P_{\hat{\mathbf{x}}i}\hat{z}_i'\right) \le -\sum_{i=1}^{N}\begin{pmatrix}\mu\lambda_{\mathbf{Q}2\min} - \mu\left\|L_i\right\| \\ -\left\|P_{\mathbf{x}i}\right\|C_i' - \left\|P_{\mathbf{x}i}\right\|\end{pmatrix}\left\|\hat{z}_i'\right\|^2$$
$$+ \sum_{i=1}^{N}\mu\left\|P_{\mathbf{x}i}\right\|^2\left\|L_i\right\|\left\|\tilde{z}_i'\right\|^2 + \sum_{i=1}^{N}\sum_{p=1}^{n}2\left\|P_{\mathbf{x}i}\right\|y_{ip}'^{\,2} \tag{D-11}$$

where $C_{1i}' = \frac{1}{2}\sum_{p=1}^{n}\left(1/\tau_{ip}^{\,2} + \left(e_{ip} + K_{ip}\right)^2 + 1\right)$.

Third dynamical system (y_{ip}'): Define the Lyapunov function candidate as $\mathbf{L}_{ip} = y_{ip}'^2/2$ for $1 \le i \le N$ and $2 \le p \le n$. Then by using (24) , (25) and $\mu \ge 1$, the first derivative is given by

$$\dot{\mathbf{L}}_{ip} = y_{ip}'(\dot{x}_{ipd}' - \dot{\bar{x}}_{ip}') \le -y_{ip}'^2/\tau_{ip} + \left|y_{ip}'\right|\left\|\dot{\bar{x}}_{ip}'\right|$$

$$\le -y_{ip}'^2/\tau_{ip} + \left|y_{ip}'\right|\sum_{s=1}^{p}\frac{1}{\mu^{p-s}}\xi_{\mathbf{x},ips}(\hat{\Pi}_{i,p-1})\left|\hat{z}_{is}'\right|$$
$$+ \left|y_{ip}'\right|\sum_{s=1}^{p}\frac{1}{\mu^{p-s}}\xi_{\mathbf{y},ips}(\hat{\Pi}_{i,p-1})\left|y_{is}'\right| + \frac{1}{\mu}\left|y_{ip}'\right|\xi_{\tilde{\mathbf{x}},ip}(\hat{\Pi}_{i,p-1})\left\|\tilde{z}_i'\right\|$$

$$\le -\left(1/\tau_{ip} - \hat{\sigma}_{ip}(\Pi_{i,p-1}, \bar{X}_{p-1})\right)y_{ip}'^2 + \sum_{s=1}^{p}y_{is}'^2 + \left\|\hat{z}_i'\right\|^2 + \left\|\tilde{z}_i'\right\|^2 \tag{D-12}$$

where $\hat{\sigma}_{ip}(\hat{\Pi}_{i,p-1}, \bar{X}_{p-1}) = \frac{1}{4}\sum_{s=1}^{p}\begin{pmatrix}\left(\xi_{\mathbf{x},ips}(\hat{\Pi}_{i,p-1})\right)^2 + \left(\xi_{\mathbf{y},ips}(\hat{\Pi}_{i,p-1})\right)^2 \\ +\left(\xi_{\tilde{\mathbf{x}},ip}(\hat{\Pi}_{i,p-1})\right)^2\end{pmatrix}$ for $2 \le p \le n$ and $\hat{\sigma}_{i1} = 0$

NN weight estimation error: Define the Lyapunov function $\mathbf{L}_{\mathbf{W}ip} = 1/\left(2\rho_{ip}\right)\tilde{W}_{ip}^{\,T}\tilde{W}_{ip}$. From (27) we have

$$\dot{\mathbf{L}}_{\mathbf{W}} = \sum_{i=1}^{N}\sum_{p=1}^{n}\frac{1}{\rho_{ip}\mu^{2(p-1)}}\tilde{W}_{ip}^T\dot{\tilde{W}}_{ip} \le \sum_{i=1}^{N}\sum_{p=1}^{n}\frac{\hat{z}_{ip}^2}{\mu^{2(p-1)}}\left(\hat{\eta}_{ip}'^M + \hat{\eta}_{ip}^M\right) \tag{D-13}$$

where $\hat{\eta}_{ip}^{M} = \left(\|W_{ip}\| + W_{ip}^{M}\right)\left(\max_{\hat{\Omega}}\|\phi_{ip}\| + W_{ip}^{M}\right)$ and $\hat{\eta}_{ip}'^{M} = \left(\|W_{ip}\| + W_{ip}^{M}\right)\max_{\hat{\Omega}}\|\phi_{ip}\|$.

Now, summing the individual Lyapunov functions, we obtain $\mathbf{L} = \sum_{i=1}^{N}\left(\|P_{\mathbf{x}i}\|^2 \mathbf{L}_{\tilde{\mathbf{x}}i} + \mathbf{L}_{\mathbf{x}i} + \mathbf{L}_{ip} + \mathbf{L}_{\mathbf{W}}\right)$ which results

$$\dot{\mathbf{L}} = \sum_{i=1}^{N}\left(\frac{d}{dt}\left(\|P_{\mathbf{x}i}\|^2 \|L_i\|\tilde{z}_i'^{T} P_{\tilde{\mathbf{x}}i}\tilde{z}_i'\right) + \frac{d}{dt}\left(\hat{z}_i'^{T} P_{\hat{\mathbf{x}}i}\hat{z}'\right) + \dot{\mathbf{L}}_{ip} + \dot{\mathbf{L}}_{\mathbf{W}}\right)$$

$$\leq -\sum_{i=1}^{N}\|P_{\mathbf{x}i}\|^2\|L_i\|\begin{pmatrix}\mu\left(\lambda_{\mathbf{Q}1i,\min} - b - bC_{1i} - 1\right) - \|P_{\tilde{\mathbf{x}}i}\|C_{2i}(X_{in}) \\ -(n-p+1)\sum_{j=1}^{N}\|P_{\tilde{\mathbf{x}}j}\| - (n-p+1)\|P_{\tilde{\mathbf{x}}i}\|\end{pmatrix}\|\tilde{z}_i'\|^2$$

$$-\sum_{i=1}^{N}\left(\mu(\lambda_{\mathbf{Q}2\min} - \|L_i\| - C_{3i}) - \|P_{\mathbf{x}i}\|C_{i1}' - \|P_{\mathbf{x}i}\| - \hat{\eta}^{M}\right)\|\hat{z}_i'\|^2$$
$$-\sum_{i=1}^{N}\sum_{p=1}^{n}\left(1/\tau_{ip} - \hat{\sigma}_{ip}^{M} - C_{4ip} - 2\|P_{\mathbf{x}i}\| - (n-p+1)\right)y_{ip}'^2 . \qquad \text{(D-14)}$$

where $\hat{\sigma}_{ip}^{M} = \max_{\hat{\Omega}}\left|\hat{\sigma}_{ip}(\Pi_{i,p-1}, \bar{X}_{p-1})\right|$ and $\hat{\eta}^{M} = \max_{i,p}(\hat{\eta}_{ip}'^{M} + \hat{\eta}_{ip}^{M})$. the value $\lambda_{\mathbf{Q}1\min}$ can be selected large when L_{ip} is appropriately chosen (for $1 \leq i \leq N$ and $1 \leq p \leq n$). Then, by selecting adequately large a_{ip} (for $1 \leq i \leq N$ and $1 \leq p \leq n$) $\lambda_{\mathbf{Q}2\min}$ can overcome the term $\|L_i\| + C_{2i}$ in the second term in (D-14). Finally, appropriate μ and sufficiently small τ_{ip} make $\dot{\mathbf{L}}$ negative semi definite (lacking NN weights errors) in the compact set $\hat{\Omega}$. These conditions are summarized as

$$\begin{aligned}&\lambda_{\mathbf{Q}1\min} \geq b + bC_{1i} + 1 \\ &\lambda_{\mathbf{Q}2\min} \geq \|L_i\| + C_{3i} \\ &1/\tau_{ip} \geq \hat{\sigma}_{ip}^{M} + C_{4ip} + 2\|P_{\mathbf{x}i}\| + (n-p+1)\end{aligned} \qquad \text{(D-15)}$$

for $1 \leq i \leq N$ and $1 \leq p \leq n$. This further implies that if the initial states are within the set $\hat{\Omega}$, then they will stay in the same set for $t \geq 0$ by using [14 and Theorem 4.8.] Consequently, $\dot{\mathbf{L}} < 0$ for $t \geq 0$ and by applying Barballat's Lemma [15] the states $\tilde{z}_{ip}'$, $\hat{z}_{ip}$, and y_{ip} asymptotically converge to zero locally while the states $\tilde{W}_{ip}$ remain bounded for

all $1 \le i \le N$ and $1 \le p \le n$.

Remark 5: In the case that g_{in} is a function of the states, matrix B_1 includes the coefficients a_{ip} (for $1 \le i \le N$ and $1 \le p \le n$). Consequently, satisfaction of conditions (D-15) is limited to a restricted class of interconnected systems.

3. Power System Stabilization Using Adaptive Neural Network-based Dynamic Surface Control

S. Mehraeen, S. Jagannathan, and M. L. Crow [1]

Abstract— *In this paper, the power system with excitation control is represented as a class of large-scale, uncertain, interconnected nonlinear continuous-time system in strict-feedback form. Subsequently dynamic surface control (DSC)-based adaptive neural network (NN) controller is designed to overcome the repeated differentiation of the control input that is observed in the conventional backstepping approach. The NNs are utilized to approximate the unknown subsystem and the interconnection dynamics. By using novel online NN weight update laws with second order error terms, the closed-loop signals are shown to be locally asymptotically stable via Lyapunov stability analysis, even in the presence of NN approximation errors in contrast with other NN techniques where a bounded stability is normally assured. Simulation results on the IEEE 14-bus power system with generator excitation control are provided to show the effectiveness of the approach in damping oscillations that occur after disturbances are removed. The end result is a nonlinear decentralized adaptive state-feedback excitation controller for damping power systems oscillations in the presence of uncertain subsystem and interconnection terms.*

Index Terms – Power System stabilization, Excitation Control, Dynamic Surface Control, Decentralized Control, Adaptive Control,

[1] Authors are with Department of Electrical and Computer Engineering, Missouri University of Science and Technology, 1870 Miner Circle, Rolla, MO 65409. Contact author: sm347@mst.edu. Research Supported in part by NSF ECCS#0624644.

I. Introduction

In the recent years, the competitive market for power generation and energy services demand a more reliable power network. Due to offshore wind generation plants and solar cells, a noticeable uncertainty in the load flows will occur in a power system thus impacting the dynamic behavior and stability. Therefore excitation control, power system stabilizer (PSS), static VAR compensators, and other power system controllers can play even more important role in maintaining dynamic performance and power system stability, and thus, increasing reliability. Centralized control strategies for ensuring performance and stability are not viable due to the sheer size of the power network which causes time delays in acquiring power system bus voltages and currents.

Decentralized control (DC) techniques [1-6], on the other hand, have been evolving for power systems so that they can achieve transient stability as well as steady state behavior in terms of damping oscillations caused by faults/disturbances. Under the DC techniques, load and frequency control methods of a multi-area interconnected power system are studied in [1-2]; however, linear power system model is used to design turbine and exciter voltage controllers. In [3], an LMI approach is chosen and sequential linear matrix inequality programming is utilized to design a power system stabilizer (PSS). In [4], by considering nonlinear power system representation, a suboptimal performance for all admissible variations of generator parameters is achieved using an LMI-based control approach.

By contrast, in [5], a decentralized neural network (NN) control of a general class of nonlinear systems in strict feedback form has been proposed for power systems by

using backstepping technique while relaxing the matching condition (where in the matching condition the interconnected terms appear in the input domain only). The method is applied to design excitation and steam turbine controls rendering state boundedness due to NN reconstruction errors while encountering repeated differentiation of the control signal due to backstepping design. In [6], a linear parameter varying (LPV) representation of the power system is chosen at each operating point via linearization and subsequently, a decentralized PSS is designed.

Dynamic surface control (DSC) [7], on the other hand, has been receiving attention in this decade [7-9]. In the DSC scheme, the well-known problem of repeated differentiation of the control signal in the backstepping design is replaced by a series of algebraic terms which simplifies the implementation. Consequently, the DSC scheme results in asymptotic stability in a semi-global manner [7] provided the system dynamics are accurately known. Further attempts in [8] provide asymptotic stabilization for a class of uncertain nonlinear systems using adaptive DSC provided the control gain coefficient matrix being unity or $g(.)=1$ (where $\dot{x}=f(x)+g(x)u$) and the system uncertainties are assumed to be linear in the unknown parameters (LIP). Hence, NN universal approximation property is asserted in [9] to relax this LIP assumption for subsystem uncertainties in order to ensure state boundedness.

In this paper, the large-scale power system with generator excitation control is represented as a nonlinear uncertain, interconnected system, in strict feedback form. Subsequently, the DSC design framework is proposed while relaxing the matching condition (i.e. the interconnected terms appear in several dynamic equations as oppose to the one where the actual control input appears). Next, NNs are introduced to approximate

both subsystem and the interconnection dynamics. Novel NN weight update laws are derived which render asymptotic stability even in the presence of NN approximation errors. Finally, simulation results on a 14-bus 5-generator power system with generator excitation control verify satisfactory performance of this controller in damping the oscillations after a disturbance has occurred.

This paper is organized as follows. First background information is given in the next section. Subsequently, power system model development as well as excitation control is introduced in Section III. The DSC state feedback design is introduced in Section IV. A numerical example is presented in Section V. Conclusions are given in Section VI.

II. Background

Consider the dynamical system $\dot{x} = f(x,t)$, where $x \in \Re^n$ representing the state vector and $u(t)$ is the input vector. Let the initial time be t_0, and the initial condition be $x_0 \equiv x(t_0)$. The state x_e is considered as an equilibrium point of the system if $f(x_e,t) = 0, t \geq t_0$.

Definition 1: An equilibrium point x_e is locally asymptotically stable at t_0 if there exists a compact set $S \subset \Re^n$ such that, for every initial condition $x_0 \subset S$, $\|x(t) - x_e\| \to 0$ as $t \to \infty$. If the compact set $x_0 \subset S$ can be made arbitrarily large and if $\|x(t) - x_e\| \to 0$ as $t \to \infty$, then the equilibrium point is semi-globally asymptotically stable.

Next, a brief background on NN is given. A general function $f(x) \in \Re$ where $x \in \Re^n$ can be written as $f(x) = W^T \phi(\bar{V}^T x) + \varepsilon(x)$ with $\varepsilon(x)$ NN denotes functional reconstruction error vector, $W \in R^{N_2 \times 1}$ and $\bar{V} \in R^{n \times N_2}$ represent target NN weight matrices.

III. Power System as an Interconnected System

In this section, a decentralized representation of a power system is obtained for nonlinear controller development. When a disturbance or fault such as a three-phase to ground occurs, the generator angles and speeds deviate from their normal operating range. Unless there is a controller to mitigate the oscillations, which bounce back and forth among multiple generators, the power system will not return to its normal operating state after the fault is removed. Generator excitation control is a means to alleviate the power system oscillations. Since the disturbance is a function of the power network voltages and angles as well as generator states, it is generally hard to design a centralized damping controller for the complex interconnected power network. Thus, in this paper, we aim at a decentralized excitation controller to mitigate the oscillations by using locally measurable states of the generator as well as its bus voltages and angles. For this controller development, the large-scale power system has to be represented in a decentralized form which is discussed next.

A. Model Development

A power system is usually modeled using a combination of differential and algebraic equations. The differential equations represent generator states (i.e. angles, speeds, and *dq* voltages E'_q and E'_d) whereas the algebraic equations represent bus active and reactive power balance relationships. For the purpose of controller design it is

desirable to have pure dynamical equations. In [12], authors have proposed an algebraic-free power system representation based on the classical generator model. In order to incorporate the generator flux-decay states, the proposed model is extended herein.

A two-axis model [13] is chosen for the purpose of power system representation. As a consequence, the generator dynamical equations are given as

$$\begin{aligned}
&\dot{\delta}_i = \omega_i;\ \omega_i = \frac{1}{M_i}\left(P_{mi} - P_{ei}\right);\\
&\dot{E}'_{qi} = \frac{1}{T_{d0i}}\left(-\frac{x_{di}}{x'_{di}}E'_{qi} + \frac{x_{di}-x'_{di}}{x'_{di}}V_{i+n}\cos(\delta_i - \psi_{i+n}) + E_{fdi}\right)\\
&\dot{E}'_{di} = \frac{1}{T_{q0i}}\left(-\frac{x_{qi}}{x'_{di}}E'_{di} + \frac{x_{qi}-x'_{di}}{x'_{di}}V_{i+n}\sin(\delta_i - \psi_{i+n})\right);\ \dot{E}_{fdi} = \frac{1}{T_{Ei}}\left(V_{Ri} - K_{Ei}E_{fdi}\right)
\end{aligned} \tag{1}$$

where δ_i is the rotor angle of the *i*-th machine, ω_i is the difference between the generator angular speed and synchronous speed, E'_{qi} and E'_{di} are generator's *dq* variables as defined in [13], E_{fdi} is the excitation voltage, and V_{i+n} and ψ_{i+n} are the generator bus voltage and phase angle, respectively, as depicted by Fig. 1. In addition,

$$P_{ei} = B_{i,i+n}V_{i+n}\left(E'_{qi}\sin(\delta_i - \psi_{i+n}) - E'_{di}\cos(\delta_i - \psi_{i+n})\right) \tag{2}$$

where *B* represents the reactance of the admittance matrix, *n* being the number of generators, and *N* denotes the number of non-generator buses in the power system as shown in Fig. 1. The bus voltage and phase angles of the power system buses are illustrated in Fig. 1 which are constrained by the set of algebraic power balance equations (neglecting resistances) as

$$\begin{aligned}
&P_{Li} + \sum_{j=1}^{n} B_{ij}V_i\left(E'_{qj}\sin(\psi_i - \delta_j) + E'_{dj}\cos(\psi_i - \delta_j)\right) + \sum_{j=n+1}^{N+n} B_{ij}V_iV_j\sin(\psi_i - \psi_j) = S_{\mathrm{P}i} = 0\\
&Q_{Li} - \sum_{j=1}^{n} B_{ij}V_i\left(E'_{qj}\cos(\psi_i - \delta_j) - E'_{dj}\sin(\psi_i - \delta_j)\right) - \sum_{j=n+1}^{N+n} B_{ij}V_iV_j\cos(\psi_i - \psi_j) = S_{\mathrm{Q}i} = 0\\
&i = n+1,\ldots,n+N
\end{aligned} \tag{3}$$

Then, taking the derivative of (3) to obtain $\dot{V}_i$ and $\dot{\psi}_i$ as

$$\frac{\partial S_{\mathrm{P}i}}{\partial t} = \frac{\partial S_{\mathrm{P}i}}{\partial V}\dot{V} + \frac{\partial S_{\mathrm{P}i}}{\partial \psi}\dot{\psi} + \frac{\partial S_{\mathrm{P}i}}{\partial \delta}\dot{\delta} + \frac{\partial S_{\mathrm{P}i}}{\partial E'_q}\dot{E}'_q + \frac{\partial S_{\mathrm{P}i}}{\partial E'_d}\dot{E}'_d = 0 \tag{4}$$

and

$$\frac{\partial S_{\mathrm{Q}i}}{\partial t} = \frac{\partial S_{\mathrm{Q}i}}{\partial V}\dot{V} + \frac{\partial S_{\mathrm{Q}i}}{\partial \psi}\dot{\psi} + \frac{\partial S_{\mathrm{Q}i}}{\partial \delta}\dot{\delta} + \frac{\partial S_{Qi}}{\partial E'_q}\dot{E}'_q + \frac{\partial S_{Qi}}{\partial E'_d}\dot{E}'_d = 0 \qquad i = n+1,\ldots,n+N \tag{5}$$

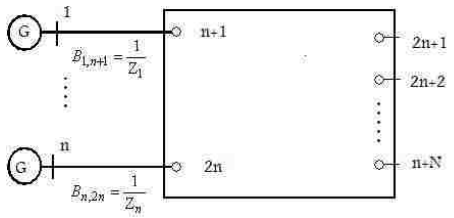

Fig.1 Power System

By using (1) for $\dot{E}'_{qi}$ and $\dot{E}'_{di}$ and solving (4) and (5) and for $\dot{V}_i$ and $\dot{\psi}_i$, we obtain a new set of dynamic equations as

$$\begin{bmatrix} A(x) & B(x) \\ D(x) & E(x) \end{bmatrix}\begin{bmatrix} \dot{V} \\ \dot{\psi} \end{bmatrix} + \left(\begin{bmatrix} C(x) \\ F(x) \end{bmatrix}\omega + R(x)\right) = 0 \tag{6}$$

where $V = [V_{n+1} \;\; V_{n+2} \;\; \ldots \;\; V_{n+N}]^T$, $\psi = [\psi_{n+1} \;\; \psi_{n+2} \;\; \ldots \;\; \psi_{n+N}]^T$, and $\omega = [\omega_1 \;\; \omega_2 \;\; \ldots \;\; \omega_n]^T$ is the generators' speed error vector. Also, define $\delta = [\delta_1 \;\; \delta_2 \;\; \ldots \;\; \delta_n]^T$, $E'_q = [E'_{q1} \;\; E'_{q2} \;\; \ldots \;\; E'_{qn}]^T$, $E'_d = [E'_{d1} \;\; E'_{d2} \;\; \ldots \;\; E'_{dn}]^T$, $E_{fd} = [E_{fd1} \; E_{fd2} \; \ldots \; E_{fdn}]^T$, $\Delta P_e = [\Delta P_{e1} \;\; \Delta P_{e2} \;\; \ldots \;\; \Delta P_{en}]^T$, and $x = [\delta^T \; \omega^T \; E_q'^T \; E_d'^T \;\; E_{fd}^T \; V^T \; \psi^T]^T$. The entities for $A_{N\times N}$, $B_{N\times N}$, $D_{N\times N}$, $E_{N\times N}$, $C_{N\times n}$, $F_{N\times N}$, $R_{2N\times 1}$, and $G_{2N\times n}$ can be derived by collecting the corresponding coefficients. Equation (6) can be rewritten in a more appropriate way as

$$\begin{bmatrix} \dot{V} \\ \dot{\psi} \end{bmatrix} = -\begin{bmatrix} A(x) & B(x) \\ D(x) & E(x) \end{bmatrix}^{-1} \left(\begin{bmatrix} C(x) \\ F(x) \end{bmatrix} \omega + R(x) \right) = a(x) \tag{7}$$

It is important to note that this step is needed only for model development and is not required for implementation.

B. Generator Representation

Next, the flux-decay model [13] of the generator is given as

$$\begin{aligned} &\dot{\delta}_i = \omega_i;\ \dot{\omega}_i = \frac{1}{M_i}(P_{mi} - P_{ei});\ \dot{E}'_{qi} = \frac{1}{T_{d0i}}\left(-E'_{qi} + (x_{di} - x'_{di})I_{di} + E_{fdi}\right) \\ &\dot{E}_{fdi} = \frac{1}{T_{Ei}}\left(V_{Ri} - K_{Ei}E_{fdi}\right) \end{aligned} \tag{8}$$

where P_{ei} is the active load at each bus, and $M_i = 2H/\omega_0$ is the i-th machine inertia. In addition, the following equalities are valid

$$P_{ei} = E'_{qi} I_{qi} + (x_{qi} - x'_{di}) I_{qi} I_{di} \tag{9}$$

and

$$I_{qi} = B_{i,i+n} V_{i+n} \sin(\delta_i - \psi_{i+n});\ I_{di} = B_{i,i+n}\left(E'_{qi} - V_{i+n}\cos(\delta_i - \psi_{i+n})\right). \tag{10}$$

Moreover, the power balance equations (3) will be simplified by employing the flux-decay assumption

$$E'_{di} = (x_{qi} - x'_{di}) I_{qi}. \tag{11}$$

In this design we assume that the mechanical power $P_{mi}\,(1 \le i \le n)$ is slowly changing compared to the other control variables; thus $\dot{P}_{mi} \approx 0$. Now define

$$x_{i1} = \delta_i - \delta_{0i};\ x_{i2} = \omega_i;\ x_{i3} = \frac{\Delta P_{ei}}{M_i};\ x_{i4} = P_{e0i} - I_{qi} E_{fdi} \tag{12}$$

where $\Delta P_{ei} = P_{e0i} - P_{ei}$ and $P_{e0i} = P_{mi}$. Consequently, the generator dynamics (8) can be rewritten in the state-space form as

$$
\begin{aligned}
&\dot{x}_{i1} = x_{i2}\ ;\ \dot{x}_{i2} = x_{i3} \\
&\dot{x}_{i3} = -\frac{x_{i3}}{T_{d0i}} + \frac{x_{i4}}{T_{d0i}M_i} + \frac{1}{T_{d0i}}\left(x_{di} - x_{qi}\right)I_{qi}I_{qi} - E'_{qi}\dot{I}_{qi} \\
&\qquad -\left(x_{qi} - x'_{di}\right)\left(\dot{I}_{qi}I_{di} + I_{qi}\dot{I}_{di}\right) \\
&\dot{x}_{i4} = I_{qi}\left(\frac{K_{Ei}}{T_{Ei}}E_{fdi} - \frac{V_{Ri}}{T_{Ei}}\right) - \dot{I}_{qi}E_{fdi}
\end{aligned}
\tag{13}
$$

The electrical diagram of the generator using the flux-decay model is depicted in Fig. 2 [13] where the voltage source and injected current are represented as $E_i = \left(\left(x_{qi} - x'_{di}\right)I_{qi} + jE'_{qi}\right)e^{\left(\delta_i - \frac{\pi}{2}\right)}$ and, $I_i = \frac{E_i}{\mathrm{Z}_i}$. According to the figure and (11), the voltage source in Fig.2 can be represented as $E_i = \left(\left(x_{qi} - x'_{di}\right)B_{i,i+n}V_{i+n}\sin(\delta_i - \psi_{i+n}) + jE'_{qi}\right)e^{\left(\delta_i - \frac{\pi}{2}\right)}$.

Then, by applying $I = Y_{\mathbf{bus}}\bar{V}$ to the power network, where $I = \begin{bmatrix} I_1 & I_2 & \dots & I_n \end{bmatrix}^T$ and $\bar{V} = \begin{bmatrix} V_{n+1}e^{\psi_{n+1}} & V_{n+2}e^{\psi_{n+2}} & \dots & V_{2n}e^{\psi_{2n}} \end{bmatrix}^T$ we obtain

$$
\begin{aligned}
&\left(\left(x_{qi} - x'_{di}\right)B_{i,i+n}V_{i+n}\sin(\delta_i - \psi_{i+n}) + jE'_{qi}\right)e^{\left(\delta_i - \frac{\pi}{2}\right)} \\
&= \sum_{k=1}^{N} Y_{\mathrm{bus},ik}V_{k+n}e^{j\psi_{k+n}}
\end{aligned}
\tag{14}
$$

which yields

$$
\begin{aligned}
&\left(x_{qi} - x'_{di}\right)B_{i,i+n}V_{i+n}\sin(\delta_i - \psi_{i+n})\sin(\delta_i) + E'_{qi}\cos(\delta_i) \\
&= \mathrm{Re}\left(\sum_{k=1}^{N} Y_{\mathrm{bus},ik}V_{k+n}e^{j\psi_{k+n}}\right)
\end{aligned}
\tag{15}
$$

and

$$
\begin{aligned}
&-\left(x_{qi} - x'_{di}\right)B_{i,i+n}V_{i+n}\sin(\delta_i - \psi_{i+n})\cos(\delta_i) + E'_{qi}\sin(\delta_i) \\
&= \mathrm{Im}\left(\sum_{k=1}^{N} Y_{\mathrm{bus},ik}V_{k+n}e^{j\psi_{k+n}}\right)
\end{aligned}
\tag{16}
$$

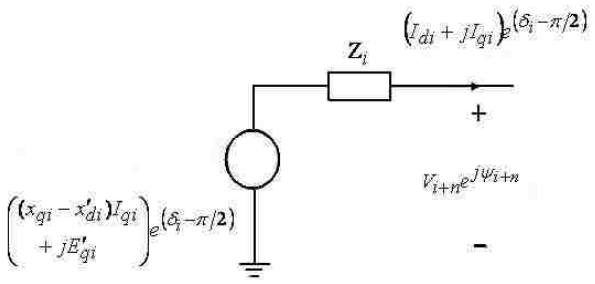

Fig.2 Generator flux-decay model

Remark 1. Here $Y_{\mathbf{bus}}$ may contain nonlinear impedances (including constant loads). Thus, even if the system $Y_{\mathbf{bus}}$ is reduced to an $n\times n$ matrix, non-generator bus voltages and angles are involved in computations. Thus, conventional $Y_{\mathbf{bus}}$ reduction techniques cannot be applied to overcome non-generator nodes.

C. Decentralized Nonlinear System Representation

The dynamical representation of the power system from (13) can be rewritten as a general class of L interconnected nonlinear subsystems in affine form as

$$\begin{cases} \dot{x}_{i1} = f_{i1}(x_{i1}) + g_{i1}(x_{i1})x_{i2} + \Delta_{i1}(\bar{X}_1) \\ \vdots \\ \dot{x}_{il} = f_{il}(X_{il}) + g_{il}(X_{il})u_i + \Delta_{il}(\bar{X}_l) \end{cases} \qquad (17)$$
$$h_i(X_{il}) = x_{i1}$$

where index i, $1\le i\le L$, represents the subsystem (generator) number, L is the number of subsystems (generators) in the power system, p, $1\le p\le l$, shows the generator state number, $l=4$ is the order of the power system according to (13), $f(.)$ and $g(.)$, represent unknown nonlinearities, $\Delta(.)$ denotes interconnected terms, with $X_{ip}=[x_{i1},\ldots,x_{ip}]^T$, $\bar{X}_p=[\breve{X}_1^T,\ldots,\breve{X}_p^T]^T$, $\breve{X}_j=[x_{1j},\ldots,x_{Lj}]^T$, $\bar{X}_0=0$ and $h_i(X_{il})$ is the subsystem output for

$1 \le i \le L$ and $1 \le p \le l$. By comparing the power system representation (13) and the general system description given by (17), it follows that $f_{i1} = f_{i2} = f_{i4} = 0$, $f_{i3} = -x_{i3}/T_{d0i}$, $g_{i1} = g_{i2} = 1$, $g_{i3} = 1/T_{d0i}M_i$, and $g_{i4} = I_{qi}$. Also, $\Delta_{i1} = \Delta_{i2} = 0$, with

$$\Delta_{i3} = \frac{1}{T_{d0i}}\left(x_{di} - x_{qi}\right)I_{qi}I_{qi} - E'_{qi}\dot{I}_{qi} - \left(x_{qi} - x'_{di}\right)\left(\dot{I}_{qi}I_{di} + I_{qi}\dot{I}_{di}\right), \tag{18}$$

$$\Delta_{i4} = -\dot{I}_{qi}E_{fdi}, \tag{19}$$

and

$$u_i = I_q\left(\frac{K_{Ei}}{T_{Ei}}E_{fdi} - \frac{V_{Ri}}{T_{Ei}}\right) \tag{20}$$

In the following, we find V and ψ as a function of the states δ, ω, and ΔP_e. Equations (15) and (16) yield expressions $E'_{qi}\cos(\delta_i)$ and $E'_{qi}\sin(\delta_i)$ as functions of δ, V, and ψ which in turn yields E'_{qi} and δ to be functions of V, and ψ as

$$E'_{qi} = \vartheta_{1i}(V,\psi),\ \delta_i = \vartheta_{2i}(V,\psi). \tag{21}$$

Consequently, by using (9), (10), and (21) the variables I_{qi} and I_{di} as well as P_{ei} can be represented as functions of V and ψ as

$$P_{ei} = \vartheta_{3i}(V,\psi) \tag{22}$$

Now, equations (11) and (21) (for $1 \le i \le L$) along with the $2N$ nodal power flow equations (3) give solutions for V and ψ in terms of δ_i for $1 \le i \le L$ as

$$V_{i+n} = \overline{\vartheta}_{1i}(\delta);\ \psi_{i+n} = \overline{\vartheta}_{2i}(\delta);\quad 1 \le i \le N \tag{23}$$

D. Interconnection Terms

In order to address the interconnection terms, the following assumption is needed for analyzing their upper bound.

Assumption 1: The excitation voltage, E_{fdi}, satisfies the following inequality [14] defined by

$$E_{fdi} \le \overline{\mathrm{K}}\left(E'_{qi} + (x_{di} - x'_{di})I_{di}\right) \tag{24}$$

where $\overline{\mathbf{K}}$ is a positive constant. Consequently, by (10) and (21) we have

$$E_{fdi} \le \vartheta_4(V, \psi) \tag{25}$$

Also, by employing (11), (21), and (25), equation (6) can be simplified to

$$\dot{V}_{i+n} \le c_{1i}(x_s);\ \dot{\psi}_{i+n} \le c_{2i}(x_s); \quad 1 \le i \le N \tag{26}$$

where $c_{1i}(.)$ and $c_{2i}(.)$ are positive nonlinear functions and $x_s = [\delta^T \quad \omega^T \quad V^T \quad \psi^T]^T$. Then, by using (22) and (23) we obtain

$$\dot{V}_{i+n} \le \bar{c}_{1i}(\delta, \omega, P_e);\ \dot{\psi}_{i+n} \le \bar{c}_{2i}(\delta, \omega, P_e); \quad 1 \le i \le N \tag{27}$$

where $\bar{c}_{1i}$ and $\bar{c}_{2i}$ are positive nonlinear functions. Now, by considering the interconnection term (18) along with (10), (23), (24), and (27) it can be shown that $\left|\Delta_{ip}\right| \le \bar{\delta}_i(\delta, \omega, \Delta P_e)$ for $3 \le p \le 4$. This step is only for model development and is not necessary for practical implementation.

Next, we show that Δ_{i3} and Δ_{i4} are zero at steady state condition. Obviously, at steady state, we have $x_{3i} = \Delta P_{ei}/M_i = 0$. Consequently, by using (18) at steady state, we obtain $\Delta_{i3s} = 1/T_{d0i}\left(x_{di} - x_{qi}\right)I_{qis}I_{qis}$ where the index "s" stands for steady state conditions. At steady state, the states x_{i1}, x_{i2}, and x_{i3} in (12) are zero. The term $(x_{qi} - x_{di})$ is zero for

round rotors and it is a small value for salient pole rotors. Therefore, $\Delta_{i3s}=0$. Also, since $\dot{x}_{3i}=0$ at steady state, we have $x_{4is}=0$. In addition, $\dot{I}_{qi}=0$ and $\Delta_{i4s}=0$. Consequently, at steady state $x_{i1}=x_{i2}=x_{i3}=x_{i4}=0$, we have $\Delta_{i3}(0)=\Delta_{i4}(0)=0$.

IV. The Decentralized DSC Controller Design

In this section, the design of the controller is now addressed. Equation (17) represents a nonlinear system in strict feedback form where a standard backstepping design can be applied. However, to overcome the repeated differentiation of virtual control inputs in backstepping, dynamic surface control design method [7] is utilized here where a first order filter is utilized instead of the derivative. However, due to the filter, additional error terms appear (i.e. y_{ip} in Fig. 3) which complicates the stability analysis. The variables used in Fig. 3 are $\Pi_{i1}=z_{i1}$ and $\Pi_{ip}=[X_{i,p-1}^T, z_{ip}, y_{ip}]^T$ where z_{ip} and y_{ip} are introduced in Fig. 3 for $1\le i\le L$ and $1\le p\le l$.

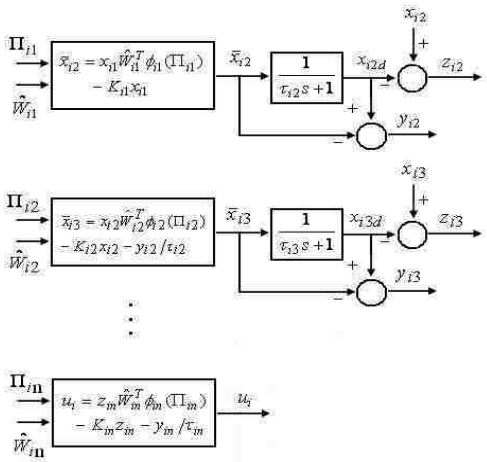

Fig.3 The DSC controller block diagram

Figure 3 illustrates the NN DSC controller design steps for the general system (17) where the interconnection and unknown nonlinear functions are present in each state dynamics. Therefore, one cannot use the assumption of matching condition. Instead, these terms have to be explicitly taken into account in the controller design which further complicates the stability analysis. Moreover, to deliver asymptotic stability, the NN weights have to be tuned appropriately. Finally, it is shown that if the following Assumptions are satisfied, the procedure shown in Fig. 3 can (semi-globally) stabilize the interconnected system (17) asymptotically where f_{ip}, g_{ip}, and Δ_{ip} are considered unknown as shown in Theorem 2.

Assumption 2: Assume that the interconnection terms in (17) are bounded above in a compact set Ω such that $\left|\Delta_{ip}(\bar{X}_p)\right| \le \sum_{j=1}^{N} \delta_{ipj}(X_{jp})$ where δ_{ipj} is an unknown function with $\delta_{ipj}(0) = 0$ for $1 \le i \le L$ and $1 \le p \le l$.

Assumption 3*:* The control gains $g_{ip}(X_{ip})$ for $1 \le i \le N$ and $1 \le p \le l$ satisfy $0 \le g_{ip}^{m} \le g_{ip}(X_{ip}) \le \bar{g}_{ip}(X_{ip})$.

Assumption 4: The nonlinear function in (17) satisfies $f_{ip}(0) = 0$ for $1 \le i \le L$ and $1 \le p \le l$.

A. Decentralized Controller Design

The DSC controller design procedure is explained now. Since there are no unknown terms in the generator state dynamics x_{i1} and x_{i2}, no NNs are utilized in the first two steps.

Step 1: Define the error as $z_{i1} = x_{i1} - x_{i1d}$ and $y_{i1} = \bar{x}_{i1} = 0$ where x_{i1d} is the desired set point for regulation. Now define $\bar{x}_{i2} = -K_{i1} z_{i1} + \dot{x}_{i1d}$ where $\bar{x}_{i2}$ is the desired virtual input to make $z_{i1} \to 0$ as $t \to \infty$. For the stabilization problem, the desired values become $x_{i1d} = \dot{x}_{i1d} = 0$. Next, the intermediate virtual input x_{i2d} is obtained by passing the desired virtual input $\bar{x}_{i2}$ through a first order filter consistent with the DSC literature [7] as

$$\tau_{i2} \dot{x}_{i2d} + x_{i2d} = \bar{x}_{i2} \tag{28}$$

Also, define $z_{i2} = x_{i2} - x_{i2d}$ and $y_{i2} = x_{i2d} - \bar{x}_{i2}$. Thus,

$$x_{i2} = z_{i2} + y_{i2} + \bar{x}_{i2} \tag{29}$$

Then, from (17) and (29), the error dynamic is given by

$$\dot{z}_{i1} = z_{i2} + y_{i2} + \bar{x}_{i2}. \tag{30}$$

Step 2: Define $\bar{x}_{i3} = -K_{i2} z_{i2} + \dot{x}_{i2d}$. By using (28), we get $\dot{x}_{i2d} = -y_{i2}/\tau_{i2}$; thus, $\bar{x}_{i3} = -K_{i2} z_{i2} - y_{i2}/\tau_{i2}$. Similarly, the intermediate virtual input x_{i3d} is obtained by passing $\bar{x}_{i3}$ through a first order filter as

$$\tau_{i3} \dot{x}_{i3d} + x_{i3d} = \bar{x}_{i3} \tag{31}$$

Define $z_{i3} = x_{i3} - x_{i3d}$ and $y_{i3} = x_{i3d} - \bar{x}_{i3}$ to obtain

$$x_{i3} = z_{i3} + y_{i3} + \bar{x}_{i3} \tag{32}$$

Thus, from (17) and (32) we have

$$\dot{z}_{i2} = z_{i3} + y_{i3} + \bar{x}_{i3} - \dot{x}_{i2d} \tag{33}$$

Step 3: Due to the presence of unknown interconnection terms in $\dot{x}_{i3}$, we use a NN approximator in the desired virtual control to approximate the unknown nonlinear dynamics. Since it is assumed that other subsystems (generators) states are not available

in subsystem (generator) *i*, the NN approximator is only a function of available states x_{i1} through x_{i4}, i.e. $\Phi_{i3}(\Pi_{i3}) = W_{i3}^T \phi_{i3}(\Pi_{i3}) + \varepsilon_{i3}$ where $\Phi_{i3}(\Pi_{i3})$ is part of unknown nonlinear function in $\dot{x}_{i3}$. In addition, the target NN weights W_{ip} and approximation error (for $1 \le i \le L$ and $1 \le p \le l$) are not known; thus, a tunable weight matrix is utilized [15] to calculate W_{ip} which results in $\hat{W}_{ip}$. Accordingly, we define the desired virtual control as $\bar{x}_{i4} = z_{i3}\hat{W}_{i3}^T \phi_{i3}(\Pi_{i3}) - K_{i3} z_{i2} + \dot{x}_{i3d}$. From (31) we obtain $\dot{x}_{i3d} = -y_{i3}/\tau_{i3}$; thus, $\bar{x}_{i4} = z_{i3}\hat{W}_{i3}^T \phi_{i3}(\Pi_{i3}) - K_{i3} z_{i3} - y_{i3}/\tau_{i3}$. Passing $\bar{x}_{i4}$ through a first order filter results in the intermediate virtual input x_{i4d} to be

$$\tau_{i4}\dot{x}_{i4d} + x_{i4d} = \bar{x}_{i4} \tag{34}$$

Define $z_{i4} = x_{i4} - x_{i4d}$ and $y_{i4} = x_{i4d} - \bar{x}_{i4}$ to obtain

$$x_{i4} = z_{i4} + y_{i4} + \bar{x}_{i4} \tag{35}$$

and

$$\dot{z}_{i3} = -\frac{x_{3i}}{T_{d0i}} + \frac{x_{i4}}{T_{d0i} M_i}(z_{i4} + y_{i4} + \bar{x}_{i4}) + \Delta_{i3} - \dot{x}_{i3d} \tag{36}$$

Step 4: Similar to step 3, in the last step, the desired virtual input is defined as

$$\bar{x}_{i5} = u_i = z_{i4}\hat{W}_{i4}^T \phi_{i4}(\Pi_{i4}) - K_{i4} z_{i4} - y_{i4}/\tau_{i4} \tag{37}$$

by using (34) to replace for $\dot{x}_{i4d}$. Note that, according to [7], there is no need for filtering the desired virtual input in the last step. Thus, z_{4i} dynamics can be written as

$$\dot{z}_{i4} = -\dot{I}_{qi} E_{fdi} + I_{qi} u_i + \Delta_{i4} - \dot{x}_{i4d} \tag{38}$$

Before proceeding, define $\bar{x}_{i1} = y_{i0} = y_{i1} = z_{i0} = K_{i0} = e_{i0} = 0$, $\tau_{i0} = \tau_{i1} = 1$ and $\tilde{W} = [\tilde{W}_{11}, \ldots \tilde{W}_{Nn}]$ where $\tilde{W}_{ip} = \hat{W}_{ip} - W_{ip}$ for $1 \le i \le L$ and $1 \le p \le l$.

B. Stability Analysis

Here, we discuss a novel NN weight update law by using the projection scheme [16] since NNs are utilized for nonlinear function approximation. An interesting property of updating the NN weights using the proposed projection scheme is the boundedness of the NN weights.

Theorem 1[16]**:** Assume that single-layer NNs are utilized to approximate the unknown nonlinearities of the system dynamics and the interconnection terms in (17). Let the NN weight tuning for the '*i*th' subsystem be provided by

$$\dot{\hat{W}}_{ip} = -\rho_{ip} z_{ip}^2 \phi_{ip}(\Pi_{ip}) - \rho_{ip} z_{ip}^2 \hat{W}_{ip} + \rho_{ip} z_{ip}^2 \chi \frac{\hat{W}_{ip}\hat{W}_{ip}^T}{\left\|\hat{W}_{ip}\right\|^2} \phi_{ip}(\Pi_{ip}) \tag{39}$$

where $\chi = 0$ *if* $\left\|\hat{W}_{ip}\right\| < W_{ip}^M$ *or* $\left\|\hat{W}_{ip}\right\| = W_{ip}^M \,\&\, \hat{W}_{ip}^T z_{ip}^2 \phi_{ip}(\Pi_{ip}) \geq 0$; $\chi = 1$ *if* $\left\|\hat{W}_{ip}\right\| = W_{ip}^M \,\&\, \hat{W}_{ip}^T z_{ip}^2 \phi_{ip}(\Pi_{ip}) < 0$; $\chi = 1$ *if* $\left\|\hat{W}_{ip}\right\| > W_{ip}^M$ for all $1 \leq i \leq L$ and $1 \leq p \leq l$, with W_{ip}^M denoting the user selected bound for the weights $\left\|\hat{W}_{ip}\right\|$. Then, the weight estimates remain within the user selected bound such that $\left\|\hat{W}_{ip}\right\| \leq W_{ip}^M$ for $t \geq 0$ provided the initial weights start within the set defined by $\left\|\hat{W}_{ip}\right\| \leq W_{ip}^M$ at $t = 0$; ■

The NN weight update law is a variant of the projection algorithm [17] wherein a quadratic term of the error is employed along with a new term $\rho_{ip} z_{ip}^2 \hat{W}_{ip}$ for relaxing the PE (Persistency of Excitation) condition. This ensures asymptotic stability in error dynamics z_{ip} and y_{ip} for all $1 \leq i \leq L$ and $1 \leq p \leq l$. The user selected bound W_{ip}^M on the NN weights can play an important role for the function approximation. Conservative bound selection (i.e. small W_{ip}^M) can result in significant reconstruction errors, which should be avoided.

This may cause the weight estimates $\hat{W}_{ip}$ to stay away from the actual weights W_{ip}. Nevertheless, the system errors regulate asymptotically to zero while the weight estimation $\hat{W}_{ip}$ are bounded.

Theorem 2: Consider the nonlinear interconnected system given by (17). Consider the Assumptions 2-4 hold and let the unknown nonlinearities in the subsystems and interconnection terms be approximated by NNs. Let the NN weight update be provided by (39), then there exist a set of control gains K_{ip} and filter time constants, τ_{ip} ,associated with the given control inputs such that the states z_{ip} and y_{ip} approach to zero asymptotically (local) for all for $1 \le i \le L$ and $1 \le p \le l$. ■

It is shown in [16] that if the Assumptions 2-4 hold and the unknown nonlinearities in the subsystems and interconnection terms are approximated by NNs the states z_{ip} and y_{ip} approach zero asymptotically for all $1 \le i \le L$ and $1 \le p \le l$ provided that the NN weight update is provided by (39) and control gains K_{ip} and filter time constants, τ_{ip} are chosen properly. In addition, from Section III, a power system satisfies Assumptions 2 through 4.

V. Simulation Results

The method introduced in Section III is utilized to design damping controller for generator excitation control. The proposed design is summarized in Table 1 and a comparison of design complexity with backstepping method is given. Note the increased complexity when dealing with the term dx'_{i4d}/dt in backstepping (in row 11). In the

Table, K_{ip} is the stabilizing design constant for $1 \le i \le n$ where n is the number of generators in the multi-machine power system and $1 \le p \le 4$.

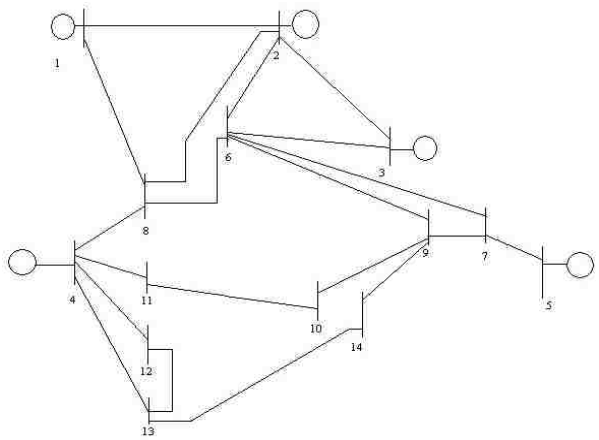

Fig. 4 The IEEE 14-bus, 5-generator power system

Also, τ_{ip} is the filter time constant at each step p for $2 \le p \le 4$. In addition, $\hat{W}_{i3}$ and $\hat{W}_{i4}$ are the NN weight estimate matrix while $\phi_{i3}(.)$ and $\phi_{i4}(.)$ are the NN activation function vector. Since there are no unknown terms in the first and second state dynamics only two NN are utilized per generator. In other words, the generator angle and speed dynamics do not require NN approximators. The IEEE 14-bus, 5-generator power system shown in Fig. 4 is considered and it is subjected to a three-phase disturbance. The generator data are given as $x'_{di} = 0.006$, $x_{di} = 0.02$, $x_{qi} = 0.019$, $T_{d0i} = 7$, $K_{Ei} = 1$, $T_{Ei} = 0.75$ for $1 \le i \le 5$ whereas $H_i = \omega_s M_i / 2 = 5$ for $i = 1,4,5$; and $H_i = 1$ for $i = 2,3$. The power system load specifications are given in Table 2. All the generators have speed governors and the excitation control is implemented by employing the DSC-based NN controller as proposed in (37) and (39). The power system loads are considered as

constants. The control objective is to damp the generators oscillations caused by a three-phase fault.

Although the stability analysis is based on the lossless power system dynamical model as described in (6), the simulations are performed using the complete power system dynamic representation with line resistances and two-axis generator model in order to evaluate the effectiveness of the representation and the controller design.

The power system modes are 11.3561, 5.9101, 2.6977, and 2.1026Hz. A three-phase disturbance is injected to the bus 1, 6, and 11 at $t = 0.2s$ and removed at $t = 0.4s$ seconds. Generators 1 through 5 are chosen for control. The control inputs u_i and weight estimate 10×1 (i.e. 10 neurons are used in the output layer) matrices $\hat{W}_{i3}$ and $\hat{W}_{i4}$ (for $1 \le i \le 5$) are obtained by using (37) and (39), respectively, where the NN weights are tuned throughout the simulations by using on-line learning. The voltage V_{Ri} is calculated using (20) and is subjected to hard limits such that the voltage satisfies $0 \le V_{Ri} \le 7$ p.u. to avoid any impractical excitation voltages E_{fdi}.

The design gains and filter time constants are chosen as follows: $K_{11} = 0.001$; $K_{21} = K_{31} = K_{41} = K_{51} = 0.0001$; $K_{12} = 0.002$; $K_{22} = K_{32} = K_{42} = K_{52} = 0.0002$; $K_{13} = 5$; $K_{23} = K_{33} = K_{43} = K_{53} = 0.5$; $K_{14} = 5.1$; $K_{24} = K_{34} = K_{44} = K_{54} = 0.51$; $\tau_{21} = .5$; $\tau_{22} = \tau_{23} = \tau_{24} = \tau_{25} = 5$; $\tau_{31} = 0.2$; $\tau_{32} = \tau_{33} = \tau_{34} = \tau_{35} = 2$; $\tau_{41} = 0.1$; $\tau_{42} = \tau_{43} = \tau_{44} = \tau_{45} = 1$; $\rho_{ip} = 0.1$ for $1 \le i \le 5$ and $2 \le p \le 4$. The weight estimate matrices $\hat{W}_{i3}$ and $\hat{W}_{i4}$ are initialized randomly for $1 \le i \le 5$. Moreover, no offline training is used to tune the weights in advance and no initial knowledge about the power system dynamics, complete knowledge of interconnection dynamics, or power system topology are needed for the controller design.

Table 1. DSC NN design procedure

Sequence		DSC	Backstepping
1	errors	$z_{i1} = x_{i1}; y_{i1} = \bar{x}_{i1} = 0$	$z'_{i1} = x_{i1}$
2	filter input	$\bar{x}_{i2} = -K_{i1} z_{i1}$	N/A
3	virtual input	$\tau_{i2} \dot{x}_{i2d} + x_{i2d} = \bar{x}_{i2}$	$x'_{i2d} = -K'_{i1} z'_{i1}$
4	errors	$z_{i2} = x_{i2} - x_{i2d}$ $y_{i2} = x_{i2d} - \bar{x}_{i2}$	$z'_{i2} = x_{i2} - x'_{i2d}$
5	filter input	$\bar{x}_{i3} = -K_{i2} z_{i2} - y_{i2}/\tau_{i2}$	N/A
6	virtual input	$\tau_{i3} \dot{x}_{i3d} + x_{i3d} = \bar{x}_{i3}$	$x'_{i3d} = -x_{i1} - K'_{i1} x_{i2} - K'_{i2} z'_{i2}$
7	errors	$z_{i3} = x_{i3} - x_{i3d}$ $y_{i3} = x_{i3d} - \bar{x}_{i3}$	$z'_{i3} = x_{i3} - x'_{i3d}$
8	filter input	$\bar{x}_{i4} = z_{i3} \hat{W}_{i3}^T \phi_{i3}(\Pi_{i3})$ $- K_{i3} z_{i3} - y_{i3}/\tau_{i3}$	N/A
9	virtual input	$\tau_{i4} \dot{x}_{i4d} + x_{i4d} = \bar{x}_{i4}$	$x'_{i4d} = z'_{i3} \hat{W}_{i3}^T \phi_{i3}(X_{i3}) - K'_{i3} z$ $- x_{i3}(-1/T_{d0i} + K'_{i2} K'_{i1} + K'_{i}$ $- K'_{i2}/T_{d0i}) \times \frac{T_{d0i} M_i}{K'_{i2} + 1}$ $- \frac{T_{d0i} M_i}{K'_{i2} + 1} z'_{i2}$
10	errors	$z_{i4} = x_{i4} - x_{i4d}$ $y_{i4} = x_{i4d} - \bar{x}_{i4}$	$z'_{i4} = x_{i4} - x'_{i4d}$
11	input	$u_i = z_{i4} \hat{W}_{i4}^T \phi_{i4}(\Pi_{i4})$ $- K_{i4} z_{i4} - y_{i4}/\tau_{i4}$	$u'_i = z'_{i4} \hat{W}_{i4}^T \phi_{i4}(X_{i4})$ $- K'_{i4} z'_{i4} - \frac{dx'_{i4d}}{dt}$
12	V_{Ri}	$V_{Ri} = T_{Ei}(u_i/I_{qi}$ $- K_{Ei}/T_{Ei} \times E_{fdi})$	$V_{Ri} = T_{Ei}(u'_i/I_{qi}$ $- K_{Ei}/T_{Ei} \times E_{fdi})$

Table 2. Power System Loads and Generations

Gen no.	P (p.u.)	Q (p.u.)	Gen no.	P (p.u.)	Q (p.u.)
1(slack)	-3.1184	0.2950	7	0.0000	0.0000
2	-0.1830	-0.4509	8	0.0760	0.0160
3	0.9420	-0.0846	9	0.5950	0.1660
4	0.1120	-0.4601	10	0.3900	0.0580
5	-0.1120	-0.3102	11	0.0350	0.0180
6	0.4780	-0.0390	12	0.0610	0.0160

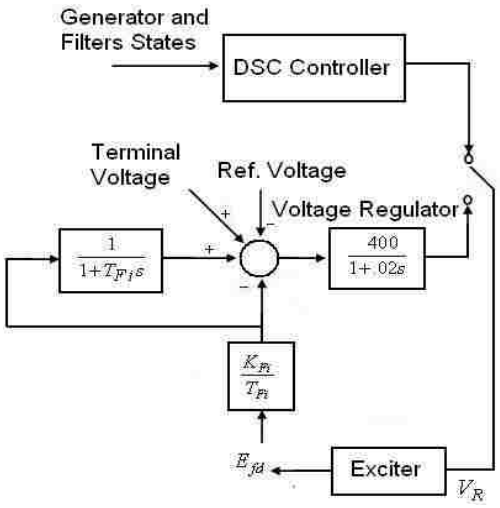

Fig. 5 Excitation/VR controller block diagram

The NN activation function is chosen as $\phi_{ip}(\Pi_{ip}) = sigmoid\,(V_{ip}{}^{T}\Pi_{ip})$ [16] for $3 \le p \le 4$ where V_{ip} is chosen at random initially and held fixed afterwards to form a set of basis functions needed for the NN approximation [10].

For comparison, the results from the DSC design are compared with a voltage regulator (VR) (in the presence of steam governor) shown in Fig. 5. The VR is designed by using conventional methods [13] defined by $G_{\mathrm{A}i}(s) = 400/(1+.02s)$ for $1 \le i \le 5$. In addition, $K_{Fi} = 0.03$ and $T_{Fi} = 10$ are employed. Figures 6 through 8 depict that a significant oscillation damping is achieved for a medium size power network by using the proposed decentralized controller when compared to the case with conventional controller.

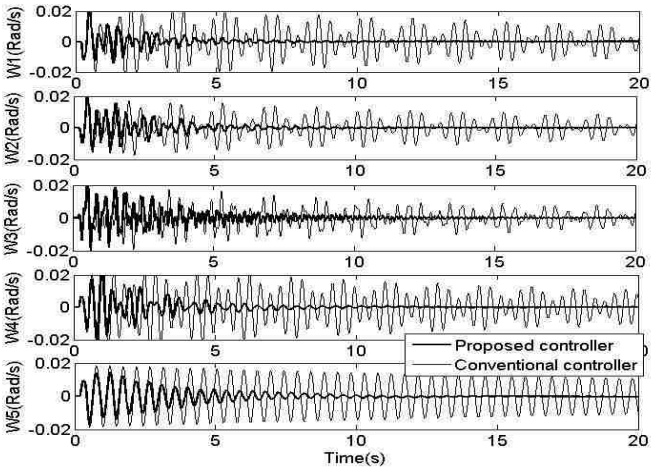

Fig. 6 Generator speeds with DSC/VR control with fault on bus 1

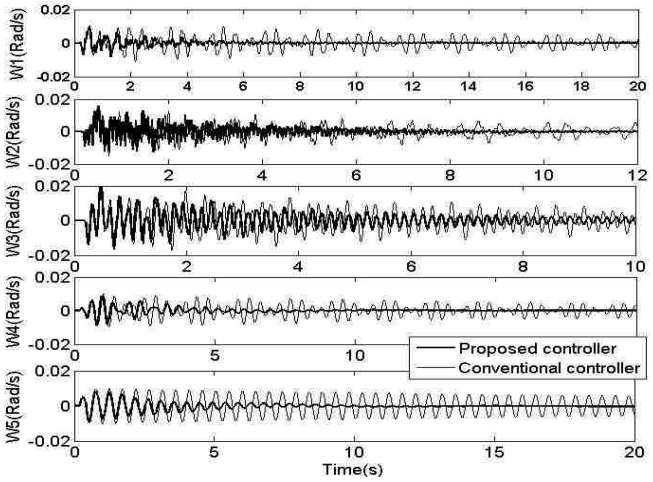

Fig. 7 Generator speeds with DSC/VR control with fault on bus 6

Moreover, Figs. 6 through 8 illustrate the robustness of the proposed controller where the oscillations from the faults occurring at different locations have been damped without changing the gains and filter time constants even when the subsystem dynamics and interconnection effects are unknown. Note, however, that damping performance

varies with the fault location. This is due to different after-fault conditions imposed on the controller.

Figure 9 shows that the variations in excitation voltages, E_{fd}, have fast transients as well as slow dynamics where the fast transients are damped in the first few seconds where the slow dynamics are due to the generator speed controller (governor) and are damped in a longer time. The NN weight estimates in Fig. 10 are bounded as expected. Overall, from these results, the proposed control is very effective in damping the oscillations even in the presence of numerous modes.

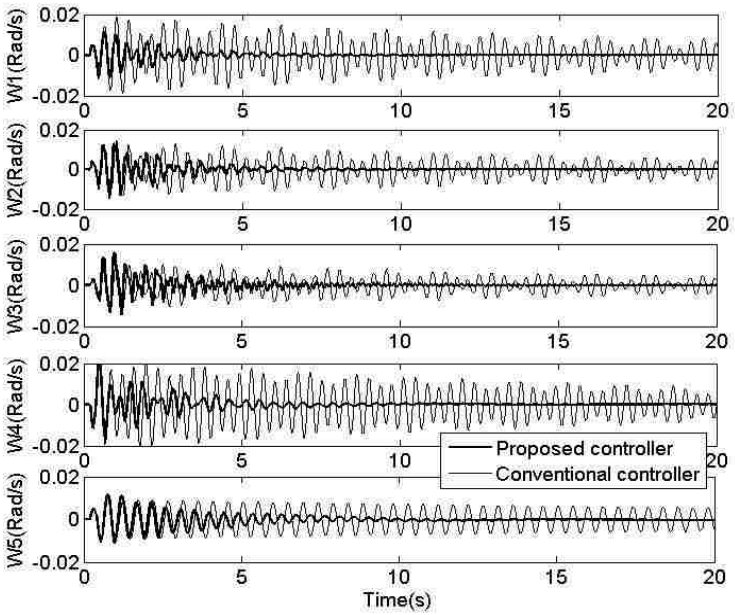

Fig. 8 Generator speeds with DSC/VR control with fault on bus 11

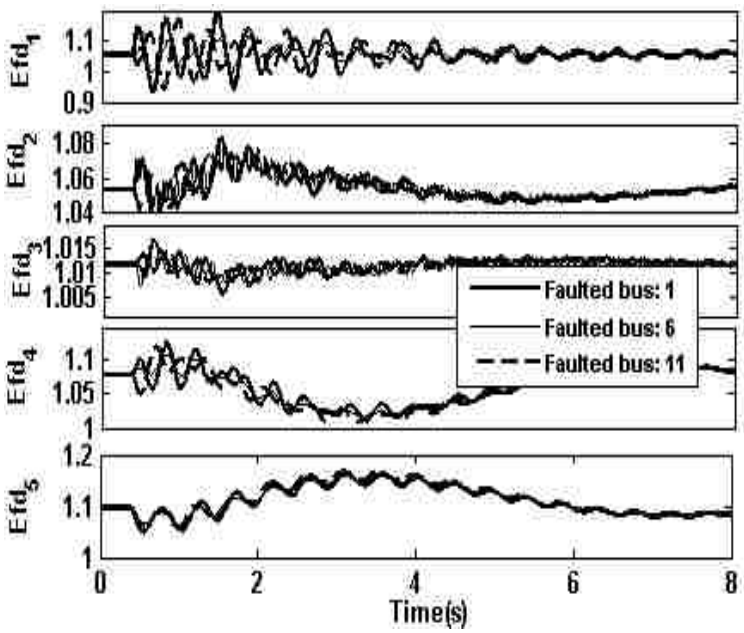

Fig. 9 Generator internal voltages with fault on bus 1, 6, and 11

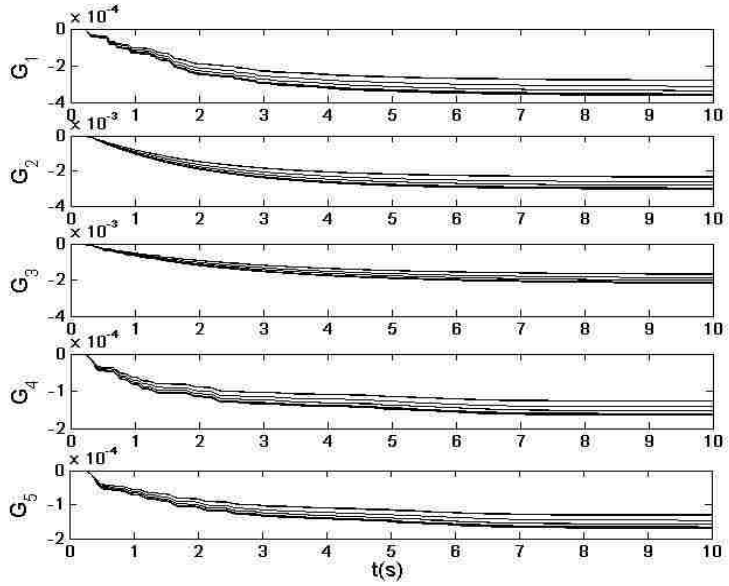

Fig. 10 Neural network weight estimates $\hat{w}_{i3}$ with fault on bus 6

VI. Conclusions

In this paper, the power system is represented as a large scale interconnected nonlinear system with uncertainties in both subsystem and the interconnection terms where the system does not satisfy the matching condition. By using a new variant of the projection scheme and dynamic surface control with NNs, the need for the repeated differentiation in the backstepping design procedure was overcome. The neural network approximation property is used to approximate the nonlinearities of the subsystems and interconnected terms. It is shown that the closed loop system is asymptotically regulated to zero with state feedback control even in the presence of NN function reconstruction errors. Simulation results on power system with generator excitation control shows the effectiveness of the approach in damping oscillations that occurs after faults in power systems.

References

[1] E. Davison and N. Tripathi, "The Optimal Decentralized Control of a Large Power System: Load and Frequency Control," *IEEE Transactions on Automatic Control*, vol. 23, no. 2, pp.:312 – 325, 1978.

[2] K. Ohtsuka, Y. Morioka, "A Decentralized Control System for Stabilizing a Longitudinal Power System Using Tieline Power Flow Measurements," *IEEE Transactions on Power Systems*, vol. 12, no. 3, pp.:1202 – 1209, 1997.

[3] G.K. Befekadu and I. Erlich, "Robust Decentralized Controller Design for Power Systems Using Matrix Inequalities Approaches," *IEEE Power Engineering Society General Meeting*, 2006.

[4] S. Xie, L. Xie, Y. Wang, and G. Guo, "Decentralized Control of Multi Machine Power Systems ith Guaranteed Performance," *Proceedings of IEE Control Theory and Appls*, vol. 147, no. 3, pp.355 – 365, May 2000.

[5] W. Liu,S. Jagannathan, G. K. Venayagamoorthy, D. C. Wunsch, M. L. Crow, L. Liu, and D. A. Cartes, "Neural Network Based Decentralized Controls of Large Scale Power Systems," *IEEE International Symposium on Intelligent Control*, pp.:676 - 681 Singapore, 1-3 October 2007.

[6] W. Qiu, V. Vittal, and M. Khammash, "Decentralized Power System Stabilizer Design Using Linear Parameter Varying Approach," *IEEE Transactions on Power Systems*, vol. 19, no. 4, pp.: 1951 – 1960, 2004.

[7] D. Swaroop, J.K. Hedrick, P.P. Yip and J.C. Gerdes; "Dynamic Surface Control for a Class of Nonlinear Systems," *IEEE Transactions on Automatic Control*, vol. 45, no. 10, pp. 1893 – 1899, Oct. 2000.

[8] P. P. Yip and J. K. Hedrick, "Adaptive Dynamic Surface Control: A Simplified Algorithm for Adaptive Backstepping Control of Nonlinear Systems," *Int. J. Control*, vol. 71, no. 5, pp. 959–979, 1998.

[9] D. Wang and J. Huang, "Neural Network-based Adaptive Dynamic Surface Control for a Class of Uncertain Nonlinear Systems in Strict-feedback Form," *IEEE Tran. on Neural Networks*, vol. 16, no. 1, pp. 195 – 202, 2005.

[10] B. Igelnik and Y. H. Pao, "Stochastic Choice of Basis Functions in Adaptive Function Approximation and the Functional-link Net," *IEEE Trans. Neural Network*, vol. 6, no. 6, pp. 1320–1329, Nov. 1995.

[11] "IEEE/CIGRE Joint Task Force on Stability Terms and Definitions, Definition and Classification of Power System Stability," IEEE *Trans. on Power Systems*, vol. 19, no. 3, pp.: 1387 - 1401, May 2004.

[12] S. Mehraeen, S. Jagannathan, M. L. Crow, "Novel Dynamic Representation and Control of Power Networks Embedded with FACTS Devices," *Proceedings of IEEE Conference on System, Man and Cybernetics*, pp.: 3171 - 3176, Oct. 2008.

[13] P.W. Sauer and M.A. Pai, *Power System Dynamics and Stability*, Prentice Hall, 1997.

[14] Y. Guo, D. J. Hill, and Y. Wang, "Nonlinear Decentralized Control of Large Scale Power Systems," *Automatica*, vol. 36, no. 9, pp. 1275-1289, 2000.

[15] F**.** Lewis**,** S**.** Jagannathan**,** S**.,** and A. Yesildirek, *Neural Network Control of Robot. Manipulators and Nonlinear Systems*, Taylor & Francis, 1998.

[16] S. Mehraeen, S. Jagannathan, and M.L. Crow, "Decentralized Control of Large Scale Interconnected Systems Using Adaptive Neural Network-based Dynamic Surface Control," *Proceedings of International Joint Conference on Neural Networks (IJCNN)*, pp.: 2058 – 2064, 14-19 June 2009.

[17] K.S. Narendra and A.M. Annaswamy, *Stable Adaptive Systems*, Dover Publications. 2005.

[18] H.K. Khalil, *Nonlinear Systems*, Prentice Hall, New Jersey, 2002.

4. Decentralized Adaptive Neural Network Control of a Class of Interconnected Nonlinear Discrete-time Systems with Application to Power Systems

S. Mehraeen, S. Jagannathan, and M. L. Crow[1]

***Abstract*—** *In this paper, a novel decentralized controller is introduced for a class of interconnected nonlinear discrete-time systems in affine form with unknown subsystem and interconnection dynamics. A single neural network (NN) is utilized in the proposed decentralized controller to overcome the unknown internal dynamics as well as the control gain matrix of each subsystem while the unknown interconnection terms are accommodated by using a mild assumption. All NN weights are tuned online by using a novel update law. By using Lyapunov techniques, all subsystems signals are shown to be uniformly ultimately bounded (UUB). Simulation results are shown on a general interconnected nonlinear discrete-time system in affine form first to show the effectiveness of the approach. Subsequently, interconnected electric power system with excitation control is considered as an example and the proposed controller is utilized to mitigate the power fluctuations after a disturbance has occurred.*

Index Terms –Decentralized Control, Neural Networks (NN), Interconnected Nonlinear Discrete-time (DT) Systems.

[1] Authors are with Department of Electrical and Computer Engineering, Missouri University of Science and Technology, 1870 Miner Circle, Rolla, MO 65409. Contact author: sm347@mst.edu. Research Supported in part by NSF ECCS#0624644.

I. Introduction

In the recent years, there has been a great interest in the decentralized control of interconnected nonlinear systems using neural networks (NNs) [1-6]. The decentralized control effort has focused mainly on nonlinear continuous-time systems [1-4] and limited effort has been applied for the discrete-time case [5][6]. Although for many applications, continuous-time controller design can be considered, in practice discrete-time control approaches are preferred for computer implementations [7] since controller designs in continuous-time become unsatisfactory when implemented using low sampled hardware. Moreover, due to sheer size of large-scale interconnected systems such as electric power systems, the feedback delays degrade the controller performance thus necessitating more decentralized control techniques. Therefore, decentralized controller development in discrete-time has to be explicitly considered for large-scale systems.

Decentralized control (DC) techniques in continuous-time [8-13] have been developed for power systems in order to obtain steady state behavior as well as transient stability by means of damping oscillations caused by disturbances. However, many authors [8-11] have not offered stability proofs except simulation results on power systems. On the other hand, in [12], a decentralized neural network (NN) control of a general class of nonlinear continuous-time systems in strict feedback form has been proposed for power systems by using backstepping when certain system dynamics are not known. Rigorous proofs are offered in this paper although the controller design is presented in continuous-time in comparison with a centralized discrete-time controller design for power systems in [14]. However, the decentralized controller development in discrete-time to treat the large-scale systems such as the power systems is not yet

undertaken due to the fact that the stability proofs in discrete-time are more involved than their continuous-time counterparts since the first difference of a Lyapunov function candidate is quadratic with respect to the states whereas it is linear for the case of continuous-time system.

Therefore, in [5] the discrete-time NN controller design for a class of interconnected nonlinear systems is considered where the interconnected terms are considered to be over bounded by a constant. Moreover, the control gain matrix is taken to be unity (i.e. $g(x)=1$). In [6] the interconnected system in discrete-time is considered and a stabilizing robust controller is proposed. However, the controller does not utilize the NN to approximate the system uncertainties.

In this work, a novel decentralized NN controller is developed for a class of interconnected nonlinear discrete-time system in Brunovsky canonical form where these restrictions are relaxed while realizing that the subsystem internal dynamics, input coefficient matrix, and the interconnected terms are unknown. A single NN is used to approximate the control gain matrix $g(x)$ as well as the subsystem internal dynamics $f(x)$ for each subsystem. By using Lyapunov stability approach, boundedness of the tracking errors as well as the NN weights are proven. Moreover, the generator excitation control problem in the electric power systems can be expressed as an interconnected nonlinear discrete-time system. Consequently, the proposed decentralized NN control approach is applied as a damping controller to reduce generator excitation voltage oscillations caused by disturbances.

This paper is organized as follows. First, the class of interconnected nonlinear discrete-time system in affine form and its associated decentralized NN controller

development are introduced in Section II. Section III presents the power system discrete-time model development, while numerical simulations and concluding remarks are provided in Sections IV and V, respectively.

II. Nonlinear Interconnected System

Consider the class of N interconnected subsystems defined as

$$\begin{aligned} x_{i1}(k+1) &= f_{i1}(x_i(k)) \\ &\vdots \\ x_{in-1}(k+1) &= f_{i,n-1}(x_i(k)) \\ x_{in}(k+1) &= f_{in}(x_i(k)) + g_i(x_i(k))u_i + \Delta_i(x) \\ y_i(k) &= x_{i1}(k) \end{aligned} \tag{1}$$

where index i represents the subsystem number, N is the number of subsystems, n is the order of the subsystem, $f_{i1}(x_i(k))$ to $f_{in}(x_i(k))$ are functions of the subsystem states and represent subsystem nonlinear internal dynamics, $g_i(x_i(k))$ is the input gain matrix, $\Delta_i(x)$ denotes interconnected terms of the subsystem 'i' with $x=[x_1^T,\ldots,x_N^T]^T$, $x_i=[x_{i1},\ldots,x_{in}]^T$ for $1\le i\le N$. Note that, the Brunovsky Canonical form is an especial case of system (1). Define the tracking error as

$$z_{ip}(k) = x_{ip}(k) - x_{ipd}(k) \tag{2}$$

for $1\le i\le N$ and $1\le p\le n$, where $x_{ipd}(k)$ is the desired trajectory for the state $x_{ip}(k)$, and $x_{id}=[x_{i1d}\ldots x_{ind}]^T$ for $1\le p\le n$. Next, define the filtered tracking error as

$$r_i(k) = [\lambda_i\ 1]^T z_i(k) \tag{3}$$

where $z_i(k)=[z_{i1}(k)\ z_{i2}(k)\ \ldots z_{in}(k)]^T$ and $\lambda_i=[\lambda_{i1}\ \lambda_{i2}\ \ldots\lambda_{i,n-1}]$. The coefficients λ_{i1} through λ_{ip} are selected such that the poles of the characteristic equation $\zeta(q)=\lambda_{i1}+\lambda_{i2}q+\cdots+\lambda_{i,n-1}q^{n-2}+q^{n-1}$ are inside the unit disc. Note that for system stabilization, the desired

values become $x_{ipd} = 0$ for $1 \le p \le n$. Before we proceed, the following mild assumptions and definition are needed.

Assumption 1: Let the interconnection terms in (1) be bounded above in a compact set Ω such that

$$|\Delta_i(x)|^2 \le \sum_{j=1}^{N} \delta_{ij}(r_j) \le \delta_{0i} + \sum_{j=1}^{N} \gamma_{ij} r_j^{\,2} \tag{4}$$

where δ_{0i} and γ_{ij} are known small positive constants for $1 \le i \le N$ and $1 \le j \le n$ in contrast with [5].

Assumption 2: The input gain $g_i(x_i(k))$ of each subsystem in (1) is bounded away from zero and is overbounded in the compact set Ω. Without loss of generality, we assume that it is positive and satisfies

$$0 < g_{i\min} \le |g_i(x_i(k))| \le g_{i\max} \tag{5}$$

in a compact set Ω where $g_{i\min}$ and $g_{i\max}$ are positive real constants.

Remark 1: Assumptions 1 and 2 are standard in the control literature [16].

Definition. (*Uniform Ultimate Bounded (UUB)*)[20]. Consider the dynamical system $\dot{x} = f(x)$ with $x \in \Re^n$ being a state vector. Let the initial time be t_0 and initial condition be $x_0 = x(t_0)$. Then, the equilibrium point x_e is said to be UUB if there exists a compact set $S \subset \Re^n$ so that for all $x_0 \in S$ there exists a bound B and a time $T(B, x_0)$ such that $\|x(t) - x_e\| \le B$ for $\forall t > t_0 + T$.

Next the decentralized controller development is introduced.

A. Controller Design

In this part we develop a NN controller which employs the filtered tracking error and NN function approximation capability and a novel NN weight estimate tuning scheme. The stability criterion is then elaborated to show the stability of the filtered tracking error as well as NN weight estimates.

Starting with (3), the filtered tracking error dynamic can be written by using (1) and (2) as

$$r_i(k+1) = [\lambda_i \ 1]^T z_i(k+1) = g_i(x_i(k)) \times \left(\frac{f_{in}(x_i(k)) - x_{ind}(k+1) + \sum_{p=1}^{n-1} \lambda_{ip} (f_{ip}(x_i(k)) - x_{ipd}(k+1)}{g_i(x_i(k))} + u_i + \frac{\Delta_i(X)}{g_i(x_i(k))} \right) .$$

The ideal stabilizing control input can be defined as $u_i = u_i^* = u_{id} + K_i r_i(k)$ where $u_{id} = -g_i(x_i(k))^{-1} \left(f_{in}(x_i(k)) - x_{ind}(k+1) + \sum_{p=1}^{n-1} \lambda_{ip} (f_{ip}(x_i(k)) - x_{ipd}(k+1)) \right)$ to achieve asymptotically stable dynamic $r_i(k+1) = K_i r_i(k)$ where $K_i < 1$ is a positive design constant. However, in practical applications u_{id} is not available since the internal dynamics $f_{ip}(x_i(k))$ and control gain matrix $g_i(x_i(k))$ are unknown for $1 \le i \le N$ and $1 \le p \le n$. Thus, we employ NN function approximation property to approximate u_{id} as (6)

$$\begin{aligned} u_{id} &= -g_i(x_i(k))^{-1} \times \\ &\left(f_{in}(x_i(k)) - x_{ind}(k+1) + \sum_{p=1}^{n-1} \lambda_{ip} (f_{ip}(x_i(k)) - x_{ipd}(k+1)) \right) \\ &= W_i^T \rho_i(x_i, x_{id}(k+1)) - \varepsilon_i(x_i, x_{id}(k+1)) \end{aligned} \quad (6)$$

where W_i is the NN ideal weight matrix and $\varepsilon_i(.)$ is the approximation error which satisfies $\|\varepsilon_i(.)\| \le \varepsilon_{i\max}$. In practice, the ideal weights W_i and approximation error ε_i are not

available either and only an estimation of the NN weights is available. Thus, u_{id} is approximated as $\hat{u}_{id}$ by a NN to obtain the control input u_i as (7)

$$u_i = \hat{u}_{id} + K_i r_i(k) = \hat{W}_i^T \rho_i(x_i, x_{id}(k+1)) + K_i r_i(k) \tag{7}$$

where $\hat{W}_i^T$ is the NN weight estimation matrix. Define the weight estimation error as $\tilde{W}_i = \hat{W}_i - W_i$. Consequently, by using (7) and adding and subtracting u_{id} in (6), the filtered tracking error (3) dynamics becomes

$$\begin{aligned} r_i(k+1) &= [\lambda_i \ 1]^T z_i(k+1) \\ &= f_{in}(x_i(k)) - x_{ind}(k+1) + \sum_{p=1}^{n-1} \lambda_{ip} (f_{ip}(x_i(k)) - x_{ipd}(k+1) \\ &+ g_i(x_i(k)) \left(\hat{W}_i^T \rho_i + K_i r_i + u_{id} - u_{id} \right) + \Delta_i(x) \\ &= g_i(x_i(k)) \left(\tilde{W}_i^T \rho_i + \varepsilon_i + K_i r_i \right) + \Delta_i(x) \end{aligned} \tag{8}$$

Define the NN weight update law as

$$\hat{W}_i^T(k+1) = c_i \hat{W}_i(k) - c_i^{-1} \alpha_i \rho_i r_i(k+1) \tag{9}$$

where $c_i < 1$ is a design positive constant. By using $W_i(k+1) = W_i(k)$, and subtracting the ideal weights from (9), we have

$$\tilde{W}_i^T(k+1) = c_i \tilde{W}_i(k) - c_i^{-1} \alpha_i \rho_i r_i(k+1) - (I - c_i) W_i \tag{10}$$

B. Stability Analysis

In this part we prove that the nonlinear discrete-time interconnected system (1) along with controller (7) and the NN weight update law (9) are stable while the tracking errors $r_i(k)$ and weight estimation errors $\tilde{W}_i(k)$ of the individual subsystems are bounded in the presence of unknown internal dynamics $f_i(x_i(k))$, unknown control gain matrix $g_i(x_i(k))$, and unknown interconnection terms $\Delta_i(X)$ for $1 \le i \le N$. We introduce the following theorem to show the stability of the interconnected system as well as the NN

weight estimation errors. This theorem guaranties boundedness of the weight estimation errors $\tilde{W}_i(k)$ and the filtered tracking errors $r_i(k)$. Once the filtered tracking error $r_i(k)$ is proven bounded, it is treated as a bounded input $r_i(k)$ for the linear time-invariant system (3) as $\lambda_{i1}z_{i1}(k)+\cdots+\lambda_{i,n-1}z_{i1}(k+n-2)+\ z_{i1}(k+n-1)=r_i(k)$ which yields bounded results for the output $z_{i1}(k)$ for all $1\le i\le N$.

Theorem 1 ***(Discrete-time Decentralized NN Controller Stability)****: Consider the nonlinear discrete-time interconnected system given by (1). Consider the Assumptions 1 and 2 hold and that the desired trajectory* x_{ipd} *(for all* $1\le i\le N$ *and* $1\le p\le n$*) and initial conditions for system (1) are bounded in the compact set* Ω*. Let the unknown nonlinearities in each subsystem be approximated by a NN whose weight update is provided by (9). Then there exist a set of control gains* K_i *and filter tracking error coefficients* λ_i*, associated with the given control inputs (7) such that the filtered tracking error* $r_i(k)$ *as well as the NN weight estimation error* $\tilde{W}_i$ *are UUB for all* $1\le i\le N$.

Proof. Define the overall Lyapunov function candidate $L=L_W+L_r$, where $L_r(k)=\sum_{i=1}^{N}\left(\frac{r_i(k)}{\sqrt{g_i(x(k-1))}}\right)^2$ and $L_W(k)=\sum_{i=1}^{N}\frac{1}{\alpha_i}\tilde{W}_i^T(k)\tilde{W}_i(k)$. Then, the first difference of the Lyapunov function due to the first term becomes

$$\Delta L_r=\sum_{i=1}^{N}\left(\frac{r_i(k+1)}{\sqrt{g_i(x(k))}}\right)^2-\sum_{i=1}^{N}\left(\frac{r_i(k)}{\sqrt{g_i(x(k-1))}}\right)^2 \tag{11}$$

Substituting the filtered tracking error (8) into (11) and expanding the terms, we obtain

$$\begin{aligned}\Delta L_r &= \sum_{i=1}^{N} \Delta L_{ri} \\ &= \sum_{i=1}^{N} \left(\sqrt{g_{i(k)}} (\tilde{W}_i^T \rho_i(x_i) + \varepsilon_i + K_i r_i) + \Delta_i(X) \right)^2 - \sum_{i=1}^{N} \left(\frac{r_i(k)}{\sqrt{g_{i(k-1)}}} \right)^2 \end{aligned} \tag{12}$$

Next, by using (10), the first difference due to the second term in the overall Lyapunov function candidate is obtained as

$$\Delta L_W = \frac{1}{\alpha_i} \left(c_i \tilde{W}_i(k) - c_i^{-1} \alpha_i \rho_i r_i(k+1) - (I - c_i) W_i \right)^2 - \frac{1}{\alpha_i} \tilde{W}_i^T(k) \tilde{W}_i(k) \tag{13}$$

Expanding the first difference of the overall Lyapunov function candidate $\Delta L = \Delta L_r + \Delta L_W$ by using (11) and (12) to obtain

$$\begin{aligned}\Delta L \le & \sum_{i=1}^{N} \begin{pmatrix} g_i(k) \rho_i^T \tilde{W}_i \tilde{W}_i^T \rho_i + g_i(k) \varepsilon_i^2 + g_i(k) K_i^2 r_i^2 + \dfrac{\Delta_i^2}{g_i(k)} \\ + 2 g_i(k) \tilde{W}_i^T \rho_i \varepsilon_i + 2 g_i(k) \tilde{W}_i^T \rho_i K_i r_i \\ 2 \tilde{W}_i^T \rho_i \Delta_i + 2 g_i(k) \varepsilon_i K_i r_i + 2 \varepsilon_i \Delta_i + 2 K_i r_i \Delta_i \end{pmatrix} - \sum_{i=1}^{N} \left(\frac{r_i(k)}{g_i(k-1)} \right)^2 \\ & + \sum_{i=1}^{N} \begin{Bmatrix} \dfrac{c_i^2}{\alpha_i} \tilde{W}_i^T(k) \tilde{W}_i(k) + \alpha_i c_i^{-2} \rho_i^T \rho_i \left[g_i(x_i(k)) \left(\tilde{W}_i^T \rho_i(x_i) + \varepsilon_i + K_i r_i \right) + \Delta_i \right]^2 \\ + \dfrac{1}{\alpha_i} (1 - c_i)^2 \|W_i\|^2 - 2 \tilde{W}_i^T(k) \rho_i \left[g_i(x_i(k)) \left(\tilde{W}_i^T \rho_i(x_i) + \varepsilon_i + K_i r_i \right) + \Delta_i \right] \\ + 2 \left\| \tilde{W}_i \right\| \dfrac{\|c_i (1 - c_i)\|}{\alpha_i} \|W_i\| + 2 W_i^T (1 - c_i) c_i^{-1} \rho_i \left[g_i(x_i(k)) \left(\tilde{W}_i^T \rho_i(x_i) + \varepsilon_i + K_i r_i \right) + \Delta_i \right] \end{Bmatrix} \\ & - \sum_{i=1}^{N} \frac{1}{\alpha_i} \{ \tilde{W}_i^T(k) \tilde{W}_i(k) \} \end{aligned} \tag{14}$$

Applying the Cauchy-Schwarz inequality $(a_1 + a_2 + \cdots + a_n)^2 \le n(a_1^2 + a_2^2 + \cdots + a_n^2)$ and $\rho_i^T \tilde{W}_i \tilde{W}_i^T \rho_i = \tilde{W}_i^T \rho_i \rho_i^T \tilde{W}_i$, yields

$$\Delta L \le \sum_{i=1}^{N}\begin{pmatrix}\left(2+\frac{1}{g_i(k)}+4(1-c_i)c_i^{-1}+4\alpha_i c_i^{-2}\|\rho_i\|^2\right)\Delta_i^{\,2}\\ +\begin{pmatrix}1+g_i(k)+g_i(k)^2+4(1-c_i)c_i^{-1}g_i(k)^2\\ +4\alpha_i c_i^{-2}\|\rho_i\|^2 g_i(k)^2\end{pmatrix}\varepsilon_i^{\,2}+\frac{1}{\alpha_i}(1-c_i)^2\|W_i\|^2\\ +\frac{c_i(1-c_i)}{\alpha_i}\|W_i\|^2+(1-c_i)c_i^{-1}\|W_i\|^2\|\rho_i\|^2\\ +2(I-c_i)^2W_i^{\,T}\rho_i\rho_i^{\,T}W_i\\ +\begin{pmatrix}1+g_i(k)+g_i(k)^2+4(1-c_i)c_i^{-1}g_i(k)^2\\ +4\alpha_i c_i^{-2}\|\rho_i\|^2 g_i(k)^2\end{pmatrix}K_i^{\,2}r_i^{\,2}\end{pmatrix}$$
$$-\sum_{i=1}^{N}\left(\frac{r_i(k)}{\sqrt{g_i(k-1)}}\right)^2-\sum_{i=1}^{N}\frac{1-c_i}{\alpha_i}\tilde{W}_i^{\,T}(k)\tilde{W}_i(k) \qquad (15)$$
$$-\sum_{i=1}^{N}\left(g_i(k)-4(1-c_i)c_i^{-1}g_i(k)^2-4\alpha_i c_i^{-2}\|\rho_i\|^2 g_i(k)^2\right)\tilde{W}_i^{\,T}(k)\rho_i\rho_i^{\,T}\tilde{W}_i(k)$$

Note that by using Assumption 1 we have $\sum_{i=1}^{N}\beta_i|\Delta_i(x)|^2 \le \sum_{i=1}^{N}\beta_i(\delta_{i0}+\sum_{j=1}^{N}\gamma_{ij}r_j^{\,2})=\sum_{i=1}^{N}\beta_i\delta_{i0}+\sum_{j=1}^{N}\sum_{i=1}^{N}\beta_i\gamma_{ij}r_j^{\,2}=\sum_{i=1}^{N}\delta_{i0}\sum_{i=1}^{N}\sum_{j=1}^{N}\beta_j\gamma_{ji}r_i^{\,2}$ where $\beta_i=\beta_i(x_i)$ is an arbitrary real-valued function of x_i. Thus, (15) becomes

$$\Delta L \le -\sum_{i=1}^{N}\begin{pmatrix}\frac{1}{g_i(k-1)}-\sum_{j=1}^{N}\left[2+\frac{1}{g_i(k)}+4(1-c_i)c_i^{-1}+4\alpha_i c_i^{-2}\|\rho_i\|^2\right]\gamma_{ji}\\ -\begin{pmatrix}1+g_i(k)+g_i(k)^2+4(1-c_i)c_i^{-1}g_i(k)^2\\ +4\alpha_i c_i^{-2}\|\rho_i\|^2 g_i(k)^2\end{pmatrix}K_i^{\,2}\end{pmatrix}r_i^{\,2}$$
$$-\sum_{i=1}^{N}\frac{1-c_i}{\alpha_i}\|\tilde{W}_i(k)\|^2$$
$$-\sum_{i=1}^{N}\begin{pmatrix}g_i(k)-4(1-c_i)c_i^{-1}g_i(k)^2\\ -4\alpha_i c_i^{-2}\|\rho_i\|^2 g_i(k)^2\end{pmatrix}\|\rho_i\|_{\max}^2\|\tilde{W}_i(k)\|^2$$

$$+\sum_{i=1}^{N}\begin{pmatrix}\begin{pmatrix}1+g_i(k)+g_i(k)^2+4(1-c_i)c_i^{-1}g_i(k)^2\\ +4\alpha_i c_i^{-2}\|\rho_i\|^2 g_i(k)^2\end{pmatrix}\varepsilon_i^{\,2}+\frac{1}{\alpha_i}(1-c_i)^2\|W_i\|^2\\ +\frac{c_i(1-c_i)}{\alpha_i}\|W_i\|^2+(1-c_i)c_i^{-1}\|W_i\|^2\|\rho_i\|^2+2(I-c_i)^2W_i^{\,T}\rho_i\rho_i^{\,T}W_i\\ +\left(2+\frac{1}{g_i(k)}+4(1-c_i)c_i^{-1}+4\alpha_i c_i^{-2}\|\rho_i\|^2\right)\delta_{0i}\end{pmatrix} \qquad (16)$$

Therefore, $\Delta L \le 0$ in (16) provided the following conditions hold

$$|r_i| > \sqrt{\frac{C'_{i\varepsilon}}{C'_{ir}}}\,, \tag{17}$$

or

$$\left\|\tilde{W}_i^T(k)\right\| > \sqrt{\frac{C'_{i\varepsilon}}{C'_{iw}}} \tag{18}$$

where

$$C'_{i\varepsilon} = \begin{pmatrix} 1 + g_{i\max} + g_i(k)^2 + 4(1-c_i)c_i^{-1}g_{i\max}{}^2 \\ + 4\alpha_i c_i^{-2}\|\rho_i\|^2 g_i(k)^2 \end{pmatrix}\varepsilon_{i\max}{}^2 + \frac{1}{\alpha_i}(1-c_i)^2\|W_i\|^2$$
$$+ \frac{c_i(1-c_i)}{\alpha_i}\|W_i\|^2 + (1-c_i)c_i^{-1}\|W_i\|^2\|\rho_i\|_{\max}^2 + 2(I-c_i)^2\|W_i\|^2\|\rho_i\|_{\max}^2 \quad ,$$
$$+ \left(2 + \frac{1}{g_{i\min}} + 4(1-c_i)c_i^{-1} + 4\alpha_i c_i^{-2}\|\rho_i\|_{\max}^2\right)\delta_{0i}$$

$$C'_{ir} = \frac{1}{g_{i\max}} - \sum_{j=1}^{N}\left[2 + \frac{1}{g_{i\min}} + 4(1-c_i)c_i^{-1} + 4\alpha_i c_i^{-2}\|\rho_i\|_{\max}^2\right]\gamma_{ji}$$
$$- \begin{pmatrix} 1 + g_{i\max} + g_{i\max}{}^2 + 4(1-c_i)c_i^{-1}g_{i\max}{}^2 \\ + 4\alpha_i c_i^{-2}\|\rho_i\|_{\max}^2 g_{i\max}{}^2 \end{pmatrix}K_i{}^2 \quad ,$$

$C'_{iw} = \dfrac{1-c_i}{\alpha_i} + C'_{i\rho w}$, and

$C'_{i\rho w} = \left(g_{i\min} - 4(1-c_i)c_i^{-1}g_{i\max}{}^2 - 4\alpha_i c_i^{-2}\|\rho_i\|_{\max}^2 g_{i\max}{}^2\right)\|\rho_i\|_{\max}^2$. This guaranties the boundedness of the weight estimation error $\tilde{W}_i(k)$ and filtered tracking error $r_i(k)$ which in turn shows that the tracking errors $z_i(k)$ are UUB for all $1 \le i \le N$ as explained. ■

Hence, the Lyapunov stability analysis shows that the proposed NN controller guarantees that the closed-loop signals are UUB with the bounds given by (17) and (18). Note that the design constant c_i should be chosen close to one to retain a small bound. In the next section, the proposed controller is applied to achieve stability of the interconnected power systems.

III. Case Study

"Power system stability is the ability of an electric power system, for a given initial operating condition, to regain a state of operating equilibrium after being subjected to a physical disturbance, with most system variables bounded so that practically the entire system remains intact" [17]. There must be a controller to mitigate the oscillations after a fault is occurred such that the power network goes back to its normal operating condition after the fault. Generator excitation control is a means to mitigate the power system oscillations. Since the disturbance is a function of the power network voltages and angles as well as generator states, it is generally hard to design a centralized damping controller in the large-scale power system.

In this section, we aim at designing a discrete-time decentralized generator excitation controller to damp the oscillations by using generator measurable states in an interconnected power system consisting of multiple generators.

A. Power System Model Development

A power system is usually modeled using a combination of differential and algebraic equations. For control design it is desirable to have pure dynamical equations. In [18], authors have proposed a continuous-time algebraic-free power system representation based on the generator classical model. In order to incorporate the generator flux decay states, the proposed model can be extended.

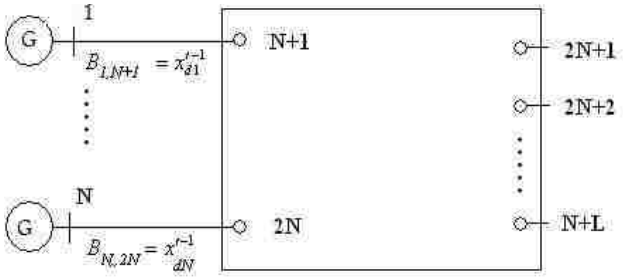

Fig.1 Power System

The two-axis model [18] is chosen for controller design. Then, the generator dynamical equations are given as

$$\begin{aligned}
\dot{\delta}_i &= \omega_i \\
\dot{\omega}_i &= \frac{1}{M_i}\left(P_{mi} - P_{ei}\right) \\
\dot{E}'_{qi} &= \frac{1}{T_{d0i}}\left(-\frac{x_{di}}{x'_{di}}E'_{qi} + \frac{x_{di}-x'_{di}}{x'_{di}}V_{i+N}\cos(\delta_i - \psi_{i+N}) + E_{fdi}\right) \\
\dot{E}'_{di} &= \frac{1}{T_{q0i}}\left(-\frac{x_{qi}}{x'_{di}}E'_{di} + \frac{x_{qi}-x'_{di}}{x'_{di}}V_{i+N}\sin(\delta_i - \psi_{i+N})\right)
\end{aligned} \tag{19}$$

where δ_i is the rotor angle of the *i*-th machine, ω_i is the difference between the generator angular speed and synchronous speed ω_s, E'_{qi} and E'_{di} are generator *dq* variables as defined in [19], E_{fdi} is the excitation voltage, $M_i = 2H/\omega_0$ is the *i*-th machine inertia, P_{ei} is the generator output electric power, P_{mi} is the mechanical power , and V_{i+N} and ψ_{i+N} are the generator bus voltage and phase angle, respectively, as depicted by Fig. 1 with *N* and *L* represent the number of generators (subsystems) and the number of non-generator buses in the power system, respectively . In addition

$$P_{ei} = B_{i,i+N}V_{i+N}\left(E'_{qi}\sin(\delta_i - \psi_{i+N}) - E'_{di}\cos(\delta_i - \psi_{i+N})\right), \tag{20}$$

where *B* represents the reactance of the admittance matrix. The voltages and phase angles of the power system buses shown in Fig. 1 are constrained by the following set of algebraic power balance equations (neglecting resistances) as

$$P_{Li} + \sum_{j=1}^{N} B_{ij} V_i \left(E'_{qj} \sin(\psi_i - \delta_j) + E'_{dj} \cos(\psi_i - \delta_j) \right) + \sum_{j=l+1}^{L+N} B_{ij} V_i V_j \sin(\psi_i - \psi_j) = S_{\mathrm{P}i} = 0 \tag{21}$$

$$Q_{Li} - \sum_{j=1}^{N} B_{ij} V_i \left(E'_{qj} \cos(\psi_i - \delta_j) - E'_{dj} \sin(\psi_i - \delta_j) \right) - \sum_{j=N+1}^{L+N} B_{ij} V_i V_j \cos(\psi_i - \psi_j) = S_{\mathrm{Q}i} = 0 \tag{22}$$

$$i = l+1, \ldots, N+L$$

Then, taking the derivative of (21) and (22) to obtain $\dot{V}_i$ and $\dot{\psi}_i$ terms, we have

$$\frac{\partial S_{\mathrm{P}i}}{\partial t} = \frac{\partial S_{\mathrm{P}i}}{\partial V} \dot{V} + \frac{\partial S_{\mathrm{P}i}}{\partial \psi} \dot{\psi} + \frac{\partial S_{\mathrm{P}i}}{\partial \delta} \dot{\delta} + \frac{\partial S_{\mathrm{P}i}}{\partial E'_q} \dot{E}'_q + \frac{\partial S_{\mathrm{P}i}}{\partial E'_d} \dot{E}'_d = 0 \tag{23}$$

and

$$\frac{\partial S_{\mathrm{Q}i}}{\partial t} = \frac{\partial S_{\mathrm{Q}i}}{\partial V} \dot{V} + \frac{\partial S_{\mathrm{Q}i}}{\partial \psi} \dot{\psi} + \frac{\partial S_{\mathrm{Q}i}}{\partial \delta} \dot{\delta} + \frac{\partial S_{Qi}}{\partial E'_q} \dot{E}'_q + \frac{\partial S_{Qi}}{\partial E'_d} \dot{E}'_d = 0 \tag{24}$$

for $i = l+1, \ldots, N+L$.

By using dynamic equations (20) for $\dot{E}'_{qi}$ and $\dot{E}'_{di}$ and solving equations and for $\dot{V}_i$ and $\dot{\psi}_i$, we obtain a new set of dynamic equations as

$$\begin{bmatrix} A(x) & B(x) \\ D(x) & E(x) \end{bmatrix} \begin{bmatrix} \dot{V} \\ \dot{\psi} \end{bmatrix} + \left(\begin{bmatrix} C(x) \\ F(x) \end{bmatrix} \omega + R(x) + G(x).E_{fd} \right) = 0 \tag{25}$$

where

$V = [V_{N+1} \quad V_{N+2} \quad \ldots \quad V_{N+L}]^T$, $\psi = [\psi_{N+1} \quad \psi_{N+2} \quad \ldots \quad \psi_{N+L}]^T$, , $\omega = [\omega_1 \quad \omega_2 \quad \ldots \quad \omega_N]^T$ is the generators speed vector, $R(.)$, and $G(.)$ are nonlinear functions of the states. In (25)

$x = [\delta^T \quad \omega^T \quad E_q'^T \quad E_d'^T \quad V^T \quad \psi^T]^T$, where $\delta = [\delta_1 \quad \delta_2 \quad \dots \quad \delta_N]^T$, $E_q' = [E_{q1}' \quad E_{q2}' \quad \dots \quad E_{qN}']^T$, $E_d' = [E_{d1}' \quad E_{d2}' \quad \dots \quad E_{dl}']^T$, and $\Delta P_e = [\Delta P_{e1} \quad \Delta P_{e2} \quad \dots \quad \Delta P_{eN}]^T$. The entries for $A_{L\times L}$, $B_{L\times L}$, $D_{L\times L}$, $E_{L\times L}$, $C_{L\times N}$, $F_{L\times L}$, $R_{2L\times 1}$, $G_{2L\times N}$ can be derived by collecting the corresponding coefficient. Equation (25) can be rewritten in a more appropriate way as

$$\begin{aligned}\begin{bmatrix}\dot{V}\\ \dot{\psi}\end{bmatrix} &= -\begin{bmatrix}A(x) & B(x)\\ D(x) & E(x)\end{bmatrix}^{-1}\left(\begin{bmatrix}C(x)\\ F(x)\end{bmatrix}\omega + R(x) + G(x).E_{fd}\right)\\ &= a(x) + b(x)E_{fd}\end{aligned} \tag{26}$$

It is important to note that this step is needed for model development only and is not required for implementation.

B. Generator Model

In order to analyze the stability of the generator, the flux-decay model [19] is chosen. Then, the generator dynamical equations are given as

$$\begin{aligned}\dot{\delta}_i &= \omega_i\\ \dot{\omega}_i &= \frac{1}{M_i}(P_{mi} - P_{ei})\\ \dot{E}_{qi}' &= \frac{1}{T_{d0i}}\left(-E_{qi}' + (x_{di} - x_{di}')I_{di} + E_{fdi}\right)\end{aligned} \tag{27}$$

In addition, the following equalities are valid

$$P_{ei} = E_{qi}'I_{qi} + (x_{qi} - x_{di}')I_{qi}I_{di} \tag{28}$$

and

$$\begin{aligned}I_{qi} &= B_{i,i+N}V_{i+N}\sin(\delta_i - \psi_{i+N})\\ I_{di} &= B_{i,i+N}\left(E_{qi}' - V_{i+N}\cos(\delta_i - \psi_{i+N})\right)\end{aligned} \tag{29}$$

Moreover, the power balance equations will be simplified by employing the flux-decay assumption as

$$E'_{di} = (x_{qi} - x'_{di}) I_{qi} \tag{30}$$

In this design we assume that the mechanical power $P_{mi}\,(1 \le i \le N)$ is slowly changing compared to the other control variables; thus, $\dot{P}_{mi} \approx 0$. Define,

$$\begin{aligned} x_{i1} &= \delta_i - \delta_{0i} \\ x_{i2} &= \omega_i \\ P_{e0i} &= P_{mi} \\ \Delta P_{ei} &= P_{e0i} - P_{ei} \\ x_{i3} &= \frac{\Delta P_{ei}}{M_i} \end{aligned} \tag{31}$$

where P_{e0i} is the steady state generator electric output power. Consequently, the generator dynamics (31) can be rewritten as

$$\begin{aligned} \dot{x}_{i1} &= x_{i2} \\ \dot{x}_{i2} &= x_{i3} \\ \dot{x}_{i3} &= -\frac{x_{i3}}{T_{d0i}} + \frac{I_{qi} u_i}{M_i T_{d0i}} + \Delta_i \end{aligned} \tag{32}$$

where

$$u_i = -E_{fdi} \tag{33}$$

and

$$\Delta_i = \frac{1}{T_{d0i}} \left(x_{di} - x_{qi}\right) I_{qi} I_{qi} - E'_{qi} \dot{I}_{qi} - \left(x_{qi} - x'_{di}\right)\left(\dot{I}_{qi} I_{di} + I_{qi} \dot{I}_{di}\right) + \frac{P_{e0i}}{M_i T_{d0i}} \tag{34}$$

Define $\Delta_{0i} = P_{e0i} / (M_i T_{d0i})$ and $\Delta_{1i} = \frac{1}{T_{d0i}} \left(x_{di} - x_{qi}\right) I_{qi} I_{qi} - E'_{qi} \dot{I}_{qi} - \left(x_{qi} - x'_{di}\right)\left(\dot{I}_{qi} I_{di} + I_{qi} \dot{I}_{di}\right).$

In [18] authors have shown that

$$\left|\Delta_{1i}\right| \le \upsilon_i(x), \tag{35}$$

where $\upsilon_i(.)$ is a nonlinear function of the generator states, $x = [x_1\ x_2\ \ldots\ x_N]^T$, $x_i = [x_{i1}\ x_{i2}\ \ x_{i3}]^T$, and that $\Delta_{1i} = 0$ at steady state conditions, that is, when $x = 0$.

Knowing that the steady-state conditions result $r_i = 0$ and vice versa, we can assume that $|\Delta_{1i}(k)|^2 \le \sum_{j=1}^{N} \gamma_{ij} r_j^{\,2}(k)$ for $1 \le i \le N$, where γ_{ij} is a positive constant and $r_i(k)$ is the filtered tracking error defined in (3). Since Δ_{0i} is a constant, Assumption 1 is satisfied for interconnected power systems.

C. Power System Dynamical Model in Discrete-time

The generator representation in discrete-time can be obtained by discretizing the continuous-time representation (32) as

$$\begin{aligned} x_{i1}(k+1) &= Tx_{i2}(k) + x_{i1}(k) \\ x_{i2}(k+1) &= Tx_{i3}(k) + x_{i2}(k) \\ x_{i3}(k+1) &= \frac{-Tx_{3i}(k)}{T_{d0i}} + T\Delta_i + g_i u_i + x_{i3(k)} \end{aligned} \tag{36}$$

where T is the time step and $g_i = T \cdot I_{qi} / (M_i T_{d0i})$. Note that for this system, *n=3* since the generator (subsystem) has third order dynamics. The power system representation in discrete-time (36) is similar to system (1) with $f_{i1}(x_i(k)) = Tx_{i2}(k) + x_{i1}(k)$, $f_{i2}(x_i(k)) = Tx_{i3}(k) + x_{i2}(k)$, $f_{i3}(x_i(k)) = -Tx_{i3}(k)/T_{d0i} + x_{i3}(k)$, $g_i(x_i(k)) = T \cdot I_{qi} / (M_i T_{d0i})$, and $T\Delta_i$ is the interconnection term where $x_i(k) = [x_{i1}(k), x_{i2}(k), x_{i3}(k)]^T$ and $x = [x_1\ x_2 \ldots x_N]^T$. Also, recall that Assumptions 1 and 2 ($g_i = T \cdot I_{qi} / (M_i T_{d0i})$ and g_i is bounded away from zero and $|g_i|_\infty$ exists) hold for the power system as explained earlier.

Remark 2: It is worth mentioning that in the generator dynamics with $g_i(x_i(k))$ and $f_{i3}(x_i(k))$ in (36) are known only if the generator parameters T_{d0i} and M_i as well as the generator current I_{qi} are known a priori. In a practical scenario, these values are not

accurately known. Thus, NN controller (7) and (9) can be utilized in the control input to improve the overall interconnected power system stability in the absence of the mentioned values. In practice, while generator angle, speed and power are measured, obtaining I_{qi} requires knowledge of $B_{i,i+N}$, according to (29).

Remark 3: If the generator values mentioned in Remark 2 $f_i(.)$ and $g_i(.)$ are known, the control input is simplified as

$$u_i = v_i = -g_i^{-1}\left(f_{i3}(x_i(k)) + \lambda_{i1}x_{i1}(k+1) + \lambda_{i2}x_{i2}(k+1) - K_i r_i(k)\right). \tag{37}$$

IV. Simulation Results

Example 1. Consider the following fourth order-subsystem interconnected nonlinear discrete-time system to demonstrate the effectiveness of the NN controllers developed in this work as

$$\begin{aligned}
x_{11}((k+1)T) &= x_{11}(kT)\\
x_{12}((k+1)T) &= f_{12}(x_{11}, x_{12}) + g_{12}(x_{11}, x_{12})u_1\\
&\quad + .01\times(x_{21}^{\ 2}(kT) + x_{22}^{\ 2}(kT) + x_{31}^{\ 2}(kT) + x_{42}^{\ 2}(kT))\\
x_{21}((k+1)T) &= x_{21}(kT)\\
x_{22}((k+1)T) &= f_{22}(x_{21}, x_{22}) + g_{22}(x_{21}, x_{22})u_2\\
&\quad + .1\times(x_{11}^{\ 2}(kT) + x_{32}^{\ 2}(kT) + x_{41}^{\ 2}(kT) + x_{42}^{\ 2}(kT))\\
x_{31}((k+1)T) &= x_{31}(kT)\\
x_{32}((k+1)T) &= f_{32}(x_{31}, x_{32}) + g_{32}(x_{31}, x_{32})u_3\\
&\quad + .1\times(x_{11}^{\ 2}(kT) + x_{12}^{\ 2}(kT) + x_{22}^{\ 2}(kT) + x_{42}(kT))
\end{aligned}$$

$$\begin{aligned}
x_{41}((k+1)T) &= x_{41}(kT)\\
x_{42}((k+1)T) &= f_{42}(x_{41}, x_{42}) + g_{42}(x_{41}, x_{42})u_4\\
&\quad + .1\times(x_{11}^{\ 2}(kT) + x_{12}^{\ 2}(kT) + x_{22}^{\ 2}(kT) + x_{32}^{\ 2}(kT))
\end{aligned}$$

where

$$f_{12}(x_{11}, x_{12}) = \frac{-1}{16}\left(x_{11}(kT)/(1 + {x_{12}}^2(kT))\right) + x_{12}(kT);$$
$$f_{22}(x_{21}, x_{22}) = \frac{-3}{16}\left(x_{21}(kT)/(1 + {x_{22}}^2(kT))\right);$$
$$f_{32}(x_{31}, x_{32}) = \frac{-3}{16}\left(x_{31}(kT)/(1 + {x_{32}}^3(kT))\right);$$
$$f_{42}(x_{41}, x_{42}) = \frac{-1}{16}\left(x_{41}(kT) \times (1 + {x_{42}}^3(kT))\right);$$

and

$$g_{12}(x_{11}, x_{12}) = 1 + 0.5\sin({x_{12}}^2(kT)) ;$$
$$g_{22}(x_{21}, x_{22}) = 1 + 0.25\sin(x_{12}(kT) + x_{22}(kT)) ;$$
$$g_{32}(x_{31}, x_{32}) = 1 + 0.5\sin(x_{32}(kT)) ;$$
$$g_{42}(x_{41}, x_{42}) = 1 + 0.25\sin(x_{41}(kT)) + 0.25\cos(x_{42}(kT)) ;$$

with sampling interval T being 1ms. The objective of each subsystem controllers is to make each subsystem state track a desired trajectory defined as $x_{11d}(kT) = 0.1\sin(0.1kT)$, $x_{21d}(kT) = 0.1\sin(0.02kT), x_{31d}(kT) = 0.1\sin(0.1kT)$, $x_{41d}(kT) = 0.1\sin(0.01kT)$. Then, controller (7) along with NN weight update law (9) is utilized to achieve this goal. The weight estimate matrices $\hat{W}_i$ are initialized at zero for $1 \le i \le 4$. Moreover, no offline training is used to tune the weights in advance even though the nonlinear system and the interconnection dynamics are not needed for the controller design. The NN activation function is chosen as $\rho_i(x_i, x_{id}(k+1)) = sigmoid\,(V_i^T[x_i, x_{id}(k+1)]^T)$ [20] where V_i is chosen at random initially and held fixed afterwards to form a set of basis functions needed for the NN function approximation [21].

The initial values are $x_{11} = 1; x_{12} = 1;$ $x_{21} = 1.5; x_{22} = 1;$ $x_{31} = 1; x_{32} = 2;$ $x_{41} = 2; x_{42} = 1$. The design gains are taken as $K_1 = K_2 = K_3 = K_4 = 0.01;$ $\alpha_1 = \alpha_2 = \alpha_3 = \alpha_4 = 0.2;$ $\lambda_1 = \lambda_2 = \lambda_3 = \lambda_4 = 0.01$. The simulation is performed under two different values $c_i = .9$ and $c_i = 1$ for $1 \le i \le 4$. It is shown by the simulation that $c_i < 1$ gives smaller NN.

Case 1($c_i = .9$*):* The satisfactory performance of the controller is depicted in Fig. 2 where the states eventually converge to a close proximity of the desired trajectory indicating the boundedness of the tracking errors as concluded in the Theorem 1. Figure 3 illustrates the NN control inputs.

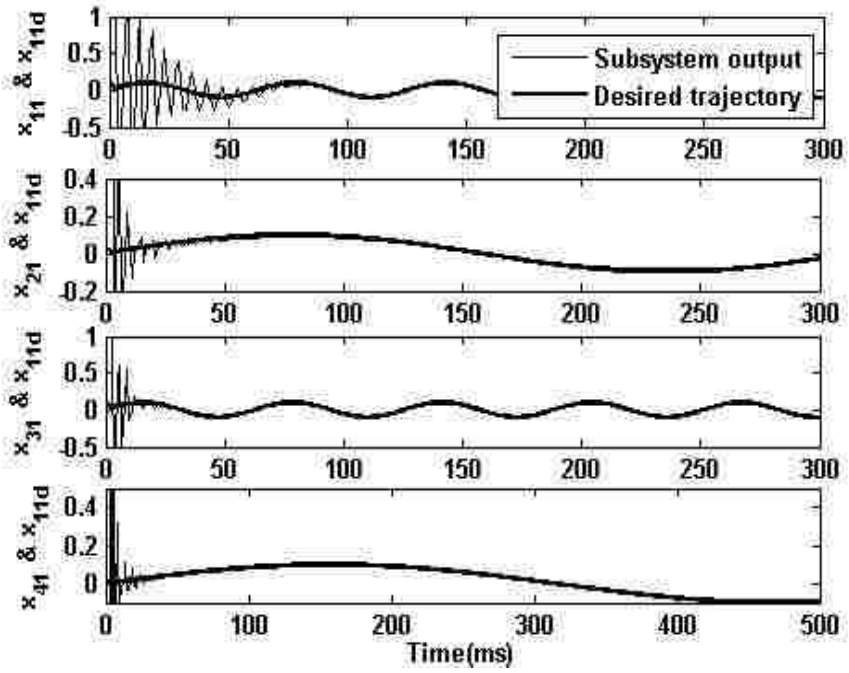

Fig.2 Interconnected systems states x_{i1} and desired trajectories x_{i1d} for $1 \le i \le 4$ with $c_i = .9$

Also, Fig. 4 shows the representative NN weights. These results are as expected according to Theorem 1 where the NN weights stay bounded and converge to small values. In order to evaluate the neural network performance the function

$$\delta_{21}(k) = W_i^T \rho_i(x_i) + \varepsilon_i = -g_i(x(k))^{-1}\left(f_{i3}(x_i(k)) - x_{i2d}(k+1) + \lambda_{i1} z_{i1}(k+1)\right) \tag{38}$$

and its corresponding NN approximation $\hat{W}_i^T \rho_i$ are depicted in Fig. 5. The NN appear to approximate the function satisfactorily.

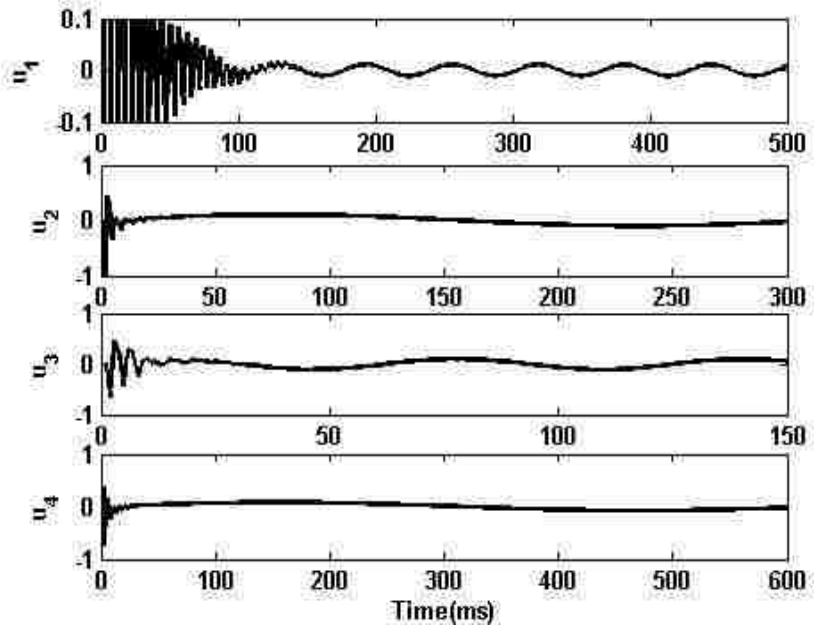

Fig.3 Interconnected systems control inputs with $c_i = .9$

Case 2($c_i = 1$): Case 1 is repeated here with the update law (9) with $c_i = 1$ for $1 \le i \le 4$. Although the controller performance is almost the same as in case 1, as shown in Figs 6 and 7, certain NN weight estimates increase to higher values than in the previous case (Fig. 8). The function approximation error with $c_i = .9$ is less than that of $c_i = 1$ depicted in Figs. 9, according to Fig 10. Larger values of weight estimates can cause over approximation of the nonlinear function throughout the simulation.

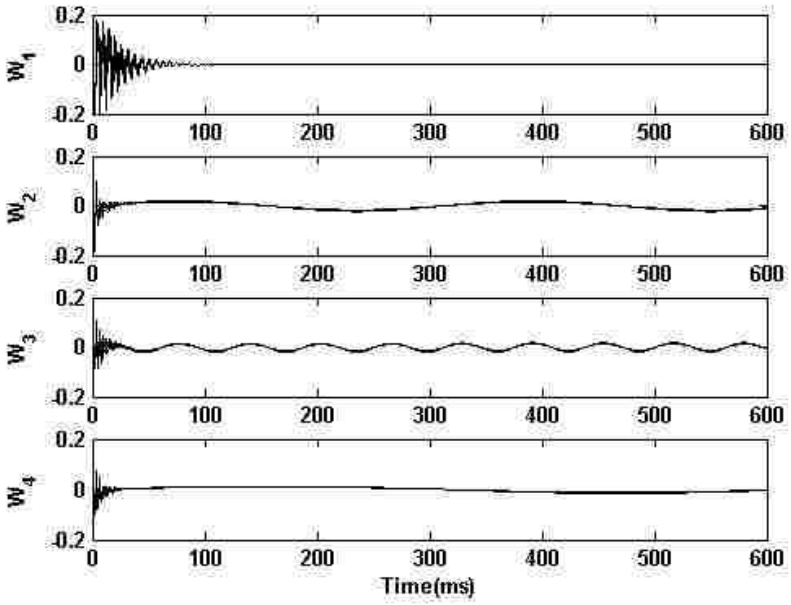

Fig.4 NN weight estimates $\hat{W}_i$ for $1 \le i \le 4$ with $c_i = .9$

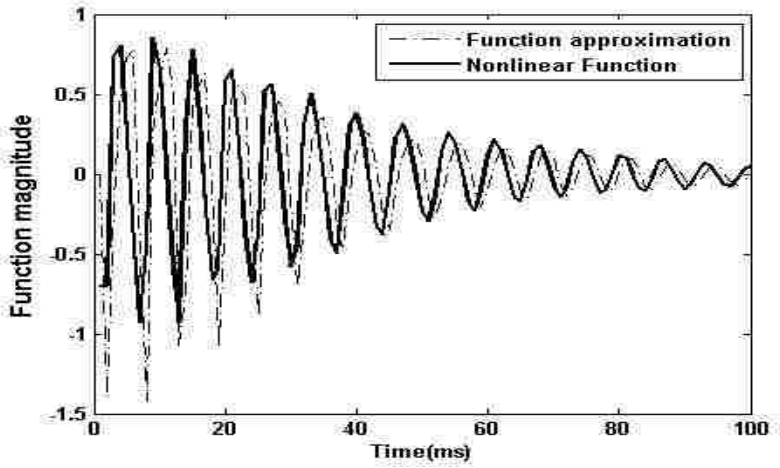

Fig.5 Actual nonlinear function and NN approximation for $\delta_{21}(k)$ introduced in (43) with $c_i = .9$

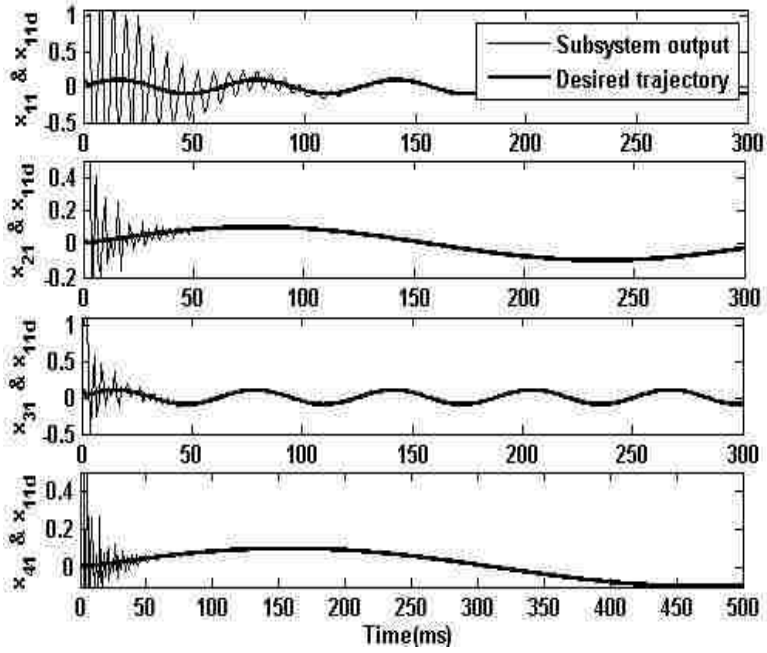

Fig.6 Interconnected systems states x_{i1} and desired trajectories x_{i1d} for $1 \le i \le 4$ when with $c_i = 1$

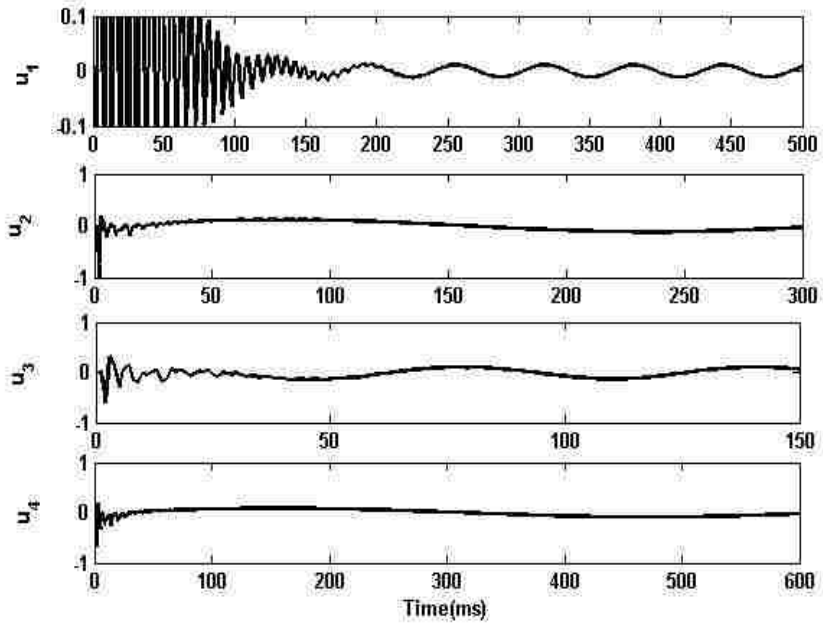

Fig.7 Interconnected systems control inputs with $c_i = 1$

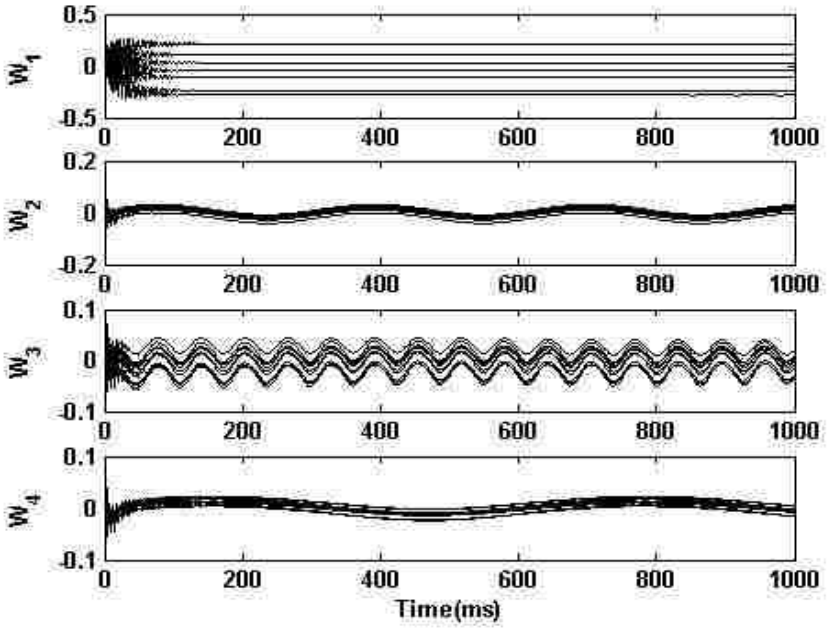

Fig.8 NN weight estimates $\hat{w}_i$ for $1 \le i \le 4$ with $c_i = 1$

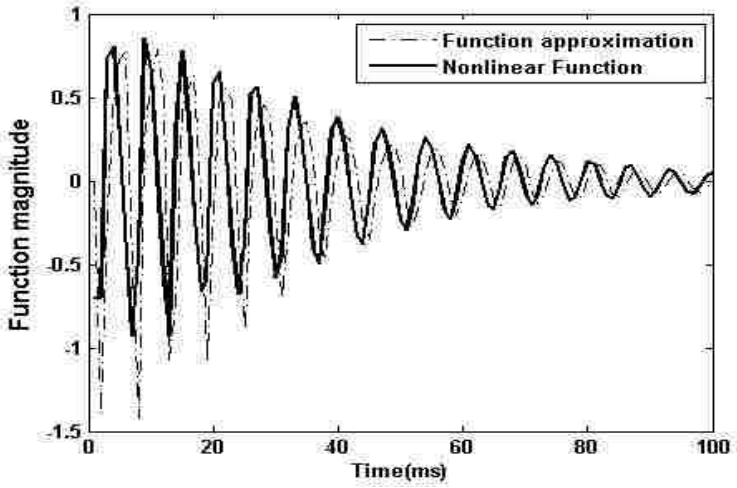

Fig.9 Actual nonlinear function and NN approximation for $\delta_{21}(k)$ introduced in (43) with $c_i = 1$

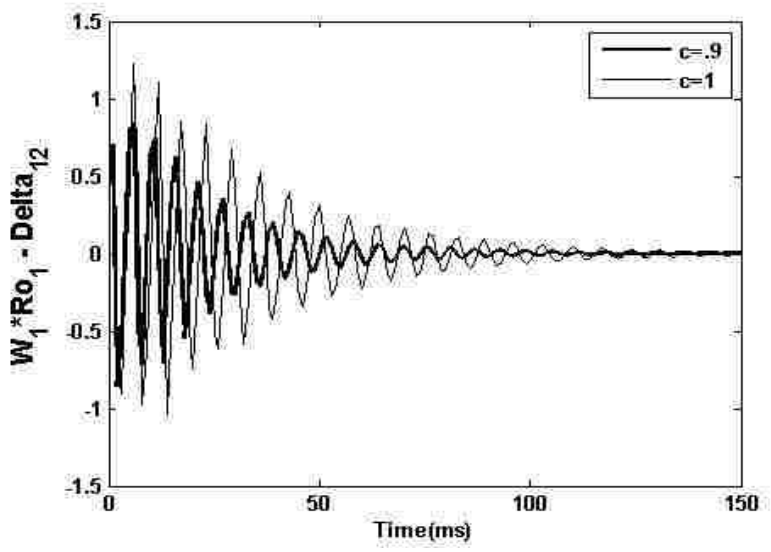

Fig.10-NN function approximation error for $\delta_{21}(k)$ introduced in (38) with $c_i = .9$ and $c_i = 1$

Example 2. The method introduced in Section III is now utilized to design power system damping controller with generator excitation control. The 3-bus, 2-generator power system shown in Fig. 11 is considered and is subjected to a three-phase disturbance on bus 3. The generator data are given as $x'_{di} = 0.3$, $x_{di} = 0.02$, $x_{qi} = 0.019$, $T_{d0i} = 7$, $1 \le i \le 2$ whereas $H_1 = \omega_s M_1/2 = 5$ and $H_2 = \omega_s M_2/2 = 1$. Both generators have speed governors and the excitation control is implemented by employing the discrete-time NN controller as proposed in (7) with update law (9) where $K_1 = K_2 = 0.001$, $\lambda_1 = \lambda_2 = [0.0001\ 0.0001]^T$, $\alpha_1 = \alpha_2 = 0.0001$, and $c_1 = c_2 = 1$. In addition, $\hat{W}_i$ (for $1 \le i \le 2$) is the NN weight estimate matrix while $\rho_i(.)$ is the NN activation function vector for the subsystems.

Similar to the previous example, the weight estimate matrices $\hat{W}_i$ are initialized at zero for $1 \le i \le 2$. The NN activation function is chosen as $\rho_i(x_i, x_{id}(k+1)) =$

$sigmoid(V_i^T[x_i, x_{id}(k+1)]^T)$ [20] where V_i is chosen at random initially and held fixed afterwards to form a set of basis functions needed for the NN approximation [21].The power system loads are considered as constants. In the simulation, time step of $T = 0.005s$ is chosen. The control objective is to damp the generators oscillations caused by a three-phase fault.

Although the stability analysis is based on the lossless power system dynamical model as described in (26), the simulations employ the entire power system dynamics with line resistances. A two-axis generator model is utilized in order to evaluate the effectiveness of the controller design.

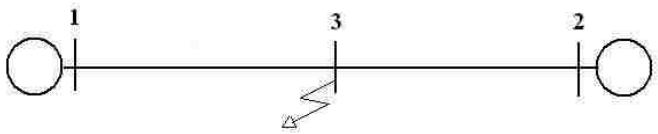

Fig.11 Power system topology

A three-phase disturbance is injected to the bus 3 at $t = 0.2s$ and removed at $t = 0.4s$ seconds. Generators 1 and 2 are chosen for control. The damping control starts once fault occurs. The neural networks have 10 neurons in the output layer where biases are considered and the NN weights are tuned throughout the simulations by using on-line learning. The voltage E_{fdi} is calculated using (33) and is subjected to hard limits such that the voltage satisfies $0.5 \le E_{fdi} \le 5$ p.u. to avoid any impractical excitation voltages E_{fdi} .

Moreover, no offline training is used to tune the weights in advance. No initial knowledge about the interconnection dynamics or power system topology is needed for the controller design.

The simulation is performed under three scenarios; a) excitation control using (7) and (9) when the generator values mentioned in Remark 2 are unknown; b) excitation control by using (37) (when the generator values are known); and c) steam governor only. Note that for (a) and (b), steam governor is also active. Figure 12 shows the damping performance of the proposed controller (case a) as compared to cases b and c whereas Fig. 13 represents the excitation voltages E_{fd} for the cases (a) and (b). Satisfactory damping performance of the proposed controller can be observed from Fig. 11as predicted by Theorem 2 while the excitation voltages are within practical accepted limits as shown in Fig. 13. The weight estimation matrices (Fig. 14) $\hat{W}_i$ (for $1 \le i \le 2$) are bounded as expected from Theorem 2. When the generator values T_{d0i}, M_i, I_{qi} are known, the control effort is a little lower than when the values are unknown while the damping performances are just slightly different. Thus, the NN controller is capable of overcoming unknown dynamics in nonlinear systems almost equally in the absence of knowledge of system parameters.

V.Conclusions

In this paper, the decentralized nonlinear discrete-time system is considered and control design for tracking problem is addressed to guarantee the boundedness of the large-scale system states. The design employs NN function approximation property to approximate the control gain matrix and internal dynamics of subsystems. There is no

offline NN training and all parameters are tuned online. By using Lyapunov techniques it is shown that the subsystems states as well as NN weight estimation errors are UUB with small bounded error. The interconnected power system can be expressed as an interconnected nonlinear dynamic system. Simulation results are performed on power systems with excitation control to verify the theoretical conjectures.

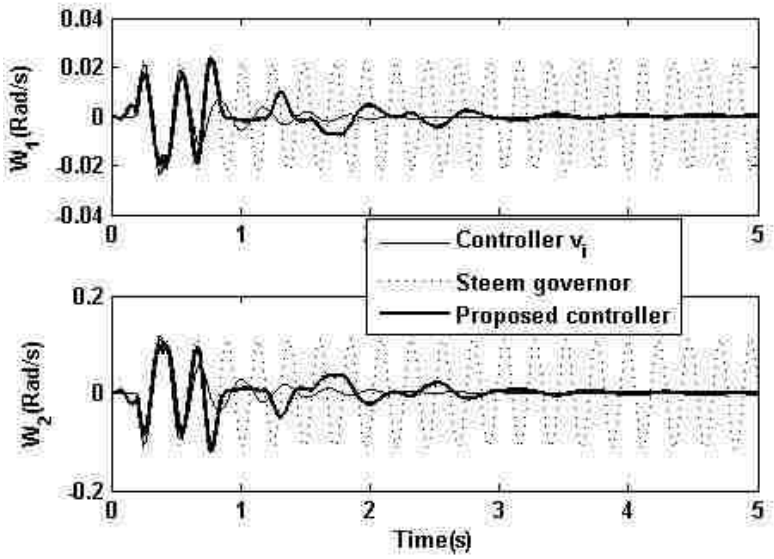

Fig. 12 Generator speeds with discrete-time control with fault on bus 3

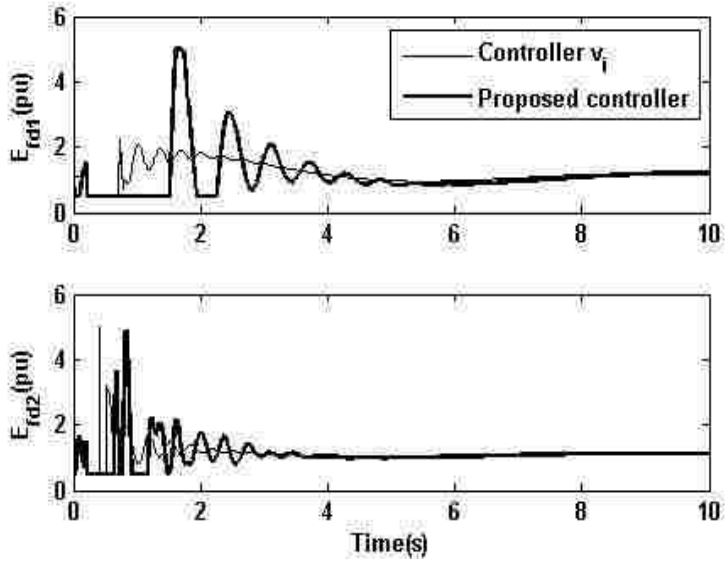

Fig. 13 Generator excitation voltages with the proposed controller

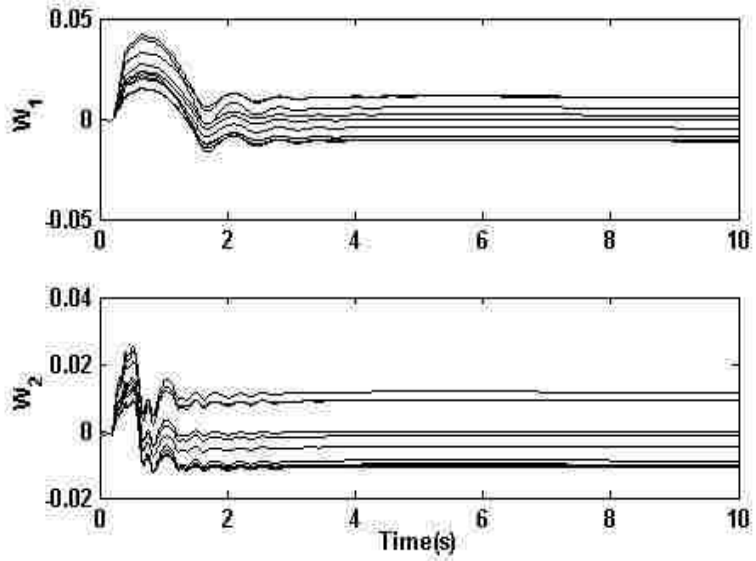

Fig. 14 NN weight estimates $\hat{W}_i$ for $1 \le i \le 2$

References

[1] S.N. Huang, K.K. Tan, and T.H. Lee, "Nonlinear Adaptive Control of Interconnected Systems Using Neural Networks," *IEEE Transactions on Neural Networks*, vol. 17, no. 1, pp.: 243 - 246, Jan. 2006.

[2] Y. Liu and X.Y. Li, "Decentralized Robust Adaptive Control of Nonlinear Systems with Unmodeled Dynamics," *IEEE Transactions on Automatic Control*, vol. 47, no. 5, pp.:848 – 856, May 2002.

[3] J. Zhou and C. Wen, "Decentralized Backstepping Adaptive Output Tracking of Interconnected Nonlinear Systems," *IEEE Transactions on* Automatic Control, vol. 53, no. 10, pp.: 2378 – 2384, Nov. 2008.

[4] Z. Jiang, "Decentralized and Adaptive Nonlinear Tracking of Large-scale Systems via Output Feedback," *IEEE Transactions on Automatic Control*, vol. 45, no. 11, pp.:2122 – 2128, Nov. 2000.

[5] S. Jagannathan "Decentralized Discrete-Time Neural Network Controller for a Class of Nonlinear Systems with Unknown Interconnections," *Proceedings of the 2005 IEEE International Symposium on Intelligent Control*, pp.: 268 – 273, 2005.

[6] E. Gyurkovics and T. Takacs, "Stabilization of Discrete-time Interconnected Systems Under Control Constraints", *IEE Proceedings on Control Theory and Applications*, vol. 147, no. 2, pp.: 137 – 144, March 2000.

[7] Y. H. Lin and K. S. Narendra , "A New Error Model for Adaptive Systems," *IEEE Transactions on Automatic Control*, vol. 25, no. 3, pp.: 585-587, June 1980.

[8] E. Davison and N. Tripathi, "The Optimal Decentralized Control of a Large Power System: Load and Frequency Control," *IEEE Transactions on Automatic Control*, vol. 23, no. 2, pp.:312 – 325, 1978.

[9] K. Ohtsuka and Y. Morioka, "A Decentralized Control System for Stabilizing a Longitudinal Power System Using Tie line Power Flow Measurements," *IEEE Transactions on Power Systems*, vol. 12, no. 3, pp.:1202 – 1209, 1997.

[10] G.K. Befekadu and I. Erlich, "Robust Decentralized Controller Design for Power Systems Using Matrix Inequalities Approaches," *IEEE Power Engineering Society General Meeting*, 2006.

[11] S. Xie, L. Xie, Y. Wang, and G. Guo, "Decentralized Control of Multi Machine Power Systems with Guaranteed Performance," *Proceedings of IEE Control Theory and Appls*, vol. 147, no. 3, pp.:355 – 365, May 2000.

[12] W. Liu,S. Jagannathan, G. K. Venayagamoorthy, D. C. Wunsch, M. L. Crow, L. Liu, and D. A. Cartes, "Neural Network Based Decentralized Controls of Large Scale Power Systems," *IEEE International Symposium on Intelligent Control*, pp.:676 – 681, October 2007.

[13] W. Qiu, V. Vittal, and M. Khammash, "Decentralized Power System Stabilizer Design Using Linear Parameter Varying Approach," *IEEE Transactions on Power Systems*, vol. 19, no. 4, pp.: 1951 – 1960, 2004.

[14] C.M. Lim and T. Hiyama, "Self-tuning Control Scheme for Stability Enhancement of Multi Machine Power Systems," *IEE Proceedings on Generation, Transmission and Distribution*, vol. 137, no. 4, pp.: 269 – 275, July 1990.

[15] S. Jagannathan, *Neural Network Control of Nonlinear Discrete-time Systems*, CRC Press, April 2006.

[16] J.T. Spooner and K.M. Passino, "Decentralized Adaptive Control of Nonlinear Systems Using Radial Basis Neural Networks," *IEEE Transactions on Automatic Control*, vol. 44, no. 11, pp.: 2050 – 2057, Nov. 1999.

[17] P. Kundur, J. Paserba, V. Ajjarapu, G. Andersson, A. Bose, C. Canizares, N. Hatziargyriou, D. Hill, A. Stankovic, C. Taylor, Van T. Cutsem, and V. Vittal, "Definition and Classification of Power System Stability IEEE/CIGRE Joint Task Force on Stability Terms and Definitions," *IEEE Transactions on Power Systems*, vol. 19, no. 3, pp.:1387 – 1401, Aug. 2004.

[18] S. Mehraeen, S. Jagannathan, and M. L. Crow, "Novel Dynamic Representation and Control of Power Networks Embedded with FACTS Devices," *Proceedings of IEEE Conference on System, Man and Cybernetics*, pp.: 3171-3176, Oct. 2008.

[19] P.W. Sauer and M.A. Pai, *Power System Dynamics and Stability*, Prentice Hall, 1997.

[20] F. Lewis, S. Jagannathan, S., and A. Yesildirek, *Neural Network Control of Robot. Manipulators and Nonlinear Systems*, Taylor & Francis, 1998.

[21] B. Igelnik and Y. H. Pao, "Stochastic Choice of Basis Functions in Adaptive Function Approximation and the Functional-link Net," *IEEE Trans. Neural Network*, vol. 6, no. 6, pp.: 1320–1329, Nov. 1995.

5. Decentralized Near Optimal Control of a Class of Interconnected Nonlinear Discrete-time Systems by Using Online Hamilton-Bellman-Jacobi Formulation

S. Mehraeen and S. Jagannathan[1]

***Abstract*—** *In this paper, the direct neural dynamic programming technique is utilized to solve the HJB (Hamilton Jacobi-Bellman) equation forward-in-time for the decentralized near optimal control of nonlinear interconnected discrete-time systems in affine form with known subsystem and unknown interconnection dynamics. The optimal controller design consists of two NNs; an action NN that is aimed to provide a nearly optimal control signal, and a critic NN which evaluates the performance of the system. All NN parameters are tuned online for both the NNs. By using Lyapunov techniques all subsystems signals are shown to be uniformly ultimately bounded (UUB) and that the synthesized subsystems inputs approach their corresponding near optimal control inputs with small bounded error. Simulation results are shown on an interconnected system to show the effectiveness of the approach.*

Index Terms –Decentralized Control, Neural Networks (NN), Optimal Control, Hamilton-Jacobi-Bellman (HJB), Nonlinear Discrete-time (DT) Systems.

[1] Authors are with Department of Electrical and Computer Engineering, Missouri University of Science and Technology, 1870 Miner Circle, Rolla, MO 65409. Contact author: sm347@mst.edu. Research Supported in part by NSF ECCS#0624644.

I. Introduction

Online approximators such as neural networks (NN) have been widely used in the controller design of nonlinear systems; however, they are mostly utilized to achieve stability [1]. An optimal control policy is necessary to stabilize the system in an optimal manner when the control costs have to be considered in addition to the system stability. Therefore, in the optimal control formulation, the objective of the controller is to minimize a cost function comprising of the states of the system and the control input [2]. The optimal control of linear systems is well-known and can be obtained by solving the Riccati equation [2]. However, the optimal control of nonlinear discrete time systems often requires solving the nonlinear Hamilton-Jacobi-Bellman (HJB) equation.

The HJB equation is more difficult to solve due to a lack of a closed-form solution and therefore recently offline methods have been developed to solve the discrete-time HJB equation [3][4]. These solutions are based on policy-value iterations for centralized discrete-time nonlinear systems to solve the nonlinear HJB partial difference/differential equation. Subsequently, neural networks (NN) are utilized to approximate the unknown nonlinear functions. In [3], the authors approximate the cost function with a Taylor series expansion under the assumption of small perturbation and propose an iterative algorithm to find the optimal control policy. In [4], the authors employ heuristic dynamic programming [5] in an iterative based offline solution. In general, the offline methods with NNs require lengthy iterative procedures to obtain a closed form solution for a region of interest in the state space.

By contrast, online approximator based controller designs are presented in [5-7] to address the HJB solution forward-in-time without involving the difficulties in iterative

offline training methodology. These methods are referred to as forward dynamic programming (FDP) or adaptive critic designs (ACD). In [6-7], the optimal control law and cost function are approximated by online parametric structures, such as NN's where the methods are verified by numerical simulations without presenting the convergence proof. The tracking problem with HJB solution is proposed in [8-11]. In [8] the tracking problem is addressed through linearization of the tracking error equations, whereas in [9] receding horizon optimal control is presented. The inverse optimal control [10] and offline direct calculation of the infinite horizon HJB equation [11] are among the recent approaches to the optimal tracking problem.

On the other hand, there has been a great interest in the decentralized control of a class of interconnected nonlinear systems using NNs. The decentralized control effort has focused mainly on stabilization and tracking for nonlinear continuous-time systems [12-16] and limited effort for affine nonlinear discrete-time systems [17][18]. The discrete-time proofs are much involved than their continuous-time counterpart since the first difference of a Lyapunov function candidate is quadratic with respect to the states whereas it is linear for the case of continuous-time system. To the best knowledge of the authors, no work is currently done on the optimal control of nonlinear decentralized discrete-time systems in affine form.

In this work the direct neural dynamic programming (DNDP) approach is utilized for the optimal regulation and tracking of nonlinear interconnected discrete-time systems in affine form by solving the HJB equation online and forward-in-time. The NNs are used to approximate the critic as well as the action networks where the optimal control signal is approximated while minimizing the cost function based on the information provided by

the critic in the presence of the unknown interconnection terms but known subsystems dynamics. Additionally, overall closed-loop stability of the nonlinear decentralized system is presented.

This paper is organized as follows. First, the class of interconnected nonlinear discrete-time system is introduced in Section II. In Section III, background information of the HJB optimal methodology and the online methodology for the HJB-based optimal control are introduced for interconnected systems. Then, numerical simulations and concluding remarks are provided in Sections IV and V, respectively.

II. Nonlinear Interconnected System

Consider the class of N interconnected subsystems defined as

$$\begin{aligned} &x_{i1}(k+1) = x_{i2}(k) \\ &\vdots \\ &x_{in-1}(k+1) = x_{in}(k) \\ &x_{in}(k+1) = f_i(x_i(k)) + g_i(x_i(k))u_i + \Delta_i(X) \\ &y_i(k) = x_{i1}(k) \end{aligned} \tag{1}$$

where index i represents the subsystem number, N is the number of subsystems, n is the order of the subsystem, $f_i(x_i(k))$, represents subsystem internal nonlinear dynamics, $g_i(x_i(k))$ is the input gain matrix, $u_i(k)$ is the subsystem control input, $\Delta_i(x)$ denotes interconnected terms of the subsystem 'i' with $x = [x_1^T, \ldots, x_N^T]^T$, $x_i = [x_{i1}, \ldots, x_{in}]^T$ for $1 \le i \le N$. Define the tracking error

$$z_{ip}(k) = x_{ip}(k) - x_{ipd}(k) \tag{2}$$

for $1 \le i \le N$ and $1 \le p \le n$, where $x_{ipd}(k)$ is the desired trajectory for state $x_{ip}(k)$, and $x_{i,p+1,d}(k) = x_{ipd}(k+1)$ for $1 \le p \le n-1$. Note that for the stabilization problem the desired values become $x_{ipd} = 0$ for $1 \le p \le n$. Next, define the filtered tracking error

$$r_i(k) = [\lambda_i \ 1]^T z_i(k) \tag{3}$$

where $z_i(k) = [z_{i1}(k) \ z_{i2}(k) \ \ldots z_{in}(k)]^T$ and $\lambda_i = [\lambda_{i1} \ \lambda_{i2} \ \ldots \lambda_{i,n-1}]$. The coefficients λ_{i1} through $\lambda_{i,n-1}$ are selected such that the poles of the characteristic equation $\zeta(q) = \lambda_{i1} + \lambda_{i2} q + \cdots + \lambda_{i,n-1} q^{n-2} + q^{n-1}$ are inside the unit disc. Before we proceed, the following definition and mild assumptions are needed.

Definition 1. (*Uniform Ultimate Bounded (UUB)*)[19]: Consider the dynamical system $\dot{x} = f(x)$ with $x \in \Re^n$ being a state vector. Let the initial time be t_0 and initial condition be $x_0 = x(t_0)$. Then, the equilibrium point x_e is said to be UUB if there exists a compact set $S \subset \Re^n$ so that for all $x_0 \in S$ there exists a bound B and a time $T(B, x_0)$ such that $\|x(t) - x_e\| \le B$ for $\forall t > t_0 + T$.

Assumption 1: Let the interconnection terms in (1) be bounded above in a compact set Ω such that

$$|\Delta_i(x)|^2 \le \sum_{j=1}^{N} \delta_{ij}(r_j) \le \sum_{j=1}^{N} \gamma_j r_j^{\ 2} \tag{4}$$

where γ_j is known small positive constants for $1 \le i \le N$ in contrast with [17].

Assumption 2: The input gain of each subsystem $g_i(x_i(k))$ in (1) is bounded away from zero and is bounded above in the compact set Ω. Without loss of generality, we assume that it satisfies

$$0 < g_{i\min} \le g_i(x_i(k)) \le g_{i\max} \tag{5}$$

in a compact set Ω where $g_{i\min}$ and $g_{i\max}$ are positive real constants.

Remark 1: Assumptions 1 and 2 are standard in the control literature [15].

Next, the decentralized optimal controller development is introduced.

III. Decentralized Optimal Control

In this section our goal is to find optimal control inputs $u_i(k)$ for $1 \le i \le N$ that can stabilize the interconnected system (1) while minimizing the infinite horizon system cost function

$$\begin{aligned} \bar{J}(x(k)) &= \sum_{j=k}^{\infty} \left(Q(x(j)) + u^T(x(j)) R u(x(j)) \right) \\ &= Q(x(k)) + u^T R u + \bar{J}(x(k+1)) \end{aligned} \tag{6}$$

where $Q(x) \in \Re^+$ is a positive definite function of the large-scale system states, $R \in \Re^{N \times N}$ is positive definite design matrix, and $u(x(k)) = [u_1(k), \ldots, u_N(k)]^T$ where $u_i(k)$ is only a function of the *i*th subsystem states (for $1 \le i \le N$). In addition to stabilizing the nonlinear system (1), the control input $u(k)$ must make the cost function (6) finite. In other words, $u(k)$ must be admissible.

Definition 2. *(Admissibility)* : The control input $u(k)$ is admissible with respect to the penalty function $Q(x) \ge 0$ and control energy penalty $u^T(k) R u(k)$ function if a) u is continuous; b) $u(x)|_{x=0} = 0$; c) $u(x)$ stabilizes system (1); and d) $\bar{J}(x(0), u, k) = \sum_{j=0}^{\infty} \left(Q(x(j)) + u^T R u \right) \le \infty$.

Moving on, this optimal control problem provides an optimal control input $u^*(x(k))$ such that $\bar{J}(u^*(k)) \le \bar{J}(u(k))$ for $\forall u(k)$. The minimizing control input $u^*(k)$ is found by using the stationary condition [2] as $\partial \bar{J}(k)/\partial u(k) = 0$, and routine calculation shows that

$$u^*(k) = -\frac{1}{2} R^{-1} g(x(k))^T \frac{\partial \bar{J}(k+1)}{\partial x(k+1)} \tag{7}$$

where $g(x(k)) = [\bar{g}_1{}^T(x_1(k)),\ldots,\bar{g}_N{}^T(x_N(k))]^T$ and $\bar{g}_i(x_i(k))_{n\times 1} = [0,\ldots,g_i(x_i(k))]^T$ for $1 \le i \le N$. From (6) and (7), we can observe that the large-scale cost function $\bar{J}(k)$ and the optimal control $u^*(k)$ (and its components $u_i{}^*(k)$ for $1 \le i \le N$) are in general functions of all large-scale system states. However, in the decentralized control strategy, only the corresponding subsystem states (such as $x_i(k)$) are available for designing the controller $u_i(k)$ for $1 \le i \le N$. By selecting proper $Q(x)$ and R decoupling the cost function (6) is possible which is presented next.

Lemma 1. *(Existence of Subsystem Cost Functions): Consider the interconnected nonlinear system (1) and associated cost function (6). Let $Q(x)$ be found satisfying*

$$Q(x) = \sum_{i=1}^{N} Q_i(x_i) \tag{8}$$

where each $Q_i(x_i)$ is a positive definite function. Then, the following results are obtained.

a) There exist positive definite matrices R_i such that $\bar{J}(x(k)) \ge \sum_{i=1}^{N} J_i(x_i(k))$ where $J_i(x_i(k)) = \sum_{j=k}^{\infty} \left(Q_i(x_i(j)) + u_i^T(j) R_i u_i(j)\right)$ is a cost function of subsystem states and control input for $1 \le i \le N$.

b) If there exists $R = diag(R_1,\ldots,R_N)$ *where* R_i *is positive definite matrix for* $1 \le i \le N$ *, then the large-scale optimal policy* $u^*(x(k))$ *in (7) can be obtained via individual subsystem optimal policies* $u_i^*(x(k))$ *where* $u^*(x(k)) = [u_1^*(x_i(k)),\ldots,u_N^*(x_i(k))]^T$ *.*

Proof. Part a) Starting from equation (6) and using (8), we have

$$\begin{aligned} \bar{J}(x(k)) &\ge \sum_{j=k}^{\infty}\left(Q(x(j)) + \lambda_{\min}(R)u^T(j)u(j)\right) \\ &= \sum_{j=k}^{\infty}\sum_{i=1}^{N}\left(Q_i(x_i(j)) + \lambda_{\min}(R)u_i^T(j)u_i(j)\right) \end{aligned} \quad . \tag{9}$$

where $\lambda_{\min}(.)$ is the minimum singular value . By defining $R_i = \lambda_{\min}(R)I_{n\times n}$, we obtain (10).

$$\begin{aligned} \bar{J}(x(k)) &\ge \sum_{j=k}^{\infty}\sum_{i=1}^{N}\left(Q_i(x_i(j)) + u_i^T(j)R_iu_i(j)\right) \\ &= \sum_{i=1}^{N}\sum_{j=k}^{\infty}\left(Q_i(x_i(j)) + u_i^T(j)R_iu_i(j)\right) \\ &= \sum_{i=1}^{N} J_i(x_i(k)) \\ &= \sum_{i=1}^{N}\left(Q_i(x_i(k)) + u_i^T(k)R_iu_i(k) + J_i(k+1)\right) \end{aligned} \tag{10}$$

Note that (10) results $\max\left(\bar{J}(x(k))\right) \ge \max\left(\sum_{i=1}^{N} J_i(x_i(k))\right)$ where $J_i(x_i(k)) = \sum_{j=k}^{\infty}\left(Q_i(x_i(j)) + u_i^T(j)R_iu_i(j)\right)$ is positive definite, and thus, the cost function for subsystem "i" (for $1 \le i \le N$) exist provided that large-scale cost function $\bar{J}(x(k))$ is well-defined.

Part b) In the case of diagonal matrix R, the cost function (6) becomes

$$\begin{aligned} \bar{J}(x(k)) &= \sum_{i=1}^{N} J_i(x_i(k)) \\ &= \sum_{i=1}^{N}\left(Q_i(x_i(k)) + u_i^T(k)R_iu_i(k) + J_i(k+1)\right) \end{aligned} \tag{11}$$

where $R = diag(R_1,\ldots,R_N)$. In this case the optimal control solution (7) becomes

$$u^*(k) = -\frac{1}{2}R^{-1}g(x(k))^T\left[\frac{\partial \bar{J}(k+1)}{\partial x_1(k+1)},\ldots,\frac{\partial \bar{J}(k+1)}{\partial x_N(k+1)}\right] \tag{12}$$

According to (11), the term $\partial \bar{J}(k+1)/\partial x_i(k+1)$ in (12) is only a function of $x_i(k+1)$. Thus, by expanding (12), we obtain $u^*(x(k)) = [u_1^*(x(k)),\ldots,u_N^*(x(k))]^T$ where

$$u_i^*(k) = -\frac{1}{2}R_i^{-1}\bar{g}_i(x_i(k))^T\frac{\partial J_i(k+1)}{\partial x_i(k+1)} \tag{13}$$

which is the optimal policy corresponding to the subsystem cost function

$$J_i(x_i(k)) = \sum_{j=k}^{\infty}\left(Q_i(x_i(j)) + u_i^T(j)R_iu_i(j)\right) \tag{14}$$

■

Remark 2: From part (b) of Lemma 1, if the subsystem optimal policy $u_i^*(k)$ is found, the optimal control input $u(k)$ can be found for the large-scale interconnected system. Even then it is still a difficult problem since the interconnection terms for each subsystem is a function of all the states of the large-scale system.

From Lemma 1, the optimal control problem can be divided into subsystem optimal control problems. However, finding a solution for the optimal policy (13) is still generally hard due to the solution of the HJB equation and presence of unknown interconnection terms. Here we use NN to approximate the cost function (14) and optimal policy (13) and present a forward-in-time solution. The unknown interconnection terms are overcome by augmenting the control input with a feed forward term comprising of subsystem states similar to the problem of tracking. Therefore, for each subsystem the design consists of an action network which is designed to produce a nearly optimal control signal, and a critic

network which evaluates the performance of the system. The augmented term is also introduced in this section. By using the universal approximation property of NN's [1], the control input (13) and cost function (14) can be represented by neural networks as

$$J_i(k) = W_{ci}{}^T \phi_i(x_i(k)) + \varepsilon_{ci} \tag{15}$$

and

$$u_i(k) = u_i^*(k) = W_{a\,i}{}^T \psi_i(x_i(k)) + \varepsilon_{a\,i} + F_i(x_i(k)) \tag{16}$$

respectively, where W_{ci} and $W_{a\,i}$ are the ideal subsystem critic and action NN weights and are assumed to be bounded with bounds $\|W_{ci}\| \le W_{ciM}$, $\|W_{a\,i}\| \le W_{a\,iM}$, ε_{ci} and $\varepsilon_{a\,i}$ are the bounded approximation errors which satisfy $|\varepsilon_{ci}| \le \varepsilon_{ciM}$, $|\varepsilon_{a\,i}| \le \varepsilon_{a\,iM}$, $\phi_i(.)$ and $\psi_i(.)$ are the vector activation functions for the critic and action networks, respectively[1], and $F_i(x_i(k))$ is a known function added to help overcome the effect of interconnection terms which will be defined shortly. Before we discuss the critic and action networks, the following assumption is required.

Assumption 3: The critic network approximation error satisfies $\left|\partial \varepsilon_{ci}(x_i(k+1))/\partial x_i(k+1)\right| \le \bar{\varepsilon}_{cM}$ in the compact set Ω for $1 \le i \le N$.

A. The Critic Network Design

The objective of the optimal control law is to stabilize the system (1) while minimizing the cost functions (14). Since the cost function (14) is analytically not available it is approximated by a NN and written as (15); however, in practice the NN ideal weights are not available. Consequently, the cost function $J_i(k)$ is approximated by

$$\hat{J}_i(k) = \hat{W}_{ci}{}^T(k) \phi_i(x_i(k)) \tag{17}$$

where $\hat{W}_{ci}$ is the estimated values for the ideal weights W_{ci} and $\phi_i(.)$ is the vector of activation functions which are chosen to be basis sets and thus are linearly independent. Define the augmented matrices and cost function $\hat{\mathbf{J}}(k)$ as

$$\mathbf{W}_c = \begin{bmatrix} W_{c1} & & 0 \\ & \ddots & \\ 0 & & W_{cN} \end{bmatrix},\ \hat{\mathbf{W}}_c = \begin{bmatrix} \hat{W}_{c1} & & 0 \\ & \ddots & \\ 0 & & \hat{W}_{cN} \end{bmatrix},\ \mathbf{\Phi} = \begin{bmatrix} \phi_1 & & 0 \\ & \ddots & \\ 0 & & \phi_N \end{bmatrix},\ \boldsymbol{\varepsilon}_c = \begin{bmatrix} \varepsilon_{c1} & & 0 \\ & \ddots & \\ 0 & & \varepsilon_{cN} \end{bmatrix}, \text{ and}$$

$$\hat{\mathbf{J}}(k) = \hat{\mathbf{W}}_c^{\ T}(k)\mathbf{\Phi}(x(k)). \tag{18}$$

Define the critic error as

$$\mathbf{E}_c(k) = \mathbf{Q}(k-1) + \hat{\mathbf{W}}_c^{\ T}(k)\Delta\mathbf{\Phi}(k) \tag{19}$$

where

$$\Delta\mathbf{\Phi}(k) = \mathbf{\Phi}(x(k)) - \mathbf{\Phi}(x(k-1)) \tag{20}$$

and $\mathbf{Q} = \begin{bmatrix} Q_1 + u_1^{\ T} R_1 u_1 & & 0 \\ & \ddots & \\ 0 & & Q_N + u_N^{\ T} R_N u_N \end{bmatrix}$. Then the critic error dynamics become

$$\mathbf{E}_c(k+1) = \mathbf{Q}(k) + \hat{\mathbf{W}}_c^{\ T}(k+1)\Delta\mathbf{\Phi}(k+1) \tag{21}$$

By selecting the critic weight update law as [20]

$$\hat{\mathbf{W}}_c(k+1) = \Delta\mathbf{\Phi}(k+1)\left(\Delta\mathbf{\Phi}^T(k+1)\Delta\mathbf{\Phi}(k+1)\right)^{-1} \times \left(\alpha_c \mathbf{E}_c^{\ T}(k) - \mathbf{Q}^T(k)\right) \tag{22}$$

the critic error becomes

$$\mathbf{E}_c(k+1) = \alpha_c \mathbf{E}_c(k) \tag{23}$$

where $\alpha_c = \begin{bmatrix} \alpha_{c1} & & 0 \\ & \ddots & \\ 0 & & \alpha_{cN} \end{bmatrix}$ with α_{ci} being a design constant for $1 \le i \le N$. From (11) and

(15) we obtain

$$\begin{aligned}\mathbf{Q}(k) &= -\mathbf{W}_c{}^T\boldsymbol{\Phi}(k+1) + \mathbf{W}_c{}^T\boldsymbol{\Phi}(k) - \boldsymbol{\varepsilon}_c(k+1) + \boldsymbol{\varepsilon}_c(k) \\ &= -\mathbf{W}_c{}^T\Delta\boldsymbol{\Phi}(k+1) - \Delta\boldsymbol{\varepsilon}_c(k+1)\end{aligned} \tag{24}$$

where $\Delta\boldsymbol{\varepsilon}_c(k+1) = \boldsymbol{\varepsilon}_c(k+1) - \boldsymbol{\varepsilon}_c(k)$. Define weight estimation error to be $\tilde{\mathbf{W}}_\mathbf{c} = \mathbf{W}_\mathbf{c} - \hat{\mathbf{W}}_\mathbf{c}$. By using (24), (22), and (21) it can be concluded that

$$\begin{aligned}&\tilde{\mathbf{W}}_c{}^T(k+1)\Delta\boldsymbol{\Phi}(k+1) = \\ &-\alpha_c\left(\mathbf{Q}(k-1) + \hat{\mathbf{W}}_c{}^T(k)\Delta\boldsymbol{\Phi}(k)\right) - \Delta\boldsymbol{\varepsilon}_c(k+1)\end{aligned} \tag{25}$$

Then, by replacing $\mathbf{Q}(k-1)$ by a similar term as in (24) we obtain

$$\begin{aligned}&\Delta\boldsymbol{\Phi}^T(k+1)\tilde{\mathbf{W}}_c(k+1) = \\ &+\alpha_c\Delta\boldsymbol{\Phi}^T(k)\tilde{\mathbf{W}}_c(k) + \alpha_c\Delta\boldsymbol{\varepsilon}_c(k) - \Delta\boldsymbol{\varepsilon}_c(k+1)\end{aligned} \tag{26}$$

As a result, the dynamics of the weight estimation errors can be obtained as

$$\begin{aligned}&\tilde{\mathbf{W}}_c(k+1) = \alpha_c\Delta\boldsymbol{\Phi}(k+1)(\Delta\boldsymbol{\Phi}^T(k+1)\Delta\boldsymbol{\Phi}(k+1))^{-1} \times \\ &\left(\Delta\boldsymbol{\Phi}^T(k)\tilde{\mathbf{W}}_i(k) + \Delta\boldsymbol{\varepsilon}_c(k)\right) \\ &-\Delta\boldsymbol{\Phi}(k+1)(\Delta\boldsymbol{\Phi}^T(k+1)\Delta\boldsymbol{\Phi}(k+1))^{-1}\Delta\boldsymbol{\varepsilon}_c(k+1)\end{aligned} \tag{27}$$

The following technical results are needed before we proceed.

Definition 3: *Linear Independent Functions* [24]. A set of functions $\phi(k) = \{\phi_\ell(k)\}_1^{L:}$ is said to be linearly independent if $\sum_{\ell=1}^{L} c_\ell\phi_\ell(x) = 0$ implies that $c_1 = \cdots = c_L = 0$.

Lemma 2. Let $\mu(k)$ be an admissible control for system (1). If the set $\boldsymbol{\Phi}(k) = \{\boldsymbol{\Phi}_\ell(k)\}_1^{L:}$ is linearly independent, then the set $\Delta\boldsymbol{\Phi}(k+1) = \{\boldsymbol{\Phi}_\ell(k+1) - \boldsymbol{\Phi}_\ell(k)\}_1^N$ is also linearly independent.

Proof: Since, $\mu(k)$ is an admissible control, we have $x(\infty) = 0$, and thus, $\boldsymbol{\Phi}(x(\infty)) = 0$. Then, by observing $\boldsymbol{\Phi}(x(\infty)) - \boldsymbol{\Phi}(x(j)) = \sum_{k=j}^{\infty}(\boldsymbol{\Phi}(x(k+1)) - \boldsymbol{\Phi}(x(k)))$ and using contradiction the proof can be completed.

Remark 3. The matrix $\Delta\mathbf{\Phi}^T(k)\Delta\mathbf{\Phi}(k)$ is invertible provided $x(k)\neq 0$. Note from (14) and (18) that the cost function becomes zero only when $x(k)=0$. Thus, once the system states have converged to zero, the cost function approximation can no longer be updated. This can be expressed as persistency of excitation (PE) requirement for the inputs to the cost function approximator (18) where the subsystem states must be persistently exiting long enough such that the critic network learns the optimal cost function. Also, the PE condition ensures the existence of minimum values for the activation function ϕ_i.

Next, we show that the critic error (21) and the critic network estimation error (27) are UUB.

Theorem 1: *Consider the nonlinear discrete-time interconnected system given by (1). Let* $\mu_i(k)$ *be an initial admissible control input for the ith subsystem of the nonlinear interconnected discrete-time system. Let the overall cost function of the interconnected system,* $\hat{\mathbf{J}}(k)$, *be approximated by NNs as defined in (18) whose weight update law is provided by (22). Then, the critic errors (19) and critic weight estimation errors* $\tilde{\mathbf{W}}_c$ *are UUB.*

Proof: Consider the Lyapunov candidate

$$\mathbf{V}_c(k)=\mathbf{E}_c(k)^T\mathbf{E}_c(k)+\Delta\mathbf{\Phi}_{\min}^2 tr\{\tilde{\mathbf{W}}_c{}^T\tilde{\mathbf{W}}_c\} \tag{28}$$

where $\Delta\mathbf{\Phi}_{\min}^2$ is a positive constant and satisfies $\Delta\mathbf{\Phi}_{\min}^2\leq\left\|\Delta\mathbf{\Phi}^T(k+1)\Delta\mathbf{\Phi}(k+1)\right\|$. The existence of $\Delta\mathbf{\Phi}_{\min}^2>0$ is ensured by the PE condition described in Remark 3. Also, note that by admissibility of the control input, we can assume $\max\left\|\Delta\mathbf{\Phi}(k)\right\|$ exists. By calculating the first difference of $\mathbf{V}_c(k)$ and using $\Delta\mathbf{\Phi}_{\max}\geq\left\|\Delta\mathbf{\Phi}(k)\right\|$ we have

$$\Delta \mathbf{V}_c(k) = -(1-\|\alpha_c\|^2)\|\mathbf{E}_c(k)\|^2 - (\Delta\mathbf{\Phi}^2_{\min} - 4\|\alpha_c\|^2\Delta\mathbf{\Phi}^2_{\max})\|\tilde{\mathbf{W}}_c(k)\|^2 + (2+4\|\alpha_c\|^2)\varepsilon^2_{cM} \tag{29}$$

where ε^2_{cM} is the bound on the approximation error $\boldsymbol{\varepsilon}_c$ such that $\|\boldsymbol{\varepsilon}_c\| \le \varepsilon_{cM}$. The first difference of the Lyapunov function is less than zero provided

$$|\mathbf{E}_c| > \sqrt{\frac{(2+4\alpha^2_{ci})\varepsilon^2_{cM}}{1-\|\alpha_c\|^2}} \quad or \quad \|\tilde{\mathbf{W}}_c(k)\| > \sqrt{\frac{(2+4\alpha^2_{ci})\varepsilon^2_{cM}}{\Delta\mathbf{\Phi}^2_{\min} - 4\|\alpha_c\|^2\Delta\mathbf{\Phi}^2_{\max}}}$$

and the gain is chosen as $\|\alpha_c\|^2 < \min\{1, \frac{\Delta\mathbf{\Phi}^2_{\min}}{4\Delta\mathbf{\Phi}^2_{\max}}\}$.

Remark 4: It is interesting to observe that the NN weight update law (21) resembles the least squares update rule commonly used in offline ADP [3][4]; however, instead of summing over a mesh of training points [3][4], the update (21) represents a sum over the system's time history stored in $E_c(k)$. Thus, the update (21) uses data collected in real time instead of data formed offline [3][4].

Remark 5: The results of Theorem 1 are drawn under the assumption of a fixed admissible control policy which is relaxed in the following section.

B. The Action Network Design for Stabilization

The action network obtains the optimal control input which minimizes the approximated cost function (15). Note that the basis function $\psi_i(.)$ needs to be the gradient of the basis function $\phi_i(.)$ of the critic NN since the optimal control (16) depends on the gradient of the cost function according to (13). It is shown in [3] that the gradient of a linearly independent set is also linearly independent.

Remark 6. According to (13) the action network of subsystem 'i' estimates the derivative of the corresponding cost function $J_i(x_i(k))$ presented in (15) as (30)

$$\begin{aligned}&\partial J_i(k+1)/\partial x_i(k+1) = W_{ci}{}^T(k)\,\partial\phi_i(x_i(k+1))/\partial x_i(k+1)\\&+\partial\varepsilon_{ci}(x_i(k+1))/\partial x_i(k+1)\end{aligned} \tag{30}$$

which is a function of $x_i(k+1)$. Unlike the optimal control of affine systems [20], the term $x_i(k+1)$ for the interconnected system is not only a function of subsystem states but also, according to (1), is a function of the interconnection term $\Delta_i(.)$, which is a function of entire state vector $x(k)$. However, the action NN is only a function of subsystem states $x_i(k)$. Consequently, the action network will not able to approximate the optimal policy in (13) accurately due to the need for the entire state vector which is not available. Thus, this term must be transformed appropriately so that the augmented term in (16) can be used to compensate the effects of the interconnection term such that the stability proof can be performed in the presence of the interconnection term.

In order to elaborate on the effect of $\Delta_i(.)$ in the analysis, first we consider (30). In this analysis, we use Taylor series expansion of (30)

$$\begin{aligned}\xi_i(x(k+1)) &= \frac{\partial\phi_i^T(k+1)}{\partial x_i(k+1)}W_{ci}(k) + \frac{\partial\varepsilon_i(k+1)}{\partial x_i(k+1)}\\&= x_i(k+1)^T\nabla\xi_i + x_i(k+1)^T\nabla^2\xi_i x_i(k+1)^T + \cdots\end{aligned} \tag{31}$$

where ∇ is the gradient and ∇^2 is the Hessian matrices and the effect of the interconnection terms are assumed negligible in the second term and afterwards due to small γ_i for $1 \le i \le N$. Thus the higher order terms can be approximated as functions of subsystem only with small approximation error. Then, $\xi_i(x(k+1))$ can be rewritten as

$$\begin{aligned}\xi_i(x(k+1)) &\approx [x_{i1}(k+1)\ \ldots\ x_{in}(k+1)]\overline{\beta}_i + C_i(x_i(k)) + \sigma_i \\ &= [x_{i2}(k)\ \ldots\ f_i(x_i) + g_i(x_i)u_i + \Delta_i(X)]\overline{\beta}_i + C_i(x_i(k)) \\ &= \beta_i(x_i) + \overline{\beta}_{in} g_i(x_i)u_i + \overline{\beta}_{in}\Delta_i(X) + C_i(x_i(k)) + \sigma_i\end{aligned} \tag{32}$$

where $\overline{\beta}_i = \nabla\xi\big|_{x_i = x_{i0}}$ is the equilibrium point, $\overline{\beta}_i = [\overline{\beta}_{i1} \ldots \overline{\beta}_{in}]^T$, $\beta_i(x_i) = [x_{i2}(k)\ \ldots x_{in}(k)][\overline{\beta}_{i1}\ \ldots \overline{\beta}_{i,n-1}]^T$, $C_i(x_i)$ represents the higher order terms, and σ_i is a bounded term representing the terms with the higher order interconnection terms. Thus,

$$\begin{aligned}&-\frac{1}{2}R_i^{-1}\overline{g}_i(x_i(k))^T\left(\frac{\partial\phi_i(k+1)}{\partial x_i(k+1)}W_{ci}(k) + \frac{\partial\varepsilon_i(k+1)}{\partial x_i(k+1)}\right) \\ &= -\frac{1}{2}R_i^{-1}g_i(x_i(k))\begin{pmatrix}\beta_i(x_i) + \overline{\beta}_{in}(x_{i0})g_i(x_i)u_i \\ + \overline{\beta}_{in}(x_{i0})\Delta_i(x) + C_i(x_i(k))\end{pmatrix} \\ &= \overline{\sigma}_i(x_i) - \frac{1}{2}R_i^{-1}g_i(x_i(k))\overline{\beta}_{in}(x_{i0})\Delta_i(x) + \sigma_i\end{aligned} \tag{33}$$

where $\overline{\sigma}_i = -\frac{1}{2}R_i^{-1}g_i(x_i(k))\left(\beta_i(x_i) + \overline{\beta}_{in}(x_{i0})g_i(x_i)u_i + C_i(x_i(k))\right)$. Consequently, (31) can be expressed as (33) with $\overline{\sigma}_{i(x_i)}$ a function of local states and the interconnection term appearing with the local system states. Only $\overline{\sigma}_{i(x_i)}$ in (33) can be approximated by the action NN (i.e. $\overline{\sigma}_i(x_i) = W_{ai}{}^T(k)\psi_i(k) - \varepsilon_{ai}(k) + F_i(k)$), and thus, from (33) and rearranging the terms we obtain

$$\begin{aligned}&W_{ai}{}^T(k)\psi_i(k) - \varepsilon_{ai}(k) + F_i(k) - \frac{1}{2}R_i^{-1}g_i(k)\overline{\beta}_{in}(x_{i0})\Delta_i(k) \\ &+ \frac{1}{2}R_i^{-1}g_i(k)\frac{\partial\phi_i(k+1)}{\partial x_i(k+1)}W_{ci}{}^T(k) + \frac{1}{2}R_i^{-1}g_i(k)\frac{\partial\varepsilon_i(k+1)}{\partial x_i(k+1)} = 0\end{aligned} \tag{34}$$

This step is important when analyzing the action network error and plays a role in the stability analysis as will be shown. Transforming the partial derivative to (34) helps to include the effects of the interconnection term while still ensuring that the closed-loop system is bounded.

Next, equation (16) calculates the optimal policy through using a NN. In practice, the NN ideal weights and approximation errors are unknown and only an estimate of the weights is available. Thus,

$$\hat{u}_i(k) = \hat{W}_{a\,i}{}^T \psi_{a\,i}(x_i(k)) + F_i(x_i(k)) \tag{35}$$

where $\hat{W}_{a\,i}$ is the estimated values of the ideal weights $W_{a\,i}$. The function $F_i(x_i(k))$ is added to help overcome the effect of the interconnection terms in the large-scale nonlinear system and is defined as

$$F_i(x_i(k)) = g_i(x_i(k))^{-1}(f_i(x_i(k)) + [0\ \lambda_i]^T z_i) \tag{36}$$

Define the weight estimation error for the action NN as $\tilde{W}_{ai} = \hat{W}_{ai} - W_{ai}$ and the action error as

$$\begin{aligned} e_{a\,i}(k) &= \hat{W}_{a\,i}{}^T(k)\hat{\psi}_i(x_i(k)) + F_i(x_i(k)) \\ &\quad + \frac{1}{2} R_i^{-1} \bar{g}_i(x_i(k))^T \frac{\partial \phi_i(k+1)}{\partial x_i(k+1)} \hat{W}_{ci}(k) \end{aligned} \tag{37}$$

Subtracting (34) from (35) yields

$$\begin{aligned} e_{a\,i}(k) &= -\tilde{W}_{a\,i}{}^T(k)\psi_i(k) + \varepsilon_{a\,i}(k) \\ &\quad + \sigma_i - \frac{1}{2} R_i^{-1} g_i(k) \bar{\beta}_{in}(x_{i0}) \Delta_i(k) \\ &\quad - \frac{1}{2} R_i^{-1} g_i(k) \frac{\partial \phi_i(k+1)}{\partial x_{in}(k+1)} \tilde{W}_{ci}(k) \\ &\quad - \frac{1}{2} R_i^{-1} g_i(k) \frac{\partial \varepsilon_i(k+1)}{\partial x_{in}(k+1)} \end{aligned} \tag{38}$$

Also, define the action NN weight update law as

$$\hat{W}_{a\,i}(k+1) = \hat{W}_{a\,i}(k) - \alpha_{a\,i} \frac{\psi_i(k) e_{a\,i}(k)}{\psi_i{}^T(k)\psi_i(k) + 1} \tag{39}$$

which yields

$$\tilde{W}_{a\,i}(k+1)=\tilde{W}_{a\,i}(k)+\alpha_{a\,i}\frac{\psi_i(k)e_{a\,i}(k)}{\psi_i^{\,T}(k)\psi_i(k)+1} \tag{40}$$

From (38) and (40) we obtain

$$\begin{aligned} e_{a\,i}(k+1)=&-\tilde{W}_{a\,i}^{\,T}(k)\psi_i(k+1)-\alpha_{a\,i}\frac{\psi_i(k)\psi_i(k+1)e_{a\,i}(k)}{\psi_i^{\,T}(k)\psi_i(k)+1}\\ &+\varepsilon_{a\,i}(k+1)+\sigma_i(k+1)-\frac{1}{2}R_i^{-1}g_i(k+1)\bar{\beta}_{in}(x_{i0})\Delta_i(k+1)\\ &-\frac{1}{2}R_i^{-1}g_i(k+1)\frac{\partial\phi_i(k+2)}{\partial x_i(k+2)}\tilde{W}_{ci}(k+1)\\ &-\frac{1}{2}R_i^{-1}g_i(k+1)\frac{\partial\varepsilon_i(k+2)}{\partial x_i(k+2)} \end{aligned} \tag{41}$$

Lemma 3: *(Admissibility).* Let $u_{i0(k)}$ be an initial admissible control input for the subsystem 'i' of the controllable system (1). Then, there exists a positive constant α_{ai} such that the subsystem control policy (35) with parameter update (39) ensures that the future control sequence provides stabilizing policies for the nonlinear system (1).

Proof: Steps follow similar to [20].

C. Filtered Tracking Error and Stability Analysis

By using the subsystem dynamics (1) and control input (35), the filtered tracking error dynamic defined in (3) is given by

$$\begin{aligned} &r_i(k+1)=f_i(x_i(k))+[0\ \lambda_i]^T z_i+\\ &g_i(x_i(k))\left(\hat{W}_{a\,i}^{\,T}\psi_{a\,i}(k)+F_i(x_i(k))\right)+\Delta_i(X)\\ &=g_i(x_i(k))\left(\tilde{W}_{a\,i}^{\,T}(k)\psi_{a\,i}(k)+W_{a\,i}^{\,T}\psi_{a\,i}(x_i(k))\right)+\Delta_i(X) \end{aligned} \tag{42}$$

In this part we show that the nonlinear discrete-time interconnected system (1) along with controller (35), critic network (17), and given neural network weight update laws is stable and the filtered tracking error and weight estimation errors (27) and (40) of the individual subsystems are bounded, even in the presence of the unknown interconnection terms $\Delta_i(x)$ for $1\le i\le N$.

Remark 7. The subsystem action error in (38) is different from the action error in [20] in the sense that it contains the interconnection term which has to be explicitly considered. As a result, a suitable Lyapunov function (which is a different Lyapunov from what is used in [20]) has to be considered to overcome the interconnection term effect.

Theorem 2: *Consider the nonlinear discrete-time interconnected system given by (1). Let* $\mu_i(k)$ *be an initial admissible control input for the ith subsystem of the nonlinear interconnected discrete-time system* for $1 \le i \le N$. *Consider the Assumptions 1 through 3 hold and that the initial conditions for system (1) are bounded in the compact set* Ω. *Let the weight tuning for the critic and action networks be provided by (22) and (39), respectively. Then, the critic error (19), the action error (37), and regulation error* $r_i(k)$ *along with the weight approximation errors of the critic and action network are all uniformly ultimately bounded (UUB) for all k ≥ k + T0. In addition,* $u_i \to u_i^* + \varepsilon_b$.

Proof: Define the overall Lyapunov function candidate

$$V(k) = \sum_{i=1}^{N} V_i(k) = \sum_{i=1}^{N} \frac{\overline{\psi}_i \Delta\phi_{i\min}^2 \alpha_{ci}{}^2 \alpha_{ai}}{3(\psi_{i\max}^2 + 1)} L_{ri}(k) + \sum_{i=1}^{N} V_{ci}(k) + \sum_{i=1}^{N} V_{a\,i}(k) + \sum_{i=1}^{N} V_{wi}(k) \tag{43}$$

Where $L_{ri} = \left(r_i(k) \Big/ \sqrt{g_{i(k-1)}}\right)^2$, $V_{a\,i}(k) = \alpha_{a\,i}\alpha_{ci}{}^2 \dfrac{\Delta\phi_{i\min}^2}{\psi_{i\max}^2 + 1} e_{a\,i}{}^2(k)$, $V_{wi}(k) = 8\overline{\psi}_i \Delta\phi_{i\min}^2 \alpha_{ci}{}^2 \tilde{W}_{a\,i}{}^T(k) \tilde{W}_{a\,i}(k)$, $\overline{\psi}_i = [\max \psi_i(k) / \min \psi_i(k)]^2$, in the compact set Ω and $V_{ci}(k) = e_{ci}{}^2(k) + \Delta\phi_{i\min}^2 \tilde{W}_{ci}{}^T \tilde{W}_{ci}$ with $e_{ci}(k) = Q_i(k-1) + \hat{W}_c{}^T(k)\Delta\phi_i(k)$, $\tilde{W}_{ci} = W_{ci} - \hat{W}_{ci}$, $\Delta\phi_{i\min}^2 \le \left\|\Delta\phi_i{}^T(k+1)\Delta\phi_i(k+1)\right\|$, and $\Delta\phi_i(k) = \phi_i(k) - \phi_i(k-1)$. Then, the first difference of the Lyapunov function due to the first term in (43) becomes

$$\sum_{i=1}^{N}\Delta L_{ri}=\sum_{i=1}^{N}\left(\frac{r_i(k+1)}{g_{i(k)}}\right)^2-\sum_{i=1}^{N}\left(\frac{r_i(k)}{g_{i(k-1)}}\right)^2 \tag{44}$$

Substituting (42) into (44) and using Cauchy-Schwartz inequality $(a_1+a_2+\cdots+a_n)^2 \le n(a_1{}^2+a_2{}^2+\cdots+a_n{}^2)$, we obtain

$$\Delta L_{ri}\le\sum_{i=1}^{N}\left(3\psi_i{}^T\tilde{W}_{ai}\tilde{W}_{ai}{}^T\psi_i+3\psi_i{}^TW_{ai}W_{ai}{}^T\psi_i+3\frac{\Delta_i{}^2}{g_i(k)}\right)-\sum_{i=1}^{N}\left(\frac{r_i(k)}{g_i(k-1)}\right)^2 \tag{45}$$

By using Assumption 1 and noting that $\sum_{i=1}^{N}\sum_{j=1}^{N}\gamma_j r_j{}^2=\sum_{i=1}^{N}\sum_{j=1}^{N}\gamma_i r_i{}^2=\sum_{i=1}^{N}N\gamma_i r_i{}^2$ we obtain

$$\Delta L_{ri}\le\sum_{i=1}^{N}\left(3\psi_i{}^T\tilde{W}_{ai}\tilde{W}_{ai}{}^T\psi_i+3\psi_i{}^TW_{ai}W_{ai}{}^T\psi_i\right)-\sum_{i=1}^{N}\left(\frac{1}{g_{i\max}}-\frac{3N\gamma_i}{g_{i\min}}\right)r_i{}^2(k) \tag{46}$$

Next, by using (40), the first difference due to the second term in the overall Lyapunov and using Cauchy-Schwartz inequality function candidate is obtained as

$$\begin{aligned}\Delta V_{a\,i}(k)=&\alpha_{a\,i}\alpha_{ci}{}^2\frac{\Delta\phi_{i\min}^2}{\psi_{i\max}^2+1}\times\\&\left(\begin{array}{l}7\alpha_{ai}^2\left(\frac{\psi_i{}^T(k)\psi_i(k+1)}{\psi_i{}^T(k)\psi_i(k)+1}\right)^2e_{ai}^2(k)+7\sigma_i{}^2(k+1)\\+7\left(\varepsilon_{ai}{}^2(k+1)+\psi_i(x_i(k+1))^T\tilde{W}_{a\,i}{}^T(k)\tilde{W}_{a\,i}{}^T(k)\psi_i(x_i(k+1))\right)\\+\frac{7}{4}\frac{\partial\varepsilon_{ci}(k+2)}{\partial x_{in}(k+2)}{}^T\bar{g}_i{}^T(k+1)(R_i{}^{-1})^2\bar{g}_i(k+1)\frac{\partial\varepsilon_{ci}(k+2)}{\partial x_{in}(k+2)}\\+\frac{7}{4}\tilde{W}_{ci}{}^T(k+1)\frac{\partial\phi_i{}^T(k+2)}{\partial x_{in}(k+2)}\bar{g}_i{}^T(k+1)(R_i{}^{-1})^2\bar{g}_i(k+1)\times\\\quad\frac{\partial\phi_i{}^T(k+2)}{\partial x_{in}(k+2)}\tilde{W}_{ci}(k+1)\\+\frac{7}{4}\bar{g}_i{}^T(k+1)(R_i{}^{-1})^2\bar{g}_i(k+1)\bar{\beta}_{in}{}^2(x_{i0})\Delta_i{}^2(k+1)-e_{ai}{}^2(k)\end{array}\right)\end{aligned} \tag{47}$$

The interconnection term $\Delta_i{}^2(k+1)$ in (47) can be expanded by using Assumption 1 and $\sum_{j=1}^{N}\sum_{l=1}^{N}\gamma_j\gamma_l r_l{}^2=\sum_{j=1}^{N}\gamma_j\left(\sum_{l=1}^{N}\gamma_l\right)r_j{}^2$. Consequently,

$$
\begin{aligned}
&\left|\Delta_i(x(k+1))\right|^2 \le \sum_{j=1}^{N}\gamma_j {r_j}^2(k+1)\\
&\le \sum_{j=1}^{N}\gamma_j\left[g_j(x_j(k))\left(\tilde{W}_{a\,j}{}^T\psi_{a\,j}(k)+W_{a\,j}{}^T\psi_{a\,j}(k)\right)+\Delta_j(x)\right]^2\\
&\le \sum_{j=1}^{N}\gamma_j\left\{\begin{array}{l}3{g_j}^2(k)\tilde{W}_{a\,j}{}^T\psi_{a\,j}\psi_{a\,j}{}^T\tilde{W}_{a\,j}\\+3{g_j}^2(k)W_{a\,j}{}^T\psi_{a\,j}\psi_{a\,j}{}^T W_{a\,j}+3\sum_{l=1}^{N}\gamma_l {r_l}^2(k)\end{array}\right\}\\
&\le \sum_{j=1}^{N}\left\{\begin{array}{l}3\gamma_j{g_j}^2(k)\tilde{W}_{a\,j}{}^T\psi_{a\,j}\psi_{a\,j}{}^T\tilde{W}_{a\,j}\\+3\gamma_j{g_j}^2(k)W_{a\,j}{}^T\psi_{a\,j}\psi_{a\,j}{}^T W_{a\,j}\end{array}\right\}+3\gamma_j\sum_{l=1}^{N}\gamma_l {r_j}^2(k)
\end{aligned}
\tag{48}
$$

Moreover, the term $\tilde{W}_{ci}{}^T(k+1)\tilde{W}_{ci}(k+1)$ in (47) can be expanded by using the update law (22) as shown below

$$
\begin{aligned}
&\tilde{W}_{ci}{}^T(k+1)\tilde{W}_{ci}(k+1) \le 2{\alpha_{ci}}^2\left(\tilde{W}_{ci}{}^T(k)\Delta\phi_i(k)+\Delta\varepsilon_{ci}(k)\right)\\
&(\Delta\phi_i{}^T(k+1)\Delta\phi_i(k+1))^{-1}\Delta\phi_i{}^T(k+1)\\
&\Delta\phi_i(k+1)(\Delta\phi_i{}^T(k+1)\Delta\phi_i(k+1))^{-1}\left(\Delta\phi_i{}^T(k)\tilde{W}_{ci}(k)+\Delta\varepsilon_{ci}(k)\right)\\
&+2(\Delta\phi_i{}^T(k+1)\Delta\phi_i(k+1))^{-1}\Delta\phi_i{}^T(k+1)\times\\
&\Delta\phi_i(k+1)(\Delta\phi_i{}^T(k+1)\Delta\phi_i(k+1))^{-1}\Delta^2\varepsilon_{ci}(k+1)\\
&\le 4{\alpha_{ci}}^2\left\|\tilde{W}_{ci}\right\|^2+4{\alpha_{ci}}^2{\Delta\varepsilon_{ci}}^2(k)+2{\Delta\phi_{i\max}}^{-2}{\Delta\varepsilon_{ci}}^2(k+1)
\end{aligned}
\tag{49}
$$

Next, the first difference of the Lyapunov function due to the third term in (43) is obtained by using (40) and expanding the terms as

$$
\begin{aligned}
&\Delta V_{wi}(k)=8\overline{\psi}_i\Delta\phi_{i\min}^2{\alpha_{ci}}^2\times\\
&\left(\alpha_{ai}^2\frac{\psi_i{}^T(k)\psi_i(k){e_{ai}}^2(k)}{\left(\psi_i{}^T(k)\psi_i(k)+1\right)^2}+2\alpha_{ai}\{\frac{\tilde{W}_{a\,i}{}^T(k)\psi_i(k)e_{ai}(k)}{\psi_i{}^T(k)\psi_i(k)+1}\}\right)
\end{aligned}
\tag{50}
$$

The action error $e_{ai}(k)$ in (50) can be expanded by using (38) as

$$
\begin{aligned}
&2\tilde{W}_{a\,i}(k)\psi_i(k)e_{ai}(k)=2\tilde{W}_{a\,i}{}^T(k)\psi_i(k)\times\\
&\left(\begin{array}{l}-\psi_i{}^T(k)\tilde{W}_{a\,i}(k)+\varepsilon_{a\,i}(k)+\sigma_i(k)-\frac{1}{2}R_i^{-1}g_i(k)\overline{\beta}_{in}(x_{i0})\Delta_i(k)\\-\frac{1}{2}R_i^{-1}\overline{g}_i{}^T(k)\frac{\partial\phi_i(k+1)}{\partial x_{in}(k+1)}\tilde{W}_{ci}(k)-\frac{1}{2}R_i^{-1}\overline{g}_i{}^T(k)\frac{\partial\varepsilon_i(k+1)}{\partial x_{in}(k+1)}\end{array}\right)
\end{aligned}
\tag{51}
$$

By using Cauchy-Schwartz inequality and taking norms we obtain

$$
\begin{aligned}
&2\tilde{W}_{\mathrm{a}\,i}(k)\psi_i(k)e_{ai}(k)\\
&\le -\frac{3}{4}\Xi_{ai}(k)^2 + 4(\varepsilon_{\mathrm{a}\,i}(k)+\sigma_i(k)+A_{1i}(k))^2\\
&+(R_i^{-1})^2 g_i{}^2(k)\bar{\beta}_{in}{}^2(x_{i0})\Delta_i{}^2(k)\\
&+\left(R_i^{-1}\right)^2 g_i{}^2(k)\left\|\frac{\partial\phi_i(k+1)}{\partial x_{in}(k+1)}\right\|^2\left\|\tilde{W}_{ci}(k)\right\|^2
\end{aligned}
\tag{52}
$$

where $\Xi_{ai}(k)=\tilde{W}_{\mathrm{a}\,i}{}^T(k)\psi_i(k)\psi_i{}^T(k)\tilde{W}_{\mathrm{a}\,i}(k)$ and $A_{1i}(k)=\varepsilon_{\mathrm{a}\,i}(k)+\ \sigma_i(k)-\frac{1}{2}R_i^{-1}\bar{g}_i{}^T(k)\frac{\partial\varepsilon_i(k+1)}{\partial x_{in}(k+1)}$.

Finally, following the same steps to obtain (29) for individual subsystems, the first difference due to the last term in (43) can be written as

$$
\begin{aligned}
&\Delta V_{ci}(k)=-(1-\alpha_{ci}{}^2)\left\|e_{ci}(k)\right\|^2-(\Delta\phi_{\min}^2-4\alpha_{ci}{}^2\Delta\phi_{\max}^2)\left\|\tilde{W}_{ci}(k)\right\|^2.\\
&+(2+4\alpha_{ci}{}^2)\varepsilon_{cM}^2
\end{aligned}
\tag{53}
$$

In order to conclude the math, the first difference of (43) can be summarized by using (46), (48),(49), (52), and (53).

$$
\begin{aligned}
&\Delta V_i(k)\le\\
&-B_{eai}e_{ai}{}^2(k)-B_{\Xi ai}\Xi^2{}_{ai}(k)\\
&-(1-\alpha_{ci}^2)e_{ci}{}^2(k)-B_{Wci}\left\|\tilde{W}_{ci}(k)\right\|^2-B_{ri}r_i{}^2(k)+B_{\varepsilon i}\\
&=-B_{eai}e_{ai}{}^2(k)-B_{\Xi ai}\Xi_{ai}(k)^2\\
&-(1-\alpha_{ci}^2)e_{ci}{}^2(k)-B_{Wci}\left\|\tilde{W}_{ci}(k)\right\|^2-B_{ri}r_i^2(k)+B_{\varepsilon i}
\end{aligned}
\tag{54}
$$

where

$$
B_{eai}=\alpha_{\mathrm{a}\,i}\alpha_{ci}{}^2\frac{\Delta\phi_{i\min}^2}{\psi_{i\max}^2+1}-7\alpha_{ai}^2\left(\frac{\psi_i{}^T(k)\psi_i(k+1)}{\psi_i{}^T(k)\psi_i(k)+1}\right)^2-9\bar{\psi}_i\Delta\phi_{i\min}^2\alpha_{ci}{}^2\alpha_{ai}^2\frac{\psi_i{}^T(k)\psi_i(k)}{\left(\psi_i{}^T(k)\psi_i(k)+1\right)^2},
\tag{55}
$$

$$
\begin{aligned}
B_{\Xi ai}=&\frac{9\bar{\psi}_i\Delta\phi_{i\min}^2\alpha_{ci}{}^2\alpha_{ai}}{\psi_i{}^T(k)\psi_i(k)+1}-\frac{7\Delta\phi_{i\min}^2\alpha_{\mathrm{a}\,i}\alpha_{ci}{}^2}{\psi_{i\max}^2+1}\frac{\psi_i{}^T(k+1)\psi_i(k+1)}{\psi_i{}^T(k)\psi_i(k)}-\frac{\bar{\psi}_i\Delta\phi_{i\min}^2\alpha_{ci}{}^2\alpha_{ai}}{\psi_{i\max}^2+1}\\
&-\sum_{j=1}^{N}\alpha_{\mathrm{a}\,j}\alpha_{cj}{}^2\frac{\Delta\phi_{j\min}^2}{\psi_{j\max}^2+1}\frac{7}{4}(R_j^{-1})^2 g_j{}^2(k+1)\bar{\beta}_{jn}{}^2(x_{j0})3\gamma_i g_i{}^2(k),
\end{aligned}
\tag{56}
$$

$$B_{Wci} = \Delta\phi_{i\min}^2 - 4\alpha_{ci}^2\Delta\phi_{i\max}^2 - 7\alpha_{a\,i}\alpha_{ci}{}^4\,\frac{\Delta\phi_{i\min}^2}{\psi_{i\max}^2+1}\left\|\frac{\partial\phi_i(k+2)}{\partial x_{in}(k+2)}\right\|^2 g_i{}^2(k+1)(R_i^{-1})^2$$

$$-\left(R_i^{-1}\right)^2 g_i{}^2(k)\left\|\frac{\partial\phi_i(k+1)}{\partial x_{in}(k+1)}\right\|^2\frac{8\overline{\psi}_i\Delta\phi_{i\min}^2\alpha_{ci}{}^2\alpha_{ai}}{\psi_i{}^T(k)\psi_i(k)+1}, \tag{57}$$

$$B_{ri} = \frac{\overline{\psi}_i\Delta\phi_{i\min}^2\alpha_{ci}{}^2\alpha_{ai}}{(\psi_{i\max}^2+1)}\left(\frac{1}{3g_{i\max}}-\frac{3N\gamma_i}{g_{i\min}}\right)-\sum_{j=1}^{N}\frac{8\overline{\psi}_j\Delta\phi_{j\min}^2\alpha_{cj}{}^2\alpha_{aj}}{\psi_j{}^T(k)\psi_j(k)+1}(R_j{}^{-1})^2 g_j{}^2(k)\overline{\beta}_{jn}{}^2(x_{j0})\gamma_i$$

$$-\left[\sum_{j=1}^{N}\frac{\Delta\phi_{j\min}^2\alpha_{a\,j}\alpha_{cj}{}^2}{\psi_{j\max}^2+1}\frac{7}{4}(R_j{}^{-1})^2 g_j{}^2(k+1)\overline{\beta}_{jn}{}^2(x_{j0})\right]3\gamma_i\left(\sum_{l=1}^{N}\gamma_l\right), \tag{58}$$

and

$$B_{\varepsilon i} = \alpha_{a\,i}\alpha_{ci}{}^2\,\frac{\Delta\phi_{i\min}^2}{\psi_{i\max}^2+1}\times$$

$$\left(\begin{array}{l}
+7\left(\varepsilon_{ai}{}^2(k+1)\right)+\frac{7}{4}\frac{\partial\varepsilon_{ci}(k+2)}{\partial x_{in}(k+2)}{}^T\; g_i{}^2(k+1)(R_i{}^{-1})^2\;\frac{\partial\varepsilon_{ci}(k+2)}{\partial x_{in}(k+2)}\\
+\frac{7}{4}\alpha_{ci}{}^2\left\|\frac{\partial\phi_i(k+2)}{\partial x_{in}(k+2)}\right\|^2 g_i{}^2(k+1)(R_i{}^{-1})^2\left(4\alpha_{ci}{}^2\Delta\varepsilon_{ci}{}^2(k)+2\Delta\phi_{i\max}{}^{-2}\Delta\varepsilon_{ci}{}^2(k+1)\right)\\
+\left[\sum_{j=1}^{N}\alpha_{a\,j}\alpha_{cj}{}^2\;\frac{\Delta\phi_{j\min}^2}{\psi_{j\max}^2+1}\frac{7}{4}(R_j{}^{-1})^2 g_j{}^2(k+1)\overline{\beta}_{jn}{}^2(x_{i0})\right]3\gamma_i g_i{}^2(k)W_{a\,i}{}^T\psi_{a\,i}\psi_{a\,i}{}^T W_{a\,i}\\
+\frac{\overline{\psi}_i\Delta\phi_{i\min}^2\alpha_{ci}{}^2\alpha_{ai}}{(\psi_{i\max}^2+1)}\psi_i{}^T W_{ai}W_{ai}{}^T\psi_i+7\sigma_i{}^2(k+1)
\end{array}\right)$$

$$+\left(\alpha_{ai}\frac{8\overline{\psi}_i\Delta\phi_{i\min}^2\alpha_{ci}{}^2}{\psi_i{}^T(k)\psi_i(k)+1}\right)\left(\varepsilon_{a\,i}(k)+\sigma_i(k)+A_1(k)+A_2(k)\right)\Xi_{ai}(k)\,. \tag{59}$$
$$+(2+4\alpha_{ci}^2)^2\varepsilon_{cM}^2$$

It can be seen from (54) that the Lyapunov function is negative outside the bound

$$\begin{aligned}
&|e_{ci}| > \sqrt{\frac{B_{\varepsilon i}}{(1-\alpha_{ci}^2)}}\quad or\quad \left\|\tilde{W}_{ci}(k)\right\| > \sqrt{\frac{B_{\varepsilon i}}{B_{Wci}}}\;\; or\\
&|e_{ai}| > \sqrt{\frac{B_{\varepsilon i}}{B_{eai}}}\quad or\quad \left\|\Xi_{ai}(k)\right\| > \sqrt{\frac{B_{\varepsilon i}}{B_{\Xi ai}}}\; or\; \left\|r_i(k)\right\| > \sqrt{\frac{B_{\varepsilon i}}{B_{ri}}}
\end{aligned} \tag{60}$$

provided that the following conditions are satisfied:

$$\alpha_{ci}^2 \le \min\{1, \left(\begin{array}{l} \dfrac{2\Delta\phi_{i\max}^2}{\Delta\phi_{i\min}^2} + \left(R_i^{-1}\right)^2 g_{i\max}{}^2 \left\| \dfrac{\partial \phi_i(k+1)}{\partial x_{in}(k+1)} \right\|^2 8\overline{\psi}_i \\ + 7\dfrac{1}{\psi_{i\max}^2 + 1} \left\| \dfrac{\partial \phi_i(k+2)}{\partial x_{in}(k+2)} \right\|^2 g_{i\max}{}^2 (R_i^{-1})^2 \end{array} \right)^{-1} \} \tag{61}$$

$$\alpha_{a\,i} \le \min\{1, \frac{\alpha_{ci}{}^2 \Delta\phi_{i\min}^2}{\left(7\psi_{i\max}^4 + 9\overline{\psi}_i \Delta\phi_{i\min}^2 \alpha_{ci}{}^2 \psi_{i\max}^2\right)\left(\psi_{i\max}^2 + 1\right)}\} \tag{62}$$

$$\gamma_i \le \min\left\{ \left(\frac{\frac{4}{21}\overline{\psi}_i \Delta\phi_{i\min}^2 \alpha_{ci}{}^2 \alpha_{ai}}{\left(\psi_{i\max}^2 + 1\right) g_{i\max}{}^2 \sum_{j=1}^{N} \alpha_{a\,j} \alpha_{cj}{}^2 \frac{\Delta\phi_{j\min}^2}{\psi_{j\max}^2 + 1} (R_j^{-1})^2 g_{j\max}{}^2 \overline{\beta}_{jn} (x_{j0})^2} \right)^{-1}, \right.$$

$$\left. \begin{array}{l} \dfrac{\overline{\psi}_i \Delta\phi_{i\min}^2 \alpha_{ci}{}^2 \alpha_{ai}}{(\psi_{i\max}^2 + 1)} \dfrac{1}{3 g_{i\max}} \div \\ \left(\begin{array}{l} \displaystyle\sum_{j=1}^{N} \frac{8\overline{\psi}_j \Delta\phi_{j\min}^2 \alpha_{cj}{}^2 \alpha_{aj}}{\psi_j{}^T(k)\psi_j(k) + 1} (R_j^{-1})^2 g_{j\max}{}^2 \overline{\beta}_{jn}{}^2 (x_{j0}) \\ + \dfrac{21}{4} \left[\displaystyle\sum_{j=1}^{N} \frac{\Delta\phi_{j\min}^2 \alpha_{a\,j} \alpha_{cj}{}^2}{\psi_{j\max}^2 + 1} (R_j^{-1})^2 g_{j\max}{}^2 \overline{\beta}_{jn}{}^2 (x_{j0}) \right] \left(\displaystyle\sum_{l=1}^{N} \gamma_l \right) \\ + \dfrac{\overline{\psi}_i \Delta\phi_{i\min}^2 \alpha_{ci}{}^2 \alpha_{ai}}{(\psi_{i\max}^2 + 1)} \dfrac{3N}{g_{i\min}} \end{array} \right) \end{array} \right\} \tag{63}$$

Note that in order to satisfy (63) the design gains α_{ai} and α_{ci} (for $1 \le i \le N$) must be sufficiently small. Thus, using standard Lyapunov extensions [1], it can be concluded that $\Delta V_i(k)$ is less than zero outside a bound resulting the cost and control errors as well as the weight estimation errors to be UUB. Since the errors $e_{ai}(k)$ and $e_{ci}(k)$ are UUB and converge to a bound, it follows that $\left\| u_i - u_i^* \right\| \le \varepsilon_b$ as $k \to \infty$ with ε_b being a positive constant. ■

Remark 8. According to Remark 3, the value of $\overline{\psi}_i$ can be bounded by ensuring that the subsystem states are persistently exciting.

Remark 9. According to Remark 6, the action network of subsystem 'i' is approximating the derivative of the corresponding cost function $J_i(x_i(k))$ (the critic network) which requires the state vector $x(k)$. If $\Delta_i(x)$ can be overbounded by a small positive constant (i.e. $|\Delta_i(x)|^2 \le \gamma_i$) in the compact set Ω, the effect of the interconnection terms can be modeled by a constant, and thus, the action network approximation error ε_{ai} is reduced since the action NN need not use the entire state vector $x(k)$. Under such a strong assumption, Theorem 2 is simplified to the case of a centralized control [20] and the requirement of known $f_i(x_i(k))$ is relaxed. Also, the control policy (35) is simplified to

$$u_i(k) = \hat{W}_{ai}{}^T \psi_{ai}{}^T (x_i(k)). \tag{64}$$

By contrast, Theorem 2 is proven by considering Assumption 1 where the interconnection terms $\Delta_i(x)$ can grow in a quadratic manner.

D. The Action Network Design for Tracking

Consider interconnected system (1) where the subsystem output is to track the desired trajectory $x_{i1d}(k)$. Consequently, in the error system (2), $x_{ipd}(k)$ can be obtained by using the advanced values of the desired trajectory $x_{i1d}(k)$ for $1 \le i \le N$ and $1 \le p \le n$. That is

$$x_{ipd}(k) = x_{i1d}(k + p - 1). \tag{65}$$

Thus, the error dynamics can be written as

$$\begin{aligned} z_{i1}(k+1) &= z_{i2}(k) \\ &\vdots \\ z_{in-1}(k+1) &= z_{in}(k) \\ z_{in}(k+1) &= f_i(x_i(k)) + g_i(x_i(k))u_i + \Delta_i(x) - x_{ind}(k+1) \end{aligned} \tag{66}$$

which resembles the stabilization problem with the states being the errors z_{ip} defined in (2) for $1 \le i \le N$ and $1 \le p \le n$.

Before we proceed, the following Assumption is required.

Assumption 4: The desired trajectory $x_{ipd}(k)$ (for $1 \le i \le N$ and $1 \le p \le n$) is bounded for $k \in R^+$.

In order to use the results of Theorem 2 necessary changes have to be made in the definitions and variables which are discussed next. First, the overall cost function (6) and subsystem cost function $J_i(x_i(k))$ (in (14)) are redefined as

$$\begin{aligned} \bar{J}_z(k) &= \sum_{j=k}^{\infty} \left(Q(z(j)) + u^T(z(j)) R u(z(j)) \right) \\ &= Q(z(k)) + u^T(z(k)) R u(z(k)) + \bar{J}_z(k+1) \end{aligned} \tag{67}$$

and

$$J_{zi}(z_i(k)) = \sum_{j=k}^{\infty} \left(Q_i(z_i(j)) + u_i^T(j) R_i u_i(j) \right) \tag{68}$$

where $z = [z_1 \; z_2 \; \ldots \; z_N]^T$. Then, the critic and action NNs become functions of the errors z_{ip} in the tracking problem. That is,

$$\hat{J}_i(k) = \hat{W}_{ci}^T(k) \phi_i(z_i(k)), \tag{69}$$

$$e_{ci}(k) = Q_i(z_i(k-1)) + \hat{W}_{ci}^T(k) \Delta\phi_i(k), \tag{70}$$

and

$$\begin{aligned} &\hat{W}_{ci}(k+1) = \Delta\phi_i(z_i(k+1)) \left(\Delta\phi_i^T(z_i(k+1)) \Delta\phi_i(z_i(k+1)) \right)^{-1} \times \\ &\left(\alpha_{ci} e_{ci}^T(k) - Q_i^T(z_i(k)) \right) \end{aligned}. \tag{71}$$

Similar to Section II-A the matrix form of (69) through (71) are $\hat{\mathbf{J}}(k) = \hat{\mathbf{W}}_c^T(k) \boldsymbol{\Phi}(z(k))$,

$\mathbf{E}_c(k) = \mathbf{Q}(k-1) + \hat{\mathbf{W}}_c^T(k)\Delta\mathbf{\Phi}(k)$, and

$$\hat{\mathbf{W}}_c(k+1) = \Delta\mathbf{\Phi}(k+1)\left(\Delta\mathbf{\Phi}^T(k+1)\Delta\mathbf{\Phi}(k+1)\right)^{-1} \times \left(\alpha_c \mathbf{E}_c{}^T(k) - \mathbf{Q}^T(k)\right)$$

where the matrices are defined similar to what previously introduced; besides, $\hat{\mathbf{J}}(k) = [\hat{J}_1(k) \ldots \hat{J}_N(k)]^T$ and $\mathbf{E}_c(k) = [e_{c1}(k) \ldots e_{cN}(k)]^T$.

Also, the optimal policy (13) becomes

$$u_i^*(k) = -\frac{1}{2} R_i^{-1} g_i(x_i(k))^T \frac{\partial J_i(k+1)}{\partial z_i(k+1)} \tag{72}$$

which in turn yields (33) to be

$$\begin{aligned} &-\frac{1}{2} R_i^{-1} \overline{g}_i(x_i(k))^T \left(\frac{\partial \phi_i(k+1)}{\partial z_i(k+1)} W_{ci}(k) + \frac{\partial \varepsilon_i(k+1)}{\partial z_i(k+1)} \right) \\ &= W_{a\,i}{}^T(k)\psi_i(x_i(k), z_i(k)) - \varepsilon_{a\,i}(k) + F_i(x_i(k)) + \sigma_i \end{aligned} \tag{73}$$

where $\sigma_i = -\frac{1}{2} R_i^{-1} g_i(x_i(k)) \begin{pmatrix} \overline{\beta}_{in}(z_{i0}) g_i(x_i) u_i - x_{ind}(k+1) \\ + C_i(z_i(k+1)) \end{pmatrix}$.

Define the action network

$$u_i(k) = \hat{W}_{a\,i}{}^T \psi_{a\,i}{}^T(x_i(k), z_i(k)) + F_i(x_i(k)) \tag{74}$$

where

$$F_i(x_i(k)) = \frac{-1}{g_i(x_i(k))} \left(f_i(x_i(k)) - x_{ind}(k+1) + [0 \ \lambda_i]^T z_i \right). \tag{75}$$

As a result, the filtered tracking error dynamics becomes

$$\begin{aligned} r_i(k+1) = {} & f_i(x_i(k)) - x_{ind}(k+1) + [0 \ \lambda_i]^T z_i + \\ & g_i(x_i(k))\left(\hat{W}_{a\,i}{}^T \psi_{a\,i}(k) + F_i(x_i(k))\right) + \Delta_i(X) \\ = {} & g_i(x_i(k))\left(\tilde{W}_{a\,i}{}^T(k)\psi_{a\,i}(k) + W_{a\,i}{}^T \psi_{a\,i}(x_i(k))\right) + \Delta_i(X) \end{aligned} \tag{76}$$

Next, define

$$e_{a\,i}(k) = \hat{W}_{a\,i}{}^{T}(k)\hat{\psi}_i(x_i(k), z_i(k)) + F_i(x_i(k)) + \frac{1}{2} R_i^{-1} \bar{g}_i(x_i(k))^T \frac{\partial \phi_i(k+1)}{\partial z_i(k+1)} \hat{W}_{ci}(k) \tag{77}$$

and

$$\hat{W}_{a\,i}(k+1) = \hat{W}_{a\,i}(k) - \alpha_{a\,i} \frac{\psi_i(k) e_{a\,i}(k)}{\psi_i{}^{T}(k)\psi_i(k) + 1} \tag{78}$$

Finally, the critic and action weight estimation errors are defined as $\tilde{W}_{ci} = \hat{W}_{ci} - W_{ci}$ and $\tilde{W}_{ai} = \hat{W}_{ai} - W_{ai}$, respectively. After the changes (67) through (78) we introduce the following Theorem.

Theorem 3: *Consider the nonlinear discrete-time interconnected system given by (66). Let* $\mu_i(k)$ *be an initial admissible control input for the ith subsystem of the nonlinear interconnected discrete-time system* for $1 \le i \le N$. *Consider the Assumptions 1 through 4 hold and that the initial conditions of the system are bounded in the compact set* Ω. *Let the weight tuning for the critic and action networks be provided by (71) and (78), respectively. Then, the critic error (70), the action error (77), and the filtered tracking error* $r_i(k)$ *along with the weight estimation errors of the critic and action network of each subsystem are all uniformly ultimately bounded (UUB) for all k ≥ k + T₀. In addition,* $u_i \to u_i^* + \varepsilon_b$.

Proof: The proof follows the same steps as in the proof of Theorem 2 by considering the following positive definite Lyapunov candidate

$$V(k) = \sum_{i=1}^{N} V_i(k) = \sum_{i=1}^{N} \frac{\overline{\psi}_i \Delta \phi_{i\,\min}^2 \alpha_{ci}{}^2 \alpha_{ai}}{3(\psi_{i\,\max}^2 + 1)} L_{ri}(k) + \sum_{i=1}^{N} V_{ci}(k) + \sum_{i=1}^{N} V_{a\,i}(k) + \sum_{i=1}^{N} V_{wi}(k) \tag{79}$$

where $L_{ri} = \left(r_i(k) \Big/ \sqrt{g_{i(k-1)}}\right)^2$, $V_{ai}(k) = \alpha_{ai}\alpha_{ci}{}^2 \frac{\Delta\phi_{i\min}^2}{\psi_{i\max}^2 + 1} e_{ai}{}^2(k)$, $V_{wi}(k) = 8\overline{\psi}_i \Delta\phi_{i\min}^2 \alpha_{ci}{}^2 \tilde{W}_{ai}{}^T(k)\tilde{W}_{ai}(k)$, $\overline{\psi}_i = [\max \psi_i(k) / \min \psi_i(k)]^2$, in the compact set Ω and $V_{ci}(k) = e_{ci}{}^2(k) + \Delta\phi_{i\min}^2 \tilde{W}_{ci}{}^T \tilde{W}_{ci}$ with $\Delta\phi_{i\min}^2 \le \left\| \Delta\phi_i{}^T(k+1)\Delta\phi_i(k+1) \right\|$, and $\Delta\phi_i(k) = \phi_i(k) - \phi_i(k-1)$. The proof is completed by expanding the terms, using (74) through (78), and following the same steps as in the proof of Theorem 2. ■

Remark 10. Note from (69) and (78) that if e_{ai} approaches zero, the cost function (69) and update law (78) are not active, that is, the critic network (69) and control policy (74) stop approaching to the optimal values. Thus, once the tracking error has become negligible, the weight matrices associated with the cost function as well as optimal policy are no longer updated. Similar to Remark 3, this can be viewed as a persistency of excitation (PE) requirement [1] for the inputs to the networks. Thus, the tracking error states $z(k)$ must be persistently exiting long enough for the cost function and optimal control policy to be obtained. Also, the PE condition ensures the existence of minimum values for the activation functions ϕ_i and ψ_i.

IV. Simulation Results

Example 1. (Stabilization) To demonstrate the effectiveness of the optimal controllers developed in this work on the interconnected systems, the following fourth order-subsystem interconnected nonlinear discrete-time system is considered as

$$
\begin{aligned}
x_{11}((k+1)T) &= x_{11}(kT) \\
x_{12}((k+1)T) &= f_{12}(x_{11}, x_{12}) + g_{12}(x_{11}, x_{12})u_1 \\
&\quad + .01 \times (x_{21}{}^2(kT) + x_{22}{}^2(kT) + x_{31}{}^2(kT) + x_{42}{}^2(kT)) \\
x_{21}((k+1)T) &= x_{21}(kT) \\
x_{22}((k+1)T) &= f_{22}(x_{21}, x_{22}) + g_{22}(x_{21}, x_{22})u_2 \\
&\quad + .1 \times (x_{11}{}^2(kT) + x_{32}{}^2(kT) + x_{41}{}^2(kT) + x_{42}{}^2(kT)) \\
x_{31}((k+1)T) &= x_{31}(kT) \\
x_{32}((k+1)T) &= f_{32}(x_{31}, x_{32}) + g_{32}(x_{31}, x_{32})u_3 \\
&\quad + .1 \times (x_{11}{}^2(kT) + x_{12}{}^2(kT) + x_{22}{}^2(kT) + x_{42}(kT))
\end{aligned}
$$

$$
\begin{aligned}
x_{41}((k+1)T) &= x_{41}(kT) \\
x_{42}((k+1)T) &= f_{42}(x_{41}, x_{42}) + g_{42}(x_{41}, x_{42})u_4 \\
&\quad + .1 \times (x_{11}{}^2(kT) + x_{12}{}^2(kT) + x_{22}{}^2(kT) + x_{32}{}^2(kT))
\end{aligned}
$$

where

$$
\begin{aligned}
f_{12}(x_{11}, x_{12}) &= \frac{-1}{16}\left(x_{11}(kT)/(1 + x_{12}{}^2(kT))\right) + x_{12}(kT); \\
f_{22}(x_{21}, x_{22}) &= \frac{-3}{16}\left(x_{21}(kT)/(1 + x_{22}{}^2(kT))\right); \\
f_{32}(x_{31}, x_{32}) &= \frac{-3}{16}\left(x_{31}(kT)/(1 + x_{32}{}^3(kT))\right); \\
f_{42}(x_{41}, x_{42}) &= \frac{-1}{16}\left(x_{41}(kT) \times (1 + x_{42}{}^3(kT))\right);
\end{aligned}
$$

and

$$
\begin{aligned}
g_{12}(x_{11}, x_{12}) &= 1 + 0.5\sin(x_{12}{}^2(kT)) ; \\
g_{22}(x_{21}, x_{22}) &= 1 + 0.25\sin(x_{12}(kT) + x_{22}(kT)) ; \\
g_{32}(x_{31}, x_{32}) &= 1 + 0.5\sin(x_{32}(kT)) ; \\
g_{42}(x_{41}, x_{42}) &= 1 + 0.25\sin(x_{41}(kT)) + 0.25\cos(x_{42}(kT)) ;
\end{aligned}
$$

with sampling interval T being 1s. The objective of each subsystem controller is to make the system states x_{i1} (for $1 \le i \le 4$) regulate to zero in a near optimal manner as proposed. The initial values of the states are given by $x_{11} = 1;\ x_{12} = 1;\ x_{21} = 1.5;\ x_{22} = 1;\ x_{31} = 1;\ x_{32} = 2;$ $x_{41} = 2;\ x_{42} = 1$. Note that the interconnection term bound coefficient $\gamma = [\gamma_1\ \gamma_2\ \gamma_3\ \gamma_4]$ (for $1 \le j \le 4$) can be written as $\gamma = [.01\ .1\ .1\ .1]$. Three cases are considered:

Case a) The non-optimal stabilizing controller defined by $u_i = \frac{-1}{g_i}\left[f_i + \lambda_{i1} z_{i2}(k) - K_i * r_i(k)\right]$ is considered where $\lambda_1 = \lambda_2 = \lambda_3 = \lambda_4 = 0.01$ and $K_1 = K_2 = K_3 = K_4 = 0.5$.

Case b) The optimal policy (64) is considered. The design gains are $\alpha_{ci} = 2e-5$ and $\alpha_{a\,i} = 1e-5$ for $1 \le i \le 4$. Note that by the control policy (64) the internal dynamics $f_i(x_i)$ need not be known provided that the interconnection terms are overbounded by a small constant as mentioned in Remark 8.

Case c) The proposed optimal controller (35) for $1 \le i \le 4$ along with the weight update laws (22) and (39) are utilized for critic and action networks, respectively. The design gains are $\alpha_{ci} = 2e-5$ and $\alpha_{a\,i} = 1e-5$ for $1 \le i \le 4$.

According to Remark 3 persistently exciting state errors are required to achieve optimal values of critic and action weight matrices. In order to provide persistency of excitation in the cases b and c in the stabilization problem, the simulation has been performed by using the a destabilizing control input to the system near origin such that the critic and action networks can benefit from nonzero control errors over a longer time. Then, the destabilizing controller is removed and the trained critic and action networks are used to control the subsystems optimally.

Moreover, the critic weights are initialized randomly whereas the action network weights start from zero. Both action and critic errors are approximated by NNs with polynomials activation functions where the critic network utilizes an even 6th order polynomials to assure positive values for cost function whereas the action network uses a fifth order polynomial since it should resemble the derivative of the critic network.

The performance of the three controllers are depicted in Fig. 1in terms of the subsystems states by using the trained values of critic and action NNs after the destabilizing controller is removed. Each subsystem has two states which eventually converge to the origin. Figure 2 illustrates the NN control inputs for the three controllers. These stable results are as predicted by Theorem 2. Also, Fig. 3 shows the large-scale interconnected system cost function defined by $\bar{J}(x(k)) = \sum_{j=k}^{M} \left(Q(x(j)) + u^T(j) R u(j) \right)$, where $u(k) = [u_1(k), \ldots, u_N(k)]^T$, $Q(x(j)) = x^T Q x$, $Q = I_{8\times 8}$, and $R = I_{4\times 4}$. Figure 4 shows the convergence of the action NN to the optimal policy through the action error (37) where the proposed optimal input converges to the optimal policy provided by the critic network in a long training time when the subsystems are perturbed. Finally, Fig. 5 shows the convergence of the critic NN error according to (19) in the training time.

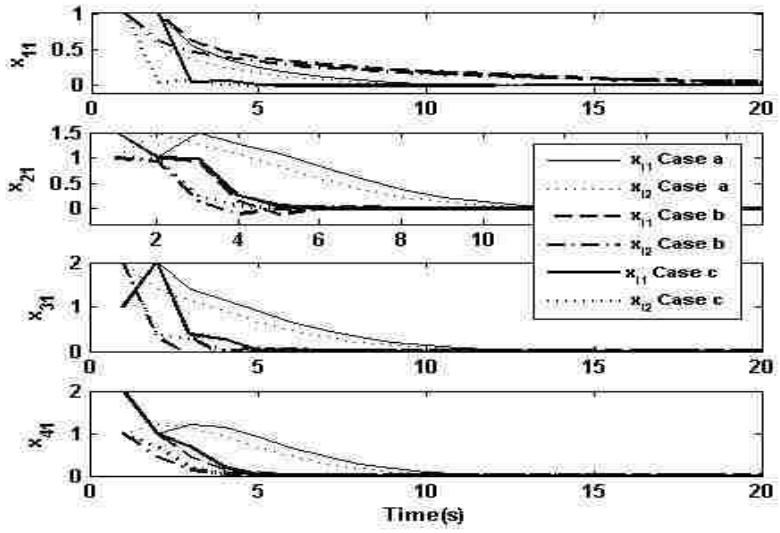

Fig.1 Interconnected systems states x_{i1} with optimal and non-optimal controller for $1 \le i \le 4$

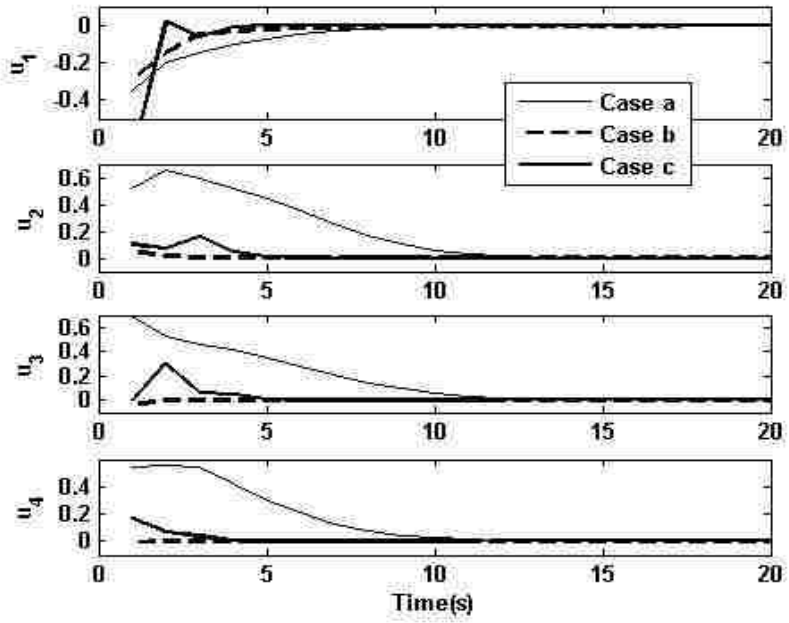

Fig.2 Control inputs

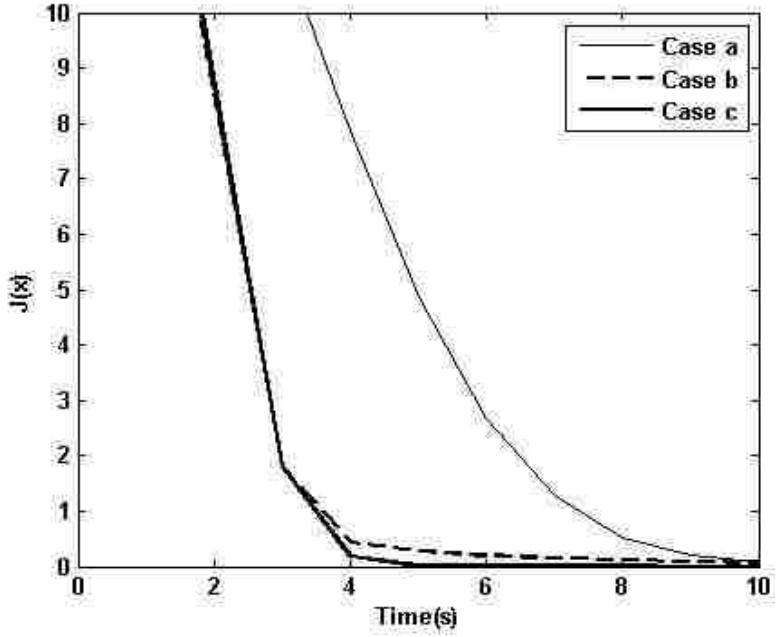

Fig.3 Cost function for the stabilization problem

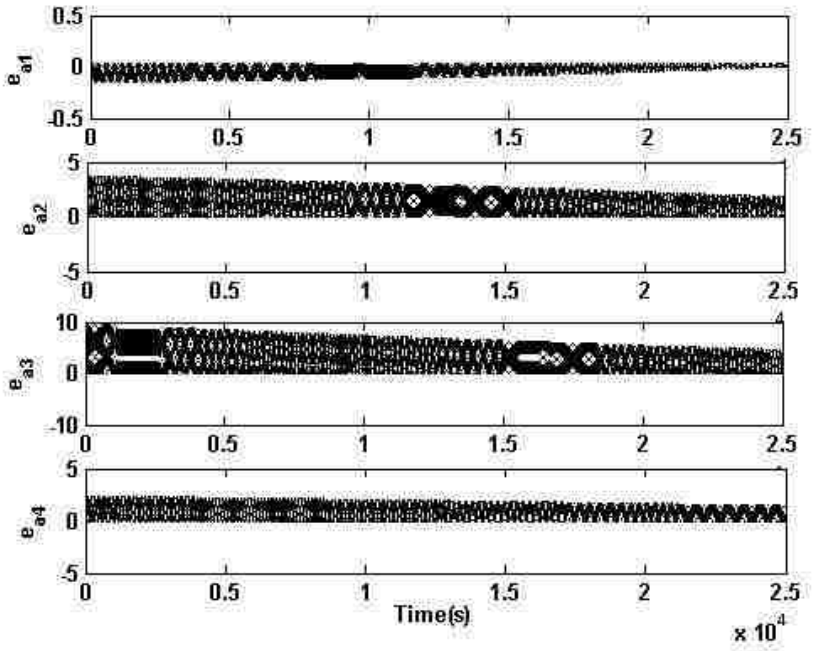

Fig.4 Action NN error for stabilization problem

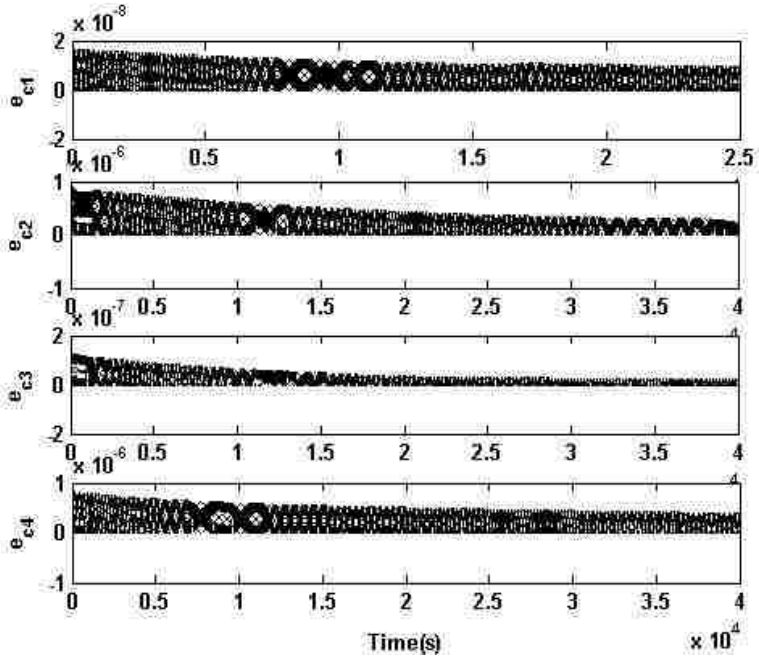

Fig.5 Critic NN error for stabilization problem

Example 2. The interconnected discrete-time system of Example 1 is now considered for tracking. The desired trajectories for the individual subsystems are given below.

$x_{11d}(kT) = 0.3\sin(0.1kT)$, $x_{21d}(kT) = 0.3\sin(0.02kT)$ $x_{31d}(kT) = 0.3\sin(0.1kT)$, $x_{41d}(kT) = 0.3\sin(0.01kT)$.

The subsystem outputs $x_{i1}(kT)$ are to follow the corresponding desired trajectory $x_{i1d}(kT)$. The control policy (74) along with the weight updates (71) and (78) are utilized for tracking problem with the subsystem critic and action network gains are $\alpha_{ci} = 2e-5$ and $\alpha_{ai} = 1e-6$ for $1 \le i \le 4$. The satisfactory tracking performance results are then shown in Fig. 6 where the subsystem outputs track the desired trajectories by using the optimal control policy (74). Figure 7 shows the control inputs. The observations confirm the results of Theorem 3 where the tracking error is bounded and the proposed control policy converges to the optimal policy provided by critic network. In Fig. 8 the control error (77) is illustrated where Fig. 9 shows the critic error (70). Similar to the previous example, a destabilizing controller provided persistency of excitation for a period of time and then it is removed where the final critic and action NN weights are used to provide the optimal tracking shown in Figs 6 and 7.

V.Conclusions

In this paper, the optimal control of discrete-time nonlinear decentralized system via online HJB methodology is considered and control design for stabilization and tracking problem is addressed. In specific, direct neural dynamic programming technique is utilized to solve the HJB (Hamilton Jacobi-Bellman) equation in real time and forward in time for the optimal control of decentralized affine nonlinear discrete-time systems. The design employs an action network that is aimed to provide a nearly optimal control signal, and a critic neural network which evaluates the performance of the system. The

NNs are tuned online. The optimal control input is augmented with an additional term for compensating the interconnection terms. Lyapunov techniques are employed to show that the synthesized subsystems inputs approach the optimal control inputs with small bounded error.

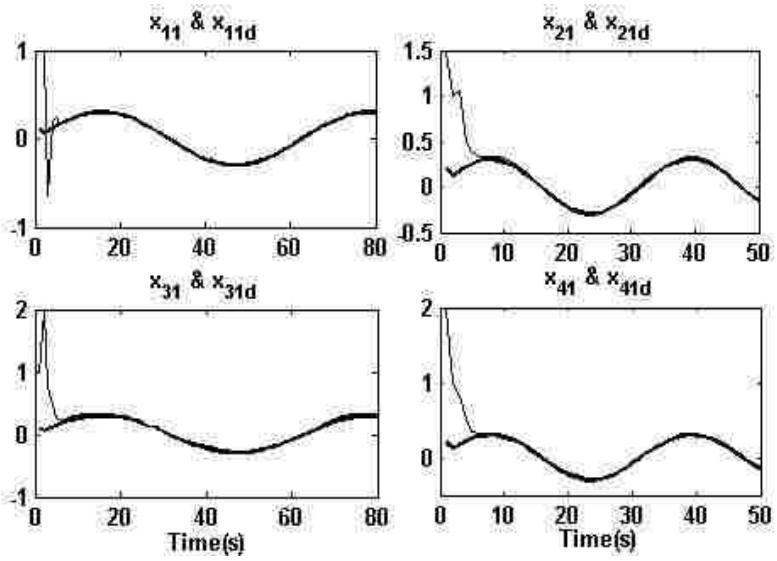

Fig.6 Interconnected systems states x_{i1} with the proposed optimal controller and desired trajectories for $1 \le i \le 4$

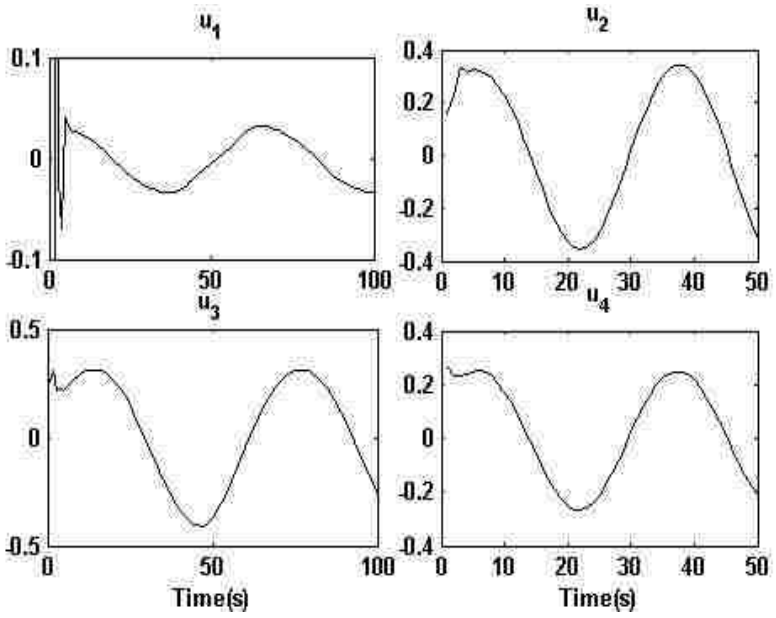

Fig.7 Interconnected systems control inputs for tracking problem

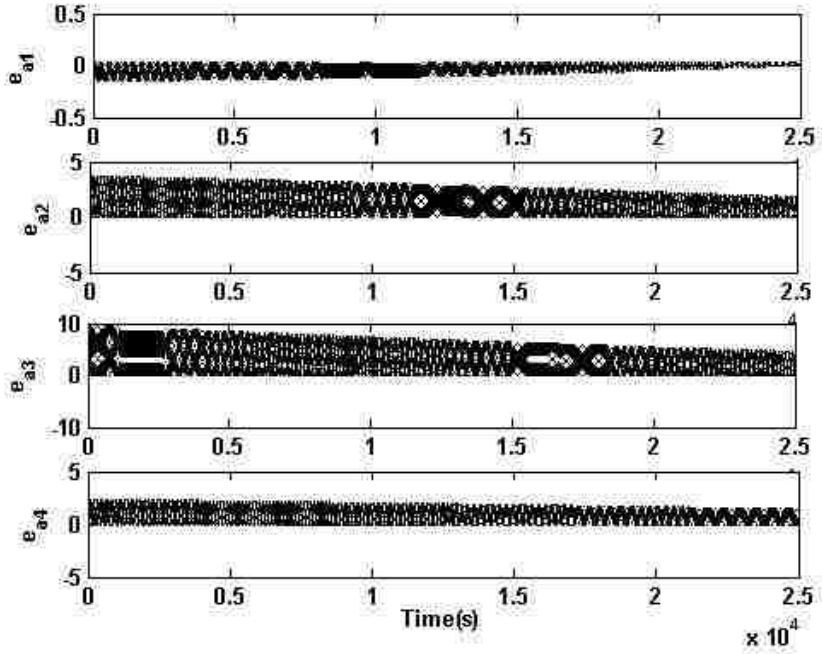

Fig.8 Action NN error for tracking problem

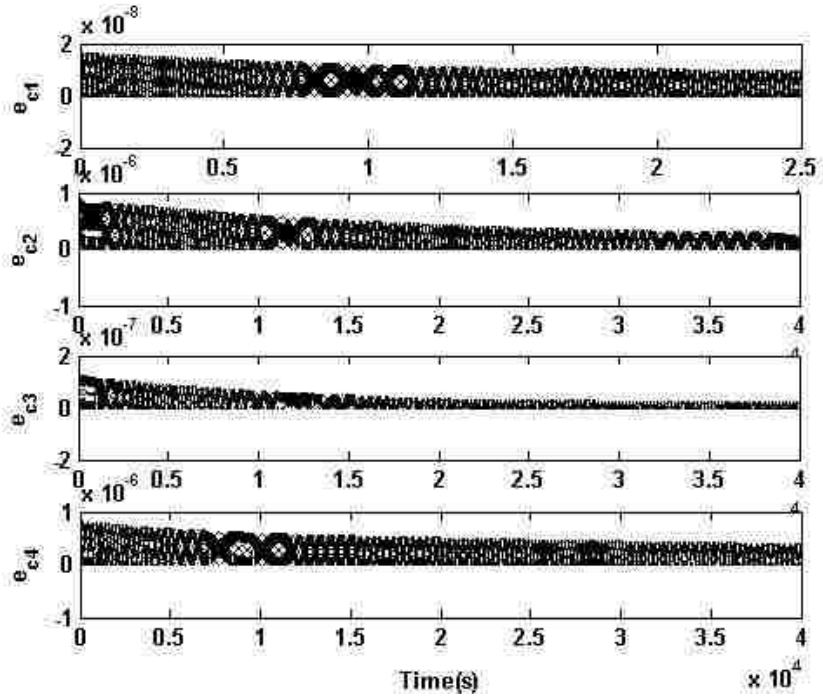

Fig.9 Critic NN error for tracking problem

References

[1] S. Jagannathan, *Neural Network Control of Nonlinear Discrete-time Systems*, CRC Press, April 2006.

[2] F. L. Lewis and V. L. Syrmos, *Optimal Control*, New York, Weily, 1995.

[3] Z. Chen and S. Jagannathan, "Generalized Hamilton–Jacobi–Bellman Formulation-based Neural Network Control of Affine Nonlinear Discrete-time Systems," *IEEE Trans. Neural Network.*, vol. 10, no. 1, pp. 90–106, Jan. 2008.

[4] A. Al-Tamimi, F.L. Lewis, and M. Abu-Khalaf, "Discrete-Time Nonlinear HJB Solution Using Approximate Dynamic Programming: Convergence Proof," *IEEE Trans. On Systems, Man, and Cybernetics—Part B*, vol. 38, pp. 943-949, Aug. 2008.

[5] J. Si, A. G. Barto, W. B. Powell, and D. Wunsch, Eds., *Handbook of Learning and Approx. Dynamics Prog.*, Wiley-IEEE Press, 2004.

[6] J. Si and Y. Wang, "Online Learning Control by Association and Reinforcement," *IEEE Trans. on Neural Networks*, vol. 12, pp. 264-276, March 2001.

[7] D. Prokhorov and D. Wunsch, "Adaptive Critic Designs," *IEEE Trans.on Neural Networks,"* vol. 8, pp. 997-1007, Sept. 1997.

[8] G. Toussaint, T. Basar and F. Bullo, "H^{∞}-optimal Tracking Control Techniques for Nonlinear Underactuated Systems," *Proc. of IEEE Conf. on Decision and Control,* pp. 2078 – 2083, 2000.

[9] D. Gu and H. Hu, "Receding Horizon Tracking Control of Wheeled Mobile Robots," *IEEE Trans. on Control Systems Technology,* vol. 14, pp. 743-49, July 2006.

[10] W. Luo, Y. C., Chu, and K. V. Ling, "Inverse Optimal Adaptive Control for Attitude Tracking of Spacecraft," *IEEE Trans. on Automatic Control,* vol. 50, pp 1693-1654, Nov. 2005.

[11] H. Zhang, Q. Wei, and Y. Luo, "A Novel Infinite-time Optimal Tracking Control Scheme for a Class of Discrete-time Nonlinear Systems Via the Greedy HDP Iteration Algorithm," *IEEE Trans. on Systems, Man, and Cybernetics—Part B,* vol. 38, pp. 937-942, Aug. 2008.

[12] S.N. Huang, K.K. Tan, and T.H. Lee, "Nonlinear Adaptive Control of Interconnected Systems Using Neural Networks," *IEEE Transactions on Neural Networks*, vol. 17, no. 1, pp. 243 - 246, Jan. 2006.

[13] Y. Liu and X.Y. Li, "Decentralized Robust Adaptive Control of Nonlinear Systems with Unmodeled Dynamics," *IEEE Transactions on Automatic Control,* vol. 47, no. 5, pp.:848 – 856, May 2002.

[14] J. Zhou and C. Wen, "Decentralized Backstepping Adaptive Output Tracking of Interconnected Nonlinear Systems," *IEEE Transactions on* Automatic Control, vol. 53, no. 10, pp.: 2378 – 2384, Nov. 2008.

[15] J.T. Spooner, K.M. Passino, "Decentralized Adaptive Control of Nonlinear Systems Using Radial Basis Neural Networks," *IEEE Transactions on Automatic Control*, vol. 44, no. 11, pp.: 2050 – 2057, Nov. 1999.

[16] W. Liu, S. Jagannathan, D.C. Wunsch, and M.L. Crow, "Decentralized Neural Network Control of a Class of Large-scale Systems with Unknown Interconnections," *proceeding of IEEE Conference on Decision and Control(CDC)*, vol. 5, pp. 4972 – 4977, 14-17 Dec. 2004.

[17] S. Jagannathan "Decentralized Discrete-Time Neural Network Controller for a Class of Nonlinear Systems with Unknown Interconnections," *Proceedings of the 2005 IEEE International Symposium on Intelligent Control*, pp.: 268 – 273, 2005.

[18] E. Gyurkovics and T. Takacs, “Stabilization of Discrete-time Interconnected Systems Under Control Constraints,” *IEE Proceedings on Control Theory and Applications*, vol. 147, no. 2, pp.: 137 – 144, March 2000.

[19] F. Lewis, S. Jagannathan, S., and A. Yesildirek, "*Neural Network Control of Robot. Manipulators and Nonlinear Systems*," Taylor & Francis, 1998.

[20] T. Dierks and S. Jagannathan, “Optimal Control of Affine Nonlinear Discrete-time Systems,” *Proceedigs of the IEEE Mediterranean Symposium on Control and Automation*, to appear in 2009.

[21] W. Rudin, *Principles of Mathematical Analysis*, 3rd *ed*, New York: McGraw-Hill, 1976.

6. Generalized Hamilton-Jacobi-Isaacs Formulation for Near Optimal Control of Affine Nonlinear Discrete-Time Systems with Application to Power Systems

S. Mehraeen, T. Dierks, S. Jagannathan, and M. L. Crow[1]

***Abstract*—** *In this paper, the nearly optimal solution for discrete-time (DT) affine nonlinear control systems in the presence of partially unknown dynamics and disturbances is considered. The approach is based on successive approximate solution of the generalized Hamilton-Jacobi-Isaacs (GHJI) equation, which appears in optimal control. Successive approximation approach using GHJI has not been applied to DT nonlinear optimal control problems. The definition of GHJI function as well as methods for updating control input and disturbance for DT nonlinear affine systems is proposed using the mild assumption of small perturbation condition and known system dynamics. Moreover, sufficient conditions for the convergence of the GHJI solution to the saddle-point are derived, and an iterative approach to approximate the GHJI equation using a neural network (NN) is presented. The result is a closed-loop optimal NN controller via off-line learning. Then, the requirement of full knowledge of the dynamics of the nonlinear DT system is relaxed by using an on-line approximator. Numerical examples including optimal control of a small power system are provided illustrating the effectiveness of the approach.*

[1] Authors are with Department of Electrical and Computer Engineering, Missouri University of Science and Technology, 1870 Miner Circle, Rolla, MO 65409. Contact author: sm347@mst.edu. Research Supported in part by NSF ECCS#0624644.

Index Terms –Neural Networks (NN), Optimal Control, Generalized Hamilton-Jacobi-Isaacs (GHJI), Nonlinear Discrete-time (DT) Systems.

I. Introduction

Closed-loop stability is often the sole purpose of many controller designs [1]. However, other objectives, such as optimality, require a control policy to stabilize the system in an optimal manner when the control cost matters in addition to the system stability. In the robust optimal control formulation, the objective of the controller is to minimize a certain cost function which represents a penalty associated with the states and control input [2] while maximizing the disturbances that the system can tolerate.

The H_∞ optimal control problem is a branch of optimal control which seeks to not only minimize a cost function, but also attenuate a worst-case disturbance [2]. Such techniques are necessary for large scale complex systems such as power networks where disturbances and faults commonly degrade the performance.

State space techniques for optimal control are derived for linear systems [3] by solving the Riccati equations in both continuous and discrete-time domain. On the other hand, the authors of [4] introduce a zero-sum two-player differential game and extended the H_∞ optimal control to nonlinear dynamic systems. In contrast, the concept of dissipativity [5] was employed to convert the H_∞ optimal control problem into an L_2-gain optimal control problem in [6]. However, the L_2-gain optimal problem requires solving the nonlinear differential or difference Hamilton-Jacobi-Isaacs (HJI) equations which is very difficult due to lack of a closed-form solution.

To overcome this problem, the continuous and discrete time problems are addressed in [7] and [8], respectively, where a smooth solution is found by solving for the

Taylor series expansion coefficients using Riccati equations. As a result, the HJI problem is reduced to solving a Riccati equation along with a sequence of linear algebraic equations. In contrast, [9] proposes an iterative based policy to successively solve the continuous-time HJI by breaking the nonlinear (in value function) partial differential equation to a sequence of linear differential equations using Galerkin techniques. However, an associated draw back of this approach is the requirement of a large number of integral calculations. A similar approach was adopted by [10] where the value function is approximated by a neural network that is trained offline using the least squares techniques.

While the continuous-time HJI problem has been under consideration [7][9][10], discrete-time HJI control problem for nonlinear systems is addressed in a limited manner. The work of [11] presents important fundamental principles concerning the HJI optimization problem via the L_2-gain optimal problem; however, no approximation strategy has been used to find a closed-form solution of the value function.

In contrast, the work in this paper seeks to extend the foundations presented in [12] by proposing a practical method for obtaining the L_2-gain near optimal control while keeping a tradeoff between accuracy and computational complexity. Using the Taylor series expansion of the value function and using a small signal perturbation assumption, a generalized Hamilton-Jacobi-Isaacs (GHJI) equation is proposed, and an iterative approach to solve the GHJI is presented. Successive solutions for the value function ensure that the value function reaches its saddle-point in a zero-sum two-player differential game where the players are system disturbances and the control input. The

successive approximations of the value function are accomplished using the approximation properties of neural networks (NN) [1] and least squares.

Next, a NN identifier is presented in this work to learn the nonlinear internal dynamics of the system. Using Lyapunov theory, it is shown that the identification errors converge to a small bounded region around the origin. Then, using the learned NN model of the internal dynamics, offline training is undertaken resulting in a novel solution to the HJI optimal control problem.

The contribution of this work is the use of a Taylor series expansion to solve the HJI equation which is more involved than the use of the Taylor series expansion to solve the HJB in [12]. For instance, additional considerations are required when solving the HJI equation to ensure the existence of a saddle-point in the zero-sum two player game where as solving the HJB equation [12] does not have such a requirement. Additionally, added complexity is introduced during the successive approximation of the HJI equation which requires an inner loop and an outer loop whereas successively approximating the HJB equation requires only a single training loop. In addition, the proposed method does not require explicit knowledge of the system internal dynamics as only an online learned NN model is utilized for the offline training in contrast to the works [8]-[12] which require the internal dynamics to be known. Additionally, convergence of the successive approximations is demonstrated while explicitly considering the identifier NN reconstruction errors.

This paper is organized as follows. First, background information for the discrete time nonlinear HJI formulation is presented in Section II. In Section III, the GHJI equation is derived, and an iterative based approach to solve the GHJI equation is

proposed. Additionally, convergence of the successive approximations is demonstrated. Then, it is shown that algebraic Riccati equation can be obtained from HJI in Section IV. Section V presents the NN implementation of the successive approximation of the GHJI equation as well as the NN identification scheme, while numerical simulations and concluding remarks are provided in Sections VI and VII, respectively.

II. Background

Consider the discrete-time affine nonlinear system

$$x_{k+1} = f(x_k) + g(x_k)u_k + h(x_k)w_k \tag{1}$$

where $x_k \in \Re^n$ is the state vector evaluated at step k, $f(.) \in \Re^n$, $g(.) \in \Re^{n\times m}$, and $h(.) \in \Re^{n\times M}$ are smooth functions defined in a neighborhood of the origin, $u_k \in \Re^m$ is the control input and $w_k \in \Re^M$ is the disturbance. Now, assume that x_{k+1} is Lipschitz on a set Ω and there is a control input such that system (1) is asymptotically stabilized. Then, our goal is to find a control input u_k which can minimize the infinite horizon cost function

$$J_k = \sum_{j=k}^{\infty}\left(Q(x_j) + u_j^T R u_j - \gamma^2 w_j^T P w_j\right) = Q(x_k) + u_k^T R u_k - \gamma^2 w_k^T P w_k + J_{k+1} \tag{2}$$

when the disturbance w_k has its worst value, i.e., w_k tries to make the cost function negative [10]. In (2), Q, R, and P are positive definite matrices, and γ is a constant. In addition to stabilizing the nonlinear system (1), the control input u_k must make the cost function (2) finite. That is, u_k must be admissible. Next, the definition of admissible control is introduced.

Definition 1. (Admissible Control): The control input u_k is called admissible with respect to the penalty function $Q(x) \geq 0$ and control energy penalty $u_k^T R u_k$, function if a) u_k is

continuous; b) $u_k(x)\big|_{x=0} = 0$; c) $u_k(x)$ stabilizes system (1); and d) $J_k(x(0),u) = \sum_{j=0}^{\infty}\left(Q(x_j) + u_j^T R u_j - \gamma^2 w_j^T P w_j\right) \leq \infty$.

Moving on, this control problem is often referred to as a zero-sum two-player differential game [4] where the two policies $u_k^*(x_k)$ and $w_k^*(x_k)$ are the solutions of (2) such that $J_k(u_k^*, w_k) \leq J_k(u_k^*, w_k^*) \leq J_k(u_k, w_k^*)$ for all u_k and w_k. The minimizing control input $u_k^*(x_k)$ and maximizing disturbance $w_k^*(x_k)$ are found using the stationary conditions [13] $\partial J_k / \partial u_k(x_k) = 0$ and $\partial J_k / \partial w_k(x_k) = 0$, and routine calculation shows $u_k^* = -\frac{1}{2} R^{-1} g(x_k)^T \frac{\partial J_{k+1}^*}{\partial x_{k+1}}$ and $w_k^* = \frac{1}{2\gamma^2} P^{-1} h(x_k)^T \frac{\partial J_{k+1}^*}{\partial x_{k+1}}$. The pair $(u_k^*(x_k), w_k^*(x_k))$ then becomes the feedback saddle-point solution of the optimization problem [4]. The necessary and sufficient condition for the existence of a solution for HJI from [2] is given in the following theorem.

Theorem 1[2]. Consider a zero-sum two-player differential game. The feedback saddle-point solution $(u_k^*(x_k), w_k^*(x_k))$ is achievable, if and only if there exists a smooth function $V_k(.) : Z \times \Re^n \to \Re$ referred as *value function* such that the HJI equation

$$\begin{aligned} V_k(x) &= \min_{u_k} \max_{w_k} \sum_{j=k}^{\infty}\left(Q(x_j) + u_j^T R u_j - \gamma^2 w_j^T P w_j + V_{k+1}(x_{k+1})\right) \\ &= \max_{w_k} \min_{u_k} \sum_{j=k}^{\infty}\left(Q(x_j) + u_j^T R u_j - \gamma^2 w_j^T P w_j + V_{k+1}(x_{k+1})\right) \\ &= Q(x_k) + u_k^{*T} R u_k^* - \gamma^2 w_k^{*T} P w_k^* + V_{k+1}(f + g u_k^* + h w_k^*) \end{aligned} \tag{3}$$

has a solution with $V_\infty(x) = 0$ where $x = x_k$. ■

Before proceeding, the following definitions are required.

Definition 2 [14]. (L_2-gain): The nonlinear system (1) with feedback control u_k and

disturbance $w_k \in l_2$ is said to have an L_2-gain less than or equal to γ if

$$\sum_{k=0}^{N}\left(Q(x_k)+u_k^T R u_k\right) \le \sum_{k=0}^{N}\gamma^2 w_k^T P w_k \tag{4}$$

with $Q(x_k)+u_k^T R u_k$ excited by the disturbance from an initial state x_0. When N approaches infinity, (4) can be rewritten as

$$\sum_{k=0}^{\infty}\left(Q(x_k)+u_k^T R u_k\right) \le \sum_{k=0}^{\infty}\gamma^2 w_k^T P w_k \ .$$

The problem of disturbance attenuation can be addressed by using the L_2-gain of a nonlinear system [11]. The disturbance w_k is locally attenuated by a real value $\gamma > 0$ if there exists a neighborhood around the origin such that $\forall w_k \in l_2$ for which the trajectories of the closed-loop system (1) starting from the origin remain in the same neighborhood, and the response $z_k \in l_2$, where $\|z_k\|^2 = Q(x_k)+u_k^T R u_k$, satisfies $\sum_{k=0}^{\infty}\left(\gamma^2 w_k^T P w_k - Q(x_k) - u_k^T R u_k\right) \ge 0$. Under these conditions, local disturbance attenuation with internal stability lends an admissible control input providing a closed-loop system with an L_2-gain less than or equal to γ [11].

Definition 3 [5]. (Finite-gain Dissipative System): The discrete-time nonlinear system (1) is said to be finite-gain dissipative with supply rate

$$W(x_k, w_k) = Q(x_k) + u_k^T R u_k - \gamma^2 w_k^T P w_k \tag{5}$$

if there exists a nonnegative function $V : \Re^n \to \Re$ called a storage function with $V(0) = 0$ such that for all $k \in Z^+$ and w_k we have $V(x_{k+1}) - V(x_k) \le W(x_k, w_k)$, or equivalently

$$V(x_{k+1}) - V(x_0) \le \sum_{j=0}^{k} W(x_j, w_j) \ .$$

The relationship between the system (1) having L_2-gain and being dissipative can be expressed by the following [11]:

a) The nonlinear system (1) has L_2-gain less than or equal γ if it is finite-gain dissipative with the supply rate (5) and $V(0) = 0$.

b) The nonlinear system (1) is finite-gain dissipative with the supply rate (5) if it has L_2-gain less than or equal to γ and is reachable from $x = 0$.

III. GHJI Equation for Nonlinear Discrete-time System

According to the optimization problem (3), the DT HJI equation becomes [11]

$V_{k+1}(f + gu_k^* + hw_k^*) - V_k(x) + Q(x_k) + u_k^{*T} R u_k^* - \gamma^2 w_k^{*T} P w_k^* = 0$ where the optimal control input u_k^* and worst case disturbance w_k^* are the solutions of optimization problem (3). Thus, the Hamiltonian function can be defined as

$$H(x_k, u_k, w_k) = V_{k+1}(f + gu_k + hw_k) - V_k(x) + Q(x_k) + u_k{}^T R u_k - \gamma^2 w_k{}^T P w_k \quad . \tag{6}$$

Note that when $H(x_k, u_k^*, w_k^*) = 0$, we have the DT HJI equation (12). According to the definition of the value function $V_k(x)$ in (3), the optimal control input u_k^* and worst disturbance w_k^* can be obtained by setting the first partial derivative of the right hand side of equation (6) with respect to u_k and w_k, respectively, equal to zero (the stationary conditions [13]) as $\partial H(x_k, u_k, w_k)/\partial u_k = 0$ and $\partial H(x_k, u_k, w_k)/\partial w_k = 0$. These equations in turn yield

$$u_k^* = -\frac{1}{2} R^{-1} g(x_k)^T \frac{\partial V_{k+1}^*}{\partial x_{k+1}} \tag{7}$$

and

$$w_k^* = \frac{1}{2\gamma^2} P^{-1} h(x_k)^T \frac{\partial V_{k+1}^*}{\partial x_{k+1}}. \tag{8}$$

Next, by substituting (7) and (8) into (12), the HJI equation becomes

$$\begin{aligned} 0 &= V_{k+1}^*(x_{k+1}) - V_k(x_k) + Q(x_k) \\ &\quad + \frac{1}{4} \frac{\partial V_{k+1}^*}{\partial x_{k+1}}^T \left(\frac{1}{\gamma^2} h(x_k) p^{-1} h(x_k)^T - g(x_k) R^{-1} g(x_k)^T \right) \frac{\partial V_{k+1}^*}{\partial x_{k+1}} \end{aligned} \tag{9}$$

Note that the differential equation (9) is nonlinear with respect to $\partial V_{k+1}^*/\partial x_{k+1}$ and in general is difficult to solve. In [12], a Taylor series expansion approach was undertaken to overcome the difficulties in finding such a value function V_{k+1}^* in the single-player Hamilton-Jacobi-Bellman optimization problem. However, no work has been done in discrete-time HJI formulation. In this paper, Taylor series expansion approach is employed to solve the DT HJI optimization.

By assuming small perturbation about the operating point x_k, we expand ΔV_k by keeping the first two terms in the Taylor series and considering the higher order terms to be negligible. It was shown in [12] that this assumption is not stringent and can be applied to quadratic cost function without making the small perturbation assumption. Thus, we obtain

$$\begin{aligned} \Delta V_k &= V(x_{k+1}) - V(x_k) = V_{k+1} - V_k \\ &\approx \nabla V_k^T (x_{k+1} - x_k) + \frac{1}{2} (x_{k+1} - x_k)^T \nabla^2 V_k (x_{k+1} - x_k) \end{aligned} \tag{10}$$

where ∇V_k and $\nabla^2 V_k$ are the gradient vector and Hessian matrix, respectively, as shown in (11) and (12) as

$$\nabla V_k = \left. \frac{\partial V(x)}{\partial x} \right|_{x=x_k} = \left[\frac{\partial V(x)}{\partial x_1} \quad \cdots \quad \frac{\partial V(x)}{\partial x_n} \right]_{x=x_k} \tag{11}$$

$$\nabla^2 V_k = \left[\begin{matrix} \frac{\partial^2 V(x)}{\partial x_1^{\,2}} & \frac{\partial^2 V(x)}{\partial x_1 \partial x_2} & \cdots & \frac{\partial^2 V(x)}{\partial x_1 \partial x_n} \\ \frac{\partial^2 V(x)}{\partial x_2 \partial x_1} & \frac{\partial^2 V(x)}{\partial x_2^{\,2}} & \cdots & \frac{\partial^2 V(x)}{\partial x_2 \partial x_n} \\ \vdots & \vdots & \ddots & \vdots \\ \frac{\partial^2 V(x)}{\partial x_n \partial x_1} & \frac{\partial^2 V(x)}{\partial x_n \partial x2} & \cdots & \frac{\partial^2 V(x)}{\partial x_n^{\,2}} \end{matrix} \right]_{x=x_k} \tag{12}$$

Next, the following lemma is stated before we proceed.

Lemma 1. Let u_k be an initial admissible control policy applied to the nonlinear discrete-time system (1) with the associated value function (3) and cost function (2) such that

$$\begin{aligned} &\nabla V_k(f_k + g_k u_k + h w_k - x_k) \\ &+ \frac{1}{2}(f_k + g_k u_k + h w_k - x_k)^T \nabla^2 V_k(f_k + g_k u_k + h_k w_k - x_k) \\ &\quad + Q(x_k) + u_k^T R u_k - \gamma^2 w_k^T P w_k = 0. \end{aligned} \tag{13}$$

Then, $J_j(x_j, u, w) = V_j$ for all $j \in Z^+$.

Proof. Substituting the dynamics (1) and using (10), we have

$$\begin{aligned} &V_\infty - V_j = \sum_{k=j}^{\infty} \Delta V_k = \sum_{k=j}^{\infty} \left(V(x_{k+1}) - V(x_k)\right) = \sum_{k=j}^{\infty} \left(V_{k+1} - V_k\right) \approx \\ &\sum_{k=j}^{\infty} \left(\begin{matrix} \nabla V_k(f_k + g_k u_k + h w_k - x_k) \\ + \frac{1}{2}(f_k + g_k u_k + h w_k - x_k)^T \nabla V_k^{\,2}(f_k + g_k u_k + h_k w_k - x_k) \end{matrix} \right). \end{aligned} \tag{14}$$

According to equation (2) we have

$$J_j(x_j, u, w) = \sum_{k=j}^{\infty} \left(Q(x_k) + u_k^T R u_k - \gamma^2 w_k^T P w_k \right). \tag{15}$$

Since u_k is an admissible control, $V_\infty = 0$, and by adding (14) to (15), we obtain

$$
\begin{aligned}
J_j(x_j,u,w)-V_j &= \sum_{k=j}^{\infty}\left(\nabla V_k(f_k+g_ku_k+hw_k-x_k)\right)\\
&+\sum_{k=j}^{\infty}\left(\frac{1}{2}(f_k+g_ku_k+hw_k-x_k)^T\nabla V_k{}^2(f_k+g_ku_k+h_kw_k-x_k)\right)\\
&+\sum_{k=j}^{\infty}\left(Q(x_k)+u_k^TRu_k-\gamma^2w_k^TPw_k\right).
\end{aligned}
\tag{16}
$$

The right hand side of (16) is zero by observing (13). Thus, $J_j(x_j,u,w)-V_j=0$. ■

Equation (13) now provides a new optimal solution for V_k^* based on new u_k^* and w_k^* which are derived next.

Definition 4. (GHJI Equation for Discrete-time Nonlinear System): Equation (13) evaluated at $V(x)|_{x=0}=0$ is defined as the GHJI equation for affine nonlinear DT system (1).

Definition 5. (Pre-Hamiltonian Function): A suitable pre-Hamiltonian function for the affine nonlinear DT system (1) is defined as

$$
\begin{aligned}
H(x_k,V_k,u_k,w_k) &= \nabla V_k(f_k+g_ku_k+hw_k-x_k)\\
&+\frac{1}{2}(f_k+g_ku_k+hw_k-x_k)^T\nabla^2V_k(f_k+g_ku_k+h_kw_k-x_k)\\
&+Q(x_k)+u_k^TRu_k-\gamma^2w_k^TPw_k.
\end{aligned}
\tag{17}
$$

Note that when $H(x_k,V_k,u_k^*,w_k^*)=0$, the GHJI equation results where u_k^* and w_k^* are the new optimal policies to be obtained. The optimal control input u_k^* and worst case disturbance w_k^* can be found by setting the first partial derivative of the equation (17) with respect to u_k and w_k, respectively, equal to zero

$$
\begin{cases}
\dfrac{\partial H(x_k,V_k,u_k,w_k)}{\partial w_k}=0\\[2ex]
\dfrac{\partial H(x_k,V_k,u_k,w_k)}{\partial u_k}=0
\end{cases}
$$

which yields

$$w_k^* = \left[2\gamma^2 P - h_k^T \nabla^2 V h_k\right]^{-1} h_k^T \left[\nabla V^T + \nabla^2 V(f_k + g_k u_k^* - x_k)\right] \tag{18}$$

and

$$u_k^* = -\left[g_k^T \nabla^2 V g_k + 2R\right]^{-1} g_k^T \left[\nabla V^T + \nabla^2 V(f_k + h_k w_k^* - x_k)\right]. \tag{19}$$

To ensure that the term $2\gamma^2 P - h_k^T \nabla^2 V h_k$ is always invertible, it is required that $\gamma^2 > \frac{1}{2}\lambda_{\max}(B)$ where $B = P^{-1} h_k^T \nabla^2 V_k h_k$. It will also be shown that selecting γ in this way guarantees the existence of a saddle-point in the zero-sum two-player game. Equations (18) and (19) may be solved together to obtain solutions in terms of the value function and system states as

$$\begin{aligned} w_k^* = &-\left(I - Y_w^{-1} h_k^T \nabla^2 V g_k Y_u^{-1} g_k^T \nabla^2 V h_k\right)^{-1} Y_w^{-1} h_k^T \times \\ &\left(\nabla V^T + \nabla^2 V(f_k - x_k) - \nabla^2 V g_k Y_u^{-1} g_k^T \left[\nabla V^T + \nabla^2 V(f_k - x_k)\right]\right) \end{aligned} \tag{20}$$

and

$$\begin{aligned} u_k^* = &-\left(I - Y_u^{-1} g_k^T \nabla^2 V h_k Y_w^{-1} h_k^T \nabla^2 V g_k\right)^{-1} Y_u^{-1} g_k^T \times \\ &\left(\nabla V^T + \nabla^2 V(f_k - x_k) - \nabla^2 V\left(h_k Y_w^{-1} h_k^T \left[\nabla V^T + \nabla^2 V(f_k - x_k)\right]\right)\right) \end{aligned} \tag{21}$$

where $Y_u = g_k^T \nabla^2 V . g_k + 2R > 0$ and $Y_w = h_k^T \nabla^2 V . h_k - 2\gamma^2 P$.

In contrast to the policies (7) and (8), the optimal control and worst-case disturbance (18) and (19) can be calculated independent of x_{k+1}. Thus, once the value function is obtained, the optimal control input and worst-case disturbance can then be implemented by using (20) and (21). However, despite its linear behavior, finding a solution for the GHJI equation is still not easy. To overcome this problem, an iterative based scheme [9][10][12] is proposed to update the disturbance and control input (18) and (19) in order to reach the optimal u_k^* and w_k^* for the discrete time GHJI problem.

The following theorem will now demonstrate that the optimal control (19) and worst case disturbance (18) ensures the existence of a saddle-point in the zero-sum two-player game.

Theorem 2. (Existence of saddle point) Let the pair (u_k, w_k^*) be an arbitrary admissible control and the worst-case disturbance inputs as provided by (18) for system (1). In addition, let the pair (u_k^*, w_k) be the optimal controller provided by (19) and an arbitrary disturbance input, respectively, for system (1). Then, the Hamiltonian function (6) satisfies $H(x_k, u_k^*, w_k) \le H(x_k, u_k^*, w_k^*) \le H(x_k, u_k, w_k^*)$.

Proof. The proof will be shown in two steps. First, it will shown that $H(x_k, u_k, w_k^*) - H(x_k, u_k^*, w_k^*) \ge 0$. By using (17), and noting that $H(x_k, u_k^*, w_k^*)$ and $H(x_k, u_k, w_k^*)$ are nothing but equation (17) rewritten in terms of w_k^* and/or u_k^*, we obtain

$$
\begin{aligned}
&H(x_k, u_k, w_k^*) - H(x_k, u_k^*, w_k^*) = \\
&\begin{pmatrix} \nabla V_k(f_k + g_k u_k + h w_k^* - x_k) + Q(x_k) + u_k{}^T R u_k - \gamma^2 w_k^{*T} P w_k^* \\ + \frac{1}{2}(f_k + g_k u_k + h_k w_k^* - x_k)^T \nabla^2 V_k (f_k + g_k u_k + h_k w_k^* - x_k) \end{pmatrix} \\
&- \begin{pmatrix} \nabla V_k(f_k + g_k u_k^* + h w_k^* - x_k) + Q(x_k) + u_k^{*T} R u_k^* - \gamma^2 w_k^{*T} P w_k^* \\ + \frac{1}{2}(f_k + g_k u_k^* + h_k w_k^* - x_k)^T \nabla^2 V_k (f_k + g_k u_k^* + h_k w_k^* - x_k) \end{pmatrix} = \\
&\left[\nabla V_k + (f_k + h_k w_k^* - x_k)^T \nabla^2 V_k\right] g_k (u_k - u_k^*) \\
&+ \frac{1}{2} u_k{}^T Y_u u_k - \frac{1}{2} u_k^{*T} Y_u u_k^*
\end{aligned}
\tag{22}
$$

Next, using (19) to replace the first term in (22) yields

$$
\begin{aligned}
H(x_k, u_k, w_k^*) - H(x_k, u_k^*, w_k^*) &= -u_k^{*T} Y_u{}^T (u_k - u_k^*) + \frac{1}{2} u_k{}^T Y_u u_k - \frac{1}{2} u_k^{*T} Y_u u_k^* \\
&= (u_k - u_k^*)^T Y_u (u_k - u_k^*).
\end{aligned}
$$

Since the matrix Y_u is positive definite it can be concluded that $H(x_k, u_k, w_k^*) - H(x_k, u_k^*, w_k^*) \geq 0$.

Next, it will be shown that $H(x_k, u_k^*, w_k) - H(x_k, u_k^*, w_k^*) \leq 0$. Similar to (22) we have

$$H(x_k, u_k^*, w_k) - H(x_k, u_k^*, w_k^*) = \left[\nabla V_k + (f_k + g_k u_k^* - x_k)^T \nabla^2 V_k\right] h_k (w_k - w_k^*) + \frac{1}{2} w_k{}^T Y_w w_k - \frac{1}{2} w_k^{*T} Y_w w_k^*.$$

Employ (18) and replace the first term in $H(x_k, u_k^*, w_k) - H(x_k, u_k^*, w_k^*)$ to obtain

$$H(x_k, u_k^*, w_k) - H(x_k, u_k^*, w_k^*) = -w_k^{*T} Y_w{}^T (w_k - w_k^*) + \frac{1}{2} w_k{}^T Y_w w_k - \frac{1}{2} w_k^{*T} Y_w u_k^* = (w_k - w_k^*)^T Y_w (w_k - w_k^*).$$

Since $\gamma^2 > \lambda_{\max}(P^{-1} h_k^T \nabla^2 V_k h_k)/2$, Y_w is negative definite. Thus, $H(x_k, u_k^*, w_k) - H(x_k, u_k^*, w_k^*) \leq 0$ and it can be concluded that $H(x_k, u_k^*, w_k) \leq H(x_k, u_k^*, w_k^*) \leq H(x_k, u_k, w_k^*)$. ■

A. Successive Approximation of the GHJI Equation

Let u_k^0 be an initial admissible control input for system (1) in the absence of disturbances w_k in a compact set Ω. The successive approximation procedure consists of a sequential set of updates for the disturbance $w_k^{(i,j)}$ in an inner loop with index *j* accompanied by a sequential set of updates for the control input $u_k^{(i)}$ in an outer loop with index *i*. The sequence starts with setting $u_k^{(i)} = u_k^0$ and $w_k^{(i,0)} = 0$ for *i=0*. Then, the pre-Hamiltonian equation (13) is solved for $V_k^{(i,j)}$ as

$$\nabla V_k^{(i,j)}(f_k + g_k u_k^{(i)} + h_k w_k^{(i,j)} - x_k) + \frac{1}{2}(f_k + g_k u_k^{(i)} + h_k w_k^{(i,j)} - x_k)^T \times$$
$$\nabla^2 V_k^{(i,j)}(f_k + g_k u_k^{(i)} + h w_k^{(i,j)} - x_k) + Q(x_k) + u_k^{(i)^T} R u_k^{(i)} \qquad (23)$$
$$-\gamma^2 w_k^{(i,j)^T} P w_k^{(i,j)} = 0.$$

The updated disturbance can now be found by using (18) as

$$w_k^{(i,j+1)} = -[h_k^T \nabla^2 V_k^{(i,j)} h_k - 2\gamma^2 P]^{-1} h_k^T \times$$
$$[\nabla V_k^{(i,j)^T} + \nabla^2 V_k^{(i,j)}(f_k + g_k u_k^i - x_k)] \qquad (24)$$

The inner loop *j* proceeds until it converges such that $V_k^{(i,j)} = V_k^{(i,j+1)} = V_k^{(i,\infty)}$.

Next, $u_k^{(i)}$ is updated according to (19) and written as

$$u_k^{(i+1)} = -[g_k^T \nabla^2 V_k^{(i,\infty)} g_k + 2R]^{-1} g_k^T \times$$
$$[\nabla V_k^{(i,\infty)^T} + \nabla^2 V_k^{(i,\infty)}(f_k + h_k w_k^{(i,\infty)} - x_k)].$$

Then, value function is found by solving (23) for $V_k^{(i,j)}$. Similar to the inner loop, the outer loop *i* proceeds until it converges such that $V_k^{(i,\infty)} = V_k^{(i+1,\infty)} = V_k^{(\infty,\infty)}$. This procedure is depicted in Fig. 1.

Theorem 3. Let $u_k^{(i)}$ an initial admissible control input for pair (*i*,*j*) on the set Ω. Then, iterating between the pair (23) and (24) ensures $V_k^{(i,j)}$ is monotonically increasing until the worst-case disturbance for the control input $u_k^{(i)}$ is found provided $\gamma^2 \geq \lambda_{\max}(B)/2$ with $B = P^{-1} h_k^T \nabla^2 V_k^{(i,j)} h_k$. That is, $V_k^{(i,j)} \leq V_k^{(i,j+1)} \leq V_k^{(i,\infty)}$ and $\lim_{j\to\infty} V_k^{(i,j)} = V_k^{(i,\infty)}$. In addition, the value function $V_k^{(i,\infty)}$ satisfies

$$\nabla V_k^{(i,j)^T}(f_k + g_k u_k^{(i)} + h_k w_k^{(i,\infty)} - x_k) + \frac{1}{2}(f_k + g_k u_k^{(i)} + h_k w_k^{(i,\infty)} - x_k)^T \times$$
$$\nabla^2 V_k^{(i,\infty)}(f_k + g_k u_k^{(i)} + h w_k^{(i,\infty)} - x_k) + Q(x_k) + u_k^{(i)^T} R u_k^{(i)}$$
$$-\gamma^2 w_k^{(i,\infty)^T} P w_k^{(i,j)} = 0$$

where

$$w_k^{(i,\infty)} = -[h_k^T \nabla^2 V_k^{(i,\infty)}.h_k - 2\gamma^2 P]^{-1} h_k^T [\nabla V_k^{(i,\infty)^T} + \nabla^2 V_k^{(i,\infty)}(f_k + g_k u_k^{(i)} - x_k)] \,.$$

Proof. First, we evaluate $\Delta V_k^{(i,j)}$ along the trajectories of

$$x_{k+1} = f_k + g_k u_k^{(i)} + h_k w_k^{(i,j+1)} \,. \tag{25}$$

From (10) we have

$$\Delta V_k^{(i,j)} \approx \nabla V_k^{(i,j)}(x_{k+1} - x_k) + \frac{1}{2}(x_{k+1} - x_k)^T \nabla^2 V_k^{(i,j)}(x_{k+1} - x_k) \tag{26}$$

Now, substituting (25) into (26) reveals

$$\Delta V_k^{(i,j)} = \nabla V_k^{(i,j)}(f_k + g_k u_k^{(i)} + h_k w_k^{(i,j+1)} - x_k) + \frac{1}{2}(f_k + g_k u_k^{(i)} + h_k w_k^{(i,j+1)} - x_k)^T \times$$
$$\nabla^2 V_k^{(i,j)}(f_k + g_k u_k^{(i)} + h_k w_k^{(i,j+1)} - x_k) \,. \tag{27}$$

Next, we rewrite the GHJI equation (13) in terms of $V_k^{(i,j)}$ along the trajectory $x_{k+1} = f_k + g_k u_k^{(i)} + h_k w_k^{(i,j)}$ as

$$\nabla V_k^{(i,j)}(f_k + g_k u_k^{(i)} + h_k w_k^{(i,j)} - x_k) + \frac{1}{2}(f_k + g_k u_k^{(i)} + h_k w_k^{(i,j)} - x_k)^T \times$$
$$\nabla^2 V_k(f_k + g_k u_k^{(i)} + h_k w_k^{(i,j)} - x_k) + Q(x_k) + u_k^{(i)^T} R u_k^{(i)} \tag{28}$$
$$-\gamma^2 w_k^{(i,j)^T} P w_k^{(i,j)} = 0.$$

Now, combining (27) and (28) renders

$$\Delta V_k^{(i,j)} =$$
$$\begin{pmatrix} \nabla V_k^{(i,j)}(f_k + g_k u_k^{(i)} + h_k w_k^{(i,j+1)} - x_k) + \frac{1}{2}(f_k + g_k u_k^{(i)} + h_k w_k^{(i,j+1)} - x_k)^T \times \\ \nabla^2 V_k^{(i,j)}(f_k + g_k u_k^{(i)} + h_k w_k^{(i,j+1)} - x_k) \end{pmatrix}$$
$$- \begin{pmatrix} \nabla V_k^{(i,j)}(f_k + g_k u_k^{(i)} + h_k w_k^{(i,j)} - x_k) + Q(x_k) + u_k^{(i)^T} R u_k - \gamma^2 w_k^{(i,j)^T} P w_k \\ + \frac{1}{2}(f_k + g_k u_k^{(i)} + h_k w_k^{(i,j)} - x_k)^T \nabla^2 V_k^{(i,j)}(f_k + g_k u_k^{(i)} + h_k w_k^{(i,j)} - x_k) \end{pmatrix}$$

and after some math we obtain

$$\begin{aligned}\Delta V_k^{(i,j)} &= -\frac{1}{2} w_k^{(i,j)^T}\left[h_k^T\left(\nabla^2 V_k^{(i,j)}\right)h_k - 2\gamma^2 P\right]w_k^{(i,j)} \\ &+ \frac{1}{2}\left[2(f_k + g_k u_k^{(i)} - x_k)^T\left(\nabla^2 V_k^{(i,j)}\right)h_k + 2\nabla V_k^{(i,j)^T} h_k\right]\left(w_k^{(i,j+1)} - w_k^{(i,j)}\right) \\ &+ \frac{1}{2} w_k^{(i,j+1)^T} h_k^T\left(\nabla^2 V_k^{(i,j)}\right)h_k w_k^{(i,j+1)} - Q(x_k) - u_k^{(i)^T} R u_k.\end{aligned} \tag{29}$$

Also, from the update law (24) we have the relation

$$\begin{aligned}&w_k^{(i,j+1)^T}[h_k^T\left(\nabla^2 V_k^{(i,j)}\right)h_k - 2\gamma^2 P] = \\ &\quad -[\nabla V_k^{(i,j)^T} + \left(\nabla^2 V_k^{(i,j)}\right)(f_k + g_k u_k^{(i)} - x_k)]^T h_k\end{aligned} . \tag{30}$$

Plugging (30) into (29) yields

$$\begin{aligned}\Delta V_k^{(i,j)} &= \frac{1}{2} w_k^{(i,j+1)^T} 2\gamma^2 P w_k^{(i,j+1)} + w_k^{(i,j+1)^T}\left[h_k^T\left(\nabla^2 V_k^{(i,j)}\right)h_k - 2\gamma^2 P\right]w_k^{(i,j)} \\ &- \frac{1}{2} w_k^{(i,j+1)^T}\left[h_k^T\left(\nabla^2 V_k^{(i,j)}\right)h_k - 2\gamma^2 P\right]w_k^{(i,j+1)} \\ &- \frac{1}{2} w_k^{(i,j)^T}\left[h_k^T\left(\nabla^2 V_k^{(i,j)}\right)h_k - 2\gamma^2 P\right]w_k^{(i,j)} - Q(x_k) - u_k^{(i)^T} R u_k^{(i)}.\end{aligned}$$

After rearranging, we have

$$\begin{aligned}\Delta V_k^{(i,j)} &= -Q(x_k) - u_k^{(i)^T} R u_k^{(i)} + \gamma^2 w_k^{(i,j+1)^T} P w_k^{(i,j+1)} + \\ &\frac{1}{2}\left(w_k^{(i,j+1)} - w_k^{(i,j)}\right)^T\left[2\gamma^2 P - h_k^T\left(\nabla^2 V_k^{(i,j)}\right)h_k\right]\left(w_k^{(i,j+1)} - w_k^{(i,j)}\right).\end{aligned} \tag{31}$$

Next, taking the infinite sum of (31) implies that

$$\begin{aligned}V_\infty^{(i,j)} - V_l^{(i,j)} &= \sum_{k=l}^{\infty}\Delta V_k^{(i,j)} = \sum_{k=l}^{\infty}(-Q(x_k) - u_k^{(i)^T} R u_k^{(i)} + w_k^{(i,j+1)^T}\gamma^2 P w_k^{(i,j+1)}) \\ &+ \sum_{k=l}^{\infty}\left(\frac{1}{2}\left(w_k^{(i,j+1)} - w_k^{(i,j)}\right)^T\left[2\gamma^2 P - h_k^T\left(\nabla^2 V_k^{(i,j)}\right)h_k\right]\left(w_k^{(i,j+1)} - w_k^{(i,j)}\right)\right) \\ &= -J_l^{(i,j+1)}(x_l, u_k^{(i)}, w_k^{(i,j+1)}) \\ &+ \sum_{k=l}^{\infty}\frac{1}{2}\left(w_k^{(i,j+1)} - w_k^{(i,j)}\right)^T\left[2\gamma^2 P - h_k^T\left(\nabla^2 V_k^{(i,j)}\right)h_k\right]\left(w_k^{(i,j+1)} - w_k^{(i,j)}\right).\end{aligned} \tag{32}$$

Since $V_\infty^{(i,j)} = 0$ equation (32) yields

$$J_l^{(i,j+1)}(x_l, u_k^{(i)}, w_k^{(i,j+1)}) = V_l^{(i,j)} + \frac{1}{2}\sum_{k=l}^{\infty}\left(\left(w_k^{(i,j+1)} - w_k^{(i,j)}\right)^T\left[2\gamma^2 P - h_k^T\left(\nabla^2 V_k^{(i,j)}\right)h_k\right]\left(w_k^{(i,j+1)} - w_k^{(i,j)}\right)\right) \tag{33}$$

.

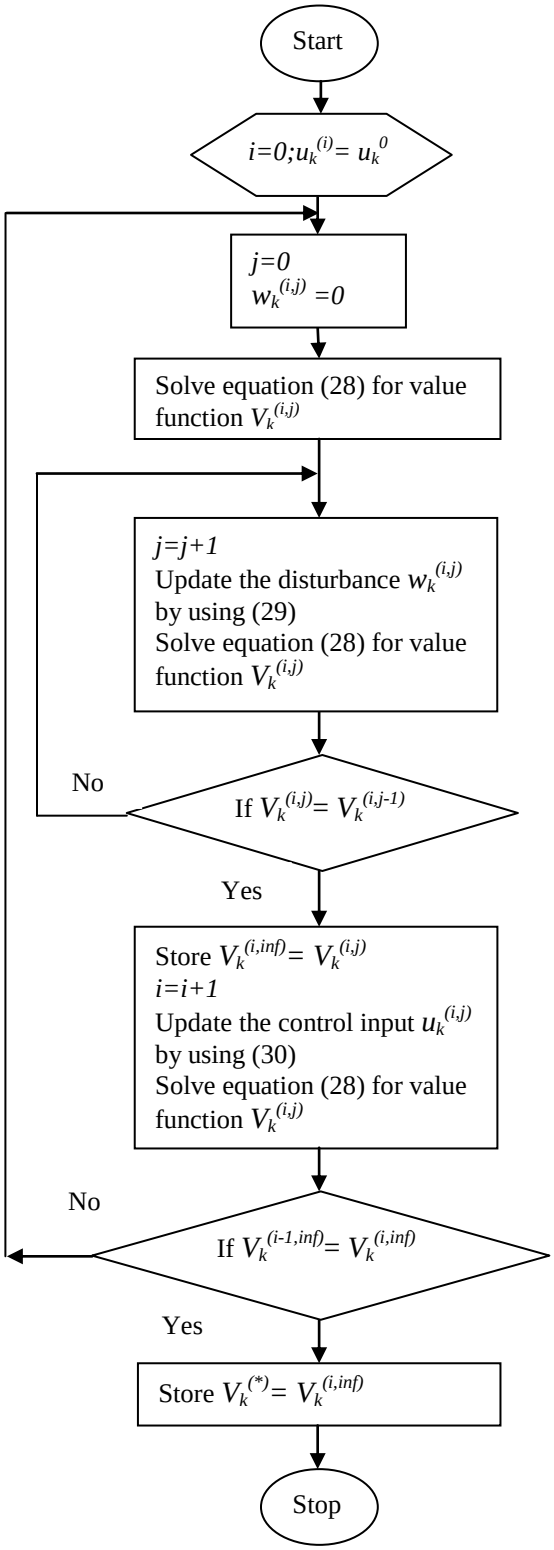

Fig. 1 Successive approximation procedure

In addition, from *Lemma 1* it is known that

$$J_l^{(i,j)}(x_l, u_l^{(i)}, w_l^{(i,j)}) = V_l^{(i,j)}. \tag{34}$$

Thus, from (33) and (34) we conclude that

$$V_l^{(i,j+1)} = V_l^{(i,j)} + \frac{1}{2}\sum_{k=l}^{\infty}\left(\left(w_k^{(i,j+1)} - w_k^{(i,j)}\right)^T\left[2\gamma^2 P - h_k^T\left(\nabla^2 V_k^{(i,j)}\right)h_k\right]\left(w_k^{(i,j+1)} - w_k^{(i,j)}\right)\right). \tag{35}$$

If $\gamma^2 > \lambda_{\max}(B)/2$, then $2\gamma^2 P - h_k^T\left(\nabla^2 V_k^{(i,j)}\right)h_k$ is positive definite, and equation (35) shows that $V_l^{(i,j+1)} \geq V_l^{(i,j)}$ which proves the first claim of the theorem. The second part of the theorem is easily shown by noting that when convergence occurs, equation (23) and (24) are solved for the same value function $V_k^{(i,\infty)}$ and disturbance $w_k^{(i,\infty)}$. Moreover, since a saddle-point exists in the zero-sum two-player game (*Theorem 2*), in a neighborhood Ω around the origin, $V_l^{(i,j)}$ has a maximum $V_l^{(i,\infty)}$ for $u_l^{(i)}$. Thus, $V_l^{(i,j)}$ continues to increase by the sequential updates (15) in the inner loop *j* until $V_l^{(i,j)} = V_l^{(i,j+1)} = V_l^{(i,\infty)}$. ■

Remark 1. In [10], H_∞ optimal control is considered for continuous-time nonlinear systems by means of obtaining the minimum γ. However, the method is based on decreasing γ by trial and error until its least value is achieved. By contrast, an explicit relationship $\gamma > \sqrt{\lambda_{\max}(B)/2}$ for the minimum γ is found here. Selection of γ in this way not only guarantees the existence of a saddle-point in the zero-sum two-player game, but also ensures convergence in the inner loop of successive approximations.

Next the convergence of the outer loop *i* is discussed.

Theorem 4. Let $u_k^{(i)}$ be an initial admissible control for pair (*i*,*j*) for system (1) on the set Ω. Then, the nonlinear system $x_{k+1} = f(x_k) + g(x_k)u_k^{(i+1)} + h(x_k)w_k^{(i,\infty)}$ has the L_2- gain less than or equal to γ. Additionally, $V_k^{(i,\infty)} \geq V_k^{(i+1,\infty)} \geq V_k^{(*)}$ and $\lim_{i\to\infty} V_k^{(i,\infty)} = V_k^{(*)}$ where $V_k^{(*)}$ solves the

GHJI equation (13). Also, if $V_k^{(i,\infty)} = V_k^{(i+1,\infty)}$, then $V_k^{(i,\infty)} = V_k^*$.

Proof. By evaluating $\Delta V_k^{(i,\infty)}$ from (10) along the trajectory of $x_{k+1} = f(x_k) + g(x_k)u_k^{(i+1)} + h(x_k)w_k^{(i,\infty)}$ and following a similar procedure as in Theorem 3, it is straight forward to show that

$$\begin{aligned}\Delta V_k^{(i,\infty)} = &-\frac{1}{2}\left(u_k^{(i+1)} - u_k^{(i)}\right)^T \left[2R + g_k^T\left(\nabla^2 V_k^{(i,\infty)}\right)g_k\right]\left(u_k^{(i+1)} - u_k^{(i)}\right) \\ &-Q(x_k) - u_k^{(i+1)^T} R u_k^{(i+1)} + \gamma^2 w_k^{(i,\infty)^T} P w_k^{(i,\infty)}.\end{aligned} \tag{36}$$

Equation (36) shows that $\Delta V_k^{(i,\infty)} \le -Q(x_k) + \gamma^2 w_k^{(i,\infty)^T} P w_k^{(i,\infty)} - u_k^{(i+1)^T} R u_k^{(i+1)}$ which, according to *Definition 2,* implies that the nonlinear system $x_{k+1} = f(x_k) + g(x_k)u_k^{(i+1)} + h(x_k)w_k^{(i,\infty)}$ has the L_2-gain less than or equal to γ and consequently is dissipative with respect to the supply rate $-Q(x_k) - u_k^{(i+1)^T} R u_k^{(i+1)} + \gamma^2 w_k^{(i,\infty)^T} P w_k^{(i,\infty)}$ according to *Definition 3*. That is, $V_{k+1}^{(i,\infty)} - V_k^{(i,\infty)} \le W(x_k, u_k^{(i)}, w_k^{(i,j)})$ where

$$W(x_k, u_k^{(i)}, w_k^{(i,j)}) = -Q(x_k) - u_k^{(i+1)^T} R u_k^{(i+1)} + \gamma^2 w_k^{(i,\infty)^T} P w_k^{(i,\infty)}.$$

For the second claim, take the infinite sum of (36) to get

$$\begin{aligned}V_\infty^{(i,\infty)} - V_l^{(i,\infty)} &= \sum_{k=l}^{\infty} \Delta V_k^{(i,\infty)} \\ &= \sum_{k=l}^{\infty}\left(-Q(x_k) - u_k^{(i+1)^T} R u_k^{(i+1)} + \gamma^2 w_k^{(i,\infty)^T} P w_k^{(i,\infty)}\right) \\ &\quad -\sum_{k=l}^{\infty}\left(\frac{1}{2}\left(u_k^{(i+1)} - u_k^{(i)}\right)^T \left[2R + g_k^T\left(\nabla^2 V_k^{(i,\infty)}\right)g_k\right]\left(u_k^{(i+1)} - u_k^{(i)}\right)\right) \\ &= -J_l^{(i+1,\infty)}(x_l, u_k^{(i+1)}, w_k^{(i,\infty)}) \\ &\quad -\sum_{k=l}^{\infty}\frac{1}{2}\left(u_k^{(i+1)} - u_k^{(i)}\right)^T \left[2R + g_k^T\left(\nabla^2 V_k^{(i,\infty)}\right)g_k\right]\left(u_k^{(i+1)} - u_k^{(i)}\right)\end{aligned}$$

Since $V_\infty^{(i,j)} = 0$ and $J_l^{(i,j)}(x_l, u_l^{(i)}, w_l^{(i,j)}) = V_l^{(i,j)}$ (from *Lemma 1*), and applying similar

reasoning used in *Theorem 2* shows

$$V_l^{(i+1,\infty)} = V_l^{(i,\infty)} - \frac{1}{2}\sum_{k=l}^{\infty}\left(u_k^{(i+1)} - u_k^{(i)}\right)^T\left[2R + g_k^T\left(\nabla^2 V_k^{(i,\infty)}\right)g_k\right]\left(u_k^{(i+1)} - u_k^{(i)}\right) \tag{37}$$

Observing $2R + g_k^T \nabla^2 V_k^{(i,\infty)} g_k > 0$, (37) shows that $V_l^{(i+1,\infty)} \le V_l^{(i,\infty)}$. Moreover, since a saddle-point exists in the considered zero-sum two-player game (*Theorem 2),* in the neighborhood Ω around the origin, $V_l^{(i,\infty)}$ has a minimum $V_l^{(*)}$ as $u_l^{(i)}$ varies. Thus, $V_l^{(i,\infty)}$ continues to decrease by the sequential updates (30) in the outer loop *i* until $V_l^{(i,\infty)} = V_l^{(i+1,\infty)} = V_l^{(*)}$. ■

Next, the admissibility of the controller is presented.

Lemma 2. (Admissibility of the controller) Let u_k^0 be an initial admissible control input for system (1) in the compact set Ω. Let the proposed successive approximation procedure of updates for the disturbance $w_k^{(i,j)}$ in the inner loop *j* and updates for the control input $u_k^{(i)}$ in the outer loop *i* is performed. Then, the control input $u_k^{(i)}$ remains admissible in each step of the outer loop *i.*

Proof. From *Theorem 3* we observe that $V_k^{(0,\infty)}$ exists and is finite in the set Ω. Also, from *Theorem 4* we observe that the positive function $V_k^{(1,\infty)}$ exists and $V_k^{(1,\infty)} \le V_k^{(0,\infty)}$. Since u_k^0 is admissible $V_k^{(0,\infty)}$ is finite and as a result $V_k^{(1,\infty)}$ is finite. Consequently, u_k^1 is admissible. By induction, admissibility of u_k^i for $2 \le i \le \infty$ is concluded. ■

Remark 2: In [12], the optimal control problem was solved by applying a Taylor series expansion of the HJB equation. In contrast, this work uses a Taylor series expansion to solve the HJI equation which is more involved than the HJB from [12]. For instance, additional considerations are required when solving the HJI equation to ensure the

existence of a saddle-point in the zero-sum two player game where as solving the HJB equation does not have such a requirement. Additionally, added complexity is introduced during the successive approximation of the HJI equation which requires an inner loop and an outer loop whereas successively approximating the HJB equation requires only a single training loop.

Remark 3: In [8], a solution to the HJI equation was found using a Taylor series to approximate the system dynamics as well as the HJI equation. As a result, the HJI problem is reduced to solving a Riccati equation along with a sequence of linear algebraic equations. In contrast, this work takes on a fundamentally different approach in forming the Taylor series expansion since we do not require a Taylor series expansion of the system dynamics. Additionally, the work of [8] does not prove that a saddle-point in the zero-sum two-player game exists using their approximation techniques whereas the saddle-point is rigorously shown to exist in this work. Finally, it is observed that [8] (and [12]) requires knowledge of the internal system dynamics $f_k(x)$ where as this requirement is relaxed in our work using the NN identifier presented after Section IV.

IV. Linear Discrete-time HJI

Next, it will be shown that discrete-time algebraic Riccati equation (DARE) for linear systems can be obtained by the proposed GHJI equation. Consider the discrete-time linear system (38) and associated value function (39)

$$x_{k+1} = Ax_k + Bu_k + Cw_k \tag{38}$$

$$V_k^{(*)} = x_k{}^T \Gamma x_k \tag{39}$$

where $x_k \in \Re^n$ is the state vector evaluated at step *k*, $A \in \Re^{n\times n}$, $B \in \Re^{n\times m}$, and $C \in \Re^{n\times M}$ are smooth functions defined in a neighborhood of the origin, $u_k \in \Re^m$ is the control input, $w_k \in \Re^M$ is the disturbance and Γ is a positive definite constant matrix.

Lemma 3. If $V_k^{(*)} = x_k{}^T \Gamma x_k$ in (39) is the value function for system (38), then $\Gamma^T = \Gamma$

Proof. This can be easily shown by obtaining the transpose of both sides of the linear HJI DARE equation (40) [18][19], knowing that *Q*, *R*, and *P* are symmetric, and for any given invertible matrix *X* we have $\left(X^T\right)^{-1} = \left(X^{-1}\right)^T$. Then,

$$\begin{aligned}\Gamma = A^T\Gamma A + Q - \begin{bmatrix}A^T\Gamma B & A^T\Gamma E\end{bmatrix}\times \\ \begin{bmatrix}R + B^T\Gamma B & B^T\Gamma E \\ E^T\Gamma B & E^T\Gamma E - \gamma^2 P\end{bmatrix}^{-1}\begin{bmatrix}B^T\Gamma A \\ E^T\Gamma A\end{bmatrix}.\end{aligned} \tag{40}$$

Assuming that the Riccati equation (40) has a unique solution yields that $\Gamma^T = \Gamma$. ■

Note that the difference between (40) and the Riccati equation obtained in [11][18][19] is the existence of input (*R*) and disturbance (*P*) gains.

Equation (39) reveals that $\nabla V_k^{*T} = 2\Gamma x_k$ and $\nabla^2 V_k^* = 2\Gamma$. Thus, the GHJI equation (13) becomes

$$\begin{aligned}&2x_k{}^T\Gamma^T(Ax_k + Bu_k^* + Cw_k^* - x_k) + (Ax_k + Bu_k^* + Cw_k^* - x_k)^T \times \\ &\quad \Gamma(Ax_k + Bu_k^* + Cw_k^* - x_k) + Q(x_k) + u_k^{*T} R u_k^* - \gamma^2 w_k^{*T} P w_k^* = 0\end{aligned}$$

or equivalently

$$\begin{aligned}&(Ax_k + Bu_k^* + Cw_k^*)^T\Gamma(Ax_k + Bu_k^* + Cw_k^*) \\ &\quad + Q(x_k) + u_k^{*T} R u_k^* - \gamma^2 w_k^{*T} P w_k^* = 0\end{aligned} \tag{41}$$

by using *Lemma 3*. The optimal policies (20) and (21) are now rewritten as

$$w_k^* = \left(C^T \Gamma C - \gamma^2 P - C^T \Gamma B \left[B^T \Gamma B + R \right]^{-1} B^T \Gamma C \right)^{-1} \times \left(- C^T \Gamma A + C^T \Gamma B \left[B^T \Gamma B + R \right]^{-1} B^T \Gamma A \right) x_k \tag{42}$$

and

$$u_k^* = \left(B^T \Gamma B + R - B^T \Gamma C \left[C^T \Gamma C - \gamma^2 P \right]^{-1} C^T \Gamma B \right)^{-1} \times \left(- B^T \Gamma A + B^T \Gamma C \left[C^T \Gamma C - \gamma^2 P \right]^{-1} C^T \Gamma A \right) x_k . \tag{43}$$

Corollary 1. The GHJI equation (41) is equivalent to the HJI DARE (40).

Proof. This can be shown by following a similar approach to [18] where matrices *R* and *P* are not identity matrices. Define

$$K = \left(C^T \Gamma C - \gamma^2 P - C^T \Gamma B \left[B^T \Gamma B + R \right]^{-1} B^T \Gamma C \right)^{-1} \times \left(- C^T \Gamma A + C^T \Gamma B \left[B^T \Gamma B + R \right]^{-1} B^T \Gamma A \right)$$

and

$$L = \left(B^T \Gamma B + R - B^T \Gamma C \left[C^T \Gamma C - \gamma^2 P \right]^{-1} C^T \Gamma B \right)^{-1} \times \left(- B^T \Gamma A + B^T \Gamma C \left[C^T \Gamma C - \gamma^2 P \right]^{-1} C^T \Gamma A \right) x_k .$$

Thus, $w_k^* = K x_k$ and $u_k^* = L x_k$. Define

$$D_{11} = B^T \Gamma B + R - B^T \Gamma C \left[C^T \Gamma C - \gamma^2 P \right]^{-1} C^T \Gamma B ,$$

$$D_{22} = C^T \Gamma C - \gamma^2 P - C^T \Gamma B \left[B^T \Gamma B + R \right]^{-1} B^T \Gamma C ,$$

$A_{11} = B^T \Gamma B + R$, $A_{22} = C^T \Gamma C - \gamma^2 P$, $A_{12} = B^T \Gamma C$, and

$A_{21} = C^T \Gamma B$. Note that $D_{11} = A_{11} - A_{12} A_{22}^{-1} A_{21}$ and $D_{22} = A_{22} - A_{21} A_{11}^{-1} A_{12}$ are the *Schur complements* of A_{11} and A_{22}, respectively. Thus [13],

$$\begin{bmatrix} D_{11}^{-1} & -A_{11}^{-1}A_{12}D_{22}^{-1} \\ -A_{22}^{-1}A_{21}D_{11}^{-1} & D_{22}^{-1} \end{bmatrix} = \begin{bmatrix} A_{11} & A_{12} \\ A_{21} & A_{22} \end{bmatrix}^{-1} .$$

Also, note that $D_{11}{}^T = D_{11}$, $D_{22}{}^T = D_{22}$, $A_{12}{}^T = A_{12}$, $A_{22}{}^T = A_{22}$, and $A_{11}{}^T = A_{11}$.

Consequently, K and L can be calculated as

$$\begin{bmatrix} L \\ K \end{bmatrix} = -\begin{bmatrix} D_{11}^{-1} & -D_{11}^{-1}A_{12}A_{22}^{-1} \\ -D_{22}^{-1}A_{21}A_{11}^{-1} & D_{22}^{-1} \end{bmatrix}\begin{bmatrix} B^T\Gamma A \\ C^T\Gamma A \end{bmatrix} = -\begin{bmatrix} A_{11} & A_{12} \\ A_{21} & A_{22} \end{bmatrix}^{-1}\begin{bmatrix} B^T\Gamma A \\ C^T\Gamma A \end{bmatrix} \quad (44)$$

Now, by using (44), equation (41) may be rewritten as

$$x_k^T \begin{pmatrix} -\Gamma + Q + A^T\Gamma A + A^T\Gamma BL + A^T\Gamma CK + \\ L^T B^T\Gamma A + L^T B^T\Gamma BL + L^T B^T\Gamma CK + K^T C^T\Gamma A + \\ K^T C^T\Gamma BL + K^T C^T\Gamma CK + L^T RL - \gamma^2 K^T PK \end{pmatrix} x_k = 0$$

or equivalently as

$$\begin{aligned} \Gamma = {} & Q + A^T\Gamma A + A^T\Gamma BL + A^T\Gamma CK + L^T B^T\Gamma A + K^T C^T\Gamma A - \\ & [L^T \quad K^T]\begin{bmatrix} R + B^T\Gamma B & B^T\Gamma C \\ C^T\Gamma B & C^T\Gamma C - \gamma^2 P \end{bmatrix} \times \\ & \begin{bmatrix} R + B^T\Gamma B & B^T\Gamma C \\ C^T\Gamma B & C^T\Gamma C - \gamma^2 P \end{bmatrix}^{-1}\begin{bmatrix} B^T\Gamma A \\ C^T\Gamma A \end{bmatrix} \\ & = Q + A^T\Gamma A + A^T\Gamma BL + A^T\Gamma CK \\ & = Q + A^T\Gamma A + [A^T\Gamma B \quad A^T\Gamma C]\begin{bmatrix} L \\ K \end{bmatrix}. \end{aligned}$$

Thus, by using (44), one can obtain

$$\begin{aligned} \Gamma = {} & Q + A^T\Gamma A \\ & -\begin{bmatrix} A^T\Gamma B & A^T\Gamma C \end{bmatrix}\begin{bmatrix} R + B^T\Gamma B & B^T\Gamma C \\ C^T\Gamma B & C^T\Gamma C - \gamma^2 P \end{bmatrix}^{-1}\begin{bmatrix} B^T\Gamma A \\ C^T\Gamma A \end{bmatrix}. \end{aligned}$$

The solution for Γ can be obtained through solving (45) iteratively [18].

$$\Gamma_{i+1} = A^T\Gamma_i A + Q - \begin{bmatrix} A^T\Gamma_i B & A^T\Gamma_i C \end{bmatrix} \times \begin{bmatrix} R + B^T\Gamma_i B & B^T\Gamma_i C \\ C^T\Gamma_i B & C^T\Gamma_i C - \gamma^2 P \end{bmatrix}^{-1} \begin{bmatrix} B^T\Gamma_i A \\ C^T\Gamma_i A \end{bmatrix} \tag{45}$$

V. NN Approximation of the Value Function

So far, we have demonstrated how to recursively solve the GHJI equation by successively updating the disturbance $w^{(i,j)}$ and control $u^{(i)}$. In addition, it was demonstrated that the optimal solution of GHJI is found by iterating between the two loops. However, a general closed-form solution for GHJI is still hard to obtain even though the GHJI equation is a linear differential equation and in general easier to solve than the original HJI equation.

Moreover, the solution for GHJI requires the internal dynamics (i.e. $f_k(x)$) to be known. In this section by using an approximator such as a NN for the internal dynamics, $f_k(x)$, we show that the value function can be obtained with a small error.

A. Successive Approximation of the Value Function using NN

First, we show how to approximate the solution of GHJI equation for the discrete-time nonlinear system by using the approximation properties of NNs and by assuming that the disturbance term $w^{(i,j)}$ and the control input $u^{(i)}$ are in feedback form. It is known that NNs can approximate smooth functions on a compact set Ω [1]. Then, we can approximate $V^{(i,j)}$ with an NN as

$$V^{(i,j)} \approx V_L(x) = \sum_{l=1}^{L} \omega_l \sigma_l(x) = W_L^T \overline{\sigma}_L(x) \tag{46}$$

where the activation function vector $\sigma_l(x)$ is continuous and zero at the origin,

$W_L = [\omega_1 \ \cdots \ \omega_L]^T$ is the vector of NN weights , $\bar{\sigma}_L = [\sigma_1 \ \cdots \ \sigma_L]^T$ is the vector of activation functions and L is number of hidden layer neurons. The NN weights are tuned to minimize the residual error (which is defined next) in least square method over a set of points within the stability region of the initial admissible control. In the $GHJI\left(V^{(i,j)}, u^{(i)}, w^{(i,j)}\right) = 0$ equation, the value function $V_k^{(i,j)}$ is replaced by V_L to obtain the residual error as

$$GHJI\left(V_L^{(i,j)} = \sum_{l=1}^{L} \omega_l \sigma_l(x), u^{(i)}, w^{(i,j)}\right) = e_L(x). \tag{47}$$

Weighted residuals [15] are used to find the least square solution for (47). The weights are determined by using

$$\langle \partial e_L(x) / \partial W_L, e_L(x) \rangle = 0. \tag{48}$$

By expanding (48) we obtain

$$\begin{aligned} &\left\langle \nabla \bar{\sigma}_L \Delta x + \frac{1}{2} \Delta x^T \nabla^2 \bar{\sigma}_L \Delta x, \nabla \bar{\sigma}_L \Delta x + \frac{1}{2} \Delta x^T \nabla^2 \bar{\sigma}_L \Delta x \right\rangle . W_L + \\ &\left\langle Q(x) + u^{(i)T} R u^{(i)} - \gamma^2 w^{(i,j)T} P w^{(i,j)}, \nabla \bar{\sigma}_L \Delta x + \frac{1}{2} \Delta x^T \nabla^2 \bar{\sigma}_L \Delta x \right\rangle = 0 \end{aligned} \tag{49}$$

where the terms $\nabla \bar{\sigma}_L$ and $\nabla^2 \bar{\sigma}_L$ are gradient vector and Hessian matrix of $\bar{\sigma}_L(x)$ with respect to x, respectively, and $\Delta x = f(x) + g(x)u(x)^{(i)} + h(x)w(x)^{(i,j)} - x$. The following lemma is needed to proceed.

Lemma 4 [12]. If the set $\{\sigma_j(x)\}_1^L = \{\sigma_1(x), \ldots, \sigma_L(x)\}$ is linearly independent, then so is the set

$$\left\{ \nabla \sigma_j^T \Delta x + \frac{1}{2} \Delta x^T \nabla^2 \sigma_j \Delta x \right\}_1^L .$$

From (49) we have

$$W_L = -\left\langle \bar{\theta}, \bar{\theta} \right\rangle^{-1} \left\langle Q(x) + u^{(i)T} R u^{(i)} - \gamma^2 w^{(i,j)T} P w^{(i,j)}, \bar{\theta} \right\rangle \tag{50}$$

where $\bar{\theta} = \{\nabla \sigma_j^T \Delta x + \Delta x^T \nabla^2 \sigma_j \Delta x / 2\}_1^L$. As a result of *Lemma 4*, $\left\langle \bar{\theta}, \bar{\theta} \right\rangle$ is full rank and invertible. Therefore, a unique solution for the weights can be obtained. In addition, the inner products in (50) can be approximated as [15]

$$\langle a(x), b(x) \rangle = \int_\Omega a(x) b(x) dx \approx \sum_{i=1}^{N} a(x) b(x) \delta x$$

where $\delta x = x_i - x_{i-1}$ is chosen small in Ω and N is large. By employing a mesh in the set Ω where the mesh size is δx, the NN weights can be found as

$$W_L = -\left(X^T X\right)^{-1} XY \tag{51}$$

where X and Y are defined as

$$X = \left[\left(\nabla \bar{\sigma}_L \Delta x + \Delta x^T \nabla^2 \bar{\sigma}_L \Delta x / 2 \right)_{x=x_1} \quad \cdots \quad \left(\nabla \bar{\sigma}_L \Delta x + \Delta x^T \nabla^2 \bar{\sigma}_L \Delta x / 2 \right)_{x=x_p} \right]^T$$

$$Y = \begin{bmatrix} \left(Q(x) + u^{(i)T} R u^{(i)} - \gamma^2 w^{(i,j)T} P w^{(i,j)} \right)_{x=x_1} \\ \vdots \\ \left(Q(x) + u^{(i)T} R u^{(i)} - \gamma^2 w^{(i,j)T} P w^{(i,j)} \right)_{x=x_p} \end{bmatrix}$$

and p is the number of points in the mesh.

Examining the weight update (51), it is observed that knowledge of x_{k+1} and thus $f_k(x)$ is required for implementation of the iterative scheme; however, it is not always possible to obtain an explicit expression for the internal dynamics $f_k(x)$ *a priori*.

B. Identification of Unknown Nonlinear Internal Dynamics

Consider the unperturbed system

$$x_{k+1} = f_k + g_k u_k . \tag{52}$$

Using the universal approximation properties of NN's [1], the smooth function $f(x)$ can be represented using a NN as

$$f(x) = W_f \psi_f(x) + \bar{\varepsilon} \tag{53}$$

where W_f represents the bounded target weight matrix, $\psi_f(x)$ is a linearly independent set of basis functions satisfying $\psi_{fMin} \le \|\psi_f(x)\| \le \psi_{fM}$ for all $x \neq 0$. It is observed that this condition is easily met with proper selection of the basis function. Additionally, $\bar{\varepsilon} = [\bar{\varepsilon}_1, \ldots, \bar{\varepsilon}_n]^T$, and $\|\bar{\varepsilon}\| \le \bar{\varepsilon}_M$ with $\bar{\varepsilon}_M$ being a positive constant.

The NN identification scheme is now defined as

$$\hat{x}_{k+1} = \hat{f}_k + g_k u_k + K\tilde{x}_k \tag{54}$$

where $\tilde{x}_k = x_k - \hat{x}_k$, K is a design constant, $\hat{f}(x) = \hat{W}_f \psi_f(x)$, and $\hat{W}_f$ is the NN approximation of W_f. Subtracting (54) from (52) reveals the identification error dynamics to be

$$\tilde{x}_{k+1} = \tilde{f}_k + \bar{\varepsilon} - K\tilde{x}_k \tag{55}$$

where $\tilde{f}_k = \tilde{W}_f^T \psi_f$ with $\tilde{W}_f = W_f - \hat{W}_f$. Let the NN tuning law be given by

$$\hat{W}_f(k+1) = \hat{W}_f(k) + \alpha \psi_f (\tilde{x}_{k+1} + K\tilde{x}_k)^T. \tag{56}$$

Then, the NN weight estimation error dynamics $\tilde{W}_f(k+1) = W_f - \hat{W}_f(k+1)$ are given by

$$\begin{aligned} \tilde{W}_f(k+1) &= \tilde{W}_f(k) - \alpha\left(\psi_f {\psi_f}^T \tilde{W}_f(k) + \psi_f \bar{\varepsilon}^T\right) \\ &= \tilde{W}_f(k) - \alpha \Delta \tilde{W} \end{aligned} \tag{57}$$

where $\Delta\tilde{W} = \psi_f \psi_f{}^T \tilde{W}_f(k) + \psi_f \bar{\varepsilon}^T$. The key feature of the update law (56) is that when $\tilde{x}_k$ in very small, that is $x_k \approx \hat{x}_k$, we can conclude that identifier (54) has learned the internal dynamics $f(x)$, that is $\hat{f}(x) \approx f(x)$. Before proceeding, the following definition is required.

Definition 6 [1]*:* An equilibrium point x_e is said to be *uniformly ultimately bounded (UUB)* if there exists a compact set $S \subset \Re^{n*}$ so that for all initial states $x_0 \in S$ there exists a bound B and a time $T(B, x_o)$ such that $\|x(k) - x_e\| \le B$ for all $k \ge k_0 + T$.

Theorem 5. Let the proposed identification scheme in (54) be used to identify (52), and let the NN update law be given by (56). Then, the state estimation errors $\tilde{x}(k)$ and NN function approximation errors $\tilde{W}_f^T \psi_f$ are *UUB***.**

Proof. Define the Lyapunov function

$$L = \frac{\alpha}{3} \tilde{x}_k{}^T \tilde{x}_k + \frac{1}{\alpha} tr\left\{\tilde{W}_f{}^T \tilde{W}_f\right\}$$

Calculating the first difference and using (55) and (57), we have

$$\begin{aligned}
\Delta L &= \frac{\alpha}{3} \tilde{x}_{k+1}{}^T \tilde{x}_{k+1} + \frac{1}{\alpha} tr\left\{\tilde{W}_f(k+1)^T \tilde{W}_f(k+1)\right\} \\
&\quad - \frac{\alpha}{3} \tilde{x}_k{}^T \tilde{x}_k - \frac{1}{\alpha} tr\left\{\tilde{W}_f{}^T \tilde{W}_f\right\} \\
&\le \alpha \left\|\tilde{f}_k\right\|^2 + \alpha \|\bar{\varepsilon}\|^2 + \alpha K^2 \|\tilde{x}_k\|^2 - \frac{\alpha}{3} \|\tilde{x}_k\|^2 \\
&\quad + \frac{1}{\alpha} tr\left\{\left(\tilde{W}_f(k) - \alpha \Delta\tilde{W}\right)^T \left(\tilde{W}_f(k) - \alpha \Delta\tilde{W}\right)\right\} - \frac{1}{\alpha} tr\left\{\tilde{W}_f{}^T \tilde{W}_f\right\} \quad .
\end{aligned}$$

After some math we obtain

$$\begin{aligned}
\Delta L &\le -\frac{\alpha}{3}(1 - 3K^2)\|\tilde{x}_k\|^2 + \alpha \left\|\tilde{W}_f \psi_f\right\|_F^2 + \alpha \bar{\varepsilon}_M{}^2 \\
&\quad + \left(2\alpha \psi_{fM}{}^2 \left\|\tilde{W}_f \psi_f\right\|_F^2 + 2\alpha \psi_{fM}{}^2 \bar{\varepsilon}_M{}^2\right) - 2\left\|\tilde{W}_f{}^T \psi_f\right\|_F^2 + 2\left\|\tilde{W}_f{}^T \psi_f\right\|_F \bar{\varepsilon}_M
\end{aligned}$$

After more manipulations we get

$$\Delta L \le -\frac{\alpha}{3}(1-3K^2)\|\tilde{x}_k\|^2 - \left(1-\alpha(2\psi_{fM}{}^2-1)\right)\left\|\tilde{W}_f{}^T\psi_f\right\|_F^2 + \bar{\varepsilon}_M{}^2\alpha(1+2\psi_{fM}{}^2)\,.$$

It can be concluded $\Delta L \le 0$ if the design parameters are selected according to $K \le 1/\sqrt{3}$, $\alpha \le 1/(2\psi_{fM}{}^2-1)$, and the following inequalities hold.

$$\left.\begin{aligned} \|\tilde{x}_k\| &\ge \sqrt{\frac{\bar{\varepsilon}_M{}^2\left(1+\alpha(1+2\psi_{fM}{}^2)\right)}{\frac{\alpha}{3}(1-3K^2)}} = b_x \quad \text{or} \\ \left\|\tilde{W}_f{}^T\psi_f\right\|_F &\ge \sqrt{\frac{\bar{\varepsilon}_M{}^2\left(1+\alpha(1+2\psi_{fM}{}^2)\right)}{\left(1-\alpha(2\psi_{fM}{}^2-1)\right)}} = b_W \end{aligned}\right\}. \tag{58}$$

As a result, the state identification error as well as the function approximation error converges to the bounds b_x and b_W uniformly. Note that b_x and b_W can be made small by choosing proper design gains and decreasing $\bar{\varepsilon}_M^2$ by means of increasing the number of hidden layer neurons [10]. ■

Corollary2. Using the proposed NN identification scheme,

$$\hat{f}_k(x) = f_k(x) - \varepsilon_f \tag{59}$$

where $\varepsilon_f = \tilde{W}_f^T\psi_f + \bar{\varepsilon}$; thus, $\|\varepsilon_f\| \le b_W + \bar{\varepsilon}_M \equiv \varepsilon_{fM}$.

Proof of *Corollary 2* is easily shown by observing (53), $\hat{f}(x) = \hat{W}_f\psi_f(x)$, and applying the bound of (58).

Next, we investigate the effect of using $\hat{f}_k(x)$ in the NN least squares training method of *Section IV-A.*

Theorem 6. Let the internal dynamics $f_k(x)$ be provided using the NN identifier (54) so that the relationship (58) holds. If the NN least squares algorithm is utilized for tuning the NN weights in order to get $\hat{f}_k(x)$ so that the value function $\hat{V}_k^*(x)$ can be constructed,

then, $\left|\hat{V}_k^*(x) - V_k^*(x)\right| \le T(|\varepsilon_f|) \le \varepsilon_M$ where *T(.)* is a function of ε_f with ε_M being a positive constant.

Proof. Similar to (46) which renders $V_k^*(x)$ when NN successive approximation algorithm converges, we approximate the function $\hat{V}_k^*(x)$ with an NN as

$$\hat{V}_k^*(x) \approx \sum_{l=1}^{L} \hat{\omega}_l \sigma_l(x) = \hat{W}_L^T \bar{\sigma}_L(x) \ . \tag{60}$$

From (50) it is easy to verify that $\hat{W}_L$ is a function of $x, \hat{f}$ where W_L is the same function of x, f as

$$\begin{aligned} \hat{W}_L &= T_1(x, \hat{f}) \\ W_L &= T_1(x, f) \end{aligned} \tag{61}$$

where $T_1(x, f) = -\left\langle \bar{\theta}(x, f), \bar{\theta}(x, f) \right\rangle^{-1} \times \left\langle Q(x) + u(x)^{(i)^T} Ru(x)^{(i)} - \gamma^2 w(x)^{(i,j)^T} Pw(x)^{(i,j)}, \bar{\theta}(x, f) \right\rangle$.

Thus, by using (46) and (61) we can rewrite $\hat{V}_k^*(x)$ and $V_k^*(x)$ as $\hat{V}_k^*(x) \approx \hat{W}_L \bar{\sigma}_L(x) = T_2(x, \hat{f})$ and $V_k^*(x) \approx W_L \bar{\sigma}_L(x) = T_2(x, f)$ where $T_2(x, f) = \bar{\sigma}_L(x) T_1(x, f)$. Consequently, by using Taylor series around the point (x, f) and $\hat{f}(x) = f(x) - \varepsilon_f$ we obtain

$$V_k^*(x) - \hat{V}_k^*(x) = T_2(x, f) - T_2(x, \hat{f}) \approx$$
$$-\left[\sum_{k_{f1}, \ldots, k_{fn}} \frac{1}{k_{f1} \ldots k_{fn}} \frac{\partial^s T_2(x, \hat{f})}{(\partial^{k_{f1}} \hat{f}_1) \ldots (\partial^{k_{fn}} \hat{f}_n)} \varepsilon_1^{k_{f1}} \ldots \varepsilon_n^{k_{fn}} \right]_{\hat{f} = f}$$

where *s* is the number of required Taylor series terms such that the Taylor series error is negligible, $\hat{f}_k - f_k = -\varepsilon_f$ from (59), $-\varepsilon_f = [\varepsilon_1, \ldots, \varepsilon_n]^T$, $\hat{f} = \left[\hat{f}_1, \ldots, \hat{f}_n\right]^T$, and k_{fi} is an integer such that $\sum_{i=1}^{n} k_{fi} = s$. Since $V_k^*(x)$ and $\hat{V}_k^*(x)$ are bounded and continuous, there exists a

positive constant δ_M such that $\left|\partial^s T_2 /((\partial^{k_{f1}} f_1)\ldots(\partial^{k_{fn}} f_n))\right| \le \delta_M$. Consequently,

$$\left|V_k^*(x) - \hat{V}_k^*(x)\right| \le \left[\sum_{k_{f1},\ldots,k_{fn}}^{s} \frac{1}{k_{f1}\ldots k_{fn}} \delta_M \varepsilon_{fM}{}^s\right].$$

Note that if $\varepsilon_{fM} < 1$, then $V_k^*(x) - \hat{V}_k^*(x)$ can be made very small. ■

VI. Simulation Case Studies

In order to verify the theoretical work introduced in this paper, a complex power system and a general nonlinear system are considered. First, a power system case study is introduced next.

The power system is chosen as a nonlinear dynamical system where the power balance equations are utilized to obtain its nonlinear dynamics. A power system is usually modeled using a combination of differential and algebraic equations. The differential equations represent generator states (i.e. angles, speeds,) whereas the algebraic equations represent bus active and reactive power balance relationships. For control design it is desirable to have pure dynamical equations. In [16], authors have proposed an algebraic-free power system representation based on the generator classical model for the power system shown in Fig.2.

This representation is appropriate to model a nonlinear power network with FACTS device as a controller. The advantage of this approach is that no algebraic equations are involved in the control design but the nonlinear behavior is retained. In the proposed approach, the power system classical model is utilized where the generators' internal voltages are held constant to develop the control approach. Then, the proposed nonlinear optimized control scheme is utilized to optimally stabilize and damp the

oscillations resulting from a disturbance by using UPFC as a controller. Finally, the results are compared with that of a conventional nonlinear backstepping controller.

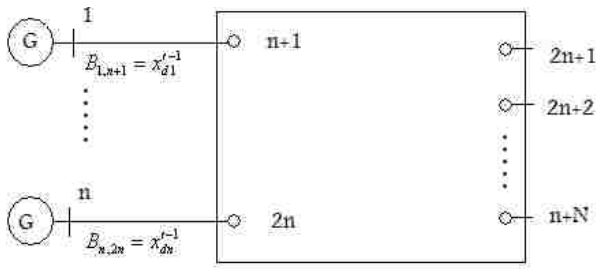

Fig.2 Power System

A. Power System Continuous-time Dynamical Model

The classical generator representation is often sufficient for the control development for mitigating inter-area oscillations since only the rotor speed deviations are of interest. In addition, the resistances of network lines are neglected. Despite this assumption made for ease of control development, the proposed control will be validated on a power system with resistances presence.

It is more convenient to represent the generator dynamical equations in the Center of Inertia (COI) coordinates as

$$\dot{\delta}_i = \omega_i$$

$$M_i\dot{\omega}_i = P_{mi} - \frac{M_i}{M_T}P_{COI} - B_{i,i+n}E_{gi}V_{i+n}\sin(\delta_i - \psi_{i+n}),\ i = 1,\ldots,n$$

where

$\delta_i = \bar{\delta}_i - \delta_0$, $\omega_i = \bar{\omega}_i - \omega_0$, $\psi_i = \bar{\psi}_i - \delta_0$, $M_T = \sum_{i=1}^{n} M_i$, $\delta_0 = 1/M_T \sum_{i=1}^{n} M_i \bar{\delta}_i$, $\omega_0 = 1/M_T \sum_{i=1}^{n} M_i \bar{\omega}_i$,

$P_{COI} = \sum_{i=1}^{n} P_{mi} - \sum_{i=n+1}^{n+N} P_{Li}$ and P_{Li} is the active load at each bus. Also, $\bar{\delta}_i$ is the rotor angle of the *i*-th machine, $\bar{\omega}_i$ is the angular speed, ω_0 is the synchronous angular speed, *B* represents the reactance of the admittance matrix, E_{gi} is the *i*-th machine internal voltage, *n* is the number of generators, $M_i = 2H/\omega_0$ is the *i*-th machine inertia, and V_{i+n} and $\bar{\psi}_{i+n}$ are the generator bus voltage and phase angle, respectively. In addition, *N* is the number of non-generator buses in the power system.

The bus voltages and phase angles of all of the power system buses are constrained by the following set of algebraic power balance equations (neglecting resistances)

$$P_{Li} + \sum_{j=1}^{N+n} B_{ij} V_i V_j \sin(\psi_i - \psi_j) = S_{\mathrm{P}i} = 0$$

$$-Q_{Li} + \sum_{j=1}^{N+n} B_{ij} V_i V_j \cos(\psi_i - \psi_j) = S_{\mathrm{Q}i} = 0;\ i = n+1, \ldots, n+N$$

where P_{Li} and Q_{Li} are the active and reactive loads on the i th bus, and $V_j = E_{gj}$; $\psi_j = \delta_j$ for $1 \le j \le n$. By using the UPFC power injection model [17] and the approach introduced in [16], the generator dynamical model can be represented as

$$\begin{cases} \dot{x}_{1i} = x_{2i} \\ M_i \dot{x}_{2i} = f_{1i} + g_{1i} x_{3i} \\ \dot{x}_{3i} = f_{2i}(x) + g_{2i}(x) u;\ \ i = 1, \ldots, n \end{cases}$$

where *n* is the number of generators. Also, UPFC dynamics is given by $\dot{\gamma} = u$ where $\gamma = V_b \cos\theta$ and $\bar{V}_b = V_b \angle(\psi_{t+n} + \theta)$ according to Fig. 3[16].

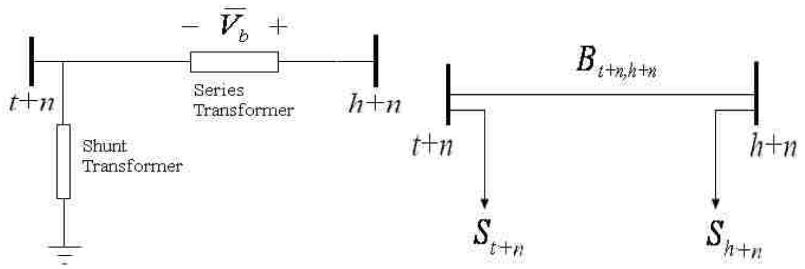

(a) (b)

Fig. 3 a) UPFC connected between two network nodes b) Injected powers to the connected buses

Then, by employing backstepping design, we obtain

$$\begin{cases} \dot{x}_{1i} = -\bar{K}_{\delta i} x_{1i} + z_{2i} \\ M_i \dot{z}_{2i} = f_{1i} + M_i \bar{K}_{\delta i} x_{2i} + g_{1i} x_{3di} + g_{1i} z_{3i} \\ \dot{z}_{3i} = f_{2i}(x) + g_{2i}(x) u - \dot{x}_{3di} \end{cases}$$

where $z_{2i} = x_{2i} - x_{2id}$, $x_{2id} = -K_{\delta i} x_{1i}$, $z_{3i} = (x_{3i} - x_{3di})$,

$$x_{3di} = \frac{1}{g_{1i}} \times [-x_{1i} - f_{1i} - M_i \bar{K}_{\delta i} x_{2i} - \bar{K}_{Z1i} z_{2i}]$$

$$\dot{x}_{3di} = \frac{1}{g_{1i}} \times [-x_{2i} - K_{Z1i} K_{\delta i} x_{2i} - \frac{K_{\delta i} M_i + K_{Z1i}}{M_i} (f_{1i} + g_{1i} x_{3i})] \ ,$$

with $\bar{K}_{\delta i}$ and $\bar{K}_{Z1i}$ are positive design constants. Next, we obtain power system discrete-time dynamics.

B. Power System Discrete-time Dynamical Model

By assuming a small time step T, the generator dynamics are approximated by

$$x_{1i}(k+1) = (1 - T\bar{K}_{\delta i}) x_{1i}(k) + T z_{2i}(k) = K_{i1} x_{1i}(k) + T z_{2i}(k)$$

where $z_{2i} = x_{2i} - x_{2id}$, K_{i1} is design constant, and

$x_{2id} = ((K_{i1} - 1)/T)x_{1i} = -\overline{K}_{\delta i} x_{1i}$. Next, observe

$$M_i z_{2i}(k+1) = Mz_{2i}(k) + Tf_{1i}(k) + TM_i K_{\delta i} x_{2i}(k) + Tg_{1i} x_{3di}(k) + Tg_{1i} z_{3i}(k)$$

where $z_{3i} = x_{3i} - x_{3di}$,

$$x_{3di} = \frac{1}{Tg_{1i}} \times [-Tx_{1i} - Tf_{1i} - TM_i \overline{K}_{\delta i} x_{2i} + (K_{2i} - M_i) z_{2i}]$$
$$= \frac{1}{g_{1i}} \times [-x_{1i} - f_{1i} - M_i \overline{K}_{\delta i} x_{2i} - \overline{K}_{Z1i} z_{2i}],$$

and K_{i1} is a design constant. Finally,

$$z_{3i}(k+1) = z_{3i}(k) + Tf_{2i}(x,k) + Tg_{2i}(x,k)u + \frac{T}{g_{1i}}[x_{2i} + K_{Z1i} K_{\delta i} x_{2i} + \frac{K_{\delta i} M_i + K_{Z1i}}{M_i}(f_{1i} + g_{1i} x_{3i})]$$

where $x = [x_{11} \quad z_{21} \quad x_{21} \quad z_{22} \quad \gamma]^T$ and the control input u_1 can be obtained as

$$u_i(k) = \frac{1}{g_{2i}(x,k)} \left(\frac{(K_3 - 1)}{T} z_{3i}(k) - f_{2i}(x,k) - \frac{1}{g_{1i}} \left[x_{2i} + K_{Z1i} K_{\delta i} x_{2i} + \frac{K_{\delta i} M_i + K_{Z1i}}{M_i}(f_{1i} + g_{1i} x_{3i}) \right] \right).$$

For the case of multiple generator/multiple UPFC control, the dynamics $z_{3i}(k+1)$ are replaced by

$$z_3(k+1) = z_{3i}(k) + Tf_3(k) + Tg_2(k)\overline{H}u_1 \tag{62}$$

where, $f_3(x) = f_2(x) - \dot{x}_{3d}$, $f_2 = [f_{21} \quad \dots \quad f_{2,n-1}]^T$, $g_2 = diag(g_{21} \quad \dots \quad g_{2,n-1})$, $x_{3d} = [x_{3d1} \quad \dots \quad x_{3d,n-1}]^T$ and $\overline{H}_{(n-1)\times 1} = [1 \quad \dots \quad 1]^T$. Additionally, we define $x_1 = [x_{11} \quad \dots \quad x_{1,n-1}]^T$, $z_3 = [z_{31} \quad \dots \quad z_{3,n-1}]^T$, $z_3 = [z_{31} \quad \dots \quad z_{3,n-1}]^T$. Moreover, note that only $n-1$ generators are chosen to be controlled. Since the n generators exist in the interconnected power network, the *n*th generator is forced to be controlled if the remaining $n-1$ speeds are controlled. Since there are fewer inputs than outputs (for $n > 2$), it is generally difficult to

find an input that makes a total Lyapunov function derivative negative definite. However, equation (62) can be stabilized by defining the control input u_1 as

$$u_i(k) = \frac{1}{\sum_{i=1}^{n-1} g_{2i}} \sum_{i=1}^{n-1} \left(\begin{array}{l} \frac{(K_3 - 1)}{T} z_{3i}(k) - f_{2i}(k) \\ -\frac{1}{g_{1i}} \times [x_{2i} + K_{Z1i} K_{\delta i} x_{2i} + \frac{K_{\delta i} M_i + K_{Z1i}}{M_i} (f_{1i} + g_{1i} x_{3i})] \end{array} \right) \tag{63}$$

In fact the control input u_i is stabilizing the dynamics defined by

$$\bar{z}_3(k+1) = \overline{H} z_3(k+1) = \overline{H}^T z_{3i}(k) + \overline{H}^T T f_3(k) + \overline{H}^T T g_2(k) \overline{H} u_1 \tag{64}$$

The stability of the individual generators can be concluded by considering the power system transient response where the generator dynamics are linear combination of the linearized model modes. For typical power systems, if the summation of the modes is equivalent to zero, stability of the individual generators can be concluded. Exceptions include topologies with unobservable modes and isolated coupled generators. With $\overline{H}^T z_3(k+1)$ converging to zero the stability of the individual generators are guaranteed by using (118) through (121) resulting in

$$\begin{bmatrix} x_{1i}(k+1) \\ z_{2i}(k+1) \end{bmatrix} = \begin{bmatrix} K_{1i} & T \\ -T & K_{2i} \end{bmatrix} \begin{bmatrix} x_{1i}(k) \\ z_{1i}(k) \end{bmatrix} + \begin{bmatrix} 0 \\ T g_{1i} \end{bmatrix} z_{3i}; 1 \le i \le n-1 \ . \tag{65}$$

By proper selection of the design constants K_{1i} and K_{2i} stability of x_{1i} and z_{2i} can be obtained. Next the above mathematical representation and the controller design is evaluated on a tractable two-generator power system.

Example 1. First, for optimal control validation, the two-generator power system shown is Fig. 4 is used and subjected to a three phase fault.

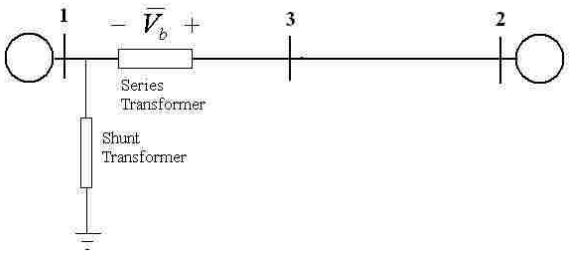

Fig. 4 Two-generator power system

The generator data is given in Table 1. The generators have speed governors with the UPFC control implemented via the power injection model. The power system loads are considered as constants. The control objective is to optimally damp the generators oscillations after the fault is cleared. Although the dynamical power system model and controller are derived based on lossless power system, the simulations are performed using the complete power system model (with line resistances) to evaluate the effectiveness of the model and the control design.

Table 1. Generators Specifications

Gen no.	1	2
x'_d	0.0023	0.0023
$H = \omega_s M/2$	5	1

In the system given by Fig. 2, the UPFC is installed on bus 1 between 1 and 3 which is found to be an appropriate placement by trial and error. A three phase short

circuit fault is applied to bus 3 at $t = 0.2s$ and removed at $t = 0.4s$ seconds. Generator 1 is chosen for control. In order to find the optimal controller, the value function is approximated by a neural network as described by (46) where a 6th-order even polynomial is chosen for the basis function with the state vector defined by $x_p = [x_{11} \quad z_{21} \quad \gamma \quad z_{31} + z_{32} \quad x_{12} \quad z_{22}]^T$. For training, a history of the power system subjected to different faults is employed instead of using a mesh formed by variation of all the states used in the literature [10].

The simulation results are depicted in Figs. 5 and 6 for oscillation damping after a fault is cleared by using an UPFC embedded with the proposed optimal controller and with standard nonlinear backstepping controller (63) where there are no other disturbances in the power system.

Subsequently, a disturbance is injected in the power system using an exponentially decaying function for the bus load where the load on bus 3 decays 0.05pu with a slow exponential rate of $\tau = 0.5s$. The results are shown in Figs. 7 and 8 where the optimal control is able to handle the load disturbance injected to the power system.

Next, a general nonlinear discrete-time system is considered and the proposed optimal controller is evaluated.

Example 2. A nonlinear system described by (66) is considered

$$\begin{bmatrix} x_1(k+1) \\ x_2(k+1) \end{bmatrix} = \begin{bmatrix} -0.8x_2(k) \\ \sin(0.8x_1(\mathrm{k}) - x_2(\mathrm{k})) + 1.8x_2(\mathrm{k}) \end{bmatrix} + \begin{bmatrix} 0 \\ -1 - x_2(\mathrm{k}) \end{bmatrix} u + \begin{bmatrix} 0 \\ 1 \end{bmatrix} w, \tag{66}$$

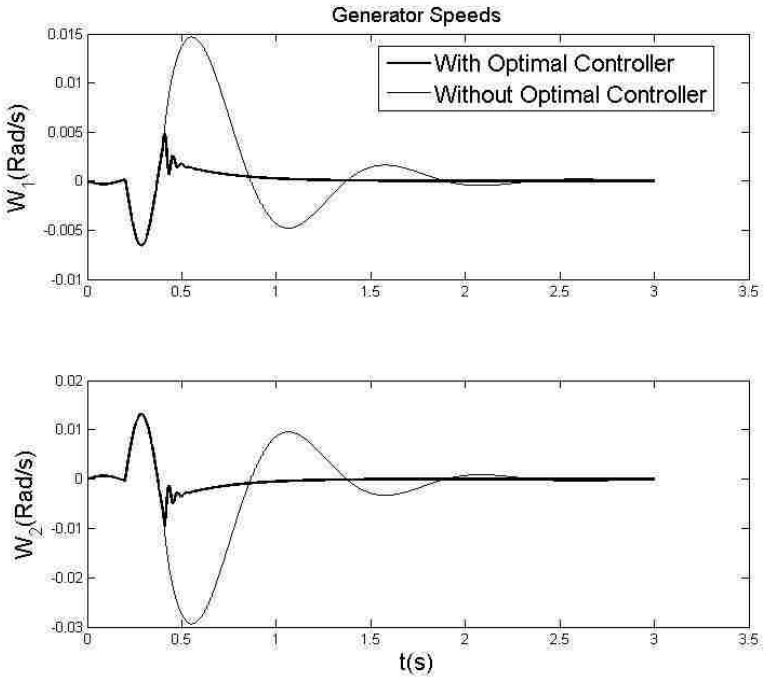

Fig. 5 Generator speeds

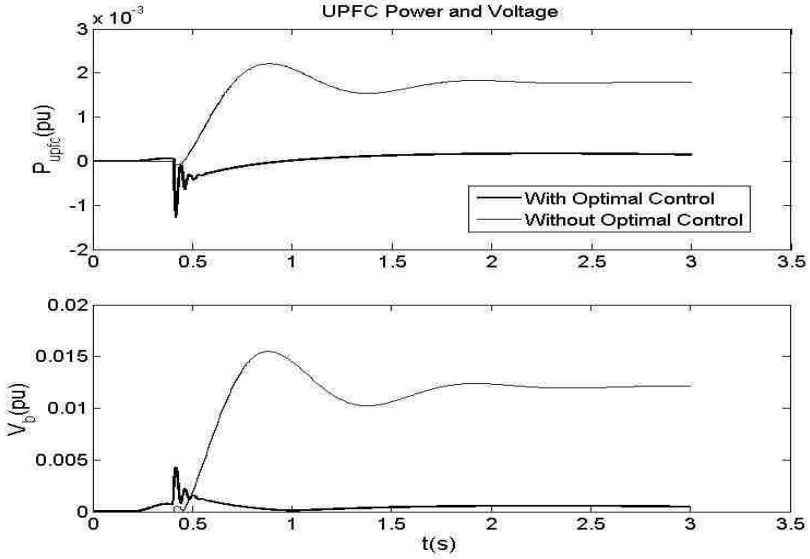

Fig. 6 UPFC injected power and series voltage

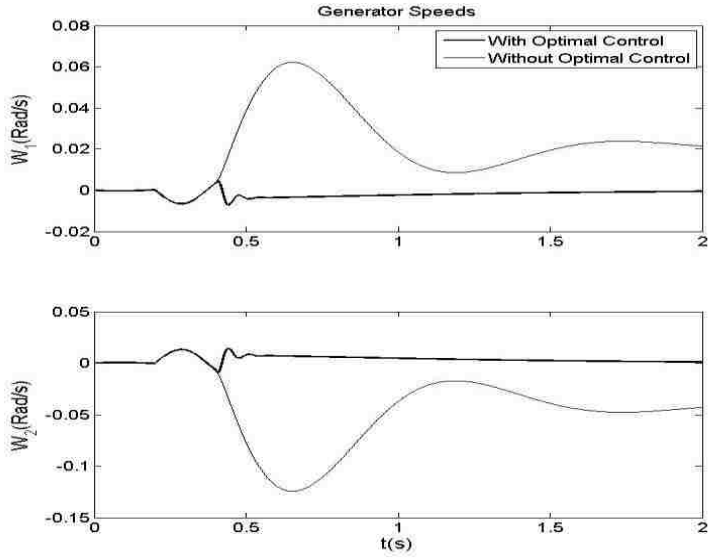

Fig. 7 Generator speeds with load disturbance

with the initial stabilizing controller is defined by $u=[1\ \ 1.5][x_1(k)\ x_2(k)]^T$. The initial conditions of (66) are taken as $x_1(0)=0.1$ and $x_2(0)=0.1$. Moreover $Q(x)=x^TQx$, *Q=1,R=P=1* , and $\gamma=20$ are used. In order to implement the NN approximator, the mesh size in the (x_1,x_2) plane is chosen to be 0.05. The region $(-0.5\le x_1\le 0.5,-0.5\le x_2\le 0.5)$ is used to train the neural network (NN). The activation functions of the NN are even polynomial functions up to tenth order in the form of $\left[x_1^2,x_1x_2,x_2^2,x_1^4,x_1x_2^3\ldots,x_2^4,\ldots,,x_1^{10}\ldots,x_2^{10}\right]$, and the control input and disturbance are updated according to the proposed procedure in Fig. 1 of *Section III-A*. The final NN weights are W_L = [2.2457 2.1128 3.3185 28.4098 38.9558 35.1154 -6.2207 -74.4427 -165.6169 -202.5626 -160.5370 9.6288 6.8831 -60.4303 -4.5262 143.2018 -5.1839 -132.6341

4.1517 -39.2125 10.0417 117.5590 309.7810 521.1991 515.7240 372.5395 35.3219 24.9638 11.1778 -79.0883 -263.6746 -430.7612 -607.4182 -532.2564 -332.3868 $]^T$.

Upon completion of the offline training, the performance of the final optimal control policy is compared to the initial stabilizing control. In the comparison, a disturbance $w = 0.05e^{-0.1k}$ is introduced into the system at *k=0*. To evaluate the overall performance of the system, the performance metric defined in [7] is utilized as

$$Attenuation(k) = \left(\sum_{j=0}^{k} \left(Q(x_j) + u_j^T R u_j \right) \right) \Big/ \left(\sum_{j=0}^{k} \gamma^2 w_j^T P w_j \right). \tag{67}$$

Fig. 9 shows the control effort of the optimal control law as well as the initial control law while Fig. 10 depicts the control attenuation associated with each policy evaluated using the metric (67). By examining Fig. 9, it is observed that the time history of the states for the initial control policy oscillates as it converges to the origin whereas with the improved control law, the states converge to the origin smoothly with no overshoots or undershoots. Additionally, examining the control signals shown in Fig. 9, the final optimal control policy exhibits significant improvements over the initial policy in terms of magnitude and smoothness. Examining Fig. 10, a significant decrease in the control effort (67) is observed when the improved optimal control law is applied to the system. Thus, the improved control policy behaves as expected.

Example 3. To demonstrate the effectiveness of the proposed nonlinear optimal method while relaxing the internal dynamics, $f(x)$, the nonlinear system in Example 2 is revisited when the $f(x)$ is unknown.

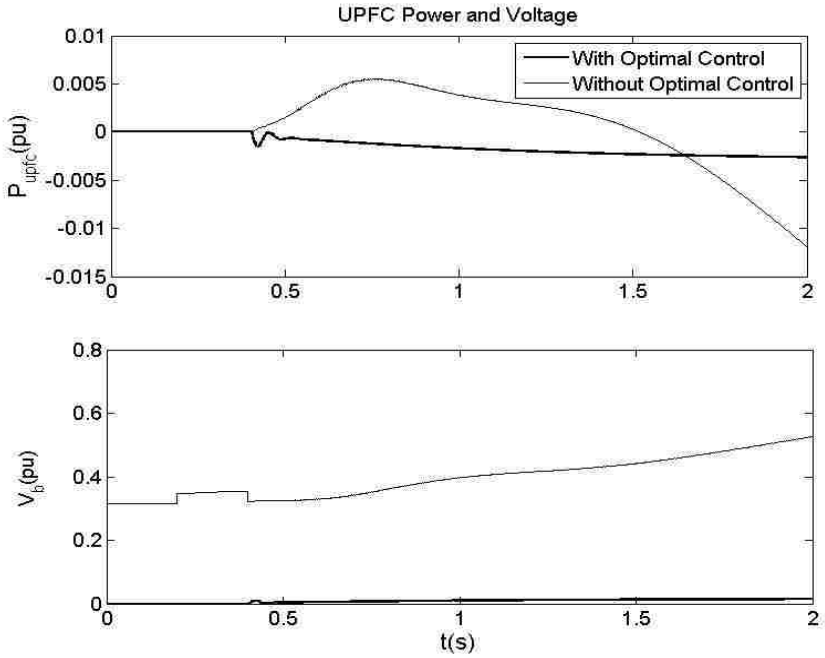

Fig. 8 UPFC injected power and series voltage with load disturbance

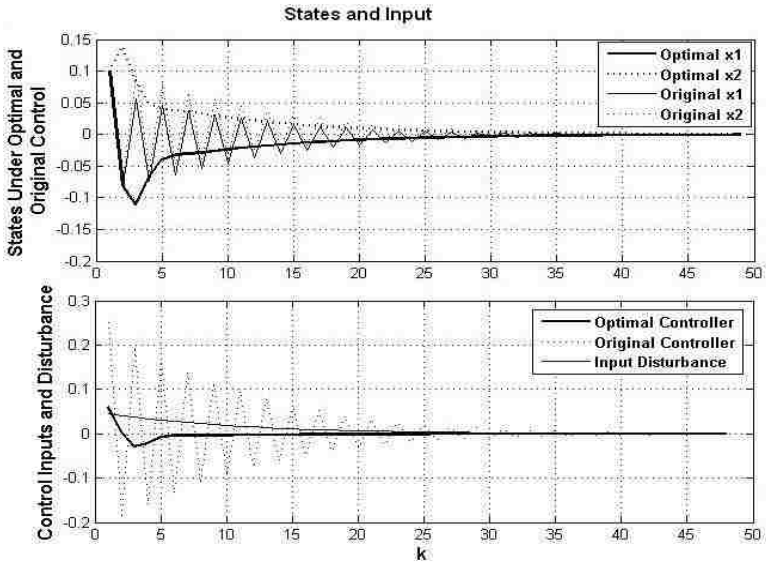

Fig. 9 Nonlinear system states and control inputs with the optimal control

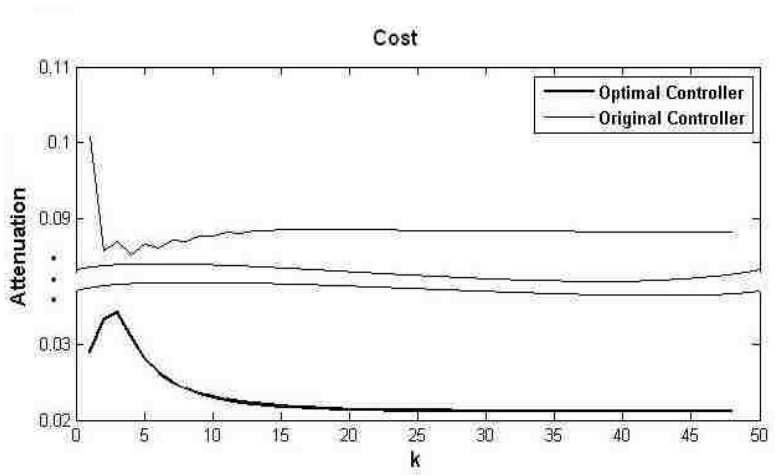

Fig. 10 Nonlinear system control cost

The internal dynamics is now approximated by $\hat{f}(x) = \hat{W}_f^T \psi_f(x)$ where the identification scheme (54) and NN weight update law (56) are applied. Te NN is comprised of 10 hidden layer neurons where the sigmoid activation function [20] is utilized. Additionally, the hidden layer weights V_f are chosen at random and kept constant during the simulation whereas the tunable weights $\hat{W}_f$ are set initially to -10. For identifier, the initial, actual, and estimated states are $x_1(0) = x_2(0) = \hat{x}_1(0) = \hat{x}_2(0) = 0.1$, respectively. The control input is designed through backstepping to let the system state $x_1(k)$ to track a desired trajectory $r(k) = \sin(k)$ which is obtained as

$$u(k) = \frac{1}{-1-x_2}\left[\begin{array}{l} -(\sin(0.8x_1 - x_2) + 1.8x_2) + \\ \frac{1}{-0.8}(r(k+2) + K_1 e_1(k+1)) + K_2 z_2 \end{array}\right]$$

where $e_1(k) = x_1(k) - r(k)$, $z_2(k) = x_2(k) - x_{2d}(k)$, and $x_{2d} = -(r(k+1) + K_1 e_1(k))/0.8$.

In addition, the design gain constants are $K_1 = 0.1, K_2 = 0.01$, and the identifier design gain constant in (54) is selected as $K = 0.01$. Then, the proposed nonlinear optimal

controller design is considered with the system with the approximated $\hat{f}(x) = \hat{W}_f^T \psi_f(x)$. The original stabilizing controller $u = [1 \quad 1.5][x_1(k) \; x_2(k)]^T$ is considered. Also, $Q(x) = x^T Q x$, *Q=1*, *R=P=1* , and $\gamma = 20;$ are used. In order to implement the NN approximator, the mesh size in the (x_1, x_2)plane is chosen to be 0.03. The region $(-0.5 \le x_1 \le 0.5, -0.5 \le x_2 \le 0.5)$ is used to train the neural network (NN). Similar to Example 2, the NN is defined with the activation functions containing even polynomial functions up to tenth order in the form of $\left[x_1^2, x_1 x_2, x_2^2, x_1^4, x_1 x_2^3 \ldots, x_2^4, \ldots, x_1^{10} \ldots, x_2^{10}\right]$, and the control input and disturbance are updated according to the proposed procedure in Fig. 1 of *Section III-A*. Upon completion of the offline training, the performance of the final optimal control policy is compared to the initial stabilizing control. Similar to Example 2, a disturbance $w = 0.05e^{-0.1k}$ is introduced to the system at *k=0*.

Fig. 11 illustrates the online identification results where the actual and identified states as well as the approximated internal dynamics $\hat{f}(x)$ and $f(x)$ are shown. Then, Fig. 12 shows the control efforts of the optimal control law as well as the initial control law while Fig. 13 shows the control attenuation associated with each policy evaluated using the metric (67). By examining Fig. 12, it is observed that the state time history and the control input for the optimal control policy with unknown $f(x)$ converges to the optimal control policy and the control input with known $f(x)$. By examining Fig. 13, the control effort (67) is also in the same range as in Example 2 when the internal dynamics $f(x)$ is known. Next, another example is employed to verify the verify that the proposed GHJI results in DARE optimal policies.

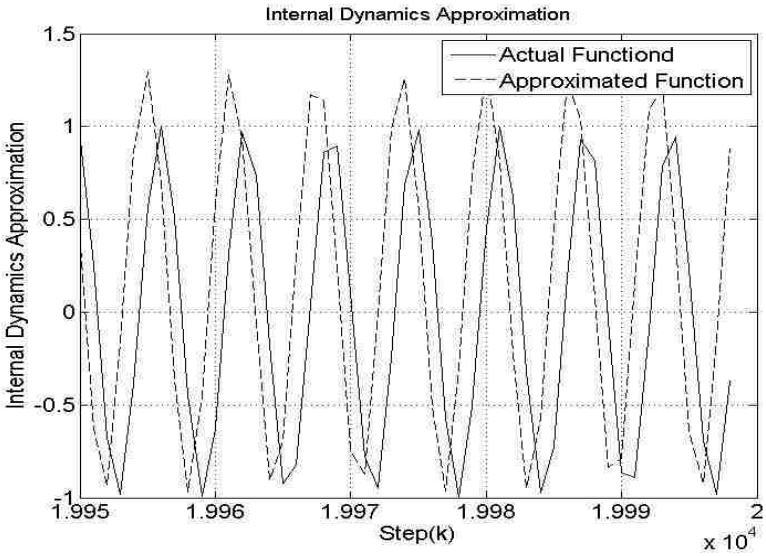

Fig. 11 Internal dynamics $f(x)$ approximation

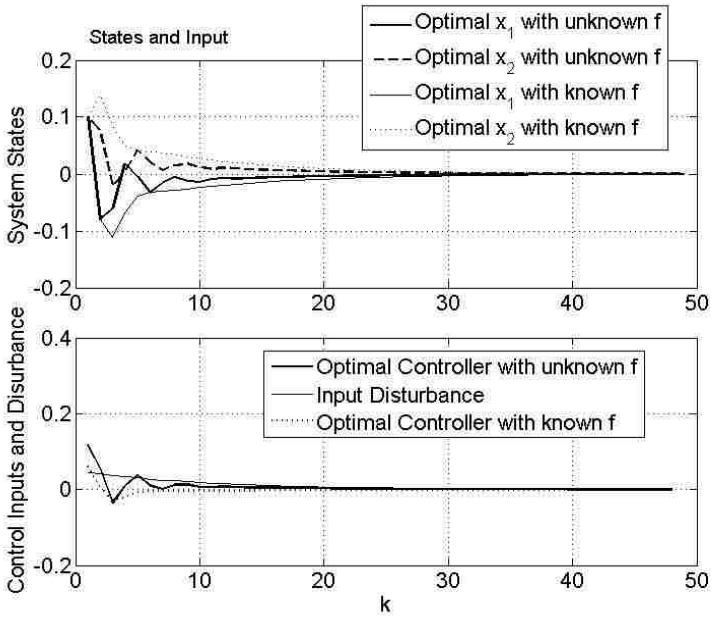

Fig. 12 Nonlinear system states and control inputs with actual $f(x)$ as well as approximated $\hat{f}(x)$

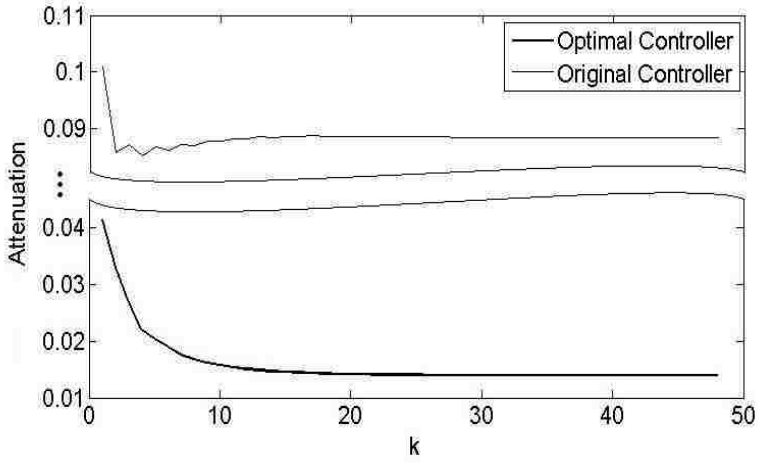

Fig. 13 Nonlinear system control attenuation with approximated $\hat{f}(x)$

Example 4. Consider the linear system described by

$$\begin{bmatrix} x_1(k+1) \\ x_2(k+1) \end{bmatrix} = \begin{bmatrix} 0 & -0.8 \\ 0.8 & 1.8 \end{bmatrix} \begin{bmatrix} x_1(k) \\ x_2(k) \end{bmatrix} + \begin{bmatrix} 0 \\ -1 \end{bmatrix} u + \begin{bmatrix} 0 \\ 1 \end{bmatrix} w. \tag{68}$$

The initial stabilizing controller is chosen to be

$$u = \begin{bmatrix} 1.5 & 1.5 \end{bmatrix} \begin{bmatrix} x_1(k) \\ x_2(k) \end{bmatrix}.$$

The initial conditions of (68) are taken as $x_1(0) = 1$ and $x_2(0) = 1$. Moreover $Q(x) = x^T Qx$ is used and *R=Q(x)=P=1,* $\gamma = 20$. In order to implement the NN approximator, the mesh size in the (x_1, x_2) plane is chosen to be 0.05. The region $(-0.5 \le x_1 \le 0.5, -0.5 \le x_2 \le 0.5)$ is used to train the NN. The NN is defined with the activation functions containing even polynomial functions up to sixth order in the form of $\left[x_1^2, x_1 x_2, x_2^2, x_1^4, x_1 x_2^3 \ldots, x_2^4, \ldots,, x_1^6 \ldots, x_2^6\right]$, and the control input and disturbance are updated according to (19) and (18). Upon completion of the offline training, the performance of

the final optimal control policy is compared to the linear DARE optimal policy (43) as well as initial stabilizing control. The DARE is solved using MATLAB where the matrix Γ is obtained as

$$\Gamma = \begin{bmatrix} 1.5074 & 1.0070 \\ 1.0070 & 3.7919 \end{bmatrix}.$$

In the comparison, a disturbance input $w = 10e^{-0.1k}$ is introduced into the system at *k=0*. The system states and the control efforts when the improved optimal controller and the original stabilizing controller were applied are shown in Fig. 14. Figure 15 shows the attenuation associated with each policy where the attenuation is defined as (67). Examining Fig. 15, a significant decrease in the control effort is observed when the improved optimal control law is applied to the system. In addition, it can be observed that the proposed nonlinear optimal controller coincides with the DARE optimal policy. Figure 16 illustrates the system trajectories with the nonlinear optimal control strategy as well as the DARE optimal controller and original controller.

These examples clearly indicate that the proposed optimal control policy renders the desired performance as expected.

VII. Conclusions

In this paper, nearly optimal solutions for discrete-time (DT) nonlinear control systems are considered. A successive approximation approach is utilized to solve the generalized Hamilton-Jacobi-Isaacs (GHJI) equation that appears in optimal control. Under a small perturbation condition, the definition of GHJI function as well as methods for updating control input and disturbance for DT nonlinear affine systems is proposed, and the associated value function is achieved.

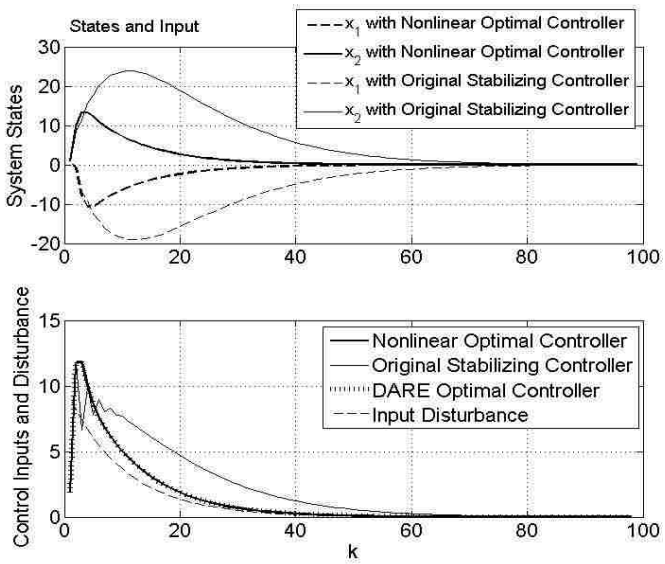

Fig. 14 Linear system states and control inputs with nonlinear and DARE optimal controllers as well as original stabilizing controller

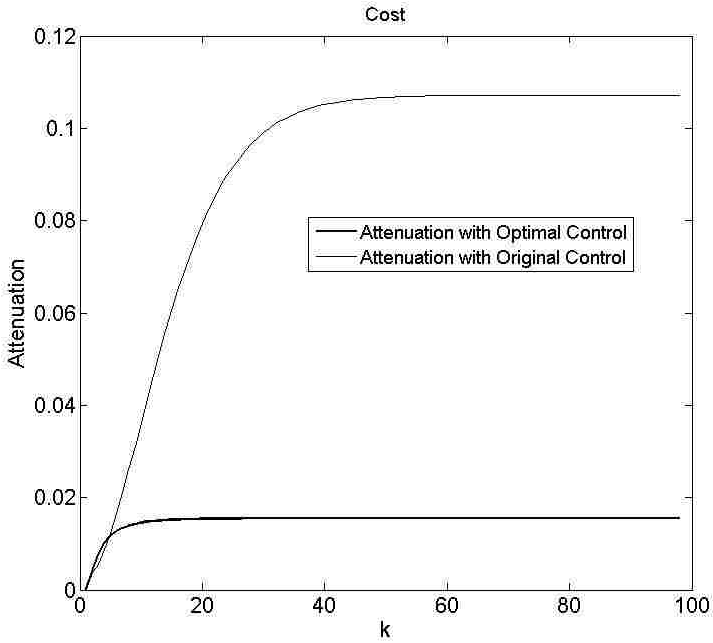

Fig. 15 Linear system control attenuation with nonlinear optimal controller and original stabilizing controller

Moreover, sufficient conditions for algorithm convergence to the saddle-point are derived. Then, a NN is employed to approximate the GHJI equation using a least squares approach. The result is a closed-loop optimal NN controller via off-line learning. Finally, by using an identifier the need for system internal dynamics is relaxed. Simulation results were also presented to verify the theoretical conjectures.

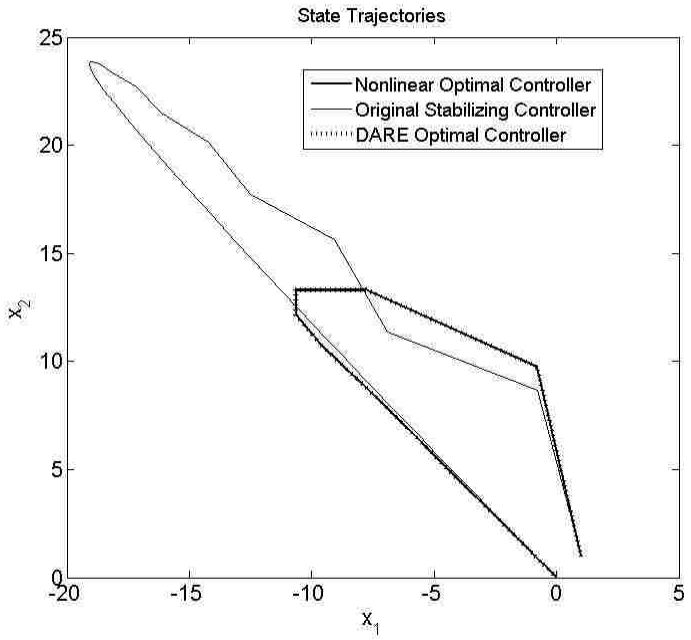

Fig. 16 Linear system trajectories with nonlinear and DARE optimal controllers as well as original stabilizing controller

References

[1] S. Jagannathan, *Neural Network Control of Nonlinear Discrete-time Systems*, CRC Press, April 2006.

[2] T. Basar and G.L. Olsder, *Dynamic Noncooperative Game Theory*, New York, Academic, 1982.

[3] J. H. Doyle, K. Glover, P. Khargonekar, and B. Francis, "State-space Solutions to Standard H_2 and H_∞ Control Problems," *IEEE Trans Automatic Control*, vol. 34, no. 8, pp. 831-847, 1989.

[4] T. Basar and P. Bernard, H_∞ *Optimal control and related minmax design problems,* Birkhäuser, 1995.

[5] J. C.Willems, "Dissipative dynamical systems part I: General theory," *Archive for Rational Mechanics and Analysis*, vol. 45, no.1, pp. 321-351, 1972.

[6] Van Der Schaft, A. J., "L2 -gain Analysis of Nonlinear Systems and Nonlinear State Feedback H_∞ Control," *IEEE Trans. Automatic Control*, vol. 37 no. 6, pp. 770-784, 1992.

[7] J. Huang and C. F. Lin, "Numerical Approach to Computing Nonlinear H_∞ Control Laws," *Journal of Guidance control and Dynamics*, vol. 18, no. 5, pp. 989-994, 1995.

[8] J. Huang, "An algorithm to solve the discrete HJI equation arising in the *L*2 gain optimization problem," *Int. J. Control*, vol. 72, no. 1, pp. 49- 57, 1999.

[9] R. W. Beard and T. W. McLain, "Successive Galerkin approximation algorithms for nonlinear optimal and robust control," *Int. J. Control*, vol. 71, no. 5, pp.717-743, 1998.

[10] M. Abu-Khalaf, F. L. Lewis, Jie Huang, "Neural Network H_∞ State Feedback Control with Actuator Saturation: The Nonlinear Benchmark Problem," *International Conference on Control and Automation (ICCA2005)*, Budapest, June 2005.

[11] W. Lin and C. I. Byrnes, "H_∞ Control of Discrete-time Nonlinear Systems," *IEEE Trans on Automatic Control*, vol. 41, no. 4, pp. 494-510, Apr 1996.

[12] Z. Chen and S. Jagannathan, "Generalized Hamilton–Jacobi–Bellman Formulation-Based Neural Network Control of Affine Nonlinear Discrete-time Systems," *IEEE Trans. Neural Network.*, vol. 10, no. 1, pp. 90–106, Jan. 2008.

[13] F. L. Lewis and V. L. Syrmos, *Optimal Control*, New York, Weily, 1995.

[14] C. A. Desoer and M. Vidyasagar, *Feedback Systems: Input-output Properties*, New York Academic, 1975.

[15] B. A. Finlayson, *The Method of Weighted Residuals and Variational Principles*, New York: Academic, 1972.

[16] S. Mehraeen, S. Jagannathan, M. L. Crow, "Novel Dynamic Representation and Control of Power Networks Embedded with FACTS Devices," *Proceedings of IEEE Conference on System, Man and Cybernetics*, Oct. 2008.

[17] Noroozian M., Angquist L., Ghandhari M., Anderson G., "Use of UPFC for Optimal Power Flow Control," *IEEE Trans. On Power Delivery,* vol. 12, no. 4, pp. 1629-1634, October 1997.

[18] A. A. Al-Tamimi, "Discrete-time Control Algorithms and Adaptive Intelligent System Designs," *PhD dissertation*, University of Texas at Arlington, 2007.

[19] A. Al-Tamimi, D. Vrabie, M. Abu-Khalaf, F.L Lewis, "Model-free Approximate Dynamic Programming Schemes for Linear Systems," *International Joint Conference on Neural Networks (IJCNN 2007),* pp.:371 – 378,12-17 Aug. 2007.

[20] Lewis F.L., Jagannathan S, Yesildirek A., *Neural Network Control of Robot Manipulators and Nonlinear Systems*," Taylor and Francis, 1999.

SECTION

2. CONCLUSIONS AND FUTURE WORK

In this dissertation, neural network (NN) control techniques were utilized in the controller design of a class of nonlinear interconnected dynamic systems with applications to power systems. In order to motivate the need for decentralized control, this work begins by introducing a novel representation of power systems, where the algebraic equations in the conventional representation of the power system are replaced by a set of differential equations. The representation is then generalized to a decentralized representation of power systems and used to implement various nonlinear control techniques starting from traditional backstepping to optimal control by solving the HJB equation forward in time.

2.1. CONCLUSIONS

In the first paper, the decentralized representation of the nonlinear power system clearly demonstrated the need for decentralized control. In the formulation, the approach taken to eliminate the algebraic equations appears to work well. If the system dynamics or nonlinearities are known beforehand, traditional backstepping-based control schemes can be utilized to deliver the desired performance. By contrast, in the second paper, the system nonlinearities and interconnection terms are assumed unknown which is typical in practical situations. Then, to overcome the repeated differentiation normally required in backstepping, dynamic surface control (DSC)–based approach is proposed. The DSC-

based approach with the proposed novel update law consisting of quadratic error terms will indeed provide asymptotic stability of the tracking error when states are available. Further, by using a linear observer introduced in the second paper, the need for state measurability is relaxed. Then, in the third paper, DSC-framework was demonstrated on a power system after the power system decentralized model is developed.

Discrete-time representation and control design are preferred for embedded computer implementation. Therefore, in the forth paper, the decentralized discrete-time controller design for unknown nonlinear interconnected system is introduced and the stringent assumption of bounded interconnected terms is relaxed. Moreover, by employing a NN the system unknown dynamics are approximated while bounded stability of the states and NN weights is guaranteed. The discrete-time decentralized representation of a power system with excitation control is developed and the proposed controller is shown to be effective on damping power system oscillations.

Further, the work of the fifth paper considers the decentralized optimal control of nonlinear interconnected systems where the HJB solution is found forward in time by using NNs with online learning strategies. The large scale system is proven to be optimally controlled and the NN weights are shown to be bounded. The work concludes by finding an offline solution for the discrete-time HJI optimal problem in the sixth paper. This final paper deals with the optimal control of nonlinear discrete-time systems in the presence of disturbances. Then, by using an iterative approach the value function is obtained. Also, the existence of the saddle-point in a zero-sum two-player differential game where the players are system disturbance and control input is proven. Next, approximation properties of neural networks (NN) and least squares are used to obtain the value function. Moreover, a NN identifier is presented in this work to learn the

nonlinear internal dynamics of the system where the obtained NN optimal policy is implemented to mitigate power systems oscillations.

2.2. FUTURE WORK

Future work should address the online discrete-time robust optimal control problem for uncertain decentralized nonlinear systems. Also, the tracking problem in the decentralized control is an open subject which is suggested as future work. Extending the HJI optimal problem to the decentralized nonlinear interconnected systems is also important to achieve optimal control of large-scale systems in the presence of disturbances.

VITA

Shabab Mehraeen was born August 26, 1972 in Tehran, Iran. He earned the Bachelor of Science degree in Electrical Engineering from Iran University of Science and Technology and Master of Science degree in Electrical Engineering from Isfahan University of Science and Technology, Iran, in 1995 and 2001, respectively. He is a member of IEEE – Institute of Electrical and Electronics Engineers and INNS – International Neural Network Society. Shahab Mehraeen received the degree of Doctor of Philosophy in December 2009.